INRES, Institut für Nutzpflanzenwissenschaften und Ressourcenschutz

Optimierung und Modellierung der Wachstumsbedingungen für die geschützte Langzeitkultivierung von *Lemna minor* L.

Dissertation

zur Erlangung des Grades

Doktor der Agrarwissenschaften (Dr. agr.)

der Agrar-, Ernährungs- und Ingenieurwissenschaftlichen Fakultät

der Rheinischen Friedrich-Wilhelms-Universität Bonn

von

Karl-Michael Schmidt

aus

Trier

Bonn 2026

Referent: Prof. Dr. Ralf Pude

1.Korreferent: Prof. Dr. Heiner Goldbach

2.Korreferent: Dr. Thomas Gaiser

Tag der mündlichen Prüfung: 08. Mai 2026

Angefertigt mit Genehmigung der Agrar-, Ernährungs- und Ingenieurwissenschaftlichen Fakultät der Universität Bonn

Results from this work were published as:

Schmidt, K. M., & Goldbach, H. E. (2022). Modelling of *Lemna minor* L. growth as influenced by nutrient supply, supplemental light, CO_2 and harvest intervals for a continuous indoor cultivation. Heliyon, *8*(12). OPEN ACCESS. https://doi.org/10.1016/j.heliyon.2022.e12194

Schmidt, K. M. (2021). Method for operating a culture facility for aquatic plants, and culture facility itself (WO2022123076A1). **European Patent Office**, filed on 13/12/2021, published on 16/06/2022 and granted on 06/11/2024 as EP 4 102 956 B1. https://data.epo.org/publication-server/pdf-document?pn=4102956&ki=B1&cc=EP&pd=20241106

To my family

If I knew exactly how this leaf came out of its branch,

I would remain silent forever, for I would know enough.

Hugo von Hofmannsthal

It is always the older that emanates the new one.

Wolfgang Pauli

Abstract:

Given the proper conditions, *Lemna spp.* rapidly produce a high amount of valuable biomass which is considered as an alternative source for feed and food. For a continuous and long-term indoor production under controlled conditions, environmental and harvest parameters have to be optimized to suppress algal growth and constantly yield a high-quality product. Experimentally assessing the effect of a larger number of parameters on the growth rate r_i is impossible due to the theoretically high number of parameter combinations. Thus, a SIMILE® - based model has been developed. This enables production parameters to be assessed individually for its effect on the growth rate r_i by a differential equation. Start values for numerical integration were taken from measured data and analytical solutions of the differential growth equation. At 400 ppm CO_2, the regrowth rate *ri* in an optimized laboratory set-up amounted to 216 g FM·$m^{-2}d^{-1}$, harvesting one third of the biomass at intervals of 5 days. In up-scaled set-ups, lower regrowth rates *ri* of about 173 g FM·$m^{-2}d^{-1}$ (Kalkar) and 190 g FM·$m^{-2}d^{-1}$ (Berlin) were obtained, because temperature and light conditions were below optimum. At 3,500 ppm CO_2, the regrowth rate *ri* in laboratory set-up increased to 323 g FM·$m^{-2}d^{-1}$ by shortening the harvest interval to three days. Maximum growth rates *ri* were obtained with an NH_4^+/NO_3^- ratio of 1/9 at 1.14 mM total N concentration. In order to account for the average frond age of the Lemna population due to the impact of cyclically repeated partial harvesting, an additional sub-model was created. There was an increase in protein content and a decrease in oxalic acid and heavy metal accumulation for younger average frond ages. These results indicate how to optimize culture conditions and partial harvest intervals. Model runs closely match the experimental data taken from the three different approaches and thus confirm the validity of the model.

Zusammenfassung

Unter geeigneten Bedingungen produzieren Lemna spp. rasch große Mengen wertvoller Biomasse, die als alternative Quelle für Futter- und Lebensmittel gilt. Für eine kontinuierliche und langfristige Indoor-Produktion unter kontrollierten Bedingungen müssen Umwelt- und Ernteparameter optimiert werden, um das Algenwachstum einzudämmen und stets ein qualitativ hochwertiges Produkt zu liefern. Eine experimentelle Bewertung des Einflusses einer größeren Anzahl von Parametern auf die Wachstumsrate r_i ist aufgrund der theoretisch hohen Anzahl an Parameterkombinationen unmöglich. Daher wurde ein SIMILE®-basiertes Modell entwickelt. Dieses ermöglicht es, Produktionsparameter einzeln auf ihren Einfluss auf die Wachstumsrate r_i mittels einer Differentialgleichung zu untersuchen. Die Startwerte für die numerische Integration wurden aus Messdaten und analytischen Lösungen der differentiellen Wachstumsgleichung entnommen. Bei 400 ppm CO_2 betrug die Wachstumsrate r_i in einem optimierten Laboraufbau 216 g $FM \cdot m^{-2}d^{-1}$, wobei ein Drittel der Biomasse in Abständen von 5 Tagen geerntet wurde. In großtechnischen Versuchen wurden niedrigere Nachwachsraten r_i von etwa 173 g $FM \cdot m^{-2}d^{-1}$ (Kalkar) und 190 g $FM \cdot m^{-2}d^{-1}$ (Berlin) erzielt, da die Temperatur- und Lichtbedingungen unter dem Optimum lagen. Bei 3.500 ppm CO_2 stieg die Wachstumsrate r_i im Laborversuch durch Verkürzung des Ernteintervalls auf drei Tage auf 323 g $FM \cdot m^{-2}d^{-1}$. Maximale Wachstumsraten r_i wurden bei einem NH_4^+/NO_3^- Verhältnis von 1/9 und einer Gesamtstickstoffkonzentration von 1,14 mM erzielt. Um das durchschnittliche Blattalter der Lemna-Population aufgrund der Auswirkungen der zyklisch wiederholten Teilernte zu berücksichtigen, wurde ein zusätzliches Teilmodell erstellt. Bei jüngerem durchschnittlichem Blattalter war ein Anstieg des Proteingehalts sowie eine Abnahme der Oxalsäure- und Schwermetallakkumulation zu beobachten. Diese Ergebnisse zeigen auf, wie die Kulturbedingungen und die Teilernteintervalle optimiert werden können. Die Modellläufe stimmen weitgehend mit den experimentellen Daten aus den drei verschiedenen Ansätzen überein und bestätigen somit die Validität des Modells.

Table of contents

ABBREVIATIONS

AFA	**A**verage **f**rond **a**ge
ATP	**A**denosin**t**ri**p**hospate
ADP	**A**denosin**di****p**hospate
BSA	**B**ovine **s**erum **a**lbumin
CPVO	**C**ommunity **P**lant **V**ariety **O**ffice
CFU	**C**olonie **f**orming **u**nit
DNA	**D**esoxyribo**n**ucleic **a**cid
DW	**D**ry **w**eight
DM	**D**ry **m**atter
DPMA	**D**eutsches **P**atent- und **M**arken**a**mt
DURAN®	Borsilicateglas
EC	**E**lectrical **c**onductivity
EDDHA	Ethylenediamine-N,N'-bis(2-hydroxyphenylacetic acid
EDTA	Ethylenediaminetetraacetic acid
EFSA	**E**uropean **F**ood **S**afety **A**gency
EPO	European Patent Office
FW	**F**resh **w**eight
FM	**F**resh **m**atter
HACCP	**H**azard **a**nalysis and **c**ritical **c**ontrol **p**oints
dH_2O	H_2O_{demin}
ICP-AES	**I**nductively **C**oupled **P**lasma **A**tom **E**mission **S**pectroscopy
LAI	**L**eaf **a**rea **i**ndex
LC-MS	**L**iquid **c**hromatography **m**ass **s**pectrometry
LED	**L**ight **e**mitting **d**iode
LHC	**L**ight **h**arvesting **c**omplex
LOM	**L**aw **o**f **m**inimum
Mbp	**M**ega **b**ase **p**airs

MS	**M**ass **s**pectrometer
MUFA	**M**ono**u**nsaturated **f**atty **a**cid
NADH	Nicotinamidadenindinukleotid
n.f.	not found
PEPC	**P**hospho**e**nol**p**yruvat**c**arboxylase
PQ	**P**lasto**q**uinone
PS	**P**hotosynthetic **s**ystem, PSI and PSII
PAR	**P**hotosynthetic **a**ctive **r**adiation
PUFA	**P**oly**u**nsaturated **f**atty **a**cid
RAPD	**R**andom **a**mplification of **p**olymorphic **D**NA
RHS	**R**oyal **h**orticultural **s**ociety
r_i	Growth rate
Rpm	**R**otation **p**er **m**inute
RUBISCO	Ribulose-1,5-Bisphosphate-Carboxylase
RuBP2	Ribulose-1,5-bisphosphat
SD	**S**tandard **d**eviation
SE	**S**tandard **e**rror
SFA	**S**aturated **f**atty **a**cid
Tanh	**Tan**gens **h**yperbolicus
TOC	**T**otal **o**rganic **c**arbon
Tp	**T**urning **p**oint
UV	**U**ltra **v**iolet
W_{max}	Capacity of population

1. INTRODUCTION

In order to ensure the feeding of the growing world's population in future decades, agricultural yields of protein crops for human food and animal feed must be increased. This requirement poses major challenges for humanity in terms of both available agricultural land and available crops. On the one hand, more efficient crop plants need to be found while the ongoing eutrophication of the water bodies via the aquifer of the cultivated areas must be avoided on the other *(Jung, 2022).* This is against the background of necessary yield increases of approximately 1.5% per year until 2050, taking into account the expected increase of the world's population to > 9 billion people *(Lee, 2011), (Sadigow, 2022), (Beltran-Peña et al., 2020)*.

For this reason, as land for cultivation will hardly increase and rather decline, ways to intensify crop production have to be found *(Hossain et al., 2020)*. One way is to use protected year-round production systems, which is challenging and needs to be optimized in order to minimize both the consumption of resources and the carbon footprint.

Considering these requirements, duckweeds (*Lemnoideae*) as floating aquatic higher plants may play a significant role in the future, given their high growth rates and protein contents.

Most genera of this plant family belong to the smallest higher plants. In large parts of south Asia, such as in India, Bangladesh and Pakistan *(Appenroth et al., 2017), Lemnoideae* are already considered as a potential food crop. However, taking into account their amino acid spectrum which has been classified to be of high quality by the WHO (World Health Organisation) *(Appenroth et al., 2017),* appropriate culture methods must be provided to obtain healthy and hygienically safe food and feed, and to optimize their nutritional value. In addition, culture methods have to be found which assure high productivity worldwide throughout the year. As *Lemnoideae* are aquatic plants, drought under field conditions will play no role if duckweeds are cultivated indoors, provided that the water is recycled, and closed systems are designed. Since 2010, it has been established that *Lemnoideae* can be cultivated on stacked racks to minimise the required floor space at Spierhof in Kalkar. With regard to year-round optimal cultivation conditions in temperate and cooler climates,

heating concepts are required that use low-caloric waste heat from industrial production processes or IT server compounds which is otherwise no longer useful for other technical applications.

Working in closed systems also allows a recycling of nutrients, and systems will need to be designed in a way that avoid any contamination.

In order to be able to economically produce duckweeds in sufficient amounts and in food-grade quality, such culture reactors and their operating procedures must be capable of a long-term stable operation. The end product must be largely free of anti-nutritional factors *(Li et al., 2022)*. Thus, the concentration of calcium oxalate and oxalic acid, as well as the accumulation of nitrate and heavy metals *(Miller, 2023), (Turck et al., 2022),* are crucial.

Two *Lemnoideae* species of the genus *Wolffia* (*Wolffia globosa* and *Wolffia arrhiza*) have already been tested and approved in Europe by the European Food Safety Authority (EFSA) as "novel food". With regard to *Lemna minor*, *Turck et al. (2022)* have demanded consolidated conditions for compliance with limits for heavy metals.

To produce sufficient quantities of *Lemnoideae*, especially *Lemna minor*, indoors, culturing can practically only be performed non-axenically. *Lemnoideae* are also known to tolerate low light. Therefore, *Lemnoideae* can be cultivated as "future crops" in a space-saving manner, even in stacks, with a minimum of additional illumination. For maximum yield and quality, the suppression of competitive algal growth is just as important as the optimisation of all culture parameters, such as nutrient concentrations and nutrient ratios, temperature, light, and additional CO_2.

For the use of *Lemnoideae* as a future protein-containing food and feed, the above-mentioned requirements must be met, and appropriate quantities produced. *Lemna minor* was selected for this study because of the highest growth rates and maximum protein yields achievable per unit of area and time.

2. LITERATURE REVIEW

2.1 Lemnoideae

2.1.1 Anatomy

Lemnoideae (duckweed, waterlentils) are floating aquatic higher plants belonging to angiosperms and monocotyledons. The first basic works on *Lemnoideae* were published by *Kaufmann (1868), Hegelmaier (1870), Hegelmaier (1871)* and *Hanstein (1871).* These mainly morphological works were related to developmental studies of the plants and were published already after the development and publication of Darwin's theory of evolution in 1859. Detailed morphological descriptions by *Hegelmaier(1870)* are still valid today.

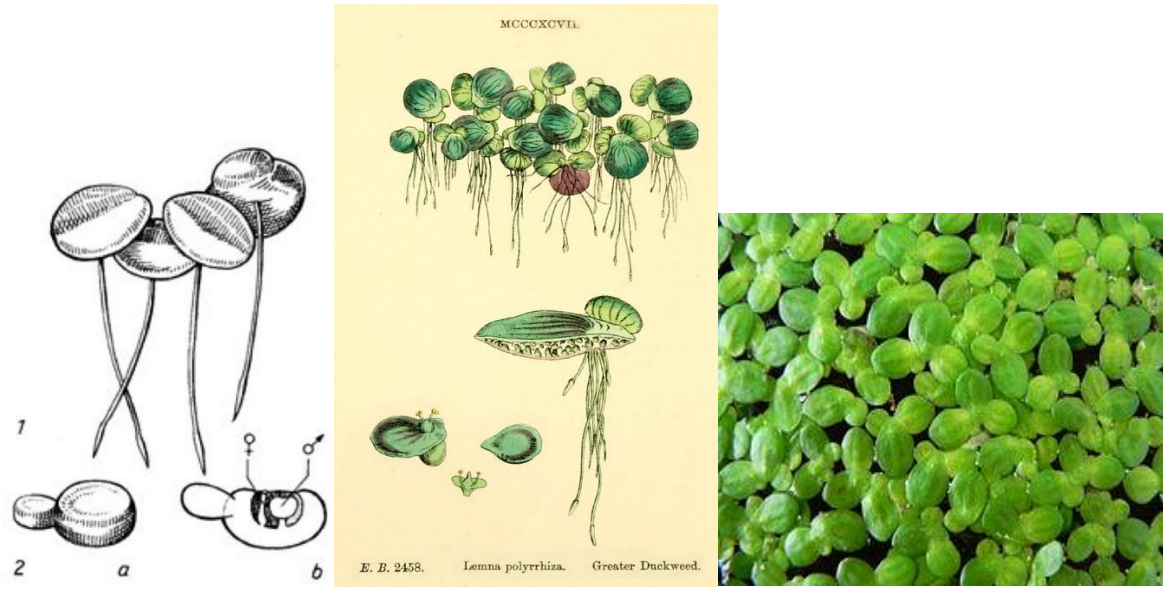

Fig. 1: The historical illustrations (left and centre) *(Appenroth & Augsten, 1996), (Brechner, 2001)* show all the characteristics of *Lemnoideae* as a higher plant; leaf, shoot axis, roots, and the diocesan organs for generative reproduction. The illustration on the right shows a current floating population of *Lemna minor*.

The relevant morphological characteristics of the species *Lemna minor* L. used for this study, compared with the further well-known genera *Spirodela polyrrhiza*, *Lemna perpusilla,* and *Lemna gibba (Andriani et al., 2019)* are shown in Table 1 as an overview.

A first varietal categorisation and registration were initiated by *Schmidt (2011)* for the species *Lemna minor* L.*, Spirodela polyrhiza,* and *Landolthia punctata*. These variety descriptions were carried out according to the provisions of the *Community Plant Variety Office CPVO* (France) at the *Institute Naktuinbouw* (Roelofarendsveen, Netherlands). Thus, a four-point

distinguishing description system had to be developed, based on the morphology of the fronds roots, colour, and structure in top view of a dense population. This approach has been accepted by the CPVO and is now included in the regular (standardized) criteria in an official questionnaire for any future applications of *Lemnoideae* (see Appendix). In this work, the cultivar *Lemna minor 'Henry DaCapo' (EU29760) 2011* was mainly used. Characteristics are described in the Appendix (Certificate on the Grant of a Community Plant Variety).

Tab. 1: Morphological characteristics of several species, *added data of *Lemna minor* species used by the author of this work, taken from the CPVO plant description (see Annex)

Characteristics	*S. polyrhiza*	*L. perpusilla*	*L. gibba*	*L. minor* *
Root				
Tip	Pointed	Pointed	Rounded	Rounded
Sheath	Not winged	Winged	Winged	Not winged
Length	10-15mm	10-20mm	10-20mm	10-20mm
Number	9-15 per frond	1 per frond	1 per frond	1 per frond
Frond				
Habit	Floating	Floating	Floating	Floating
Shape	Ovate to sub-orbicular	Obovate to oblong	Obovate	Obovate
Apex	Obtuse to rounded	Obtuse	Obtuse to rounded	Obtuse to rounded
Number	Solitary (2-5 in group)	Solitary (2-5 in group)	Solitary (2-4 in group)	Solitary (2-7 in group)
Margin	Entire	Entire	Entire	Entire
Length	8-16mm	10-15mm	7-12mm	1-8mm
Branching	Unbranching	Unbranching	Unbranching	Unbranching
Scale	Present in ventral and dorsal	Absent	Absent	Absent
Gibbous	Present	Absent	Present	Present
Nerves	Prominent, 7-12 nerves	Indistinct nerve	Indistinct nerve	Indistinct nerves
Symmetry	Symmetric	Symmetric	Asymmetric	Symmetric
Surface	Brown pigment in ventral, green in dorsal and slightly convex	Flat in dorsal and ventral	Gibbous in ventral and dorsal, brown pigment in ventral, shining in dorsal	Gibbous in vertical and dorsal, dark green

With a mother frond size of about 15mm, *Spirodela polyrhiza* is the largest among them, while *Wolffia globosa, Wolffia arrhiza,* and the newly added *Wolffia microscopica* are the smallest ones with less than one millimeter in size. A conclusion of this may be a successive reduction of morphological structures in parallel with evolutionary development *(Wang et al., 2011)*.

Improved morphological description criteria were developed by the author to distinguish between varieties within the species, and accepted by the Community Plant Variety Office (CPVO), Angers CEDEX 2, France, see Annex. *Severi & Fornasiero (1983)* found that the morphology in *Lemna minor* can also vary with the concentration of abscisic acid.

The individual capacity of a population of *Lemnoideae* is strongly dependent on its anatomy and is one of the most important parameters for obtaining maximum yields over time.

2.1.2 Geographic distribution

Under natural conditions of temperate zones, *Lemnoideae* grow vegetatively between May and October. During the transition from the long-day to short-day photoperiod, flowering and the formation of turions are induced (circadian clock) *(Miwa et al., 2006),* as mentioned above for *Spirodela polyrhiza*, *Landolthia punctata, Lemna minor,* and *Lemna gibba (Fu et al., 2017).* The influence of the photoperiod on flowering was already described by *Bünning (1967), Christensen et al. (1992), Covington et al. (2001), Doi et al. (2004), Fowler et al. (1999),* and *Datko et al. (1980),* also for *Lemna paucicostata* Hegelm. 6746. A further update of flower induction was given by *Muranaka (2022)* for *Lemna aequinoctialis,* and by *Ueno et al. (2022) for Lemna minor.*

Lemnoideae are found around the world, except for arid and arctic areas *(Appenroth & Augsten, 1996; Cheng & Stomp, 2009).* This applies to all 5 known genera. They thrive in so-called mesotrophic and eutrophic water habitats, such as quiet lakes, water ditches, but also in marshlands and ponds *(Appenroth, 1993)*. See Fig.2.
Even though duckweeds (*Lemnnoideae)* are C3-plants *(Wedge & Burris, 1982), (Bauer et al., 1983), (Bauer et al., 1976), (Bauer & Martha, 1981),* their optimal culture temperature is atypically high (about 29-31°C).

Most duckweed species are floating, often forming a closed plant cover. Only a few species are submerged, such as *Lemna trisulca (Erismann & Finger, 1967), (Leng et al., 1999).* The respective water habitats are standing or only slowly moving. Outdoors, reductions in temperatures, nutrient supply, and/or shorter day lengths lead to the formation of an overwintering bud, termed turion *(Acosta et al., 2021).* Turions store starch and sink to the bottom of the water habitat due to their higher specific weight. The storing of starch is induced by the phytohormone abscisic acid. With increasing spring temperatures, the turions rise back up, developing new fronds *(Appenroth, 1993), (Acosta et al., 2021).*

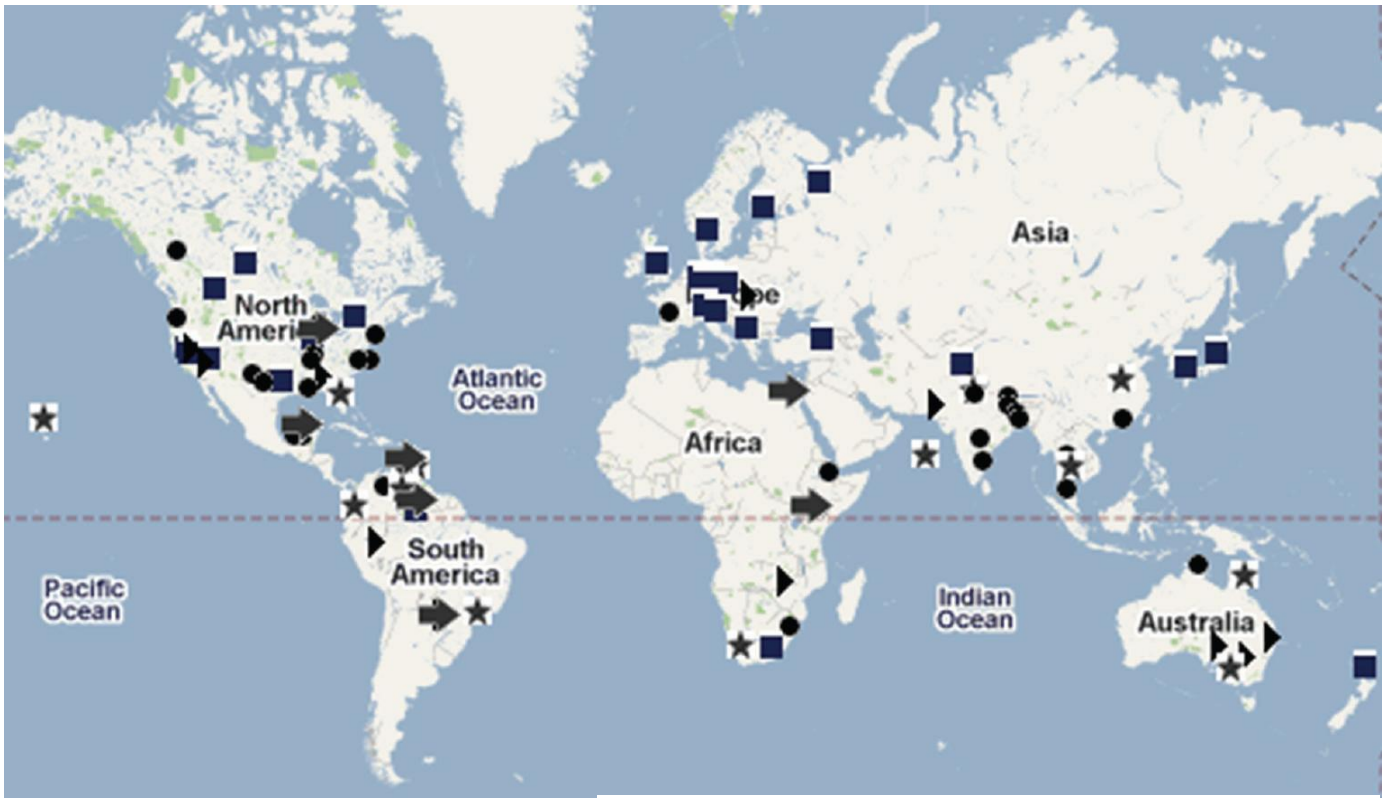

Fig. 2 Souce: Wang et al. 2011, Geographical distribution of the Lemnoideae genera

According to literature, the increase of DNA contents corresponds to the increasing latitude found in the *Pinaceae* family (*Ohri & Khoshoo, 1986),* and also to the increasing altitude observed in *Zea mays* (*Rayburn & Auger, 1990),* and is observed in the *Lemnoideae* by *Wang et al. (2010)*.

Another important species briefly mentioned is *Wolffia globosa*. As a rootless species, it shows a completely different behaviour in culture in nutrient uptake and growth *(Yang et al., 2021)*.

2.1.3 Systematics, genetics

Lemna minor belongs to the *Lemnoideae (Les et al., 2002)*. They form a subfamily within the family of *Araceae* (arum or aroid family) *(Andriani et al., 2019)*.

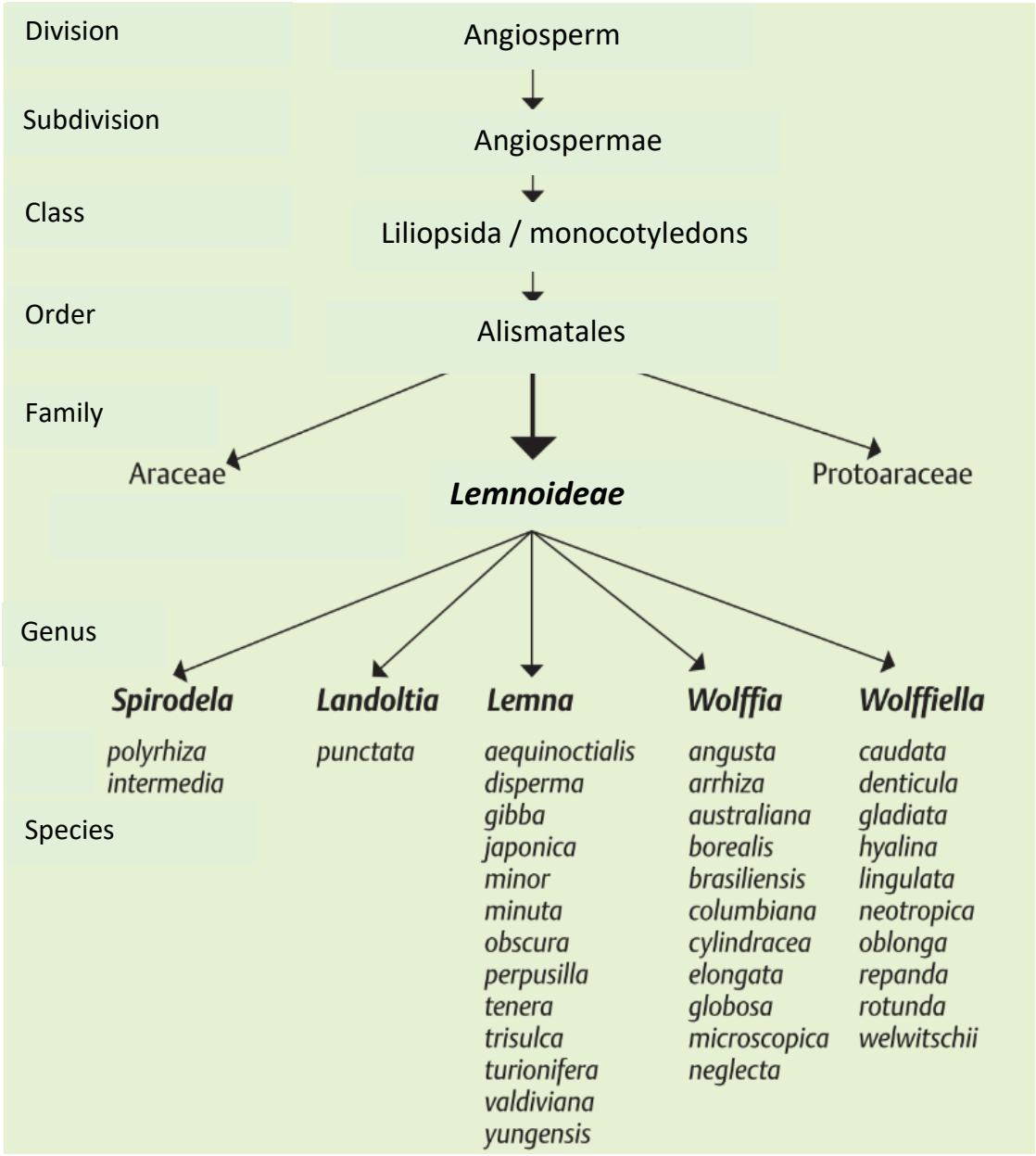

Fig. 3: Phylogenetics; Systematics of Lemnoideae, (Appenroth & Lam, 2012)

The detailed classification according to *Appenroth & Lam (2012)* is shown in Fig. 3. To this date, the family of *Lemnoideae* includes 36 species which are divided into five genera, *Spirodela, Landoltia, Lemna, Wolffia,* and *Wolffiela*. *Spirodela* is the most ancestral, while *Wolffia* is the most recent and evolved one (*Les et al., 2002; Landolt, 1992*). *Acosta et al. (2021)* presented an overview of the 36 species, as well as their corresponding genetic ancestry (Fig. 4). *Bog et al. (2019),* furthermore, deduced that all five genera are monophyletic. In this context, it is further shown which species have been frequently considered in genetic studies since 2011, particularly by *Wang et al. (2011).* Furthermore, the genome sizes of the investigated species are presented.

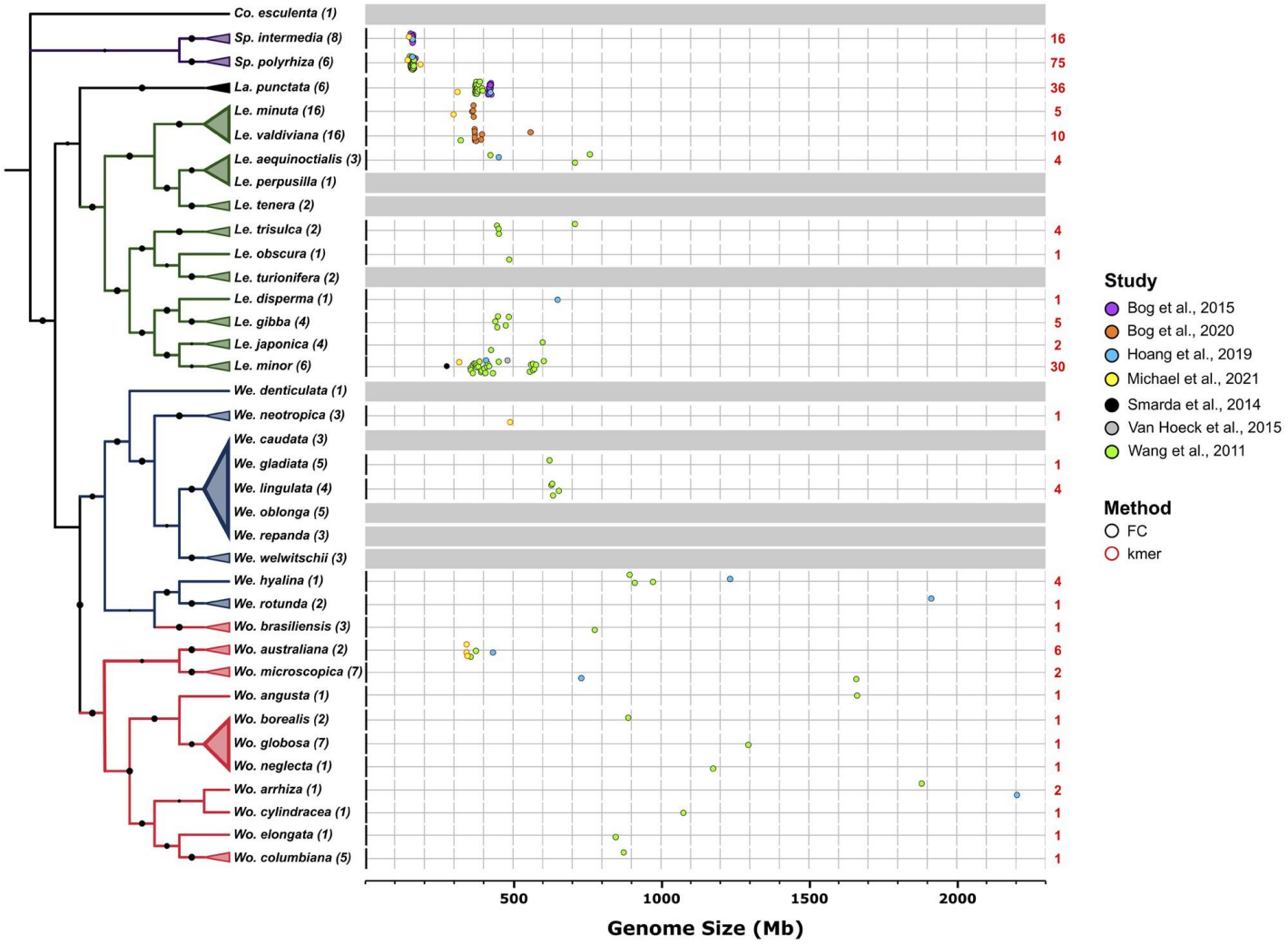

Fig. 4: Source: Acosta el al. (2021) Genome size for the currently described 36 species of Lemnoideae according to the frequency of mention in relevant basic publications of genetic studies since 2011.

The genetic classification of the individual species is widely known from *Les et al., (2002), Wang et al., (2011),* and *Hoang et al. (2019).* RAPD (DNA) analysis of genome polymorphism in *Lemnoideae* has been intensively studied by *Martirosyan et al. (2008)*. A more detailed genotyping was carried out by, e.g., *Klaus et al. (2013),* and *Xu et al. (2015),* and was further refined by *Acosta et al. (2021).* The respective genome sizes are indicated in Fig. 4, including the number of DNA base pairs contained within the haploid set of chromosomes of each of the *Lemnoideae* spp.. The approximated genome size has been mapped to the phylogenetic tree for *Lemnoideae*, combining morphological features, flavonoids, allozymes, and the DNA sequence analysis, according to *Wang et al. (2011).* With respect to the comparisons of the genome sizes, *Lemna minor* has a value of about 400Mbp. Both *Landoltia punctata* and *Lemna gibba* are near this value. *Wolffia* shows a remarkable distribution, which may vary from about

600Mbp to more than 2,200Mbp, depending on the species, which is impressive for the smallest of all *Lemnoideae*. Related to that, in the phylogeny of *Lemnoideae*, the evolution of the genome size relates to the morphological progression. *Wang et al. (2011),* and later, *Xu et al. (2015)* confirmed that the ancestral genus *Spirodela* has the smallest genome size, while the most advanced genus *Wolffia* has both the biggest genome size and the highest genetic diversity, as is shown above in Fig. 4. On this basis, it was found that this relationship correlates with morphological reduction, rather than with organism complexity within the family. This correlation is consistent with the findings in *Landolt (1986),* which showed a relationship between DNA content and degree of primitivity. The cytological variation in duckweed has been extensively studied by counting its chromosomes. It was concluded that polyploidy (2n = 20, 30, 40, 50, 60, 80) was the main intra-populational variation (*E. Landolt, 1986).* This means that polyploidy is very common, having occurred in duckweed multiple times in the past. According to this, polyploidy, transposable element mobility, insertions, deletion, and epigenome restructuring contribute to the successful development of a new species and also to changes in the genome size, see *A. R. Leitch & I. J. Leitch (2008),* and they have an immediate effect on the phenotype and the fitness of an individual, see *Otto (2007).* Polyploidy might promote the divergence during the evolution of duckweed. Changes in the genome structure may lead to a differential gene loss and to extensive changes in gene expression, see *Adams & Wendel (2005),* and may have immediate effects on the phenotype and the fitness of an individual *(Otto, 2007).* It was suggested in the past that variations in the DNA content have an adaptive significance and correlate with the environmental traits of species *(M. C. J. Bottini et al., 2000).* The first details about the life time of *Lemna minor* was published by *Caldwell (1899)*. In the meantime, *Lemnoideae* have also been fully genetically sequenced (*Fourounjian, 2020)*. Every species of *Lemnoideae* is highly invasive with a strong exponential, predominately vegetative growth *(Acosta et al., 2021), (Leng et al., 1995), (Sree et al., 2015), (Sree et al., 2020)*. Defined genetic triggers according to that were also confirmed by *Appenroth et al. (2013)* in detail.

2.2 Growth of *Lemnoideae*

2.2.1 Temperature

Optimum temperatures for highest growth rates for all *Lemnoideae* genera (see Fig.5) were determined by *Docauer (1983)* and *Landolt et al. (1987)* and more recently confirmed by *Lasfar (2007)*.

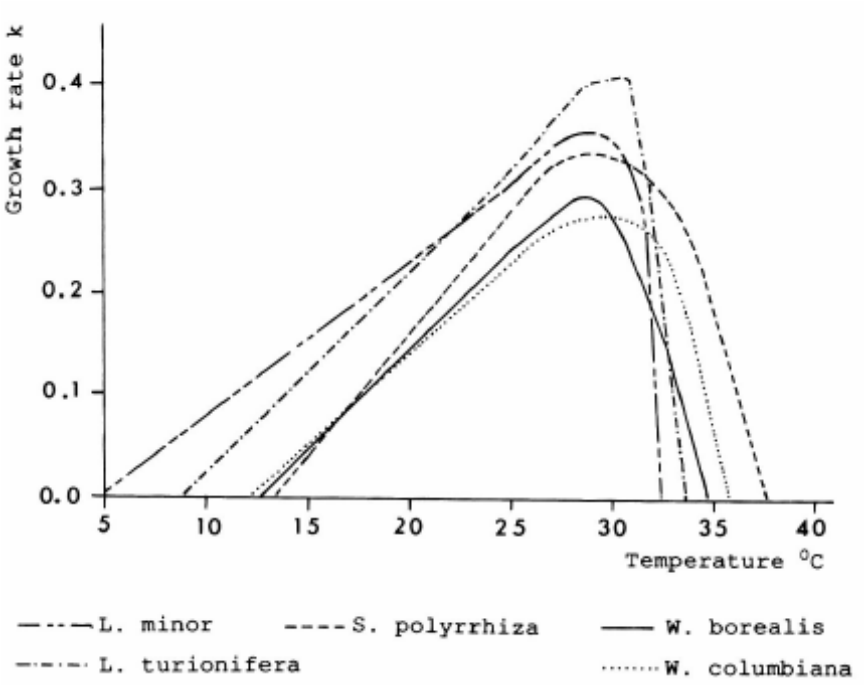

Fig. 5: Growth rate of different Lemnoideae species in relation to temperature (Docauer 1983), as illustrated in Landolt et al. (1987)

According to the cited works, the growth rate for all genera of *Lemnoideae* increases strongly with increasing temperatures, reaching its maximum within only a small temperature range between 28°C and 31°C, decreasing very steeply above this temperature. For *Lemna minor,* the optimum manifests itself at 29°C.

2.2.2 Demand of nutrients

Aligned with the known strong exponential growth of *Lemnoideae,* their consumption of nutrients is high. Thus, they were considered for the remediation of eutrophic water bodies (*Ansari & Khan, 2008), (Walsh et al., 2001), (Paolacci et al., 2021).* Data regarding their geographic origin provide initial clues to the preferred living conditions and nutrient requirements of the respective species *(Datko et al. 1980)*. The classic macronutrients, N, P and K, play an essential role in the cultivation of *Lemna*, particularly in optimizing/maximizing

the protein synthesis. Furthermore, molar ratios of N/P, N/K, and N/Mg are important. Comparing known experimental set-ups *(Petersen et al., 2021; Khvatkov et al., 2021; Devlamynck et al., 2021),* nutrient solutions were adjusted to a pH value of 6.5-6.9 considering that under non-axenic conditions the growth of competitive algae needs to be supressed. Maintaining a stable pH within the nutrient solution is a particular requirement for obtaining optimal growth conditions of an exponentially growing, non-axenically operated *Lemna* culture. *McLay (1976)* already considered the pH level of the nutrient solution to be important for an optimal growth of duckweed, mainly *Lemna minor, Spirodela oligorrhiza*, and *Wolffia arrhiza.* Because *Lemna minor* are growing so fast, they demand a high continuous supply of nutrients, considering that during their life cycle of about 28-30 days, 11+/-1 buddings take place *(Wersal & Turnage, 2021).* Different standard nutrient solutions (*Hoagland & Arnon, 1938), (Schenck & Hildebrandt, 1969), (Steinberg, 1946)* have been used by various working groups, some in modified form. The so-called N-medium was considered in *Appenroth (2015)* and *Appenroth et al. (1996)*. Fig.6 shows the growth rates of *Lemna minor* to be dependent on N and P concentrations in the nutrient solution by *Lasfar (2007)*. The maximum intrinsic growth rate of about 0.4 d^{-1} was reached above 1mg P L^{-1} (0.033 mM P) and above 2.5 mg N L^{-1} (0.178mM N), remaining nearly constant till 9.6 mg P L^{-1} (0.31 mM P) and till 28 mg N L^{-1} (2.0 mM N). Above 10 mg P L^{-1} (0.32 mM P) and above 30 mg N L^{-1} (2.14 mM N), the growth rate decreases slightly. With reference to this well-known work, it is already apparent that N and P concentrations are lower in the optimum than the classical nutrient solutions mentioned above.

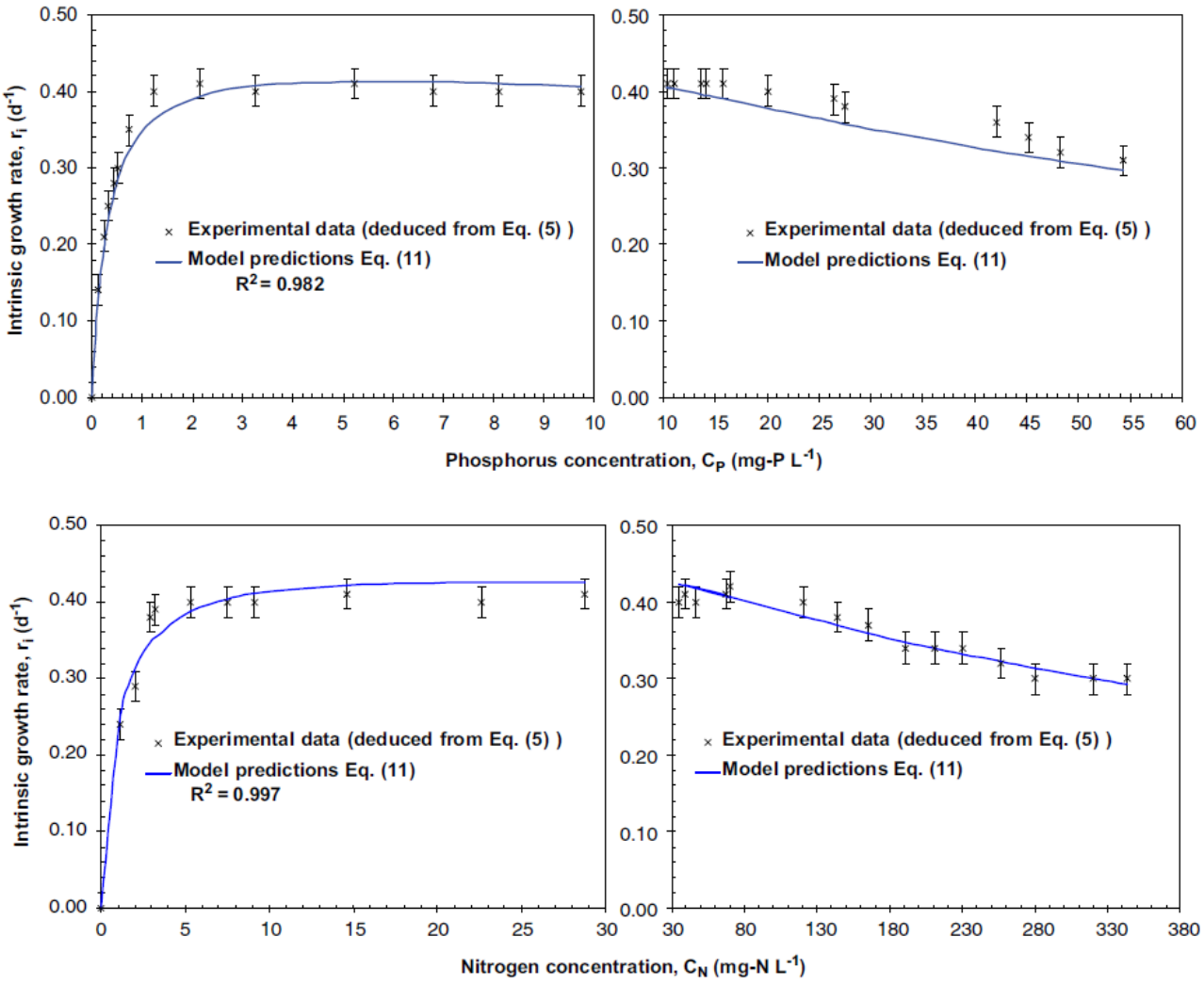

Fig.6: Growth rate of Lemna minor, dependent on N and P concentrations, aligned with model predictions by Lasfar et al. (2007)

Devlamynck et al. (2021) used a modified Steinberg *(Steinberg, 1946)* nutrient solution with 8mM of K and 10mM of N, provided mainly as KNO_3, to detect nitrate accumulation in *Lemna minor.* Other macronutrients were used in the nutrient solution, aligned mainly with the concentrations defined in standard nutrient solutions.

Tab. 2 shows ingredients linked to chlorophyll with respect to the species *Wolffia microscopica*, as well as pattern of phytosterols and elements concentration.

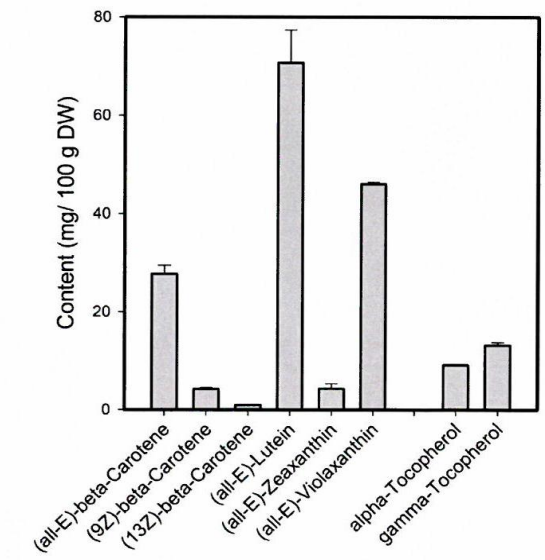

Pattern of phytosterols in *Wolffia microscopica* (Total content of sterols: 50 mg/g lipid extract).

Peak number	Sterol	Retention time [min]	Sterol composition
1	Campesterol	20.2	18%
2	Stigmasterol	20.4	15%
3	Sitosterol	20.7	53%
4	Δ5-Avenasterol	20.8	11%
5	Δ5,24(25)-Stigmastadienol*	20.9	1%
6	Cycloartenol	21.0	2%

* Tentatively identified by (relative) GC retention time and GC/MS data.

Macro elements [g/kg DW]		Micro elements [mg/kg DW]		Heavy metals [mg/kg DW]	
Ca	6.0	Fe	240	Cd	0.40
K	83	Mn	755	Pb	0.24
Mg	3.1	Cu	3.52	Hg	0.04
Na	0.30	Zn	30.8	As	0.05
P	7.04	I	0.75		
		Se	0.06		

Ash content: 165.1 ± 0.6 g/kg DW

Essential micronutrients are playing a crucial part in the chlorophyll synthesis of all genera of *Lemnoideae*. In addition to this dependency, it was noted that even a marginal dose of the element boron had an effect on the starch-protein ratio. *Camacho-Cristóbal, González-Fontes (1999)* manifested, for tobacco leaves, that boron deficiency decreases nitrate reductase activity. *Türker et al. (2017)* found, for *Lemna gibba* L., that boron deficiency decreases growth

and photosynthesis, and increases starch production. According to *Xu et al. (2011), Xu & Shen (2011), Xu et al. (2023),* both the method of cultivation and the quality of the culture water have a strong effect on the amino acid content and on the concentration of individual amino acids. It is well known that a sodium content of 5-50 mM l^{-1} within the culture water generates a higher starch content in *Lemna minor* at the expense of the protein content. *Ullah et al. (2021)* examined the effect of salt stress of *Lemna minor* and found that, at a NaCl concentration of 2g/l in the nutrient solution, the protein content was not decreasing. Decrease of protein content starts at 4g/l NaCl. *Zhao et al. (2015)* studied this effect already with an additional view on nitrate and phosphate. However, this consideration is only relevant when liquid manure is used as a sustainable source of nutrients for *Lemnoideae* cultivation.

Landolt & Kandeler (1987) found that raw protein values of up to 45% could be achieved under a strong exposition to light and a high concentration of nitrate. So far, it has been shown that the protein content varied with these cultivation parameters; see *Yu et al. (2011).* The crude protein value is usually determined according to Kjeldahl method F6,25 *(VDLUFA, 2012)*. For optimization of nutrient solutions and cultivation parameters, it is crucial to provide a precise determination of the actual pure protein concentration within the biomass. Otherwise, for example, a high nitrate concentration within the nutrient solution could keep up the additional storing of nitrates in the vacuoles during cultivation, as was shown by *Devlamynck et al. (2020)*, thus only pretending a high protein synthesis. Therefore, the Kjeldahl method requires an elimination of nitrate before analysis to yield pure protein values.

A further essential element is iron. Since *Cornelis et al. (2009)* examined strict iron uptake regulation in bacteria, *Kobayashi & Nishizawa (2012)* confirmed the same for *Lemnoideae* as higher plants. It may be expected that a high chloroplast density of the shade (low light) tolerant *Lemnoideae* requires a higher uptake of corresponding amounts of Fe compared to other species.

2.2.3 Light

The correlation between light exposure and growth rate for *Lemnoideae* is widely known.

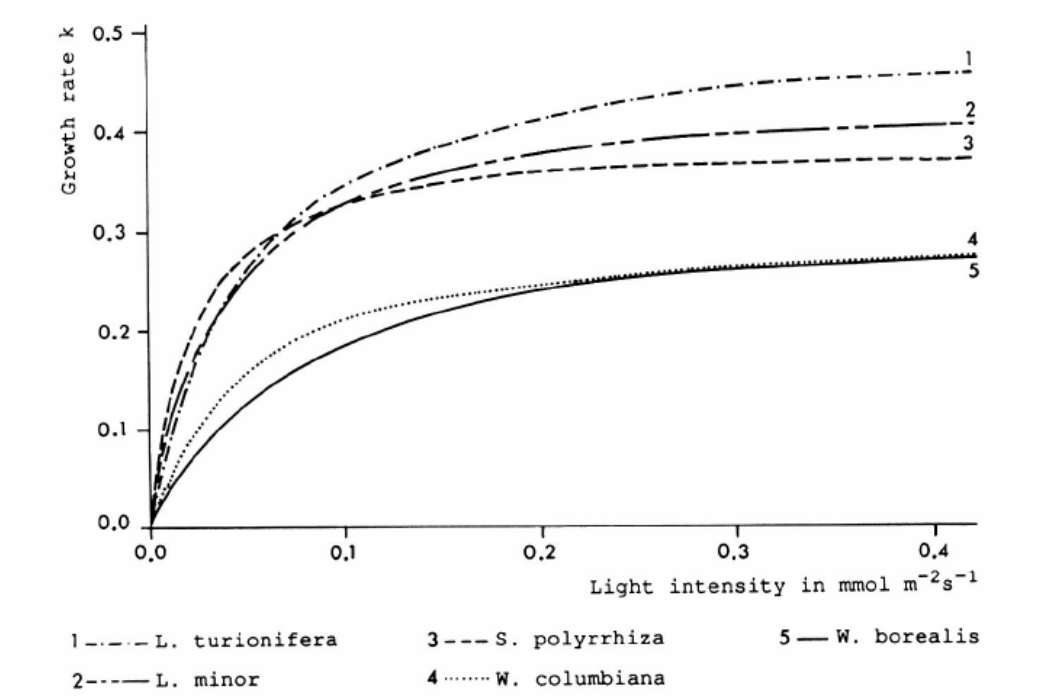

Fig. 7: Growth rate of different species in relation to light intensity (Docauer, 1983), as illustrated in Landolt et al. (1987)

Fig.7 shows the growth rates for different *Lemnoideae* species according to *Docauer (1983)* and *Landolt et al. (1987)*. The different species show very different maximum growth rates under the same light intensity. Nevertheless, the trend is always the same: up to around 100µmol m^{-2} s^{-1}, the growth rates increase linearly, only to asymptotically saturate above 100µmol m^{-2} s^{-1}. According to *Docauer (1983)* and *Landolt et al. (1987)*, the maximum growth rate for *Lemna minor* asymptotically reaches already 95% of max. between 120-160µmol m^{-2} s^{-1}. A further increase to 400µmol m^{-2} s^{-1} would increase the growth rate for only another +5%. This applies to the supplied light intensity in the PAR range as an integral over all relevant wavelengths, i.e., only in relation to the light quantity. The light quality (ratios of certain wavelengths to each other) is not taken into account here.

With respect to the correlation between photosynthetic efficiency and the C fixation mentioned above, it is noted that the stomata of *Lemnoideae* have guard cells, containing chloroplasts reacting in a light sensitive manner. However, these guard cells are inactive in their adult state, which they reach quickly, and therefore they are permanently open so that

they cease to react to light and are never confronted with draught stress *(Zeiger et al., 1987);* (*Borisjuk et al., 2018)*.

So, the lowlight tolerance expressed in most *Lemnoideae* suggests that *Lemnoideae* are using nitrate as osmoticum *(Quingyang Zhou et al., 2017; Bloom-Zandstra, Lampe, 1985)*. It has been repeatedly observed in *Lemnoideae* at laboratory and at upscaling conditions with a 1,000 m^2 cultivation surface that under extreme lowlight conditions, <50 µmol m^{-2} s^{-1} PAR, a higher chloroplast density is found coinciding with a darker green colouring *(Steward et al., 2021)*, *(Steward et al., 2020)*. *Lepedus et al., (2020)* revealed a relationship between different light quantities, growth, and PSII efficiency for *Lemna minor* and further confirmed the lowlight tolerance of *Lemna minor*.

Paolacci et al. (2021) have also found that, within the genus *Lemna*, there are even different light utilisation strategies between *Lemna minuta* and *Lemna minor*. He concluded that *Lemna minuta* displayed a higher relative growth rate under high light intensities, and *Lemna minor* exhibited a higher morphological plasticity under lowlight conditions. The light intensity series experiment by *Liebers et al. (2023)* revealed that *Lemna minor* photosynthesis was superior to *Arabidopsis thaliana* photosynthesis also under weak actinic light (420nm), suggesting that further mechanisms (besides quenching by carotenoids) might contribute to the improved photosynthetic performance of *Lemna minor*. For that reason, considering light quality in addition to light quantity would lead to further improvements of culture conditions.

In the context of light and photosynthetic efficiency, also Fe plays an important role in the respiratory chain in the functional protein ferredoxin. It is noted, however, that a continuous supply of iron is possible from various pools of the cell. *Roncel et al. (2016)* proved that iron deficiency induced a partial inhibition of photosynthetic electron transport and a high sensitivity to light. *Mattoo et al. (1984)* found that both anabolism and catabolism of proteins are photo-regulated, with degradation coupled to electron transport rather than phosphorylation.

The need for iron may slightly increase anti-proportionally to the light quantity (in PAR) under low light conditions. Because iron is also important for chlorophyll synthesis, a visible increased uptake of iron is observed. This is supported by the findings of *Merry et al. (2021)*

who discovered the same dependency for soybean, representing higher plants. Since magnesium, as a further nutrient, was indicated to be significant for photosynthesis efficiency, *Ye et al. (2019)* found magnesium-deficiency effects on pigments, photosynthesis, and the photosynthetic electron transport in the leaves and nutrient of leaf blades and veins in *Citrus sinensis* seedlings, to also have an important influence on electron transport and related photosynthetic efficiency.

2.2.4 CO_2

Lopez-Pozo et al. (2023) qualified *Lemnoideae* as novel crop for CO_2 sequestration according to its high growth rate and, consequently, high uptake rate. *Zenir et al. (2022)* examined elevated CO_2 concentrations in *Lemna minor* cultivation. They saw clear benefits, predominantly under elevated CO_2 and low nutrient supplies.

Consequently, uptake and transfer of CO_2 via the permanently open stomata, are not obstructed by any flow resistance, except for the so-called mesophyll resistance. This simplifies any possible modelling. Light-inhibition of dark respiration in *Lemna minor* L., was examined by *Fuhrer (1983) who considered this already*. CO_2, which diffuses through the stomata, is fixated (carboxylated) within the stroma of the chloroplasts by the enzyme RUBISCO (Ribulose-1,5-Bisphosphate-Carboxylase) and transferred to a C5 body (a molecule having 5 carbon atoms, Ribulose-bisphophate), forming a C6 body which disintegrates into two C3 bodies and is partly oxidised. *Ewert (2004)* basically considered modelling plant responses to elevated CO_2 by using the **L**eaf **A**rea **I**ndex (LAI) as a gas exchange interface. This seems to be relevant also for *Lemna minor* as a higher plant. *Frost-Christensen & Floto (2007)* examined the resistance to CO_2 diffusion in cuticular membranes of amphibious plants and the implication for CO_2 acquisition in detail.

2.3 Use of *Lemnoideae*

2.3.1 Feed, food

The human population is quickly growing to over $9 \cdot 10^9$ people by 2050, and a sustainable production of food in view of climate change and resource limitation is a challenge *(HPLE, 2017)*, *(Pagliuso et al., 2022)*, *(Herreo & Thornton, 2013)*, *(Porter et al., 2015)*. *Lemnoidea*e may significantly contribute to supplying food for an ever-growing population, because they

are fast-growing under the proper conditions. Their composition may even qualify them as valuable sources of proteins and essential nutrients for food and feed (see below). First novel food approvals have been granted by EFSA (European Food Safety Agency) *(see https://open.efsa.europa.eu/),* starting with the *Lemnoideae* species *Wolffia globosa* and *Wolffia arrhiza.* Species of *Lemna minor* and *Lemna gibba* followed in 2025 *(EU commission , 2025)*. A pure protein content of about 35% in dry matter is expected.

2.3.2 Nutritional Factors

2.3.2.1 Proteins

The nutritional value of duckweeds for human food is well established and has also been shown by many authors *(Appenroth et al., 2017; Appenroth et al., 2018; Chakrabarti et al., 2018).* Since the Food and Agriculture Organization of the United Nations, FAO *(see FAO 2018)* declared *Lemnoideae* to be part of food production and agriculture in the future, *De Beukelaar et al. (2019)* and *Xu et al. (2022)* also considered duckweed as a vegetable and a protein source in several food applications. *Appenroth et al. (2017)* state that *Lemnoideae* dry matter contain 20-35% pure protein, 4-7% fat and 4-10% starch, a content of essential amino acids of about 4.8% for Lys, 2.7% of Met + Cys, and 7.7% of Phe + Tyr. A comparison of all values in Tab. 3 (further below) displays that *Lemna minor* L. shows a very balanced nutritional composition, and it is, therefore, particularly suitable for uses as animal feed and human food.

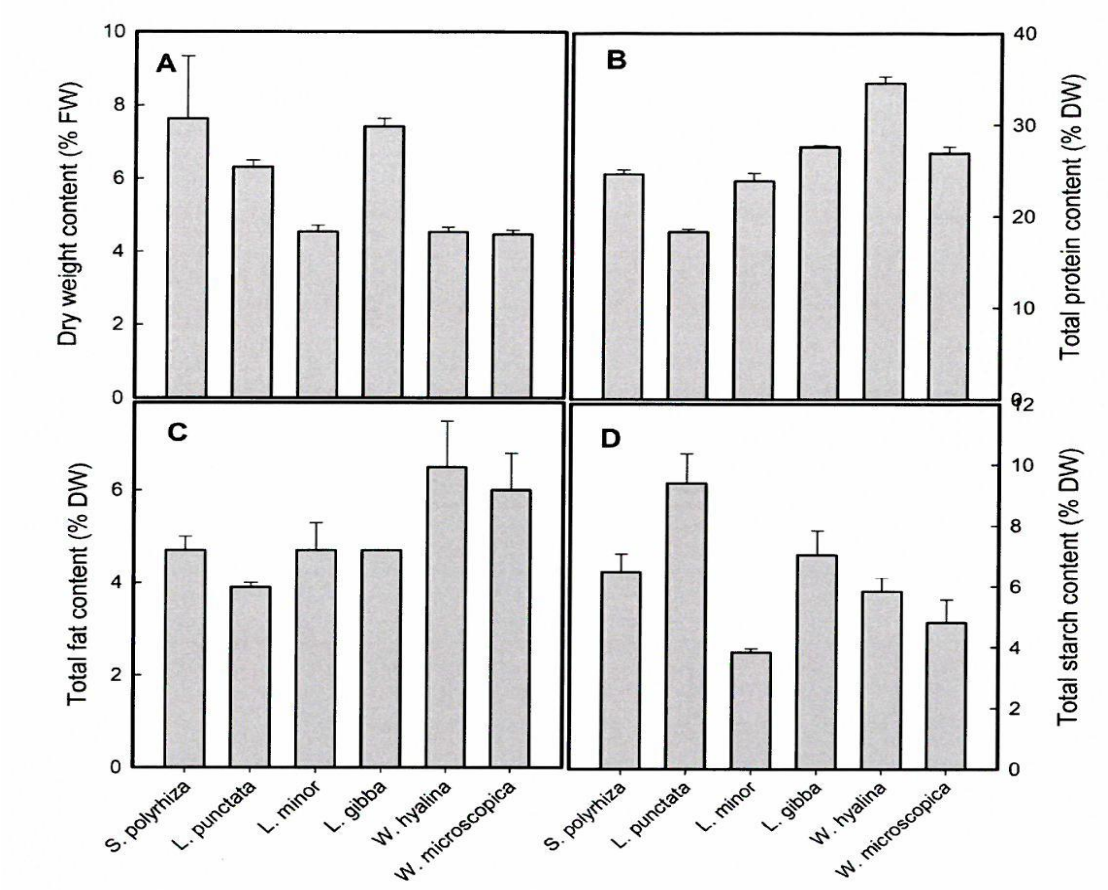

Fig.8: Appenroth et al.(2017) compared the protein, fat, and starch contents on a dry matter basis of different Lemna species.

Fig. 8 shows that dry weight contents vary between species from ca. 5% to almost 8%, with *Lemna minor* at the lower end, and *Spirodela* and *Lemna gibba* within the upper range of values. Maximum total protein, fat, and starch content was found in *Lemna hyaline*, but a higher total yield may be reached by *Lemna minor*.

Nevertheless, achievable protein content and protein value are quite dependent on the cultivation method, relate to the nutrient solution, method of operation, and influence of the statistical age of the harvested culture *(Chmilar & Laird, 2019)*.

Tab.3A: Amino acid composition of 6 different *Lemnoideae* acc. to Appenroth et al. (2017)

Amino acid composition of proteins from different duckweed species [g/ 100 g protein].

Amino acid	*Spirodela polyrhiza*	*Landoltia punctata*	*Lemna minor*	*Lemna gibba*	*Wolffiella hyalina*	*Wolffia microscopica*
CYS	0.8	1.1	0.9	0.9	1.0	1.2
MET	1.6	1.6	1.6	1.6	2.0	1.6
ASP	7.8	8.1	8.2	10.6	7.3	10.4
THR	4.2	4.1	4.0	4.0	4.2	4.7
SER	4.1	4.0	4.1	4.2	4.3	4.7
GLU	9.6	9.5	9.8	10.3	10.5	10.9
GLY	4.3	4.5	4.6	4.6	5.0	4.7
ALA	5.4	5.3	5.1	6.0	6.0	7.8
VAL	4.4	4.6	4.6	4.5	4.8	4.9
ILEU	3.3	3.5	3.7	3.4	3.9	3.7
LEU	6.8	7.3	7.3	7.2	8.0	7.7
TYR	3.1	3.1	3.1	3.2	3.8	3.3
PHE	3.97	4.5	4.4	4.3	5.1	4.2
LYS	4.2	4.1	5.0	4.2	5.8	5.7
HIS	1.6	1.6	1.5	1.6	1.7	1.7
ARG	4.7	4.7	4.8	4.9	4.7	5.2
PRO	3.5	4.1	3.8	3.9	3.7	3.6

As shown in Tab.3A, the amino acid spectrum of the smaller species, such as *Wolffia,* is slightly superior compared to the ones with larger fronds. In turn, however, the effective growth rate of their culture is lower. Still, all the different species exhibit a total distribution of high-value essential amino acids, particularly, aspartic acid, glycine, valine, and lysine.

2.3.2.2 Fatty acids

Compared to e.g. soybean, the total content of raw fat in *Lemnoideae* is comparably low, but they possess a high-value fatty acid composition like shown in tab.3B.

Monounsaturated fatty acids (MUFA) are roughly in the mid-range of values, compared to the other *Lemna* species. Polyunsaturated fatty acids (PUFA) are at the upper range of values with respect to the other varieties. The ratio of omega-6 to omega-3 fatty acids in *Lemna* is also in the middle range, compared to the other *Lemnoideae* species.

According to *Appenroth et al. (2017),* 48-71% of the lipids are polyunsaturated fatty acids with a n6/n3 ratio of 0.5 or less. This means that the proportion of omega-3 fatty acids is at least twice as high as the proportion of omega-6 fatty acids.

Tab.3B: from Appenroth et al. (2017) shows a juxtaposition of fatty acids of various species[a,b] of Lemnoideae.

Fatty acids	*S. polyrhiza*	*L. punctata*	*L. minor*	*L. gibba*	*W. hyalina*	*W. microscopica*
SFA	39.85 ± 0.01	46.23 ± 0.57	27.99 ± 0.35	28.25 ± 0.11	32.20 ± 0.05	25.07 ± 0.14
MUFA	4.40 ± 0.02	5.65 ± 0.46	4.63 ± 0.04	4.13 ± 0.03	5.32 ± 0.06	3.77 ± 0.09
PUFA	55.75 ± 0.01	48.12 ± 1.03	67.38 ± 0.31	67.62 ± 0.07	62.48 ± 0.01	71.16 ± 0.23
Sum n3	44.26 ± 0.24	32.66 ± 0.51	46.00 ± 0.06	53.08 ± 0.01	47.99 ± 0.11	44.22 ± 0.18
Sum n6	10.85 ± 0.02	14.89 ± 0.52	20.89 ± 0.12	14.23 ± 0.09	14.12 ± 0.01	26.77 ± 0.04
n6/n3 ratio	0.25 ± 0.00	0.46 ± 0.01	0.45 ± 0.00	0.27 ± 0.00	0.29 ± 0.00	0.61 ± 0.00
SC-FA (C-4 > C-10)	0.02 ± 0.00	0.01 ± 0.00	0.00 ± 0.01	0.10 ± 0.00	0.00 ± 0.01	0.00 ± 0.00
MC-FA (C-11 > C-14)	0.60 ± 0.02	0.41 ± 0.01	0.48 ± 0.03	0.62 ± 0.03	0.61 ± 0.01	0.14 ± 0.00
Single FAME > 1%						
C-16:0	29.38 ± 0.04	32.59 ± 0.16	21.33 ± 0.25	22.08 ± 0.23	22.03 ± 0.11	20.23 ± 0.13
C-18:1c9	1.71 ± 0.02	3.09 ± 0.39	1.67 ± 0.00	0.69 ± 0.01	1.08 ± 0.01	1.52 ± 0.00
C-18:2c9,c12	10.59 ± 0.01	14.36 ± 0.14	20.11 ± 0.12	12.99 ± 0.08	13.75 ± 0.01	25.42 ± 0.01
γC-18:3c6,c9,c12	0.01 ± 0.00	0.01 ± 0.00	0.52 ± 0.00	1.02 ± 0.01	0.02 ± 0.01	1.20 ± 0.01
αC-18:3c9,c12,c15	43.86 ± 0.24	32.40 ± 0.54	44.47 ± 0.10	48.60 ± 0.10	47.85 ± 0.12	39.58 ± 0.04
C-18:4c6,c9,c12,c15	0.00 ± 0.01	0.00 ± 0.00	1.16 ± 0.04	3.91 ± 0.12	0.00 ± 0.00	4.57 ± 0.13
C-22:0	0.42 ± 0.02	0.52 ± 0.01	0.37 ± 0.01	0.54 ± 0.02	2.57 ± 0.03	0.90 ± 0.00
C-24:0	3.01 ± 0.19	3.83 ± 0.02	1.32 ± 0.05	1.61 ± 0.09	1.81 ± 0.03	0.96 ± 0.00
C-26:0	0.56 ± 0.06	2.30 ± 0.31	0.46 ± 0.02	0.26 ± 0.02	0.93 ± 0.02	0.33 ± 0.01

[a] Fatty acids were separated gas chromatographically as corresponding fatty acid methyl esters (FAME).
[b] Data are expressed as mean ± SD of % total FAME.

In comparison to the above, recent studies on soybeans by *Vivar et al. (2023)* have shown an n6/n3 ratio of between 5.63 and 14.34. Above a n6/n3 ratio of 5:1 in food, the absorption of n3 (omega-3) fatty acids is nutritionally inhibited. In comparison, the soybean fatty acids profile of edible oils and fats in India exhibit an omega 6/omega 3 ratio of 2.1 in cv.s *Dalda* and *Nature fresh*, 4.7 in *Gemini*, and up to 8.6 in the variety *Fortune.* This is an unfavourable predominance of omega 6 fatty acids.

The n6/n3 ratio also plays an important role in fish feeding. It is known (*Carr et al., 2023)* that the use of soybeans in feed leads to an unfavourable, i.e., excessive n6/n3 ratio in the fish meat. Thus, the nutrition of predatory fish should not rely predominantly on soybean meal, as e.g., salmonids, have a higher need for omega 3 fatty acids than for omega 6 fatty acids. Although soybean meal carries a high portion of amino acids, the excessive amount of omega 6 fatty acids is unfavourable for human diet. So, from a holistic perspective, *Lemnoideae* therefore exhibit a higher nutritional value than soybeans because of their lower omega-6 fatty acid contents.

In order to safely recover all nutritionally valuable ingredients in *Lemnoideae*, it is necessary to harvest the plant material with as low mechanical pressure as possible. Stomata are permanently open, (*Zeiger et al. 1987* and *Borisjuk et al. 2018*), any loss of apoplastic and cytosolic solution should be prevented.

2.3.3 Antinutritional factors

In order to pass the admission tests of EFSA see *(https://open.efsa.europa.eu/questions/EFSA-Q-2020-00512), (EU Commision, 2025)* the concentration of oxalic acid (oxalate) and the tendency to accumulate heavy metals in *Lemna minor (DeKock et al., 1973), (Francesci, 1987)* has to be taken into account and should be minimized.

2.3.3.1 Oxalic acid, calcium oxalate

Calcium plays a fundamental part in membrane stability and cell integrity (*Marschner, 2012, Chapter 6.5.5).* Calcium stabilizes cell membranes by bridging phosphate and carboxylate groups of phospholipids and proteins, and it stabilizes the cell wall by binding to pectins. Calcium may be exchanged for other cations at some of these binding sites; the exchange of plasma membrane-bound Ca for Na, heavy metals, or Al may contribute to increased salt stress, heavy metal and aluminium toxicity *(Cramer, 2002; Horst et al., 2010)*.

Nevertheless, soluble oxalic acid and insoluble calcium-oxalate have been identified by EFSA *(EU Commision, 2025)* to be emerging risks, causing the formation of kidney stones *(Massey et al., 1993)* and thus need to be minimized when using *Lemnoideae* as a protein source. As an example, according to *Noonan et al. (1999),* the daily intake of oxalate in English diets is 70-150mg. In a test of several samples with a high oxalic acid content, the highest content of 120.5mg/100g was determined in a smoothie, containing 25.1% rhubarb. In another smoothie, containing 16% beetroot juice, 8% spinach, and 6% kale, a content of 78.0mg/100g was determined *(see BVL, 2017).*

Storage of calcium oxalate, especially in *Lemnoideae,* takes place in specialized idioblast cells *(Foster, 1956)* in its parenchyma *(Mazen et al. 2004)*, *(Thor, 2019).* To this date, it has been assumed that cytosolic calcium detoxification is achieved by formation of Ca oxalates *(Francesci and Schuren, 1986), (Francesci, 1987), (Francesci, 1987), (Francesci, 1989), (Li and Francesci, 1990), (Francesci, 2001), (Francesci, Horner, 1979) (Ledbetter and Porter, 1970).* *Hepler (2005)* and *Kudla et al. (2010)* emphasized, though, that Ca^{2+} is essential for the growth and development of plants, and thus the Ca has to be tightly balanced for optimum nutritional properties in *Lemnoideae*.

From *(Wang et al., 2009)* it is known that higher ratios of NH_4^+/NO_3- lower organic acid and thus oxalic acid concentrations, too.

Calcium oxalate (CaOx) crystals are widely spread across the families of higher plants *(Mazen et al., 2003; Arnott and Pautard, 1970; Gallaher, 1975; Franceschi and Horner Jr, 1980; Horner and Wagner, 1995; Nakata, 2003),* but the functioning and the formation process of calcium oxalate crystals are not fully understood yet. It is current knowledge that the process of the formation of calcium oxalate crystals is considered to be a type of cellular disposal of excessive calcium ions *(Frank, 1972; Zindler-Frank, 1975; Borchert, 1985; Borchert, 1986; Franceschi, 1989; Franceschi and Loewus, 1995; De Silva et al., 1996; Kuo-Huang and Zindler-Frank, 1998; Pennisi and McConnell, 2001; Zindler-Frank, Honow and Hesse, 2001; Volk et al., 2002).* The largest part of "tissue calcium" appears as calcium oxalate *(Gallaher et al., 1975; Gallaher and Jones, 1976*). Various studies identified ascorbic acid to be the mediating precursor of oxalic acid for the formation of crystals *(Franceschi and Horner Jr, 1979)* and also that the "crystal" idioblasts already contained the biochemical path for ascorbate synthesis *(Kostmann et al., 2001; Kostmann & Koscher, 2003),* thus rendering it wholly independent for the production of oxalic acid. It is generally assumed that idioblasts have larger proportions of endoplasmic reticulum and Golgi apparatus *(Li et al., 2003)*. It was also shown that the idioblasts, for example, of *Pistia stratiotis* are enriched with calreticulin (*Quitadamo et al., 2000), (Nakata et al., 2003).* At this point, it is referred to the genetic relationship between *Lemnoideae* and *Pistia* (see chapter 2.1.1-2.1.3), both of which belong to the family of *Araceae (Nakata et al., 2003).* At concentrations of 10-15mMol/L Ca^{2+} in the nutrient solution, calcium oxalate crystal formation is reversible (*Mazen et al., 2003).* As found by *White & Broadley (2003)* and *McAinsh & Pittman (2009)*, the concentration of Ca^{2+} in the cytosol is low (0.1-1.0 µMol).

As seen in Fig. 9 from *White & Broadley (2003), White & Broadley (2009)* these low Ca^{2+} concentrations are essential for various reasons, such as the prevention of P_i precipitation and denaturation of proteins, the competition with Mg^{2+} for binding sites, and a prerequisite for the function of Ca^{2+} as a secondary messenger. The major transporters catalysing the Ca^{2+} efflux from the cytosol to the apoplast and the endoplasmic reticulum are Ca^{2+}-ATPases, and Ca^{2+}/H+ antiporters catalyse the Ca^{2+} efflux from the cytosol to the vacuole. The latter is

energized by the proton-electron chemical gradient generated by tonoplast H^+-ATPase and H^+-PP_iase activities.

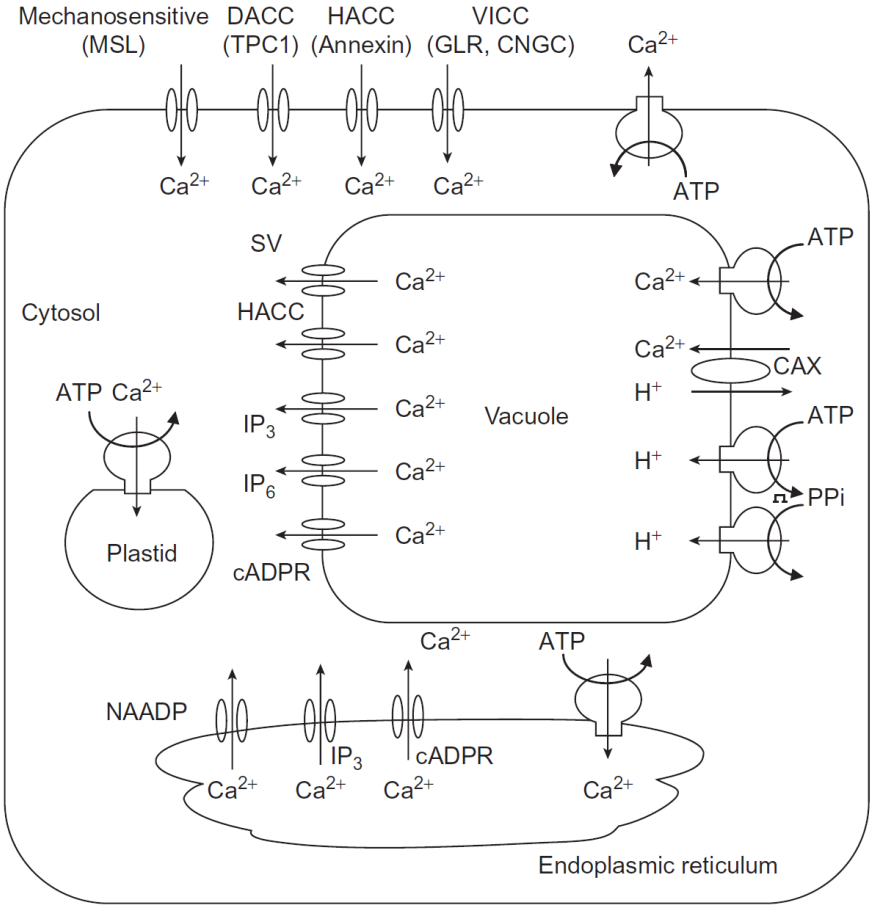

Fig. 9 Calcium transport processes in plant cells. *Adapted from White and Broadley (2003).*

Cheriyah et al. (2016), Cheriyah et al. (2013) could later verify different calcium oxalate crystal formations, both raphides and druses, in *Amorphophallus muelleri* flower at different harvest times. The same could be verified in *Lemnoideae* by *Franceschi (1987), (1989), and (2001).* It is known that high concentrations of calcium oxalate in animal feed may cause renal calculus in long-life farm animals, such as dairy cattle, etc. *(Alford et al., 2020).* Thus, a reduction of calcium oxalate amount in *Lemnoideae* is required for its use in feed and food.

2.3.3.2 Heavy metals

Lemnoideae have a strong tendency to accumulate heavy metals and thus they may be considered for remediation of agricultural and industrial effluents. *Bokhari et al. (2016)* examined this for industrial effluents in a greenhouse cultivation of *Lemna minor* L., *Megateli et al. (2009)* did so for *Lemna gibba. Hou et al. (2007)* worked on remediation of copper and

cadmium by *Lemna minor.* *Kahn et al. (2020)* considered differential bioaccumulation of selected heavy metals from wastewater by *Lemna minor*. *Khellaf & Zerdaoui (2009)* examined the growth response of *Lemna* to heavy metal pollution. *Appenroth et al. (2010)* examined effects of nickel on the chloroplasts of the duckweeds *Spirodela polyrhiza* and *Lemna minor* and their possible use in biomonitoring and phytoremediation. All these studies confirmed that *Lemna minor* shows high accumulation rates of heavy metals during growth. It can be assumed, though, that the accumulation increases with the culture period and the average age of the fronds.

2.3.3.3 Accumulation of toxic substances

Turck et al. (2022) examined the accumulation of toxins from cyanobacteria in duckweeds, because microcystins, in particular, have been reported to accumulate in *Lemna* species. This was based on detailed experiments by *Mitrovic et al. (2005)* and by *Saqrane et al. (2007).* However, such microcystins were found in axenic cultures of *Lemna*. Since the use of *Lemnoideae* as feed and food requires high yields, the cultivation needs to be performed non-axenically. However, *Yahaya et al. (2020)* already verified the controllability of pathogenic germs in *Lemna* through suitable hygienic measures.

2.3.4 Current cultivation systems

2.3.4.1 Outdoor

A highly scaled Lemna production plant intended for *Lemna* production in industrial measures was constructed and built by Parabel, Florida, USA. In order to produce large quantities of *Lemna* biomass with minimal investment and the lowest possible operating costs, an outdoor pond system was used. It needs to be considered that, in 2018, cultivation parameters were not fully understood and verified yet.

Fig.10: Upscaled outdoor Lemna production plant (Lemnature AquaFarms, formerly Parabel) in Florida, USA, with 900 acres (365 Ha). The last version was constructed in 2021.

As already mentioned, all *Lemnoideae* are hyperaccumulators, and heavy metals were introduced from the environment above the permissible limits for plant biomass due to the open construction. EFSA therefore rejected Parabel's novel food application. Furthermore, the cultivation was also subject to the influence of weather conditions and could therefore hardly be optimised. Even a small input of bird faeces leads to rapid contamination with pathogenic microorganisms. Both, consistent yields and a high-quality biomass could therefore not be achieved. The company, renamed “Lemnature AquaFarms”, therefore filed for bankruptcy in December 2023.

2.3.4.2 Indoor

A first proposal of a cultivation apparatus for continuous culturing and harvesting was published by *Erisman & Finger (1968).* Round culture tubs with a spiral bottom line were proposed, in which starting biomass was inoculated in the centre of the spiral. The area of the

spiral expanded outwards in the manner of a Fibonacci number series in order to give the exponential growth an expanding area. This concept was never continued for economic reasons.

Based on the ECOFERM project in the Netherlands, companies, such as DryGro or Hinoman, switched back to indoor farming for *Lemna* production in 2015. This initially solved the problem of contamination, for example, with heavy metals. Furthermore, contaminations/infections with pathogenic bacteria, such as *Escherichia coli*, can be suppressed or eliminated by controllable measures in indoor farming.

However, the systems were only intended for cultivation on large floor areas. This meant that the space required was large, and the energy requirement in the enclosed space for a year-round operation was immense, at least in temperate climate zones.

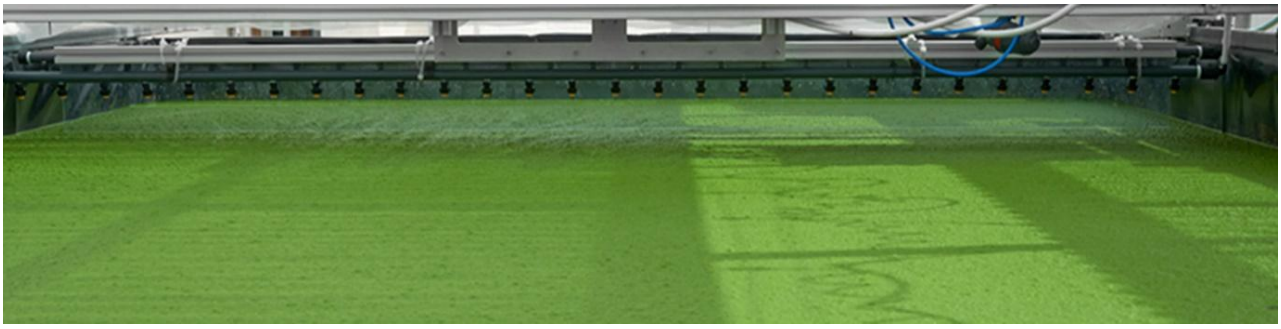

Fig.11: Hinoman indoor cultivation of Wolffia in floor based ponds.

2.4 Modelling of *Lemna* Growth

Growth of *Lemna* depends on several growth parameters, as temperature, light, nutrition and CO_2. Even the cycle time of partial harvests impact influences the obtained growth rate. Since it is impossible to consider this high amount of possible permutations of all growth parameters previously mentioned, a modelling had to be used for optimization.

Lemnoideae were used as a model system in phytobiology (*Wada & Kagawa, 2001*). Fundamental findings on photoperiodic reactions (blossom) by *Hillman (1961, 1966)* were based on fundamental experiments using the *Lemna* system. A quasi-empirical determination, for example, the so-called Malthus-Verhülst model *(Murray et al., 2011; Kot 2001; Vassilieva*

2011; Müller and Kuttler 2015; Nisbet and Gurney, 1986; Kufel et al., 2012) cannot consider all growth parameters.

Lemnoideae are currently proposed as a model plant by *Acosta et al. (2021)* and *Cao et al. (2018)* again. Recently, an integral experimental and modelling approach for *Lemna minor* was also shown by *Van Dyck et al. (2021)*

The so-called "logistic function" commonly used had formerly been based on Malthus mathematics for growing populations. This results from the fundamental differential equation in biology which says that the increase in individuals N is always proportional to the number of individuals N_0 in a population that are capable of populating

$dN \sim N_0$

The more empirical solution according to a first work by *Malthus (1798)* was firstly considered by *Charles Darwin (1838)*, and further improved for limited growth by *Verhulst (1838), (1845).* He already considered a limitation C (capacity), and thus developed the equation:

$$N(t) = \frac{C}{1+k*e^{-Ct}} \qquad \text{eq.1}$$

where k is a dynamic factor, C the possible maximum of population.

Korner et al. (2002), Bontsema et al. (2010), furthermore, considered nutrients, light, and CO_2, and *van Ooteghem (2010), Bot (1983)* (PhD University Wageningen, NL) used that in the ECOFERM project. According to this project (University of Wageningen, Netherlands), the k-factor was defined by *Frédéric et al. (2006),* considering *Docauer (1983)* and *Landolt et al. (1987),* and also confirmed by *Lasfar (2007)*, as intrinsic growth rate r_i as follows:

$$r_i = R \cdot \Theta_1^{\left(\frac{T-Top}{Top}\right)^2} \cdot \Theta_2^{\left(\frac{T-Top}{Top}\right)} \cdot \Theta_3^{\left(\frac{E-Eop}{Eop}\right)^2} \cdot \Theta_4^{\left(\frac{E-Eop}{Eop}\right)} \cdot \frac{\mathrm{CP}}{(\mathrm{CP}+\mathrm{KP})} \cdot \frac{\mathrm{KIP}}{(\mathrm{KIP}+\mathrm{CP})} \cdot \frac{\mathrm{CN}}{(\mathrm{CN}+\mathrm{KN})} \cdot \frac{\mathrm{KIN}}{(\mathrm{KIN}+\mathrm{CN})} \cdot \left(\frac{g}{gmax}\right) \qquad \text{eq.2}$$

With

T, T_{op}	Temperature (optimum Temperature)
E, E_{op}	Integral Light (Optimum Light)
C_P	concentration of P
C_N	concentration of N

K_{IP}, K_P, K_N, K_{IN}	constants for saturation and inhibition of P and N
g	growth rate for pH
g_{max}	maximum growth rate for pH
R	maximum intrinsic growth rate
Θ_i	pre-factor for light and temperature

With r_i as growth rate, a growth function for a simplified logistic function *(Lasfar, 2014); (Murray, 2011)* was used. This model was, however, not adequate to describe the entire growth process: cyclic harvesting intervals and harvesting amplitudes remained unconsidered. *Khvatkov et al. (2020)* developed an EXCEL®-based model, using adapted values from several experimental set ups. This allows refitting to measured values, but no accurate predictions were possible.

3. OBJECTIVES AND HYPOTHESES

Given the proper conditions, *Lemna spp.* rapidly produce a high amount of valuable biomass which is considered as an alternative source for feed and food. To ensure a hygienically safe production and, e.g., to avoid microbial contamination, protected cultivation is required. For a continuous and long-term indoor production under controlled conditions, culture and harvest parameters have to be optimized in order to suppress algal growth and to constantly yield a high-quality product. An experimental assessment of the effects of a large number of potentially influencing parameters, such as nutrient composition on the growth rate r_i, is impossible due to the possible number of parameter combinations. Thus, a model had to be developed where the influence of a larger number of individual parameters can be assessed individually and in combination. As *Lemnoideae* cultures have to be considered and treated as populations, the average frond age is considered to be highly important to obtain the best nutritional qualities. For any use of *Lemna* spp. For feed and food, protein concentrations, the potential hyperaccumulation of heavy metals and oxalic acid are relevant as well. Thus, the following hypotheses had to be assessed.

Hypothesis 1:

It is possible to grow *Lemna minor* L. at high rates throughout the year by optimizing nutrient supply, nutrient ratios, pH, light supply, and harvest intervals in an indoor culture system.

Hypothesis 2:

For long-term cultivation *Lemna minor* growth can be described by modelling with the aim, to optimize growth parameters, harvest intervals and harvest amounts with high accuracy.

Hypothesis 3:

The average age of the fronds in a *Lemna minor* L. culture can be influenced by optimized harvest intervals to yield maximum protein contents while minimizing the accumulation of anti-nutritional factors (oxalate and heavy metals).

4. MATERIALS AND METHODS

4.1 Laboratory setup Bonn

4.1.1 Culture trays, nutrient pumps, heating, light, CO_2

To determine the maximum biomass yield and biomass quality, both the nutrient solution and the culture parameters were optimised in a series of trials. For this purpose, the culture trials were generally set up with 6 different test elements and 4 replicates in each case, using 24 identical glass trays. In the laboratory setup, culture trays provided an aquatic culture surface of 0.018m^2 each. The trays were made of borosilicate glass (DURAN®). Any contamination of the nutrient solution by elements from the glass material could be excluded.

The circumference of the glass trays was covered with sleeves made of black foam rubber to minimize light entrance from the side and thus reduce the formation of algae.

For experiments relating to boron deficiency, the minimum molarity was $\leq$ 4.6µM. This ensured that the contribution of boron from the test tray material was merely < 47nMol/l for a cultivation time of a total of 28 days, also with a continuous pH value of 5.5. The trays were placed in an open-top growth box shown in Fig.12 and 13 with an autonomously controlled time and wavelength-controlled light and heating facility.

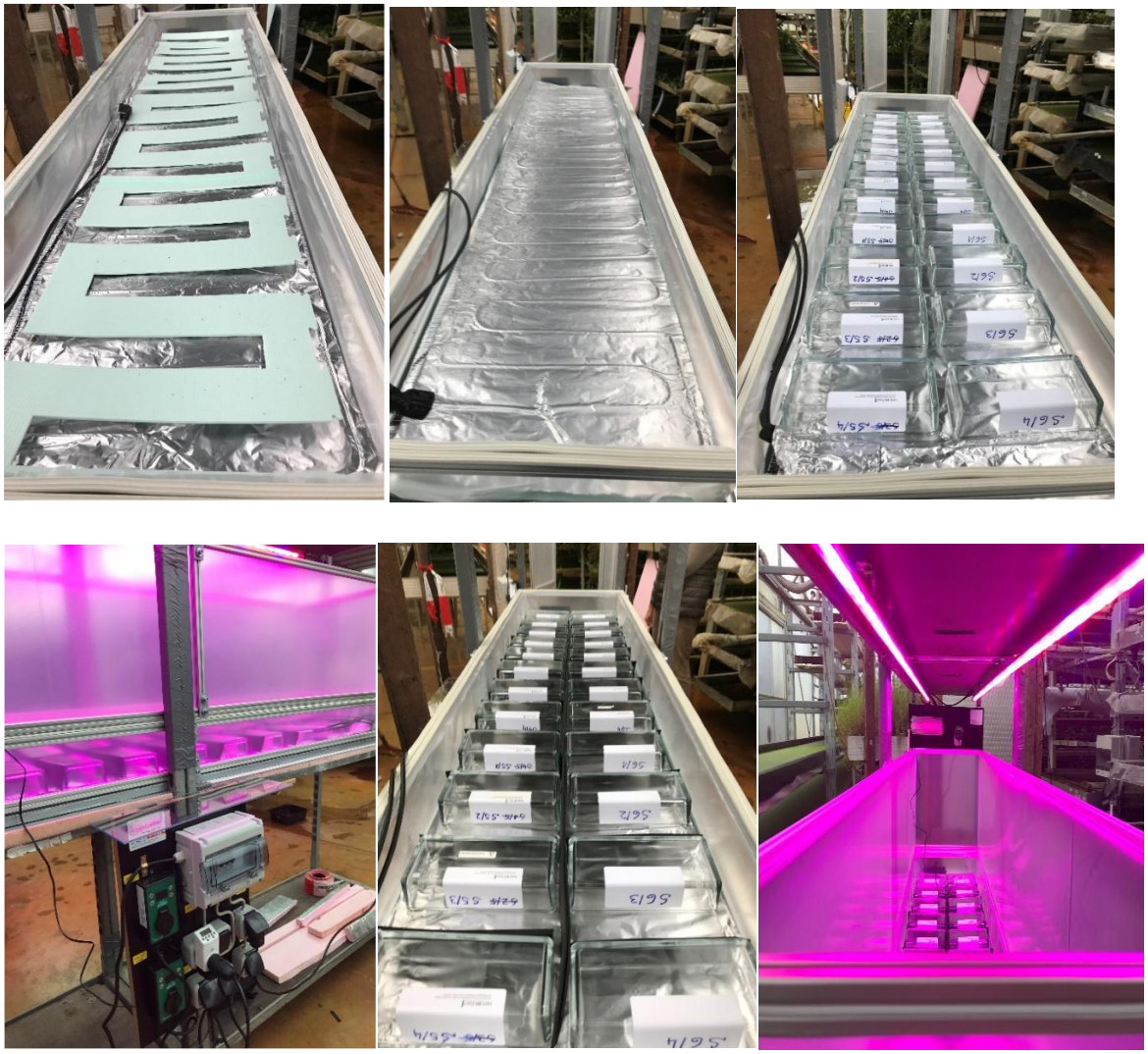

Fig. 12, Upper row: Incorporation of a sandwich heating, Lower row: Connection of temperature and light control

Fig.13: Open top growth box with independent temperature and CO_2 injection control.

Temperature control of the test elements within the open-top growth box, at 27-29°C, was uniform for all experiments. Temperature control was performed using a sandwich heating,

consisting of two separated heating mats (BioGreen by Beckmann, Allgäu, Germany) with independently regulated heating circuits. The set up was built inside the open-top growth box. The heating of the culture trays created a “non-turbulent” hot-air cushion directly above the culture trays. See Fig. 14, both circuits were sensor-controlled to ensure that both the culture water and the culture surface were maintained at the selected temperature. In addition, the open-top growth box was equipped with a controlled CO_2 gassing system with SCENTY® having a MAPEX® control flowbox, including a CO_2 feedback sensor, all made by HTK Hamburg, Germany. CO_2 concentrations of about 3,500 ppm inside the open-top box were supplied from a gas cylinder (80bar, Air Liquide, Krefeld, Germany). Gas purity was 5.0 (99.9990%), equalling food quality.

Due to the installation of electrical elements in the environment of cultured water, all controllers as well as all electrical power supplies, including the heating system, were routed via a centrally installed distribution system, and protected with a separate/additional residual current device RCD (240V, 10A, ABB AG, Germany). This equipment allowed to create average CO_2 concentrations of 3,500 ppm above the culture trays during illumination, and compare the results to ambient 400 ppm CO_2 concentrations. The flow setting was stably adjusted and programmed manually, having a hysteresis of between about 3,100 and 3,900ppm. With a time-symmetrical hysteresis, this resulted in a stable mean value in the time integral of 3,500ppm in the open-top growth box. The CO_2 sensor was arranged in a height of 30mm above the test trays, thus ensuring that the control target is met directly above the cultures. Feeding was performed using co-controlled pressure reducers by Air Liquide for gas bottles by Air Liquide. The gas quality used conformed to the purity standard 5.0 for food.

Fig. 14: Final setup in Bonn with open-top growth box under two light tables, Rhenac Greentec, Rack M-RU mobile

According to the target defined in the Introduction, all cultivation tests were run as long-term laboratory cultures. This allowed to generate and confirm similar starting data between the laboratory and upscaled conditions. About one third of the cultures was harvested from the population various times during cultivation at the indicated cycle periods. This allowed a continuous regrowth of the culture.

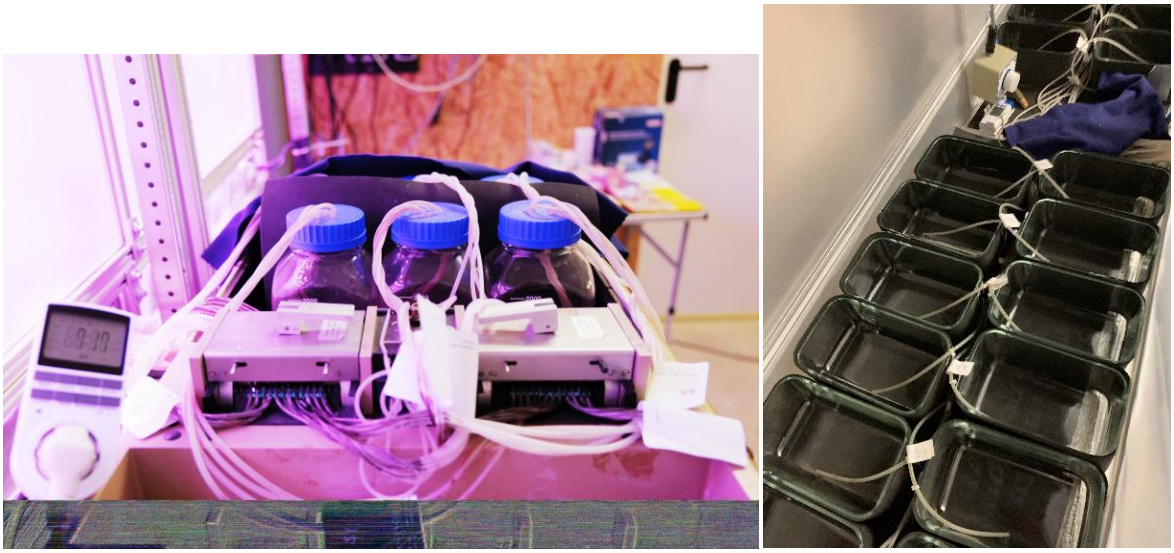

Fig.15: Scalar flow analyzer, reconstructed as a high-precision 30-channel peristaltic nutrient pump

The flow analyzer in Fig.15 was equipped with a 30-channel peristaltic pump having Tygon® tubing (Merck KG, St. Gobain) with an internal diameter of 1.2mm. In a total of 6 glass tanks,

2 litres of thoroughly mixed stock solution per treatment pertaining to the respective test element were stored in each case. The glass tanks were provided with dispensers which distributed the respective stock solution via the peristaltic pump simultaneously to all 4 replicates. The precision of the supplied nutrition solution was at ≤ 20µl/s. This allowed to precisely adapt the required amounts of nutrients via pumping intervals. Time control was set to provide the daily feeding of the stock solutions two to three times per day. This assured to closely adjust the nutrient supply, compensating the nutrient uptake during the light periods. It was controlled by measuring and recording the conductivity EC at each measuring point and for all replicates (see Fig. 16 for the detailed set up).

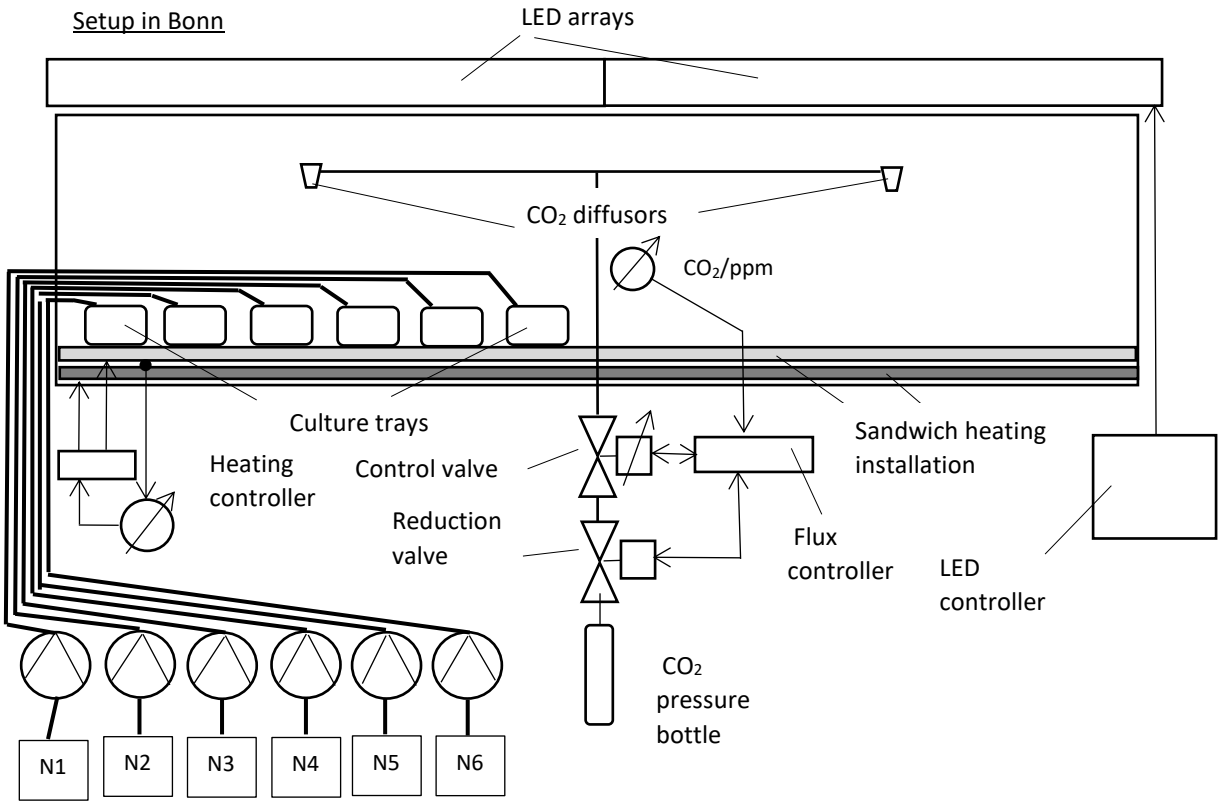

Fig. 16: Lab-set-up in Bonn in detail. The open-top grow box was installed under the light-rack installation, controlled by a LED controller for independent control of emitters of the above mentioned wavelengths. The grow box was provided with two identical CO_2 diffusors, and controlled by feedback regulation via a flux controller and a CO_2 concentration sensor. The heating consisted of a combined air convection heater and a conduction heater in sandwich construction. 6 culture trays of 0.018m^2 aquatic productive surface each and the respective micropump array for 6 different nutrient solutions per experiment are shown, with further trays for 4 replications each. A total of 24 trays was distributed randomly in the grow box (not shown). The micropumps were calibrated using a controller, and the nutrient solutions were controlled to be constant in periodic automatic re-feedings from stock solutions N1-N6 two or three times a day during the illumination growth period.

Light quantity and quality were uniform in the laboratory setup in Bonn using light tables (Mobile LED-Rack R-MU, Rhenac Green-Tech AG). The set up allowed to vary light quality (Fig. 17). The spectral lines were varied at 400nm and 440nm, and at 660nm and 730nm, respectively. White-light diodes were added for the spectral ranges of 500nm to 630nm, adding a mainly green-yellow spectrum, because green light was found to be effective in promoting plant growth *(Chen et al., 2024)*. When changing light intensities between 440nm and 660nm, the whole spectrum had to be re-adjusted for the same photon flow density of 129 µmol m^{-2} s^{-1} as follows. According to Fig.17 one also needs to consider that a photon with a shorter wavelength (e.g., 440nm) carries a higher energy than a photon at 660nm. Therefore, e.g., increasing the 440nm would increase both the photon flow density and the related higher photon energy per photon count. Therefore, the integral of photon flux needed to be readjusted when several ratios of specific wavelength were changed. Otherwise, light quantity and light quality cannot be compared.

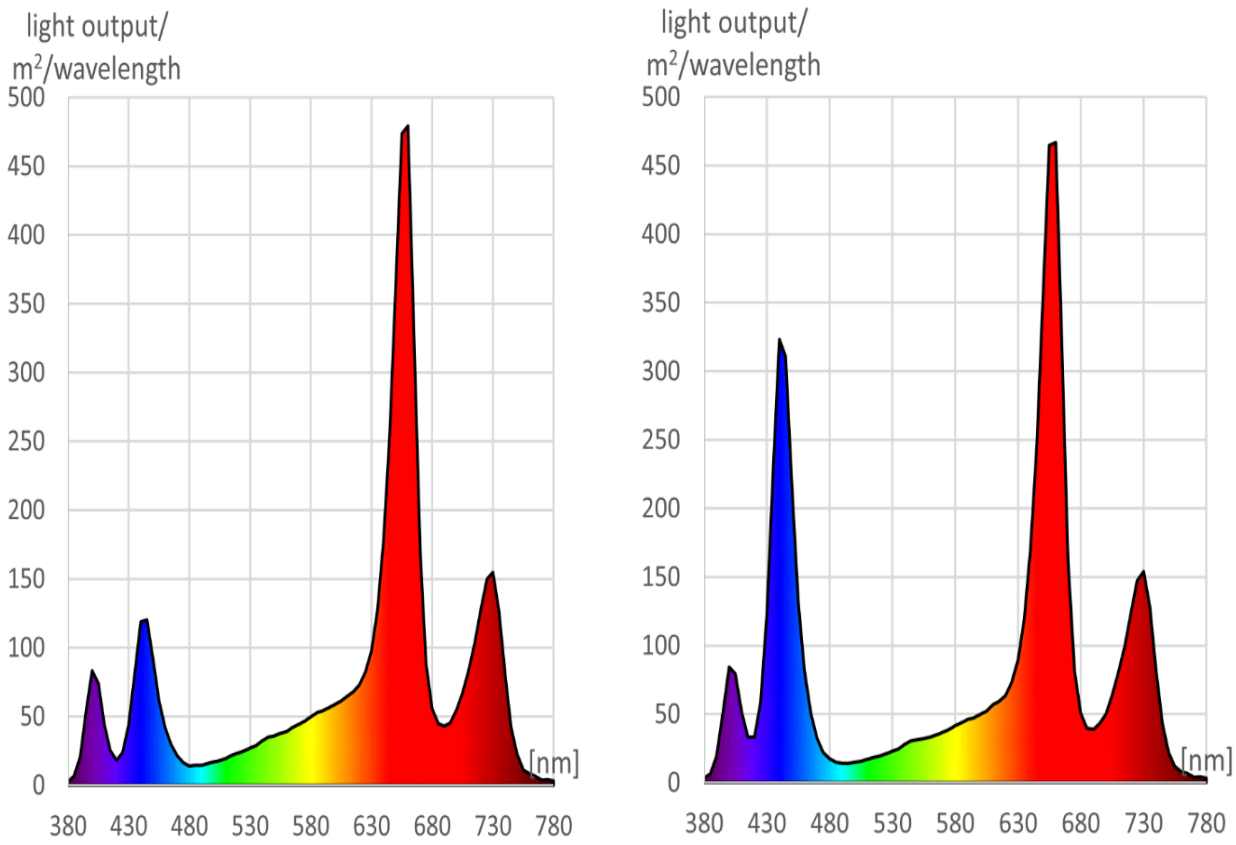

Fig.17: (left), a low-blue light spectrum with an I(440nm)/I(660nm) ratio of 1/4. Fig.17 (right) a high-blue light spectrum with an I(440nm)/I(660nm) ratio of 3/4. Light output was measured in mW•m^{-2} for each wavelength peak.

The two spectra used as different light qualities were defined as low-blue (LB) and high-blue (HB) spectra. The difference consisted in the ratio of the two spectral lines I(440nm)/I(660nm); ¼ for the low-blue and ¾ for the high-blue light spectra, measured with a photometer by GOSSEN, Mavospec Base.

This installation allowed to either operate all 24 test trays under the same illumination conditions (light quantity and quality), or 12 test trays at two different spectra or intensities, but otherwise identical experimental conditions. To this end, black radiation-absorber plates made of foam rubber were installed between the lighted areas of the two light tables up to 60mm above the cultures. Using this value and a distance to the light emission plane of 700mm, it was possible to exclude any dissipation into the respective other light table. The open gaps of 50mm above the culture trays and of 30mm towards the CO_2 sensor allowed an unobstructed gas flow. The flow was additionally controlled by measurements using a TESTO 440 having a CO_2 probe head (06321270) and a Bluetooth handle.

Wavelength-sensitive light quality and quantity were controlled using a photometer (Gossen ,Mavospec-Base 15579) with computer-aided spectral analysis for Excel®.

In addition, absolute measurements of the light quantity in PAR were performed using a LICOR LI-1500 light sensor logger and two measuring heads LICOR Quantum Q 107 010, and were separately controlled for both light tables.

4.1.2 Nutrient solution

Nutrient concentrations and nutrient ratios were varied in several experimental set ups. Total N was tested between 0.5 and 10mM, as the broadest range, resulting in various N/P, N/K, N/Mg ratios. Absolute concentrations were gradually approximated using expected values of depletion, and adjusted (at 1.14mM total N at a pH level of about 5.5-6.5) for a long-term, stable nutrient solution having low NO_3^- accumulation values and supressing any competitive growth of algae.

Tab.4: Stock solutions of mineral salts; the solutions were then diluted to the respective concentrations in the nutrient studies (see below).

Macronutrients		Oligonutrients		Micronutrients
Chemical	**Chem. formula**	**CAS no.**	**Concentration**	**Supplier**
Calcium nitrate tetrahydrate	$Ca(NO_3)_2$ 4 H_2O	13477-34-4	0.5M	Carl Roth GmbH & Co. KG
Ammonium sulfate	$(NH_4)_2SO_4$	7783-20-2	0.5M	Carl Roth GmbH & Co. KG
Potassium hydrogen phosphate	KH_2PO_4	7778-77-0	0.2M	Carl Roth GmbH & Co. KG
Potassium sulfate	K_2SO_4	7778-80-5	0.3M	Carl Roth GmbH & Co. KG
Magnesium sulfate	$MgSO_4$ $7H_2O$	10034-99-8	80mM	Merck KG
Boric acid	H_3BO_3	10043-35-3	46mM	Merck KG
Manganium chloride tetrahydrate	$MnCl_2$ $4H_2O$	13446-34-9	9.15mM	Merck KG
Zink sulfate heptahydrate	$ZnSO_4$ $7H_2O$	7446-20-0	0.7mM	Carl Roth GmbH & Co. KG
Copper sulfate	$CuSO_4$ $5H_2O$	7758-99-8	0.32mM	Carl Roth GmbH & Co. KG
Sodium molybdate	Na_2MoO_4 $2H_2O$	10102-40-6	0.496mM	Carl Roth GmbH & Co. KG
Sequestrene 138	NaFe(III)-EDDHA	16455-61-1	0.04M	Merck KG

Starting from the stock solutions in Tab.4, different nutrient solutions were obtained by dilution. On this basis, both, total N concentrations and corresponding nutrient ratios NH_4^+/NO_3^-, N/P, N/K, N/Mg have been varied. The same method was applied to obtain limitations in elementary oligo- and micronutrients, such as Mg, Fe, and B, considering *(McLay, 1976), (Szabo et al., 2005).*

The individual stock solutions were mixed with H_2O_{demin} to obtain the different nutrient solutions like shown below in Tab.5A and 5B, using a Micropipettor (ROTILABO®, 0.001-5ml Carl Roth) and a magnetic stirrer with a hotplate (ROTILABO®, MH 15, Carl Roth) at the start of the culture. As described above, 20-fold concentrated nutrient solutions were fed to the

cultures to compensate exactly for water loss by evapotranspiration and nutrient uptake (Fig. 16). The nutrient solution was re-adjusted during the light phases with the beginning of the light phase and after 8h, (and in some cases another supply during the day) to compensate for nutrient depletion. The amounts of added nutrients were based on the average nutrient concentrations in growing *Lemna* fronds and the growth rates. For example, 7/100 of the volume of nutrient solution in the culture trays at a culture water temperature of 29°C and with an average of half the maximum capacity of culture coverage had to be replaced on a daily basis.

The accumulation of manganese was studied, because manganese is an essential trace element but tends to accumulate in *Lemna* *(Liu et al., 2017).* Deficiencies were tested for the oligonutrient Mg and the micronutrients Fe and B. The concentrations of the elements Fe and B in the nutrient solutions were logarithmically reduced. For studying Fe deficiency, the concentrations for Fe were adjusted to 40µM, 20µM, 4µM treatments, and for B they were 46µM, 23µM and 4,6µM. The optimal temperature of 29°C was taken from literature data (*Landolt et al., 1987)*, (*Docauer, 1983),* which was verified in the author's own pre-runs. Each experimental treatment was performed with 4 replications. Statistics were calculated using MS Excel® software. The target values for the nutrient solutions after optimisation at all three sites were as follows:

Tab.5A: Starting nutrient solutions (mM), *(µM), after dilution.

NH_4^+/NO_3^-	NH_4^+	NO_3^-	KH_2PO_4	K_2SO_4	Mg	Ca	Fe*	B*	Mn*	Zn*	Cu*	Mo*
10/90	0.11	1.03	0.24	0.28	0.4	0.52	18	46	9.1	0.77	0.32	0.49
20/80	0.22	0.92	0.24	0.28	0.4	0.46	18	46	9.1	0.77	0.32	0.49
30/70	0.33	0.81	0.24	0.28	0.4	0.41	18	46	9.1	0.77	0.32	0.49

Tab.5B: Refeed stock solutions (mM), *(µM), replacing 50ml·tray^{-1}·d^{-1} (3mm·m^{-2}) Evapotranspiration (total volume of water body per tray 1000ml, controlled to be constant by 2-3 refeed partitions d^{-1} during photoperiod)

NH_4^+/NO_3^-	NH_4^+	NO_3^-	KH_2PO_4	K_2SO_4	Mg	Ca	Fe*	B*	Mn*	Zn*	Cu*	Mo*
10/90	2.2	20.6	4.8	5.6	8.0	10.3	360	920	182	15.4	6.4	9.8
20/80	4.4	18.4	4.8	5.6	8.0	9.2	360	920	182	15.4	6.4	9.8
30/70	6.6	16.2	4.8	5.6	8.0	8.1	360	920	182	15.4	6.4	9.8

To avoid B contaminations through the water supply, H_2O_{demin} was additionally purified by adding the boron absorber Amberlite® IRA 743 for all stock solutions at 10g/10 l. The absorber was applied for 3 days before using the water for nutrient solutions. The effect of boron deficiency was further visualized by examining the size of the fronds, the length of the roots,

and the diameter of root calyptra. The geometric dimensions were determined at a low magnification using the microscope's measuring system (Olympus CX 31 RTSF / Cellsens Entry V1, Software CellSens V1.12), and were verified using a nonius caliper (Mitutoyo).

4.1.3 Treatment of plant material: culturing, harvesting, drying, grinding

In all growth experiments, cultures were started at a coverage of about 9 or 12g FM per test tray, which corresponded to an initial coverage of 660g·m^{-2}.

The plant material used for all experiments was *Lemna minor* 'Henry DaCapo' (CPVO reg. EU2970), derived from the selection at Spierhof, Kalkar. The plants were taken from a maintenance culture before every test run and were pre-cultured in an area of 0.2m^2 at ca. 60mMol $m^{-2}s^{-1}$. Respective amounts of *Lemnoideae* were maintained in pre-culturing trays with half the concentration of nutrient solution and about 65µmol m^{-2} s^{-1}photon flow density (light quantity), but with the same light quality in order to prevent a light quality-dependent trigger to the plants when transferring them from pre-culture to the test culture. Before the inoculation of the test trays, the plants from the pre-culture were rinsed in H_2O_{demin}. The inoculation amount of 9-12g FM (fresh matter) per tray was weighed with a precision of +/- 10mg, and placed into the test trays with 1,000ml nutrient solution. The pre-cultures were always cultivated at 400ppm CO_2 at an air temperature of 22°C.

As considered in the associated modelling, repeated (cyclic) partial harvesting of 1/3 of the respective test tray was started as soon as a biomass coverage amounted to 2/3 of maximum coverage. Harvesting was continuously repeated in cycles of 5 days at 400ppm CO_2, and of cycles of 3 days at 3,500ppm CO_2.

Harvesting each tray was performed using a mesh for medical use, Flow Meshtrade™ FM-100, PP-Mesh 1/3mm x 1mm, 70% void volume (Diversified Biotech, Dedham, MA, USA). The use of an adjustable culture surface splitter to be positioned on the trays allowed the harvested partial culture surface to be highly reproducible. Four parallel replications were cultivated in each case. The fresh matter, taken from determined partial area segments (1/3 of the respective cultivation area) from each test tray, was weighed using a precision balance +/- 10mg.

After each harvest, samples were placed in pergamin sample bags (95x132, Carl Roth), dried in a dryer at 40°C for 12h, stored under dry conditions in desiccators (Exsikkator ROTILABO® Glass, DN 250, 8l; Exsikkator Star Vitrum, Carl Roth), and ground just before starting the preparation of the samples for chromatography. Grinding the respective samples was performed in 20ml HD polyethylene vials (Carl Roth), filled with the respective *Lemna* dry sample and 3 stainless-steel balls of the sizes of 8mm, 4mm, and 2mm were placed in each vial. Grinding was carried out on an excenter shaker for 20 minutes at 4Hz. This resulted in a uniform grinding with an average particle size of 20-30µm.

4.1.4 Analysing methods

PREPARATION FOR LCMS, MEASURING OF OXALIC ACID

To prepare the samples, 10mg of *Lemna* powder, weighed with a precision scale (MS104TS/00, Metteler Toledo) were incubated in 500µl ultra-pure H_2O (Milli-Q® Lab Water Solutions, Merck) at 60°C in an ultrasonic bath for 60min. A temperature of 60°C was chosen to be safe for extraction according to *Vanhaven (2018, p56), Hönow & Hesse (2002)*. After that, the samples were centrifuged at 18,200 x g and 22°C for 10min to pellet the solids. 250µl of the supernatant were transferred into a 1ml Chromabond C_{18} ec SPE column (Macherey-Nagel, Düren, Germany). The water fraction was collected in 1.5ml reaction tubes (Sarstedt, Nümbrecht, Germany), and, thereafter, the bound oxalate was eluted twice with 500µl of 50% (v/v) acetonitrile in water. Both elution fractions were pooled in one tube and mixed thoroughly, then 100µl of the sample were transferred into glass vials with inserts, and crimped shut (vials, insert and crimp caps all by Macherey-Nagel, Düren, Germany). Soluble oxalate was measured by liquid chromatography–mass spectrometry (LC 2040C 3D + FCV-20AH2 Valve Unit + LCMS 2020, Shimadzu, Duisburg, Germany). The liquid chromatography system (LC) was used without separation column to inject the sample and to maintain a steady flow of the eluent. Eluent composition was 50% acetonitrile (Ultra LC-MS grade, Carl Roth, Karlsruhe, Germany) and 50% ultra-pure water with a flow rate of 0.4ml/min. The ion source was set to an interface temperature of 350°C, a DL temperature of 250°C, and the heat block was set to 200°C. Drying gas was used with a flow of 10 l/min, and nebulising gas flow was 1.5 l/min. The MS was used in single-ion mode for a mass-to-charge ratio of 89 with the ESI in negative mode. Injection volume was 10µl. As the measurements were performed using

LC2040 only as an autosampler device, and as no column was used, there was no retention of the analytes before the MS. To ensure a stable baseline and to allow a precise peak integration, samples were injected 0.5min after starting the run. Four biological replicates of each sample were measured, and calibration of oxalate was carried out in triplicates using oxalic acid as a standard.

PROTEIN CONTENT BY BRADFORD

The pure protein content in the dried *Lemna* biomass was analyzed according to *Bradford (1976)* To extract the proteins from *Lemna* powder, 50mg of each ground sample were mixed with 1ml 0.1 M NaOH in 1.5ml reaction tubes (Eppendorf, Hamburg, Germany) on a vortex mixer (Vortex Genie 2; Scientific Industries, Bohemia, NY, USA) until the powder was suspended and neither lumps nor air pockets were visible. The mixture was then incubated for 30 minutes at room temperature on a shaking platform (DuoMax 1030; Heidolph, Schwabach, Germany) at 50rpm. After incubation, the powder was separated from the supernatant by centrifugation at 18.200 g for 30min (Centrifuge 5430R; Eppendorf, Hamburg, Germany). The supernatant was then diluted by 250 with ultrapure H_2O (Milli-Q® Lab Water Solutions, Merck), and used for further analysis. The Bradford assays were carried out in 96-well plates using the commercially available solution Roti®-Quant (Carl Roth GmbH & Co. KG, Karlsruhe, Germany) according to the manufacturer's protocol. Additionally, spiked samples with elevated concentrations of protein were prepared to correct the measurements for any protein loss during sample preparation. For these spiked samples, bovine serum albumin (BSA) (Sigma-Aldrich, Steinheim, Germany) was added to the dried *Lemna* powder before the addition of NaOH. Four of the samples were spiked with 10mg BSA, and four samples with 20mg BSA, and after that, these samples were treated the same as all other samples. For the preparation of the linear calibration, BSA was used as a standard. The plates were then measured at 595nm on an Infinite 200 PRO microplate reader (Tecan, Crailsheim, Germany), and the protein concentration was calculated from the linear regression of the calibration. One calibration was measured on each plate to ensure reproducibility between plates. Pure protein content, Pp, in % /dry matter was calculated as follows:

$$Pp = \frac{mC*dil}{Ldm} \qquad \text{eq. 3}$$

with

Pp: pure protein

mC: measured concentration by Bradford *(Bradford M.M., 1976)* resp. calibration

dil: dilution

Ldm: *Lemna* dry matter

In addition to the conventional calibration of the Bradford analysis, a correction factor between bovine albumin and *Lemna* protein was determined by linear regression of the spikes.

Both oxalic acid and protein concentrations were measured in *Lemna* dry matter samples from the cyclic (repeated) partial harvesting of cultures over 30 days of cultivation time. The different treatments with NH_4^+/NO_3^- ratios of 10/90, 20/80, and 30/70 were cultured in 4 parallel replications in each case. The different treatments with NH_4^+/NO_3^- ratios of 10/90, 20/80, and 30/70 were considered different at light qualities, but the same light quantity. The cultures were continuously exposed to 3,500ppm CO_2. FM and DM were determined and related to the contents of oxalic acid and proteins.

HEAVY METALS BY ICP

The samples from cyclic (repeated) harvests were dried and ground in the same way as described in the previous chapter. The resulting *Lemna* DM was prepared by the Aqua Regia Digestion method, DIN EN 13657:2003-01, for later ICP-AES (**I**nductively **C**oupled **P**lasma **A**tom **E**mission **S**pectroscopy). The elements listed in Table 6 were treated according to the DIN ISO 22036:2009-06 method for determining the related wavelength, linear calibration and blank calibration.

Tab.6: Methodology used for ICP

Element	Standard	Range
Cu	DIN ISO 22036:2009-06	3mg/kg in DM
Zn	DIN ISO 22036:2009-06	3mg/kg in DM
Ca	DIN ISO 22036:2009-06	3mg/kg in DM
Mg	DIN ISO 22036:2009-06	3mg/kg in DM
Na	DIN ISO 22036:2009-06	0.1mg/kg in DM
K	DIN ISO 22036:2009-06	10mg/kg in DM
Mn	DIN ISO 22036:2009-06	5mg/kg in DM
Fe	DIN ISO 22036:2009-06	5mg/kg in DM

4.1.5 Parameters for the modelling of growth and regrowth

A model for considering all growth-relevant parameters needs to be developed in a self-consistent manner from the beginning. To this end, not only the culture parameters had to be considered, but also the method for consistent partial cyclic harvesting. Any form of linearisation of the sigmoidal growth curve had to be prevented in order to exclude any under- or over-estimation for long-term cultivation.

Different to the model equation by *van den Top (2014),* the population of *Lemnoideae* grows along the differential equation of limited growth *Murray (2011); Verhulst (1845), Maltus (1807), Bacaër & Bacaër (2011)*.

$$\frac{dW(t)}{dt} = r_i \cdot W(t) \cdot (1 - \frac{W(t)}{Wmax}) \qquad \text{eq. 4}$$

with

W(t)	time-dependent development of the population
r_i	growth rate in g•m^{-2}•d^{-1}
W_{max}	capacity, maximum biomass coverage (population density) in g•m^{-2}

and with an implemented term $r_i \cdot \frac{W(t)}{Wmax}$

W_{max} in eq. 1 is the maximum biomass coverage of a specific population, the so-called capacity, which in *Lemnoideae* differs between species, and even between cultivars/lines. Because of the high number of individuals per area, the growth of biomass develops with the same mathematical dynamics as the population. Integrating the differential equation eq. 4, the analytical solution can be described as

$$W(t) = \frac{Wmax}{2} \cdot (tanh(\frac{r_i}{2} \cdot t + \frac{Wmax}{2} \cdot C) + 1) \qquad \text{eq.5}$$

with the tangens hyperbolicus (tanh) as a specific e-function

$$\tanh = \frac{sinh}{cosh} = \frac{e^x - e^{-x}}{e^x + e^{-x}}$$

The exponent x in eq. 2 relates to

$$x = (\frac{r_i}{2} \cdot t + \frac{Wmax}{2} \cdot C)$$

The complete mathematical derivation of the analytical solution by integrating the differential equation above is attached in the Appendix.

The specific constant factor C results from the so-called self-consistent mathematical solution of integration (see Appendix). The exponent *(x)* as such consists of a time-dependent term $(r_i/2)\bullet t$ and a further time-independent term $(W_{max}/2)\bullet C$. Nevertheless, this integration factor C occurs as a product to be multiplied by W_{max} in the exponential term of the e-function "tanh (tan hyperbolicus)". This strongly indicates that *C* can be interpreted and/or predicted as a species- and/or variety-dependent co-factor to be considered in the growth process of the population. It has been supported by observation of experiments for three years that each variety exhibits a different capacity W_{max} of the population under the same experimental conditions (light quality and quantity, nutrients, temperature, CO_2). For this reason, growth rates in the literature are generally indicated for a specific species *(Khvatkov et al., 2018; Lasfar et al., 2007; Petersen et al., 2021; Petersen et al., 2022; van Dyck et al., 2022).* As can be seen below, W_{max} has to be inserted into the model as one of the most important parameters. Moreover, it is possible to identify several species in "reverse-modelling" after a series of comparisons of modelling curves by applying eq. 5 if the equation is solved towards *C*.

As the growth rate r_i further depends both on the temperature (T), *(Korner et al., 2002, Bontsema et al., 2010)* and the photon flux density (E), a modified van't Hoff-Arrhenius relationship by *Lasfar et al. (2007)* was used:

$$r_i(T) \propto T \cdot \theta 1^{\left(\frac{T-Top}{Top}\right)^2} \cdot \theta 2^{\left(\frac{T-Top}{Top}\right)} \qquad \text{eq.6}$$

$$r_i(E) \propto E \cdot \theta 3^{\left(\frac{E-Eop}{Eop}\right)^2} \cdot \theta 4^{\left(\frac{E-Eop}{Eop}\right)} \qquad \text{eq.7}$$

with

T	temperature
T_{op}	optimal temperature
E	photonic energy
E_{op}	optimal photonic energy

The exponents of the temperature-related Θ_1 and Θ_2 functionals and the radiation-related Θ_3

and Θ_4 become zero when the temperature T is permanently kept at $T = T_{op}$ (T_{op} = optimal temperature) and PAR $E = E_{op}$ (E_{op} = optimal light). Therefore, near the respective optima, the values for the functionals Θ_i are 1. Therefore, under these conditions, eq. 6 and eq. 7 are accurately reduced to be simply linearly dependent

$$r_i(T) \propto T \qquad \text{eq.8}$$

$$r_i(E) \propto E \qquad \text{eq.9}$$

Thus, the modelling for a controlled indoor system becomes easy in T and E because of a linear dependency, as resulted in eq. 6 and eq. 7, if in the range near the optimum. The factors for T and E in the optimum can be set to 1, provided that T could be experimentally determined, and to lower than 1 if the system is not operated at the optimum.

The influence of the most important nutrients (N, P) on the growth rate was taken as described by *Driever et al. (2005)* and followed Michaelis Menten kinetics.

$$r_i(P,N) = \alpha P,N \cdot \frac{CP}{(CP+KP)} \cdot \frac{KIP}{(KIP+CP)} \cdot \frac{CN}{(CN+KN)} \cdot \frac{KIN}{(KIN+CN)} \qquad \text{eq.10}$$

with

$\alpha_{P,N}$	intrinsic growth rate
C_P	concentration of P
C_N	concentration of N
K_{IP}, K_P, K_N, K_{IN}	constants for saturation and inhibition of P and N.

where

K_{IP} = 101 mg P/l

K_P = 0.31 mg P/l

K_N = 0.95 mg N/l

K_{IN} = 604 mg N/l

Using eq.10 with the aforesaid 1.14mM N and 0.23mM P, the growth rates for the nutrients N and P result in $r_i(P,N) = \alpha(P,N) \bullet 0.823$. With these levels of N and P, 0.823% of the possible maximum nutrient-related growth rate can be obtained.

Since a further exposure to CO_2 is significantly effective for an optimal long-term production of *Lemnoideae,* mesophyll resistance was considered. For modelling of CO_2 transfer into the plant cells, total mesophyll resistance remains the only important factor. Fick's law was used, considering the influence of the partial pressure of CO_2 for diffusion *(Hikosaka et al., 2015)*. Thus, the complete further passage of CO_2 can be considered as total mesophyll resistance (Evans et al., 2009)

$$R_m = R_{ias} + R_{liq} \qquad \text{eq.11}$$

with

R_m: mesophyll resistance

R_{ias}: intercellular air resistance

R_{liq}: sum of liquid resistance

Liquid resistance R_{liq} itself is a sum of

$$R_{liq} = R_{wall} + R_{Plasmamembrane} + R_{Cytosol} + R_{chloroplast} + R_{Stroma} \qquad \text{eq.12}$$

This part represents all transport processes of CO_2 towards the RuBisCo(Ribulose-1,5-bisphosphat-carboxylase/-oxygenase) enzyme. *Ooteghem (2007)* confirmed the model of *Bot (1983)* to be

$$R_{CO_2} = \frac{R_{cut} * R_S}{R_{cut} + R_S} + R_{carboxilation} \qquad \text{eq.13}$$

with

R_{cut}: cuticula resistance

R_S: stomata resistance

As stomata of *Lemna are constantly open (Landolt et al., 1987) Severi & Fornasiero (1983)*, the CO_2 pathway remains constant. In the modelling, the time derivative of a constant leads to zero. Therefore, R_{CO2} remains mainly only dependent on $R_{carboxilation}$.

With regard to the contribution of $R_{carboxylation}$ in eq. 13, which is related to RuBisCo activity in C-fixation, it has to be considered that this part is dependent on light quantity *(Hawkesford et al., 2012), (Ye et al., 2023),* but it is validly assumed that it is also dependent on light quality, as the amount of photon energy influences the so-called light saturation point versus CO_2

concentration. However, as far as the photonic energy E has already been taken into account in the contribution on the growth rate $r_i(E)$ (see eq.7), this would lead to a coupled differential equation that is not trivial to solve analytically.

If all dependencies of all transport processes mentioned are taken into account, the following valid simplification can be found for the model. When considering the differential equation for growth, only the change per unit of time is important. Since the above-mentioned contributions are at best quadratic, the first derivative with respect to time would mathematically lead to a linearisation. For this reason, a comparable approach can be found for $r_i(CO_2)$, as well as for $r_i(E)$ and $r_i(T)$ in eq. 7 and 6 mentioned above, namely a linearisation dependency near the optimum.

This shows that the measurement of crop growth at 3,500ppm versus 400ppm CO_2 takes into account all of the above-mentioned transport processes for CO_2 if the outcome of these measures is refed into the modelling for $r_i(CO_2)$. This assumption/simplification is supported by the fact that the saturation of the so-called Γ-point also follows the Michaelis-Menten kinetics *(Fuhrer (1983); Frost-Christensen & Floto (2007).* Therefore, a linearisation near the optimum has also been confirmed for the $r_i(CO_2)$ part of the growth rate. Considering all aforementioned dependencies of the growth rate, r_i results in a further so-called product rule, which means that all influences of temperature, photonic energy, N/P ratio, and CO_2 are essential, independent from each other, and not replaceable,

$$r_i = r_{i0} \cdot |\alpha(r_i(T))| \cdot |\beta(r_i(E))| \cdot |\gamma(r_i(N,P))| \cdot |\delta(r_i(CO2))| \qquad \text{eq.14}$$

with

r_{i0}	possible maximum growth rate
$\alpha(r_i(T))$	α factor, contribution of temperature to the growth rate
$\beta(r_i(E))$	β factor, contribution of photonic energy to the growth rate
$\gamma(r_i(N,P))$	γ factor, contribution of nutrient ratios to the growth rate
$\delta(r_i(CO_2))$	δ factor, contribution of CO_2 concentration to the growth rate

The multiplication of every related factor mentioned above with the maximum possible growth-rate results in the specific growth-rate contribution and is termed productivity factor *pf*.

The factors *α, β, γ, δ* are each = 1 at the optimum supply, and are < 1 outside of it. This was used with the cumulation rule (product rule) for the effective growth rate r_i in the subsequent modelling. Each resulting factor for the parameters of temperature, CO_2, nutrition, and light is essential for the growth rate, and cannot be replaced or compensated by another one. The aim of all these factors is to adjust them in the cultivation as closely to 1.0 as possible.

To validate the proper model methodology, a simple cross check was done as follows:

As seen above, for example, the factor for nutrition could be adjusted very closely to 1.0, using eq. 10. Importantly, the result from the product rule of eq. 14, considering that the findings of optimisation are only 0.9 (90%) for each parameter, would only result in a $0.9^4 = 0.66$ (66%) use of the possible maximum growth potential. This clearly indicates the importance of an optimisation of each cultivation parameter possibly above 90% for a continuous near maximum yield and the accuracy of the model.

Under the constant conditions of our cultivation system operating near the optimum, this value can be considered to be constant as well, and thus can be simplified. This results in the definition of a coefficient factor for $r_i(CO_2)$, which can be determined with high accuracy by measuring, and be re-fed into the model as a valid value as the aforementioned product rule for the overall growth rate *ri*. In an abbreviated mathematical notation, this is

$$r_i = r_{i0}(\prod_{j=T,E,NP,CO2} k(r_i(j))), \qquad \text{with k = } \alpha, \beta, \gamma, \delta \text{ as specific constants} \qquad \text{eq.15}$$

As a result, the specified new growth formula of eq. 5, 14, and 15 results in

$$W(t) = \frac{Wmax}{2} \cdot (tanh(\frac{r_{i0}}{2} \cdot (\prod_{T,E,N,P,CO2} k \cdot r_i(j)) \cdot t + \frac{Wmax}{2} \cdot C) + 1) \qquad \text{eq.16}$$

Consequently, a time-dependent exponent

$$\frac{r_{i0}}{2} \cdot (\prod_{T,E,N,P,CO2} k \cdot r_i(j)) \cdot t$$

and the aforementioned time-independent exponent

$$\frac{Wmax}{2} \cdot C$$

are obtained.

The introduction of the term for r_i into eq. 5 and 16 summarises all relevant growth factors.

Since the modelling used was based on numerical integration, the analytical solution was used to obtain the extrema of the maximally possible harvest amplitude (harvest amount), keeping them within the area of quasi-exponential growth of the sigmoidal growth curve W(t). The analytical solution could provide these values by analytical curve discussion.

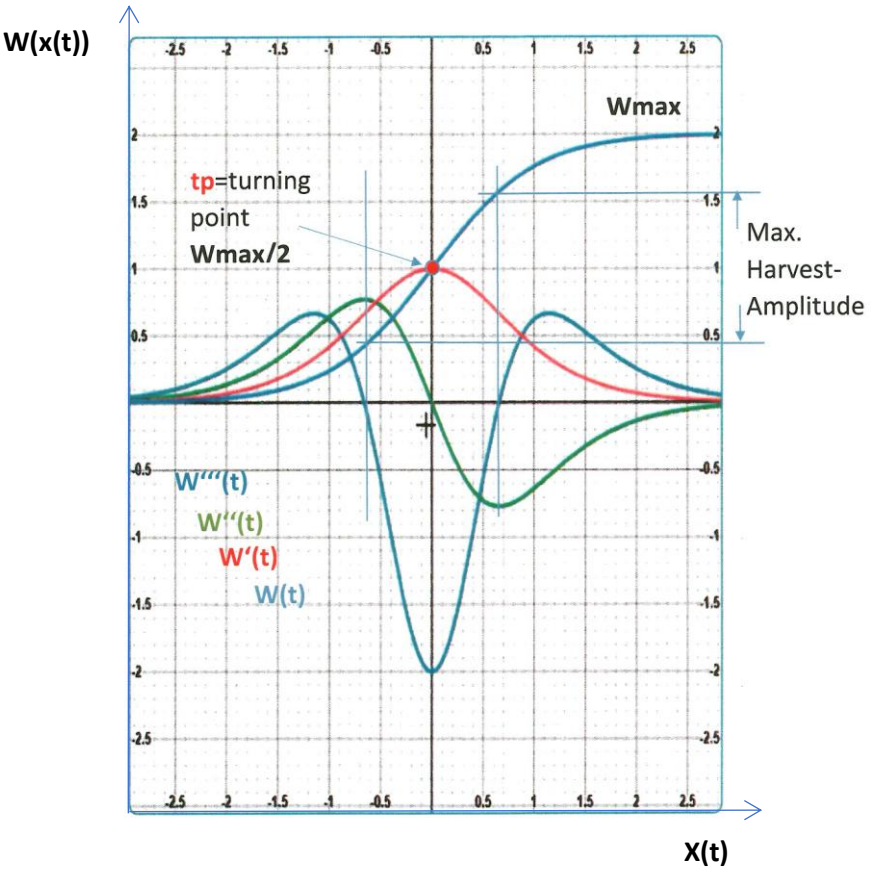

Fig.18: Curve delineating the differential equation eq.5. The sigmoidal curve of limited growth is point-symmetric around tp. The first derivation W'(t) indicated tp as the point of the maximum gradient (growth rate), which shows that tp=W_{max}/2. Furthermore, the area of quasi-linear growth extends between the maxima of the second derivation and/or zero points of the third derivation.

According to Fig.18, the area of quasi-linear growth extends between the maxima of the second derivation and/or zero points of the third derivation. An important conclusive outcome is the maximal harvest amplitude (amount of cyclic harvest from the culture), indicated above as max harvest amplitude m = 0,53•W_{max}.

W_{max} is the so-called capacity (maximum population density of fresh matter, FM).

W(t) = sigmoidal growth curve

W'(t) = first derivation, indicating the maximal growth rate at tp

W''(t) = second derivation, extrema indicating the maximal harvest amplitude of the quasi-linear growth zone in the middle of W(t)

W'''(t) = third derivation, a more precise definition of the limits of the maximal harvest amplitude as zero crossing of the function. Here it is given as $0.53 \bullet W_{max}$.

A full-scale curve sketching was used to enable the analysis of the growth system already before the start of the modelling. The analytical result of the (non-numeric) equation eq.5 and 16 is that the term $W_{max}/2$ (half the capacity) occurs twice, firstly, as a multiplication factor before the functional, and secondly, in the argument of the tangens hyperbolicus function. For this reason, the real turning point **tp** of the sigmoidal function is the point of the maximum growth rate. If conditions are kept at the optimum, such as temperature, light quality and quantity, the maximally possible harvest amplitude would be ≤ 53% of W_{max} (variety-specific maximum capacity of the population).

For a numeric integration using SIMILE® (www.Simulistics.com), the previously determined term for r_i into eq.14 and eq.15 summarises all growth-relevant factors also in a numeric integration. The model was programmed using SIMILE®, where numeric integration allows to test the influence of input parameters on growth. For a continuous culture, harvest intervals have to be optimised to ensure a continuous biomass formation and to suppress algal growth. Thus, the harvest has to be carried out around the maximum growth rate, i.e., at the turning point of the growth function. These parameters have been verified by experiments. The harvest interval was chosen to be around $W_{max}/2$ of the growth curve, as shown in Fig.18. The upper harvest point has to remain still at the quasi-linear gradient of the growth rate, which is $\leq$ 53% of W_{max}, and the harvest cycle has to be located symmetrically around the turning point tp. Thus, a factor m has to be implemented in the programming of SIMILE® within said analytically determined harvest amplitude: $m \leq 0.53$. In order to be symmetrical around tp = $W_{max}/2$, the harvesting interval can be described as:

$$|W_{harvest}| = \frac{Wmax}{2} * ((1 + m/2) - (1 - m/2)) \quad \text{Harvest amplitude (amount)} \qquad \text{eq.17}$$

Harvesting started at W1, as the upper point within the quasi-linear portion of the sigmoidal growth curve (see Figure 23), which is

$$W1 = \frac{Wmax}{2} * (1 + m/2) \quad \text{eq.18}$$

and ends at the lower point, which is the remaining biomass after harvesting.

$$W2 = \frac{Wmax}{2} * (1 - m/2) \quad \text{eq.19}$$

Modelling is impossible without any previous experimental determination of these parameters. According to our previous experience, maximum biomass production differs widely between different genera and varieties or local populations of *Lemnoideae*. Maximum biomass production per unit of area can be assessed as soon as there is an equilibrium between the growth and the decay of fronds. Considering the growth rate within the complete harvesting amplitude to be linear is an over-simplification.

When the model is performed for extended periods of cultivation, this assumption would produce inaccurate results. After every harvest, the model must calculate both the growth function and the regrowth function as a sigmoidal curve. Only at the precise turning point "t_p" does the growth rate, or also the regrowth rate r_i, reach its maximum. In contrast, the mathematically continuous sigmoidal curve will change through the harvest process to a discontinuous delta function (sawtooth function).

The numeric programming in SIMILE® was based on:

$$\mathrm{dW}_{growth} = r_i \cdot \mathrm{W(t)} \left(1 - \frac{\mathrm{W(t)}}{\mathrm{Wmax}}\right) \cdot \mathrm{dt} \quad \text{eq.20}$$

inserted as operator for the numeric integration of unlimited growth in SIMILE®. The operator r_i was considered as a subroutine for T (temperature) and E (photoperiod), the macronutrients N, P, and CO_2 were considered as pre-factors α, β, γ, δ in the effective growth rate ri,

$r_i = r_{i0}(\prod_{j=T,E,NP,CO2} k(r_i(j)))$,

with k = α, β, γ, δ, using the predetermined values for r_i(T), r_i(E), r_i(N,P), r_i(CO_2), A further operator for cyclic harvesting in SIMILE® is

$dW_{cyclic\ harvest}$ = if (W > W_$E_{cycl.}$) then (W-W_E_{Min})/dt() else 0.

A further operator for the generation of fractals as a repeated loop for the harvesting impact is:

$dW_{harvest}$ = if (Ist_harvest==1) then (W*m)/dt() else 0,

for regrowth and the next cyclic harvest. With a brief preview on the results, for a consistent understanding of the method of modelling, the following measured data were used to start the modelling, as is displayed in Tab.15. It was considered that the population mathematically follows the impact caused by cyclic harvesting with a sustainable optimal yield over time. Two cases needed to be considered:

1st Case:

Harvest amount (amplitude) and harvest time (cycle time) perfectly match the growth/regrowth conditions. The harvest amount (amplitude) is symmetrically centred around the (predetermined) point tp (maximum gradient) of the sigmoidal growth curve from the first harvest onwards. A perfect sawtooth curve, displaying the actual status of the population at every point in time, including harvest and regrowth dynamics, is obtained as shown below.

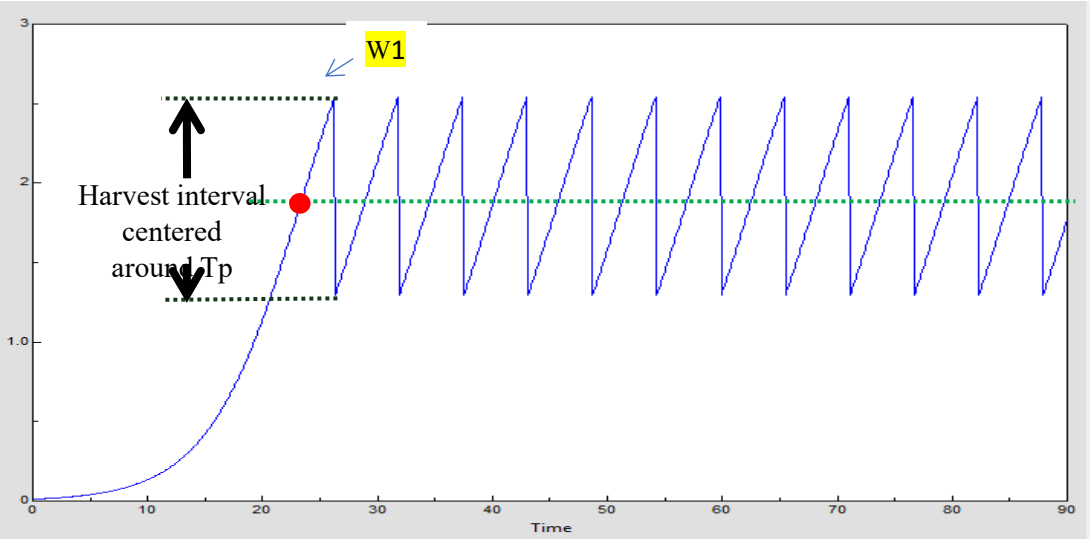

Fig.19: Repeating (cyclic) harvest impact to sigmoidal growth curve symmetrically around tp. Harvest time and harvest amount (amplitude) are fitted to optimum data of modelling.

2nd Case:

The harvest amount changes when the first harvest amount (amplitude) is not symmetrically centred around tp, but higher. The subsequent harvests are assumed to be carried out on

same 1/3 of the area. According to the model used, the culture density and the effective harvest yield would decrease with each subsequent harvest until the regrowth rate and harvest cycle time match. According to the model, this would occur as the maximum growth rate is reached at tp.

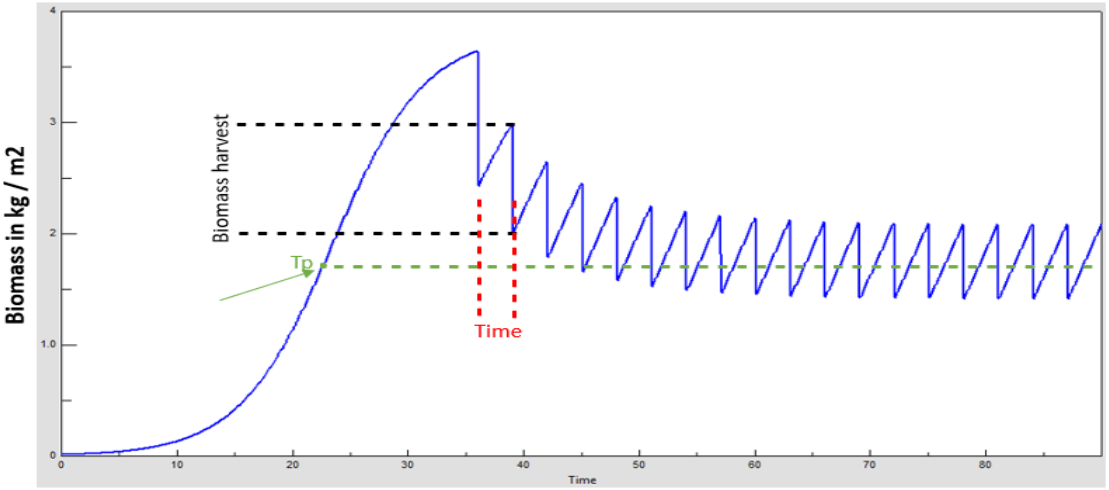

Figure 20: Prediction of a continuous decrease of the density of the culture for the 1st harvest far above tp

4.1.6 Integration of the model into an indoor photo-bioreactor

For the upscaling setup in Kalkar, fully-sized culture trays (length 27m, width 0.78m) were used for a total of three test campaigns. A total of 12 stacked culture trays in a rack (see Figure 19, left) were harvested. As the light quality was not constant from the top down at the setup in Kalkar because of added global radiation in a glass house despite additional LED illumination, the harvested yields of the individual culture trays were not useful for statistical purposes due to the heterogeneous conditions. Instead, the amount harvested was measured by adding up the contents of all the trays. This may have caused a temperature gradient from top to bottom, which could have influenced the growth rate. Also, it was not possible to perform any comparative measurements with higher CO_2 concentrations of 3,500ppm in the upscaling setups at Kalkar and Berlin.

4.1.7 Determination of the average frond age

Repeated (iterative) partial harvesting and regrowth of the *Lemna* culture significantly reduces the effective average age of the fronds. The basic analysis of a *Lemnoideae* population starts with a pre-culture having a constant initial average age ***A*** in the "undisturbed" case. Individuals that become lethal are replaced by new fronds. Such pre-cultures are much older than the lifetime of the individual *Lemnoideae* plants.

Based on this, part of this self-sustaining population needed to be harvested regularly. The repeated harvesting interval ***T*** is chosen such that, at the next harvest time, the population has reached the same population status as before harvesting.

A portion ***(1-f)*** of the crop is harvested in the process, with ***f*** as the remaining portion after harvesting. There is a correlation between the values of ***f*** and ***T***, which depends on the respective population dynamics. The average age of the new population is ***αT***. In case of a linear progression, for example, ***α*** would be ***½***.

A: average age of the fronds

α: average factor for regrowth between two harvests

ß: proportion of the old population that had died in the period

T: cyclic (repeated) harvesting interval time

αT: average age of the new population portion

1-f: harvest portion

f: remaining portion after harvesting

A_i: average age after the i-th harvest.

Simplified model:

Cultivation time remains less or equal to life time, so that A_i is independent on *β* (death rate):

Assumptions:

- Harvest portion:

$$1 - f = \frac{1}{3} \qquad \text{eq.21}$$

- Remaining portion after harvesting:

$$f = \frac{2}{3} \qquad \text{eq.22}$$

- Cyclic harvest time: $T = 3d$

$$A_i = fA_{i-1} + (f-1)\alpha T \qquad \text{eq.23}$$

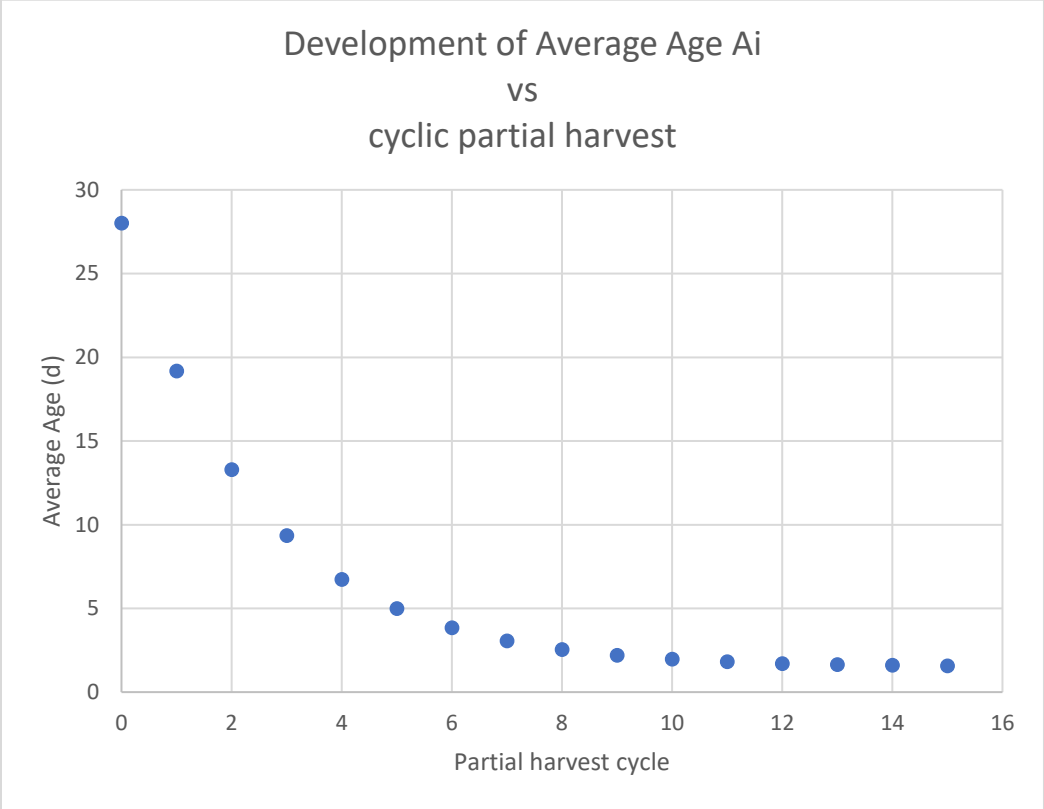

Fig. 21: Decrease of average frond age depending on a partial 1/3 harvest impact every 3 days

Extended model:

Cultivation time is longer than life time, so that A_i includes the death rate β. The author discussed this with Gunter Krauss, University Bonn.

Assumptions:

- The average age of the remaining population is

$$A_{i-1} + T \qquad \text{eq.24}$$

- The average age of the new population is

$$\alpha T$$

- The proportion of the old population is

$$f(1 - ß) \quad \text{eq.25}$$

- where *ß* is the proportion of the old population that had died in the period.
  The proportion of the new population is

$$1 - f + f\,ß \quad \text{eq.26}$$

- i.e., the compensation of the harvested *(1-f)* plus the compensation of the dead plants.

$$A_i = f\,(1 - \beta)(A_{i-1} + T) + (1 - f + f\beta)\alpha T \quad \text{eq.27}$$

Since the age remains constant in the undisturbed case *(f = 1),* the following must apply to the relative mortality rate *ß*:

$$A_i = A_{i-1}$$

i.e.

$$A_i = (1 - \beta)(A_i + T) + \beta\alpha T \quad \text{eq.28}$$

$$A_i = A_i + T - \beta A_i - \beta T + \beta\alpha T \quad \text{eq.29}$$

$$0 = T - \beta(A_i + T - \alpha T) \quad \text{eq.30}$$

$$\beta = \frac{T}{A_i + (1 - \alpha)T} \quad \text{eq.31}$$

4.2 Integration of the model into an aquaponic system: first upscaling in Berlin

4.2.1 Culture trays, light, CO_2, watering system

The first upscaling like shown in Fig.22 was located at ECF Farm Systems GmbH, Bessemerstraße 29, Berlin, Germany. A cultivation system with 6 culture trays was stacked in a rack of about 20m^2 aquatic surface, and installed in an indoor fish farming compartment of a greenhouse. Waste water, heat, and exhaust CO_2 from the fish farming facility were used for the cultivation of *Lemna*. The nutrient solution for the *Lemna* cultures was separately

supplemented with additional nutrients, as required (aquaponics). The temperature in the entire compartment was controlled to remain at 25-27°C.

Furthermore, the same composition of the resulting nutrient solution that was optimised in the lab system in Bonn was applied in the upscaled setups. The same applies to supplemental lighting. In contrast to the laboratory scale, it was only possible to approximate both temperature and photon flow density due to the influence of global radiation in this setting.

Refilling of water and nutrient solution was provided by tubes installed in each of the trays. A constant control of CO_2 introduction over the complete culturing time was not possible.

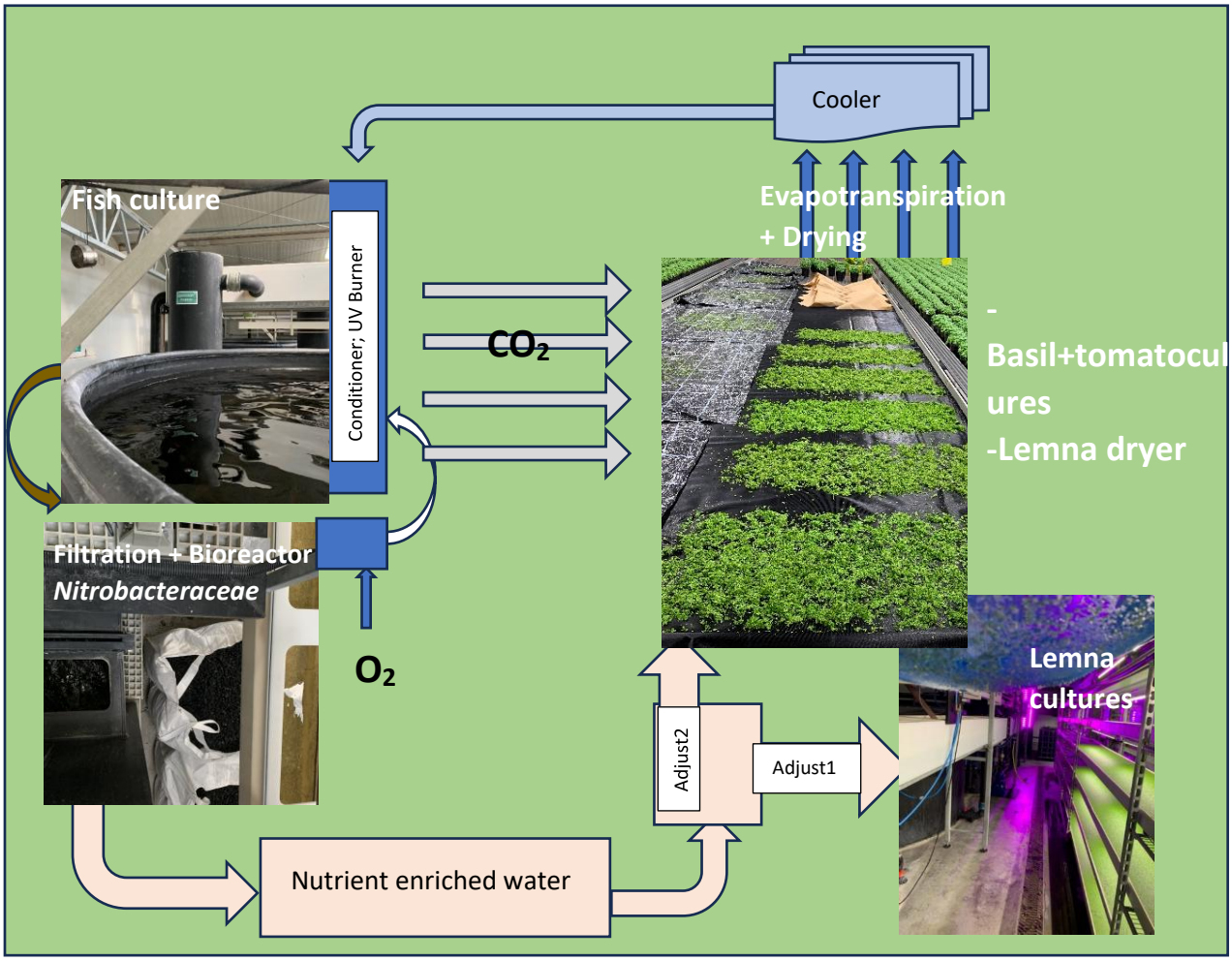

Fig. 22: Indoor aquaponic system at ECF Farm Systems, with partly closed and CO_2 cycles of the greenhouse and fish culture compartments, including use of manure from the fish culture, filtered and nitrified by a *Nitrobacteraceae* bioreactor, conditioned by oxidation, and fed as nutrient-enriched water to the plant cultures, after final adjustment of nutrient ratios and dilution; adjust1-gate for the greenhouse and adjust2-gate for the *Lemna* culture.

The cleaned and nitrified (trickle filtration with *Nitrosomonas* and *Nitrobacter* innoculation) fish slurry was permanently circulated in the fish culture system in a circulating channel that was open at the top and exposed to oxygen and subsequent UV burners at two points in the circulation. The basic nutrient solution for the *Lemna* culture system was taken from this circulating volume and introduced into the total nutrient solution that had been optimised in the laboratory setup using mineral fertilizer via adjust2-port. The CO_2 release from the fish cultures was used throughout the aquaponic system for air enrichment. Unfortunately, the CO_2 concentration at the *Lemna* cultivation site in January and February 2020 was only 2,300-3,200 ppm when the cultures were growing from an initial start after inoculation. At the time of the harvest trials beginning in May 2020, the temperature had to be limited to approx. 27°C by ventilation. The CO_2 concentrations achieved were only below 600 ppm.

Fig.23A: Preparing a culture tray, firstly, with water before introducing the stock solution diluted to 1:19 to the final concentration of the nutrient solution mentioned above.

Fig. 23B left: Start of the population on 11th Jan. 2020 (4:13 pm)
Fig. 23B center: Status of the population on 17th Jan. 2020 (11:30 am)
Fig. 23B right: Status of the population on 20th Jan. 2020 (12:41pm)

The sequence of images in Fig. 23B shows that the population reached more than 20 times the density of the start population after 9 days from inoculation, with the power of e^3=20. At that time the concentration of CO_2 was still below 2,300-3,200 ppm.

4.2.2 Nutrient solution in the first upscaling

Adapted feeding of the nutrient solution in the Berlin upscaling setup was performed manually, see Tab.7. Fish manure, as an organic component after nitrification and hygienization from the aquaponic cycle, was used as the basis for the nutrient solution. NH_4^+, as well as the elements P, K, Mg, Ca, Fe, Mn, Zn, B, Cu, S, B, Cu, and Mo were added as salts dissolved in H_2O_{bidest} to such an extent that they corresponded to the concentrations of the nutrient solution from the laboratory setup. They were adapted to the ongoing depletion *in situ*. Re-feeding the nutrient solution at the upscaling site in Berlin was performed manually. The fish manure was taken from the bottom of the tanks of the aquatic culture and treated as follows.

Tab.7: Stock solution to be added to fish manure

Fish manure, original, after biofilter/nitrification (*Nitrobacteraceae*)		**Low concentrated stock solution, after 1:3 dilution and with the addition of NH_4^+, P, K, Mg, Ca, Fe, Mn, Zn, B, Cu, Mo**	
Elements (Extraction)	mmol/l	Elements (Extraction)	mmol/l
NH_4^+	< 0.1	NH_4^+	+ 0.29
K^+	0.8	K^+	0.27 + 1.8 = 2.07
Na^+	14.1	Na^+	3.53
Ca^{2+}	1.7	Ca^{2+}	0.43
Mg^{2+}	0.6	Mg^{2+}	0.15
Si	0.2	Si	0.05
NO_3^-	10.7	NO_3^-	2.68
Cr	2.3	Cr	0.57
SO_4^{2-}	1.8	SO_4^{2-}	0.45
HCO_3	2.2	HCO_3	2.2
PO_4^{3-}	0.19	PO_4^{3-}	0.048 + 0.5 = 0.548
Fe	< 0.0004	Fe	0.036
Mn	< 0.0001	Mn	0.018
Zn	0.0002	Zn	0.00154
B	0.008	B	0.092
Cu	0.0004	Cu	0.00064
Mo	< 0.0001	Mo	0.00098
pH	7.0	pH	6.5

A further dilution with 1:1 with filtered and sterilized cistern water was used, replacing the evapotranspiration losses with water + stock solution. The NO_3^- level was balanced between 1.48mM after refill and 0.8mM before refill. So, the test installation of the *Lemna* cultures was included in the water and nutrient cycles, as shown in the Fig. 22.

4.2.3 Treatment of plant material in the first upscaling Berlin

The same plant material was used, *Lemna minor* 'Henry DaCapo' (CPVO reg. EU2970). For inoculation of the first upscaled setup in Berlin, pre-cultured plant material from the laboratory setup in Bonn was used. As considered in the associated modelling, cyclic (repeated) partial harvesting of 1/3 of the culture trays, illuminated by additional LED bars, was performed. Harvesting started as soon as a biomass coverage amounting to 2/3 of the limit coverage was reached. Harvesting was continuously repeated in cycles of 5 days and in cycles of 3 days. Said optimal cycle times were determined in the modelling by SIMILE® for

400ppm CO_2 and for 2,500ppm CO_2, and they were confirmed to be accurate in practical application. Harvesting of each tray was performed by the use of a mesh, and then the harvested biomass was transferred to a further mesh foil in a container for dewatering during a waiting time of 15 minutes. After that, the FM was weighed before being transferred to the greenhouse for drying on a plant table at about 35°C. After 24h, the biomass was weighed again for determining the Dry Matter (DM).

4.2.4 Analysing methods

Growth rates r_i in this first upscaling were determined and compared with the laboratory setup. The harvested biomass per tray was weighed in the same manner as in the laboratory setup after blotting off the adhering nutrient solution, but not dryed in order to determine FM. Deviations in the r_i-related parameters temperature, CO_2, and light from the optima resulting in the laboratory setup were considered in the model predictions from the Simile®-based adapted model, and compared with the obtained real harvest amounts in time.

4.2.5 Parameters for modelling of the first upscaling

The modelling was executed for all setups of the fully illuminated zone. In the experiments, 1/3 of the illuminated maturation zone was harvested in each harvest cycle. In order to compare laboratory measures and upscalings, the same basic growth model, as described in eq.5 was used. Only the theoretical predictions for the growth factor r_i according to eq.8 to eq.10 were replaced to result in a new r_i. Harvest amplitudes (amounts) were then correlated to both the predictions and the laboratory measures.

4.3 Integration of the model for 2nd upscaling at Kalkar

For the upscaling setup in Kalkar, fully-sized culture trays (length 27m, width 0.78m) were used for a total of three test campaigns. A total of 14 stacked culture trays in a rack (see Fig.24, left) were harvested. As light quality was not constant from the top down at the setup in Kalkar because of added global radiation despite additional LED illumination, the harvested yields of the individual culture trays were not useful for statistical purposes due to the unequal conditions. Instead, measurement of the harvested amount was performed by summing up all trays. Also, it was not possible to perform any comparative measurements with higher CO_2 concentrations for these premises.

4.3.1 Culture trays, temperature, light, CO_2

The first serial analysis was performed in test trays made of boron-silicate glass in the technicum greenhouse (type Venloblock) at Spierhof, Kalkar, Germany. The trays were randomly distributed in floating plastic trays in the rack system.

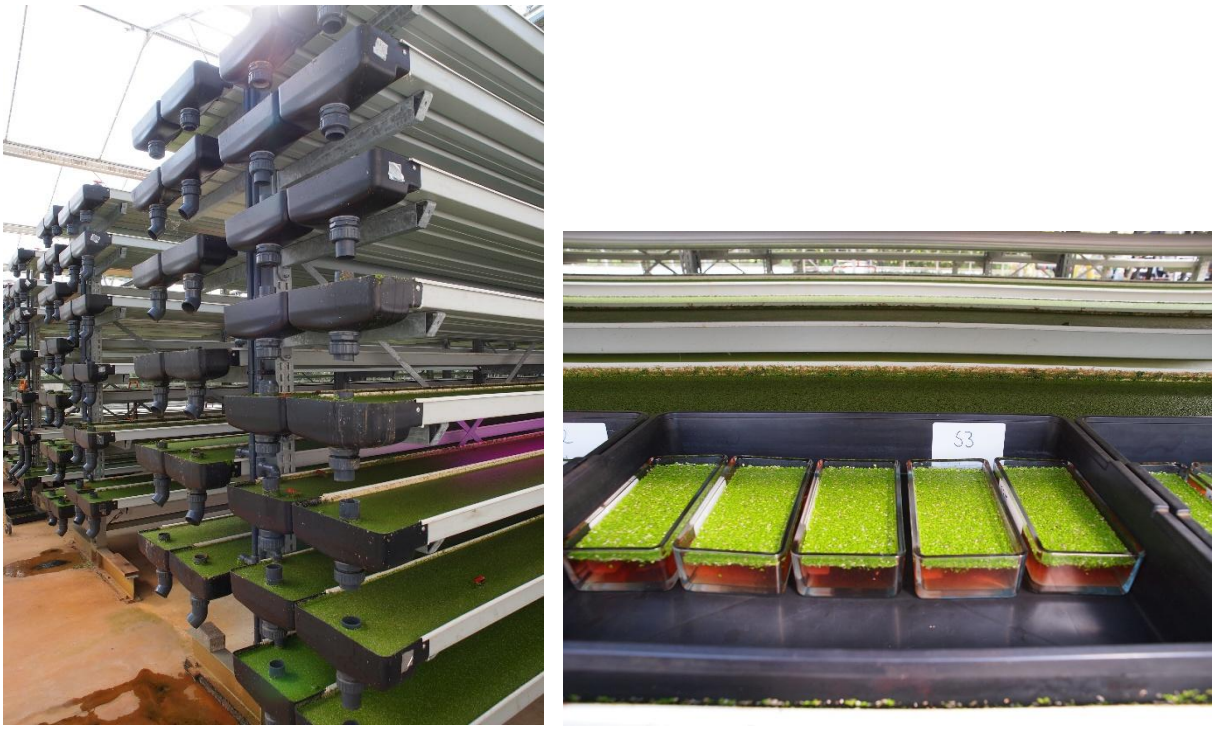

Fig. 24, left: Racks of culture trays at the Spierhof site;
Right: Floating trays with the samller test trays as a first test setup.

Every test element included 4 randomly distributed replications. Additional LED illumination was provided by an LED system (Low-Blue, by Netled, Pirkkala, Finland), dimmed down to a value of 90 µmol m^2s^{-1} PAR in the first test series, which amounted to a total value of about 120-130 µmol m^2s^{-1} PAR in the period between July and September, including any added global radiation. Both related to the results by *Lasfar (2017)* and were maintained in all subsequent experiments. For the LED light component, a 16/8 light/dark period was controlled automatically and timed as closely as possible with the global radiation photoperiod between July and September. High amounts of global radiation were limited by using an automatically controlled greenhouse shadowing system.

Light and temperature control was performed using a timer, implemented into the central greenhouse controller (Hortraco Horti, Sirius-GC + SmartLink), and was kept as synchronous as possible with the course of global radiation. Culture management within the greenhouse was non-axenic, as in all setups.

Fig.25: Left: Sprouting zone at 20-40 µmol m^2 s^{-1} PAR global radiation; Right: Maturation zone with 130 µmol m^2 s^{-1} PAR.

4.3.2 Nutrient solution

The same finally optimized nutrient solution, as shown in Tab.5A and Tab.5B was used. At the beginning of the experiments in Kalkar, the introduction of the nutrients was performed manually from the stock solution mentioned above. At a later stage, the upscaled, stacked trays in the racks that were connected to a central watering system were used. The nutrient stock solution was diluted to the same nutrient concentrations and ratios and fed into the culture trays by means of a pump and corresponding dispenser hoses. Refeeding nutrients and water were balanced with the evapotranspiration losses in the greenhouse measured at each tray.

4.3.3 Treatment of plant material

Pre-culturing was performed with the same nutrient solution ratios, but mainly diluted to half of the concentration of the experiments. In the second upscaled setup, *Cataclysta lemnata* Linnaeus (1758) sometimes appeared as a pest. This pest, also known from *Mariani et al. (2021)* lays its eggs in the floating *Lemna* culture, see Fig.26a. The resulting caterpillars pupate, wrapped in *Lemna*, see Fig.26b, and hatch as moths after approximately 30 days.

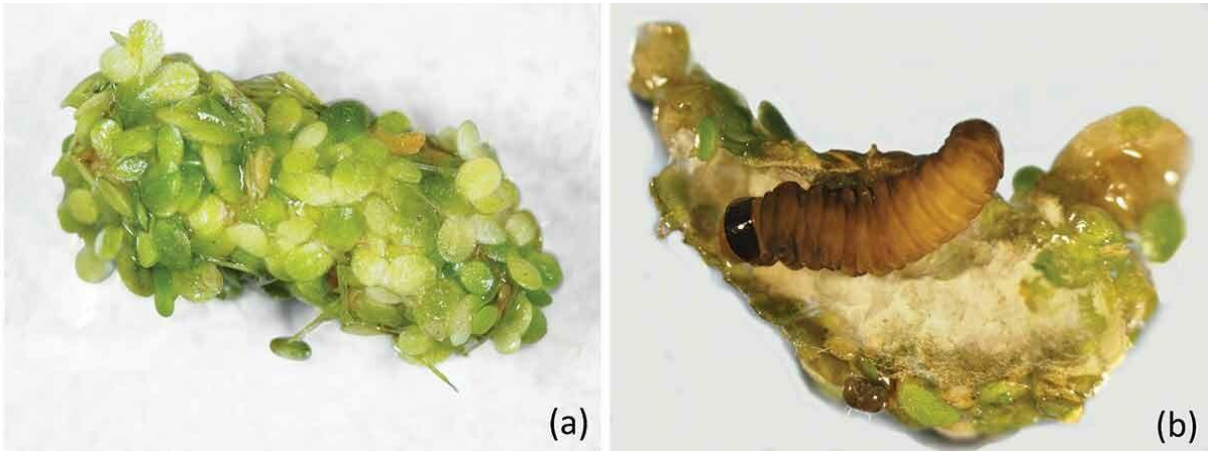

Fig.26a: Caterpillars pupate, wrapped in *Lemna*, inner portion of the pupate with hydrophonic larva Fig.26b Photos by F. Mariani (2021)

Fig.27a, Mating phase, Fig27b female moth in oviposition (Photos by F. Mariani)

In order to keep the long-term cultivated trays free from any insect larvae, especially *Cataclysta lemnata* L. *Bacillus thuringiensis* was successfully used (Xentari®). It was only necessary in the Kalkar setup, and only in the pre-culture trays. Nevertheless, infected pre-cultures were cleaned, and culture water was changed after treatment with Xentari®. Test cultivation as well as pre-culturing were performed as in all setups with single-variety cultures from *Lemna minor* L. 'Henry DaCapo' CPVO EU 29760, in order ensure a homogeneous growth rate.

4.3.4 Analysing methods

The growth rates r_i in this second upscaling were also determined and compared with the laboratory setup. The harvested biomass per tray was weighed in the same manner as in the laboratory setup after dewatering over meshes to determine FM. Deviations in the r_i-related parameters in the second upscaled setup of temperature, CO_2, and light compared to the laboratory setup were considered.

4.3.5 Parameter for modelling of the second upscaled setup

The Simile®-based model predictions and the real harvest amounts obtained were compared as well. The specific growth rate r_i for the modelling of the second upscale setup (Kalkar) resulted from the corresponding parameters, such as temperature, light, and CO_2 for the conditions mentioned in this relevant second upscale setup. The parameters for the specific growth rate r_i were determined according to the respective specific local conditions and by applying the formulae from eq.5 and eq.14.

5. RESULTS

5.1 Optimization of nutrient solution (laboratory set-up)

5.1.1 Macronutrients and oligonutrients

Absolute concentrations for N, P, K and Mg as well as nutrient ratios of NH_4^+/NO_3^-, N/K, N/P and N/Mg were compared on their influence on yield and quality. The test set-up with 5 treatments at different NH_4^+/NO_3^- ratios of 100/0, 75/25, 50/50, 25/75, 0/100, and 4 replicates obtained the following results.

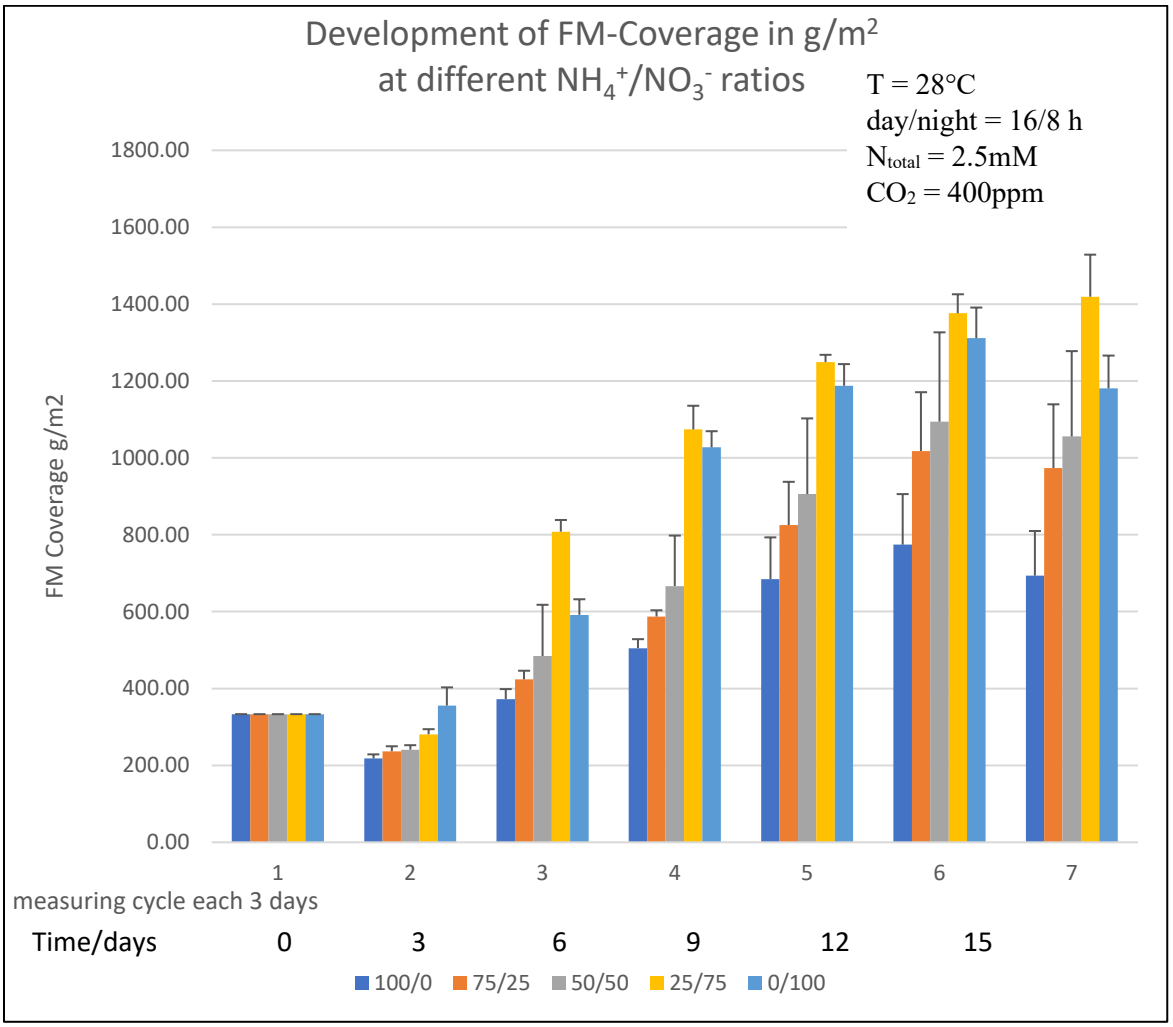

Fig.28: Growth dynamics of *Lemna minor* cultures at NH_4^+/NO_3^- ratios of 100/0, 75/25, 50/50, 25/75, 0/100.

At measuring point 1, every culture tray was equally inoculated with 333g/m^2 FM (Tray: 0.018m^2, seeding density 6g FM). Following curves were obtained by culturing conditions of T = 28°C, light/dark period = 16/8, N_{total} = 2.5mM, CO_2 = 400ppm.

The growth of the FM coverage density (g/m^2), measured every three days, without partial harvest, followed a consequent sigmoidal trend. Since the growth of biomass directly corresponds to the growth of population (numbers of individuals), all further data are related to biomass FM.

At measuring point 2, after the first 3 days, the coverage in every treatment shows a small decrease, except for the 0/100 NH_4^+/NO_3^- treatment. This is an adaption effect caused by the shift from the pre-culture at a lower N_{total} concentration to the nutrient solution of the test elements. From the 6th day onwards, all cultures in every treatment show a consequent continuous increase of their plant densities by growth for all NH_4^+/NO_3^- ratios. From measuring point 3 (6 days) until the end of the test time after 18 days, the respective increases significantly differ from each other. All treatments show a continuous common trend up to 15 days of culture period. Thereafter a decrease of frond densities was observed for all treatments, except for the NH_4^+/NO_3^- ratio of 25/75, which extends to a coverage density that is significantly higher by +20.2%, than the next lower NH_4^+/NO_3^- ratio of 0/100. In this set-up, the NH_4^+/NO_3^- ratio 25/75 shows the highest and most sustainable growth in that experimental run (see Fig.28).

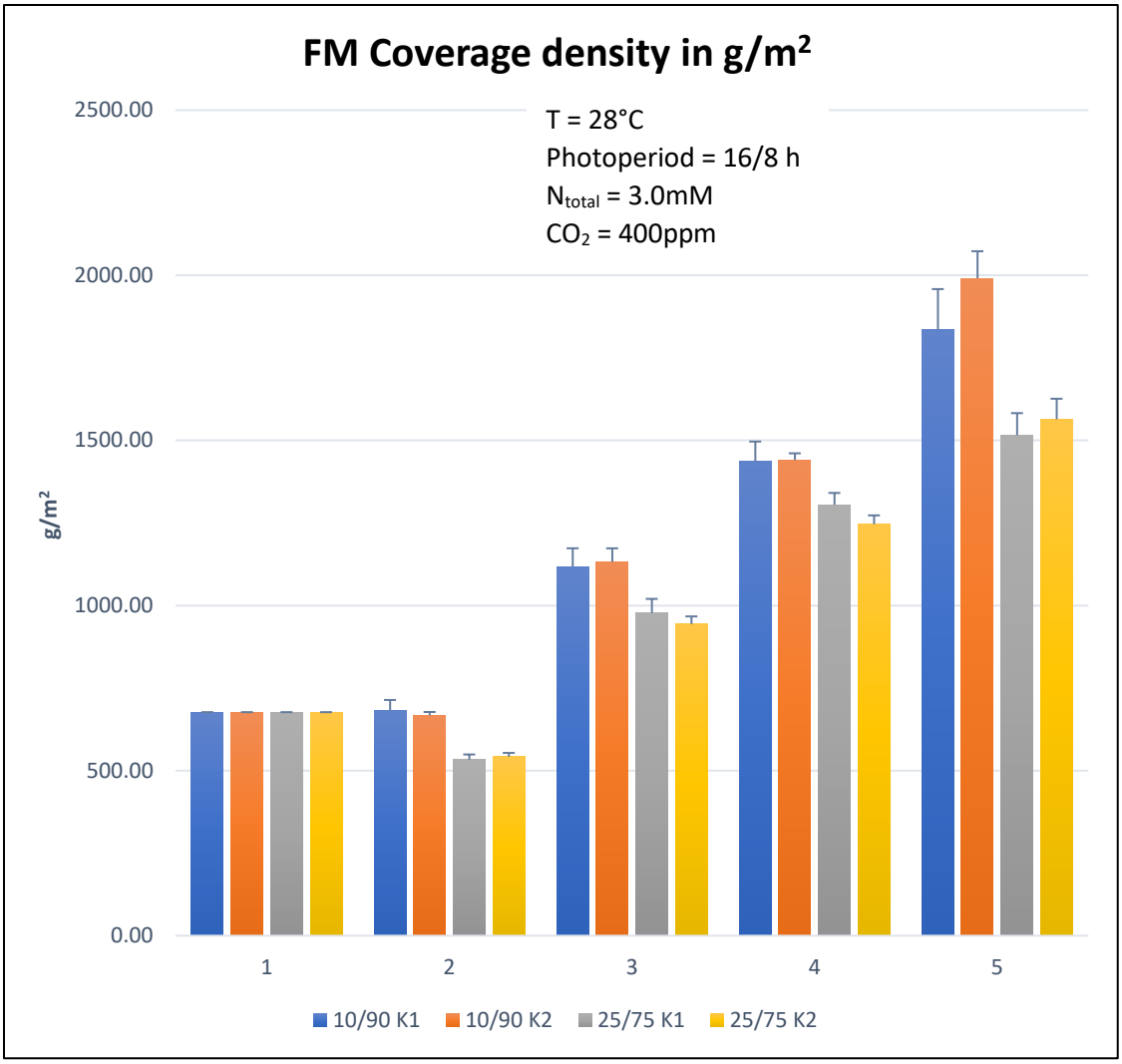

Fig.29: Refinement of the optimal NH_4^+/NO_3^- ratio of 25/75 and 10/90 at different N/K ratios. N_{total}/K ratio of N/K1 =1.85 and N/K2 =1.45 in the same run.

A further refinement of the NH_4^+/NO_3^- ratios between 25/75 and 10/90, as shown in fig.29, resulted in the highest growth rate at a NH_4^+/NO_3^- ratio of 10/90. Along this experimental run, two different N/K ratios (N/K1=1.85 and N/K2=1.45) were compared simultaneously for both NH_4^+/NO_3^- ratios, 25/75 and 10/90, and resulted in a higher growth rate for N/K2. All other nutrients were supplied at concentrations that were high enough to avoid any undersupply. Seeding density was started for that experimental run at 677g/m^2 in order to verify the trends also at a higher end coverage density at +40%, compared to the experimental run, shown in fig.28. The NH_4^+/NO_3^- ratio of 10/90 resulted in a significantly higher coverage already after 15 days of growth. This applies to both N/K1 and N/K2 ratios, compared with the NH_4^+/NO_3^- ratio of 25/75. As a further result, N/K2, as such, reached the highest coverage density at the end

of the measurement. The NH_4^+/NO_3^- ratio of 10/90 maintained pH of the nutrient solution constant over a long time.

To optimise the N/P ratio, elements at N_{total}/P ratios of 5/1, 10/1, and 20/1 were tested with 4 replicates each. The effect of an additional CO_2 supply was tested in two identical runs at concentrations of 400ppm and 3,500ppm CO_2.

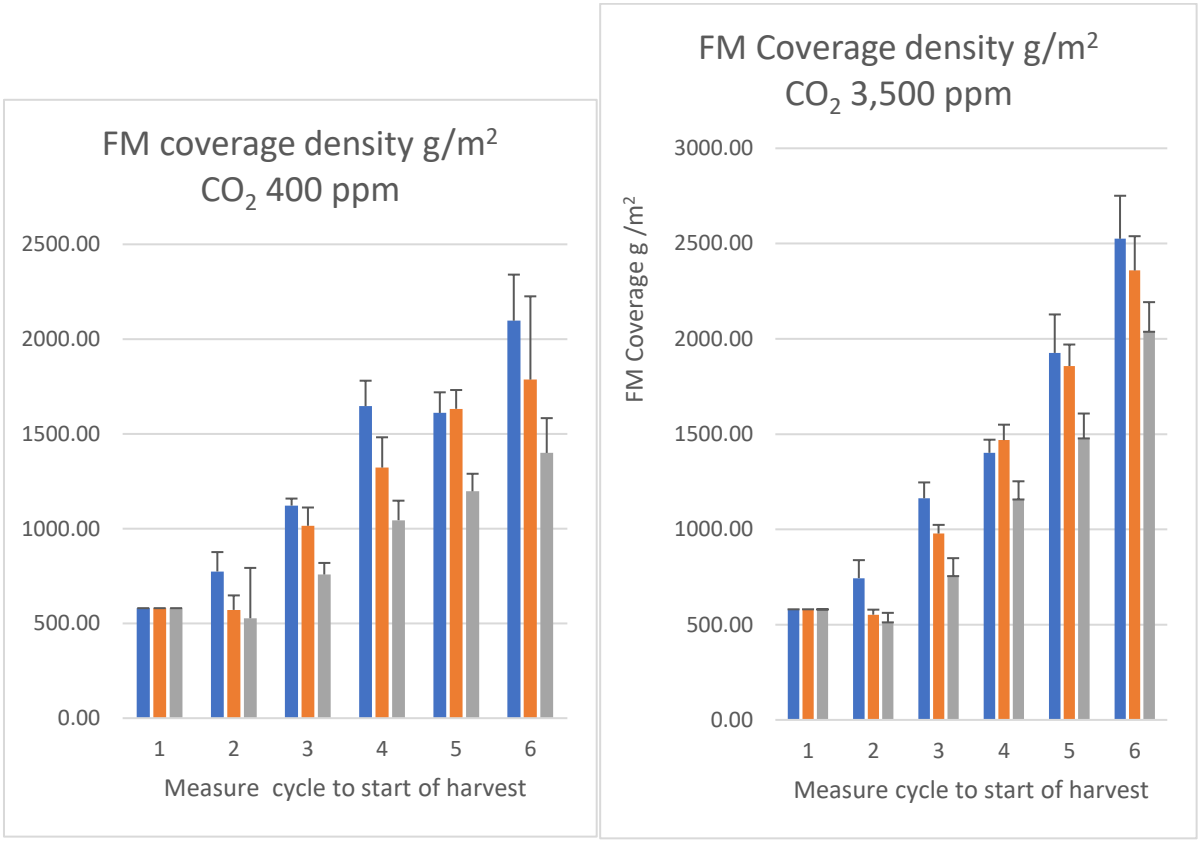

Fig.30: Optimising the N/P ratio by maximum growth to harvest starting point at 400 and 3,500ppm CO_2 and a N/P ratio of 5/1. N/P=5/1 N/P=10/1 N/P=20/1

Fig.30 shows the growth development at different N/P ratios. By testing ratios of 5/1, 10/1, and 20/1, the ratio of N/P=5/1 obtained the significantly highest growth for both CO_2 concentrations at 400ppm and 3,500ppm.

For this run, as shown in fig. 30, light intensity (spectral photon flux rate) was adjusted at 80 $\mu mol \cdot m^{-2} \cdot s^{-1}$ only. At 3,500ppm CO_2 a maximum of FM coverage of about 2,550 $g \cdot m^{-2}$ was obtained. Because C-fixation and light intensity are directly correlated, a total increase of growth over time at higher light intensities resulted at 129 $\mu mol \cdot m^{-2} \cdot s^{-1}$ as shown in fig. 59A

(further below), where a maximum FM coverage of about 4,200 $g \cdot m^{-2}$ was obtained before start of harvest.

At 129 $\mu mol \cdot m^{-2} \cdot s^{-1}$ the optimal N_{total} concentration is 1.14 mM additionally when refeeding nutrient stocks two to three times per day based on the expected nutrient uptake.

An experiment to optimize Mg supply resulted in an optimum yield at 0.288mM, as shown in fig.31.

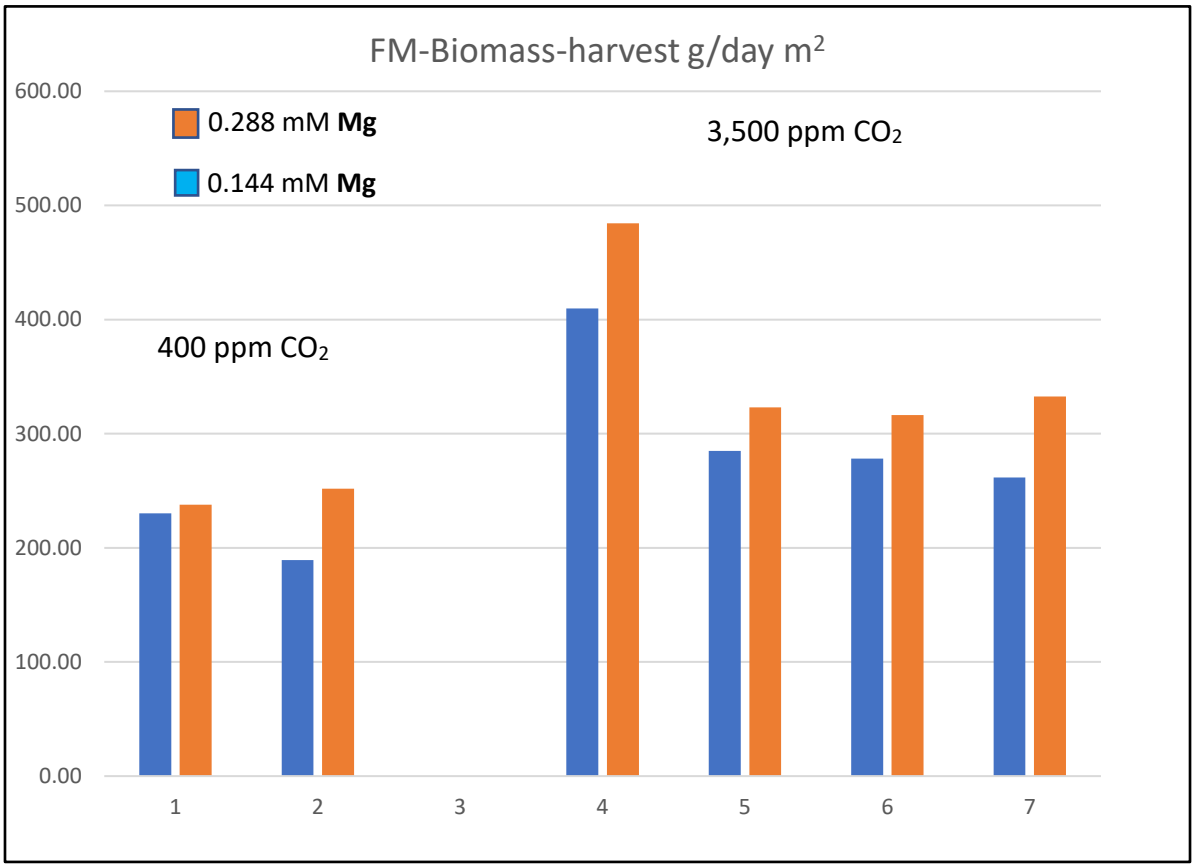

Fig.31: Comparison of two Mg concentrations at 0.144mM and 0.288mM at 400ppm and 3,500ppm CO_2; measured without statistic.

After increasing the CO_2 concentration from 400ppm to 3,500ppm and a waiting time of six days until the next harvest, the partial harvest yielded a significantly higher FM formation of 324 +/- $8 g \cdot d^{-1} \cdot m^{-2}$ from the fifth to sixth partial harvests onwards.

At that high level of regrowth and a higher Mg concentration of 0.288mM, both nutrient consumption and evapotranspiration increased. At a N_{total} of 2.5mM, the culture tended to increase its pH level on the long term.

The further refinement, as already indicated above, adapted as well to the lowered N_{total} = 1.14 mM concentration with a continuous supply of CO_2 at 3,500ppm and a NH_4^+/NO_3^- ratio of 10/90 is shown in fig.32 below.

With regard to the aforesaid N_{total} concentration, the best long-term stability of consolidated harvest was reached at 0.4mM Mg, as shown in fig.32. Long-term stability of the pH level at 6.5-6.8 was obtained at that condition. As a consequence, algae population was visibly reduced. Thus, 0.4mM Mg at N_{total} concentration of 1.14mM.

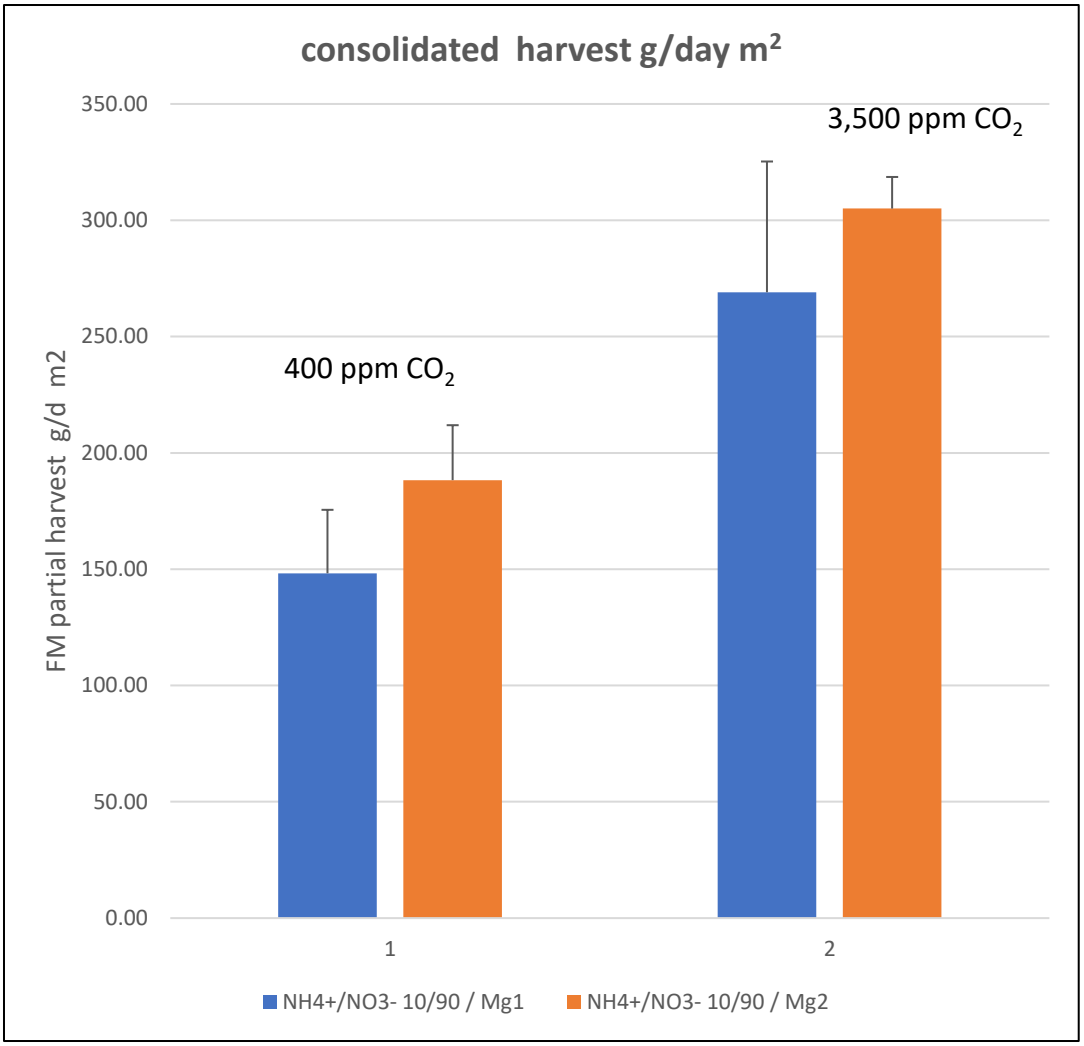

Fig.32: Final consolidated harvest amount after cultivation up to a harvest point of 30% over the tp point using an optimised NH_4^+/NO_3^- ratio of 10/90 at two further N/Mg-ratios of 1.14/0.2 and 1.14/0.4 and a further refinement of the Mg concentration.

Optimum consolidated harvest was reached with 0.4 mM Mg in both CO_2 fractions, wherein, at 3,500ppm CO_2, the increase of FM biomass yield is most significant. At 3,500ppm CO_2, a

stable consolidated long-term harvest amount of 305.02 +/- 20g·d^{-1} ·m^{-2} was obtained at N_{total} of 1.14mM. For all subsequent experiments, N_{total} concentrations of 1.14 mM, with P at 0.23 mM, and with a N/P ratio of 5/1, were used. These values were introduced into eq. 10 later for further experiments as well as into the modelling parameter set. The optimal temperature was 29°C, confirmed, as already shown, by *Landolt, Kandeler (1987)* and *Lasfar et al. (2007)*, and at an illumination of 129 µmol•m^{-2}•s^{-1} PAR.

5.1.2 Deficiencies of Fe and B

Three Fe concentrations: 40µM (NL1),20µM (NL2), and 4µM (NL3) showed no significant differences between both, low-blue (lb) and high-blue (hb) light regimes. All other nutrient concentrations were kept at the optimum in all treatments. Growth was enhanced by 3,500ppm CO_2 to test the nutrient effects at the highest possible demand. Fig.33 shows, in comparison to all cultures, an increase of coverage density for 40µM and 20µM from seeding density at measuring point 1 to start of harvest at point 2. At 4µM Fe deficiency, the coverage density until point 2 becomes a significantly lower by -24% than for 40µM and 20µM. From the first partial harvest at point 2 and any of the following, the regrowth to further harvest cycles remained significantly lower for 4µM (green and blue bars, Fig.33). By that, also the growth and regrowth rates remain constantly by -24% lower, indicating transition to deficiency.

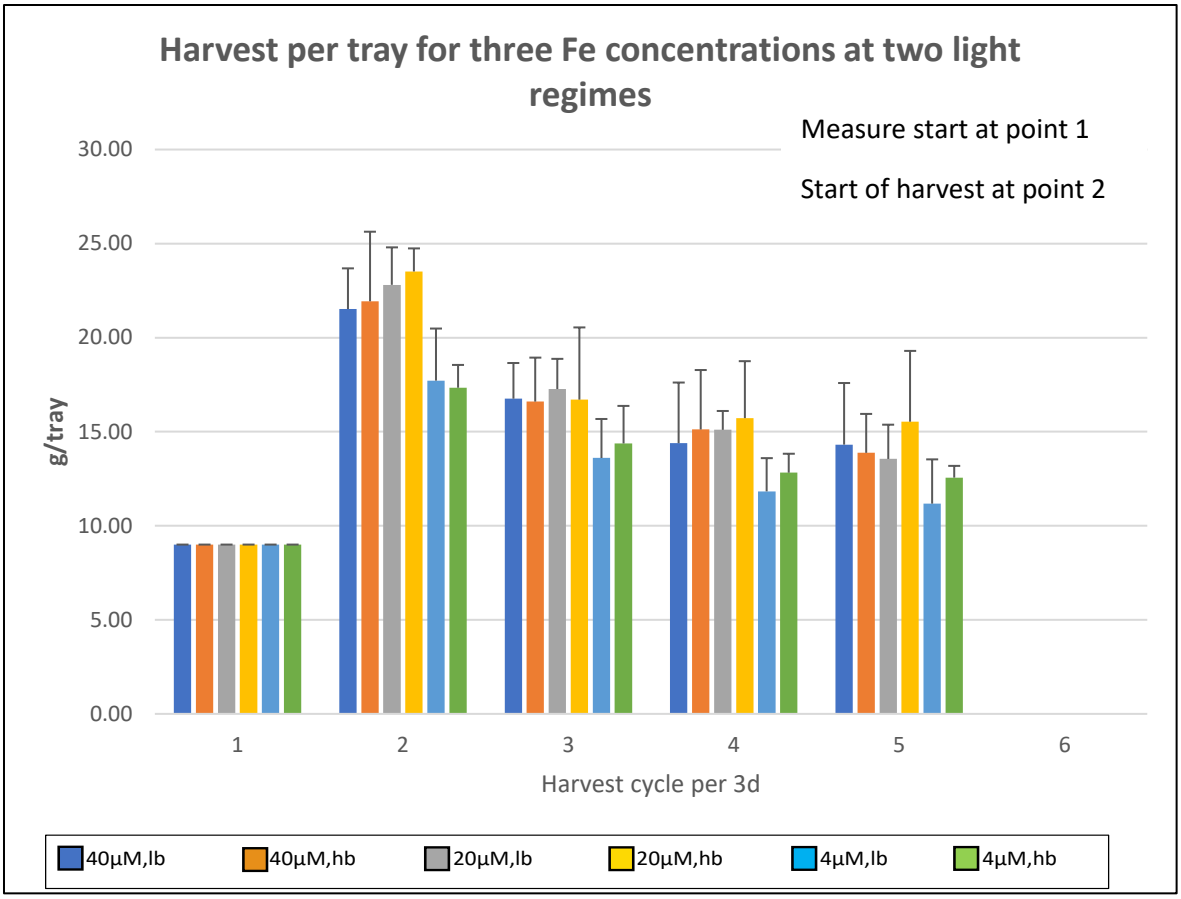

Fig. 33: Overview of the trend in all Fe- treatments. Partial repeated (cyclic) harvest amount (g FM per tray) each 3d over time, started after reaching harvest coverage at point 2, for three (40, 20, 4µM) Fe concentrations, each with a different light regime (high-blue(hb) and low-blue(lb)).

Fig.34a, -b, -c there is no significant difference between low-blue and high-blue light supply in all concentrations, not even in case of deficiency.

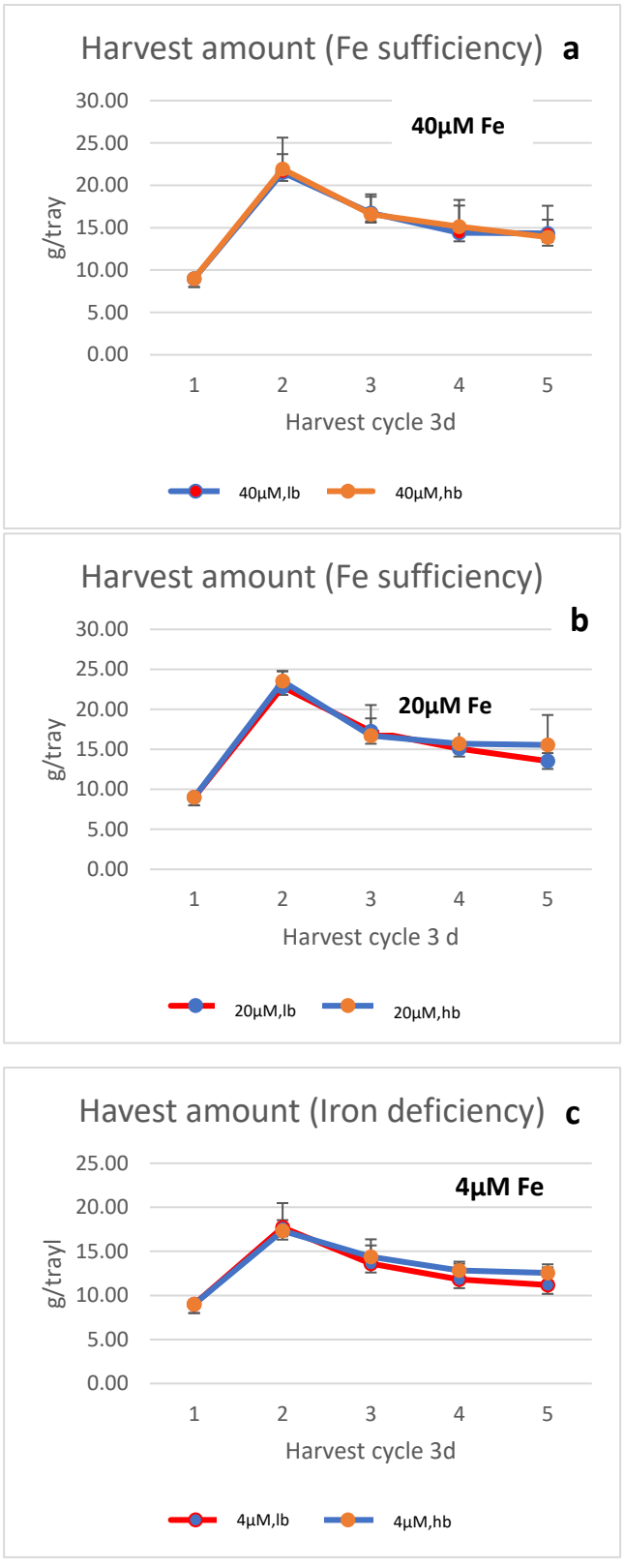

Fig.34 a, b, c.: Detailed view to the three trials at different Fe concentrations 40µM, 20µM and 4µM along a logarithmic concentration scale (40-20-04). each with a different light regime (low blue (lb) and high blue (hb).

While there was no significant difference in growth between 40 µM and 20µM, 4 µM showed a 22% total lower biomass growth (Fig.34a, b). This indicates a deficiency at 4µMol Fe.

Three treatments of B concentrations from 46µM down to 23µM and 4.6µM in a logarithmic scaling with 4 replicates each were used in this experimental run.

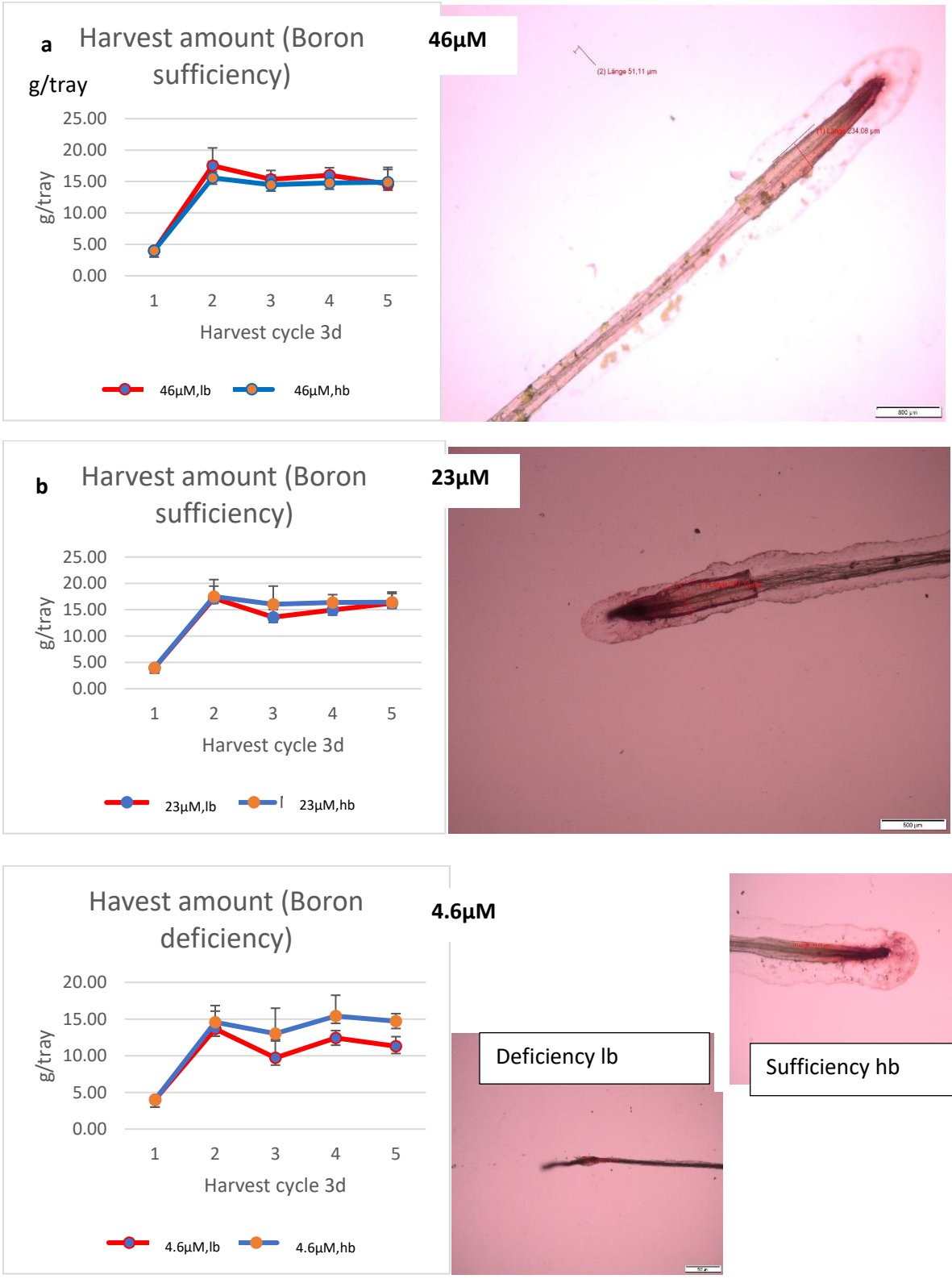

Fig.35 a, b, c.: Different B concentr. 46 µM, 23µM, 4.6 µM, each at low-blue (lb) and high blue(hb) light

White bar in Fig.35 a, b, c indicates 46µM, 23 µM and 4,6 µM.

At 46 and 23µM B, the cultures reached culture density at 1st harvest of about 17.51g FM per tray (963.05 $g \cdot m^{-2}$ FM) on average. At 4.6µM B, the culture density, after the same culture time, only reached 14,56g FM per tray (800.8 $g \cdot m^{-2}$ FM). Consolidated harvest was obtained with 46 and 23µM B at 14.89g FM per tray (818.95 $g \cdot m^{-2}$ FM) every 3 days harvest, which resulted in 272.98$g \cdot m^{-2} \cdot d^{-1}$. In contrast to Fe deficiency, B deficiency only occurred under the low-blue light regime. So, for low-blue, the consolidated harvest reached 11.30g FM per tray (621$g \cdot m^{-2}$ FM), but for high-blue it reached 14.7g per tray (808.5$g \cdot m^{-2}$ FM) every 3 days harvest, which resulted in 269.5$g \cdot m^{-2} \cdot d^{-1}$.

This result was further supported by tracking the measures of the root calyptra, since boron deficiency is significantly visible by stunted roots. Root measures were 234µm and 257µm for 46µM and 23µM of B, the same applies both for the high-blue and the low-blue regime.

At 4.6µM of B root measures were 244µm for high blue and 118µm for low blue.

This result further shows the reduction of biomass at 4.6 µM B, which is more pronounced at the low blue light regime. Thus, the B demand seems to be much lower at higher proportions of blue light.

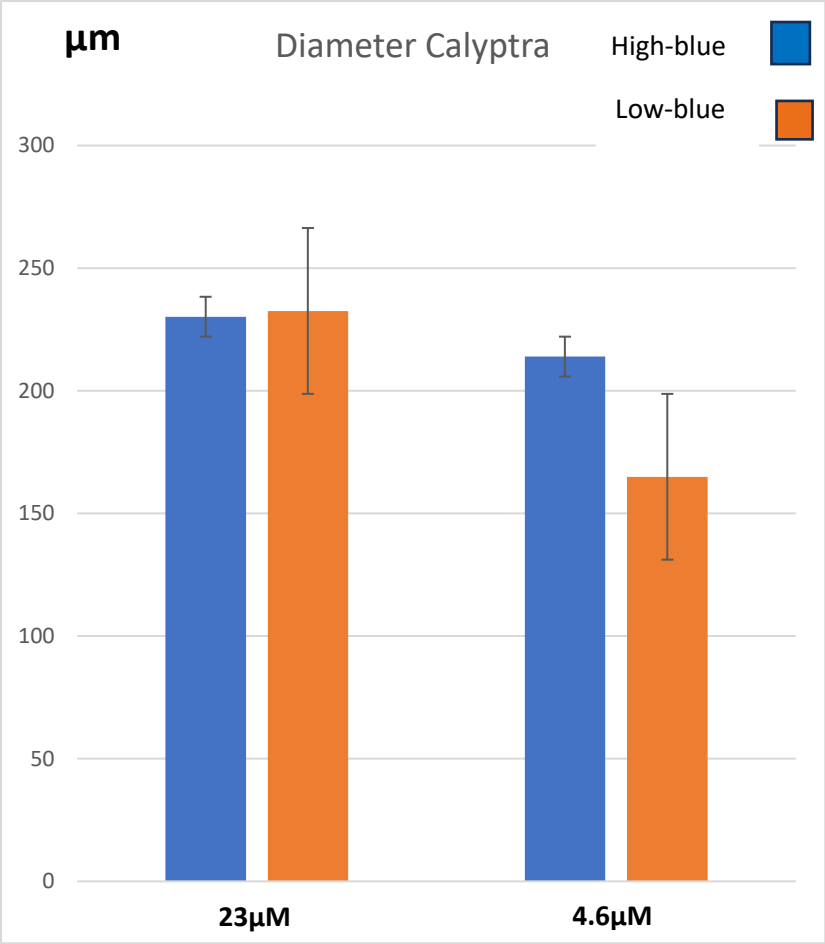

Fig.36: Diameter of calyptra and point of sufficiency at 23µM and 4.6 µM of deficiency.

Fig.36: shows that a reduction to 10%, i.e., from 46µM to 4.6µM, resulted in significant changes in both the harvest quantity (or growth rate) and the diameter of the calyptra (root tips). The calyptra was reduced to only half its usual diameter under the low B concentration.

5.1.3 Nutrient supply, algal growth and pH of the culture media

Under non-axenic culture conditions, an algae co-population, identified as *Chlorella vulgaris* (see fig.37), grew fast at N_{total} concentrations of 2.5mM, 5mM, 10mM, and 15 mM and a NH_4^+/NO_3^- ratio of 25/75, as shown in fig.38 Light condition was about 80 $\mu mol \cdot m^{-2} \cdot s^{-1}$ and temperature about 25°C.

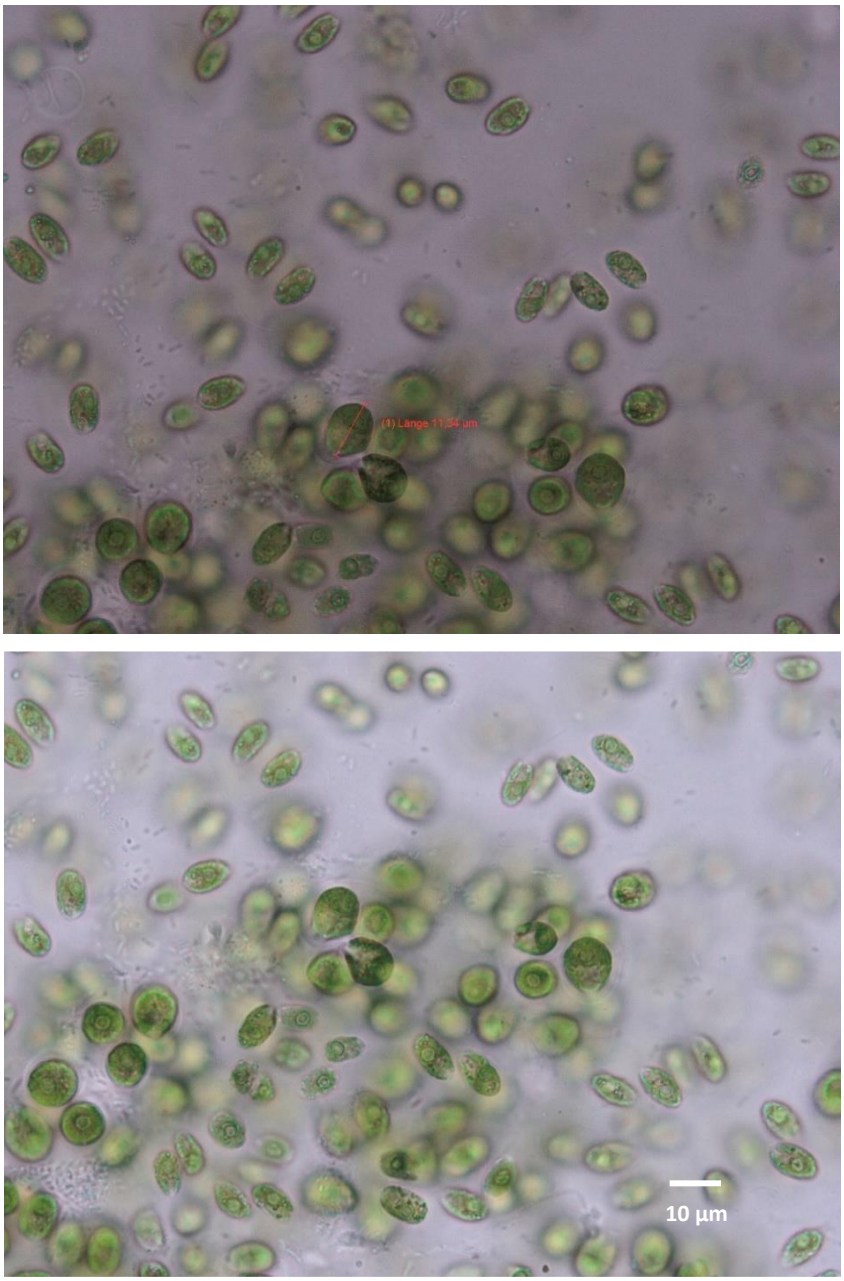

Fig.37: *Chlorella vulgaris* at 1200x magnification which measures about 11.34 µm

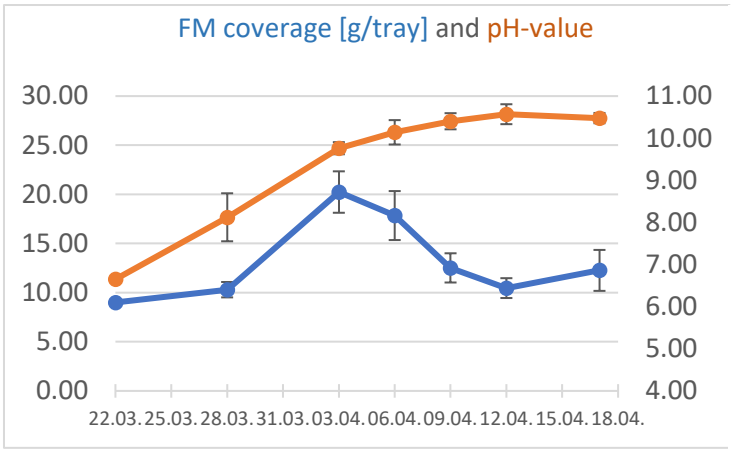

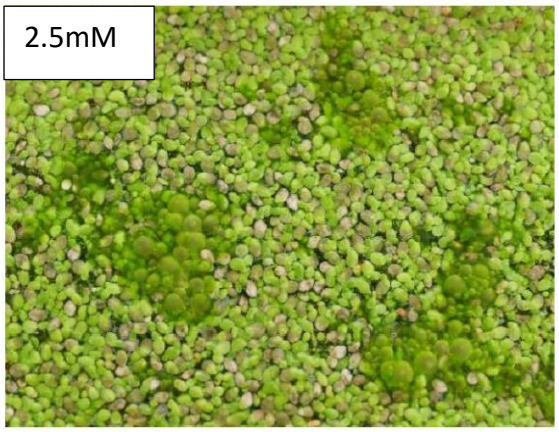

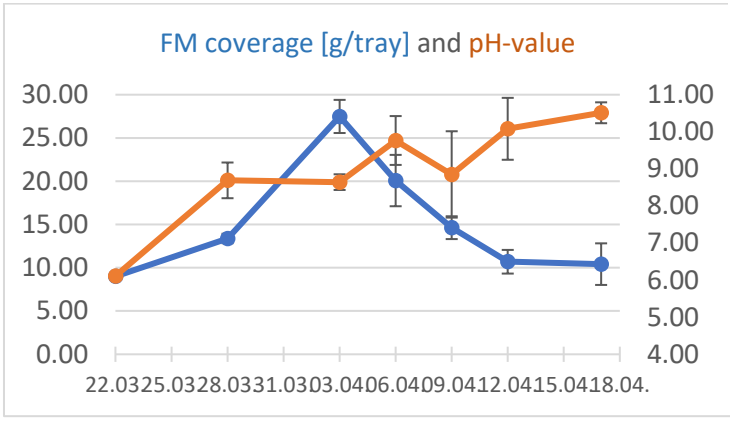

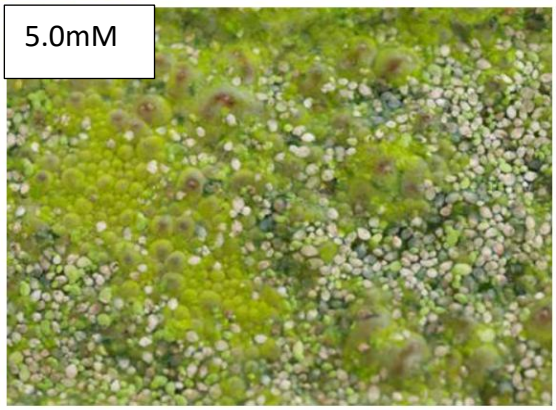

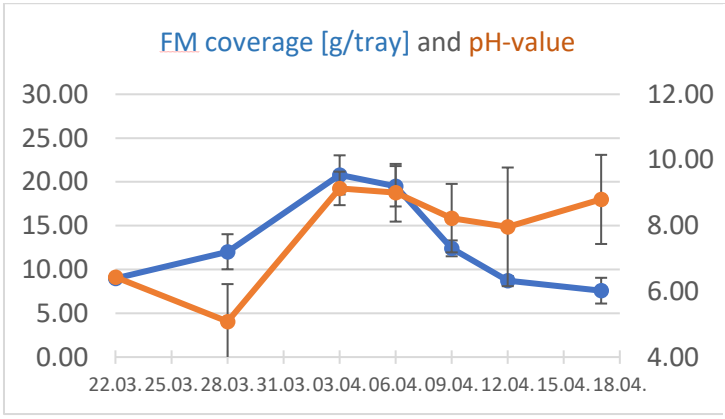

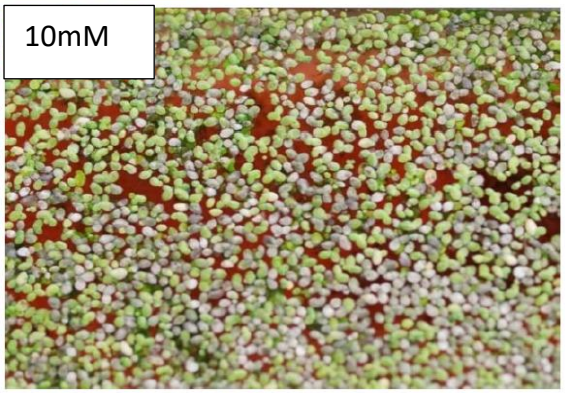

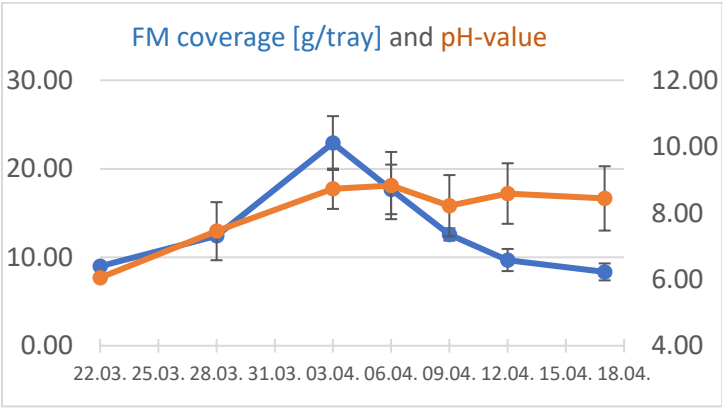

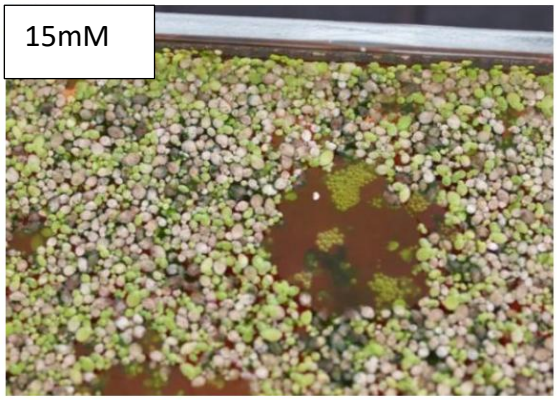

Fig.38: Development of FM and pH value for 2.5, 5.0, 10, and 15 mM of N_{total} during a 4 week culture time.

Chlorella vulgaris, a single-celled alga, grew fast under these conditions and became strongly competitive with *Lemnoideae*. As shown in Fig.38, all treatments were started at 10g FM/Tray (= 650gm^{-2}). As algae and *Lemna* spp. could not be separated, the total FM production was considered. After reaching their maximum at 12 d, *Lemna* spp. quickly degraded and died off.

The increase of the pH-level went parallel in time with a strong growth to reach maximum biomass coverage in all treatments. After reaching values above pH >9, the algal population increased and the *Lemna* population decreased and finally died off, even at a total N concentration of 2.5mM. Although this concentration is often used, the optimum of N_{total} is lower. It was found that a strong increase of pH value started before the algal bloom. At a N concentration of 1.25mM N_{total} pH remained stabile over a long period if the NH_4^+/NO_3^- ratio was kept at 10/90, but with a slight accumulation of N_{total}. So optimum was obtained at a daily consumption of 69 mmol·m^{-2}·d^{-1}.

All experiments for 20/80 and 30/70 NH_4^+/NO_3^- ratio showed high growth rates only under short-term cultivation but cultures died off after the first harvest.

A daily consumption of 69mmol·m^{-2}·d^{-1} N_{total} fits best to the maximum growth rate of 300g·d^{-1}·m^{-2}. For all subsequent experiments the nutrient solution used N_{total} concentrations resulted at 1.14mM, with P at 0.23mM, with the N/P ratio 5/1. These values are used in eq.10 (Chapter 4.1.4) and also for the final experiments and the comparison with the modelling results/estimations.

Tab.8: Resulted nutrients ratios at optimum

N_{total}/P	N_{total}/K	N_{total}/Mg	N_{total}/S	N_{total}/Ca
4.75	**1.43**	**2.85**	**4.07**	**2.11**

The obtained optimum nutrient solution was applied in all further upscaled experiments at Kalkar and Berlin.

5.2 Optimization of culture parameters

5.2.1 Temperature

The influence of temperature on growth rate could be confirmed to be exactly as reported by Lasfar (2007) and by Landolta&Kandeler (1987) with an optimum at 29°C.

At the upscaled set-ups in Kalkar and Berlin, temperature fluctuations occurred, influenced by incoming global radiation during the day and by lowering the greenhouse heating at night. Thus, the average temperature during the day ranged around 25°C (Kalkar) and 22 °C (Berlin). From *Lasfar (2007)* temperature curve field the reduction of yield can be determined by -3% for each °Kelvin below 29°C (T_{opt}).

5.2.2 Light

Total exposure to light, measured in $\mu mol \cdot m^{-2} \cdot s^{-1}$, was adjusted at two total photon flux densities (light quantity) at 80 and at 129$\mu mol \cdot m^{-2} \cdot s^{-1}$. In the laboratory set-up, 129$\mu mol \cdot m^{-2} \cdot s^{-1}$ was resulted optimum. At 80$\mu mol \cdot m^{-2} \cdot s^{-1}$ photon flux density a culture capacity W_{max} of 2,225$g \cdot m^{-2}$ was obtained at a CO_2 concentration of 3,500ppm (Fig. 30). At 129$\mu mol \cdot m^{-2} \cdot s^{-1}$, (Fig.59A) a W_{max} of 4,300 $g \cdot m^{-2}$ was obtained at same CO_2 concentration. This was considered in the list of r_i in tab.15 for modeling further below. Further differences in accumulation and slight differences in protein content were observed at different light qualities. I(440nm)/I(660nm) ratio of ¼ for low-blue and I(440nm)/I(660nm) of ¾ for high-blue resulted in visible effects, as shown further below (Fig.41, 44, 49, 50-57).

5.2.3 CO_2

Experimental results for cultivation at different CO_2 exposures were obtained for 400ppm and 3,500ppm. The consolidated harvest amount increased by up to 62% when the CO_2 concentration was raised from 400ppm to 3,500ppm (see fig. 59A). Stronger growth and regrowth were observed in any experiment if the nutrient level was continuously stabilized by sufficient refeed of nutrients.

A further side effect could be observed in the Berlin set-up using purified and nitrified fish manure in cultures which were exposed to about 2,000ppm CO_2 when N_{total} was depleted. While the N level dropped to virtually zero, *Lemna minor* grew extremely long roots of up to 500mm while root length was only 10- 20mm at N-sufficiency (Fig.39).

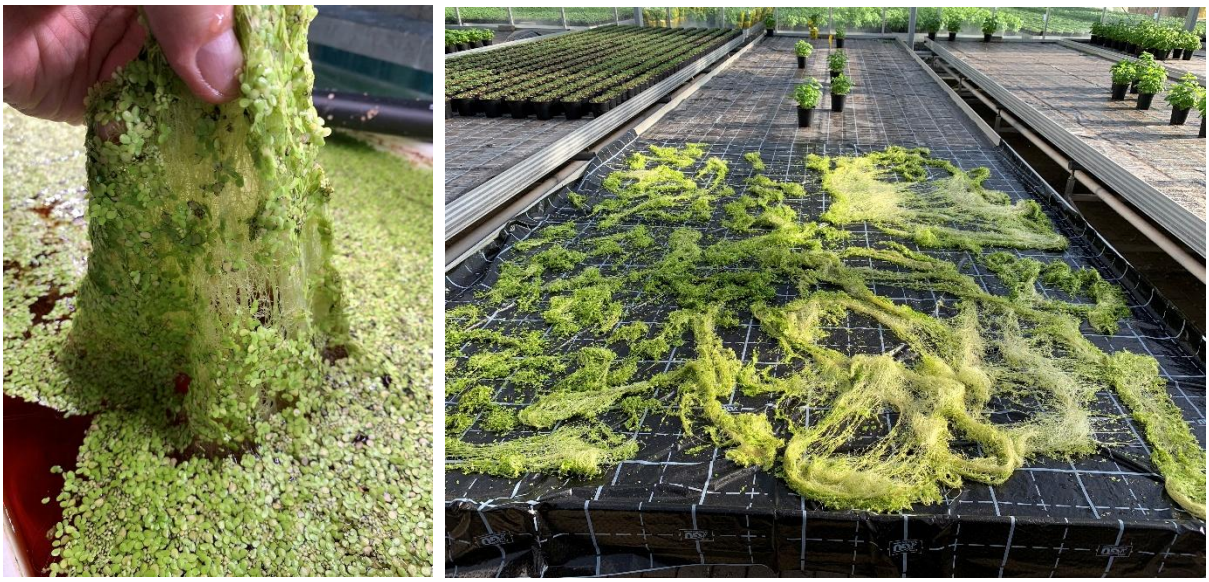

Fig. 39: Extraordinary root growth during CO_2 exposure of about 2,000 ppm when the N_{total} level ran empty.

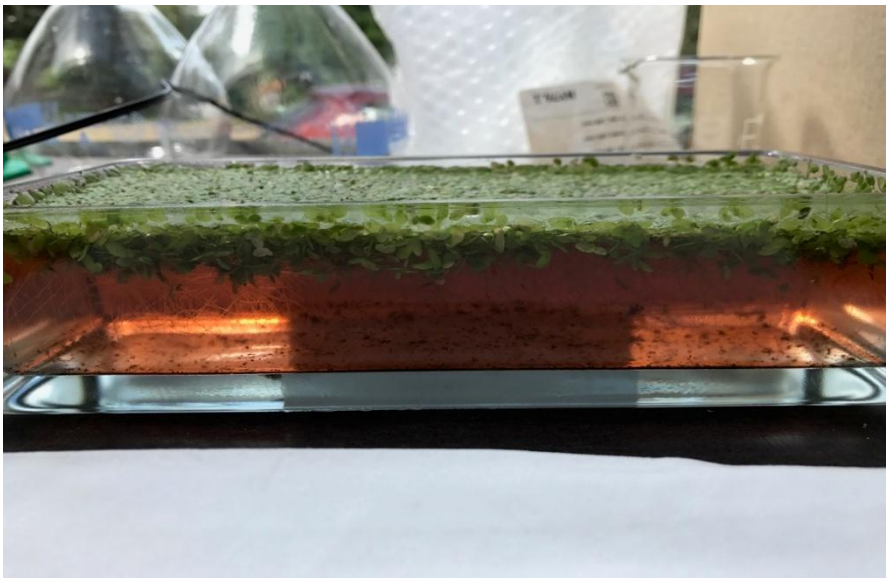

Fig.40: Side view on culture tray with maximum FM coverage density obtained at 3,500ppm CO_2 with optimum nutrient solution and 129µmol•m^{-2}•s^{-1} photon flux density.

Fig.40 shows a *Lemna* culture at maximum FM coverage (maximum capacity) of about 4,300g•m^{-2} before starting first harvest and correlates to the data shown in fig.59A further below.

As a further result, additionally supplemented CO_2 at 3,500ppm increased the dry matter content. With a NH_4^+/NO_3^- ratio of 20/80, the dry matter content was higher at 400ppm than with a 10/90 ratio. During CO_2 supplementation at 3,500ppm, a change was obtained towards

a higher dry matter content for 10/90. Fig.41 furthermore shows the highest dry matter content for 10/90 at high-blue exposure.

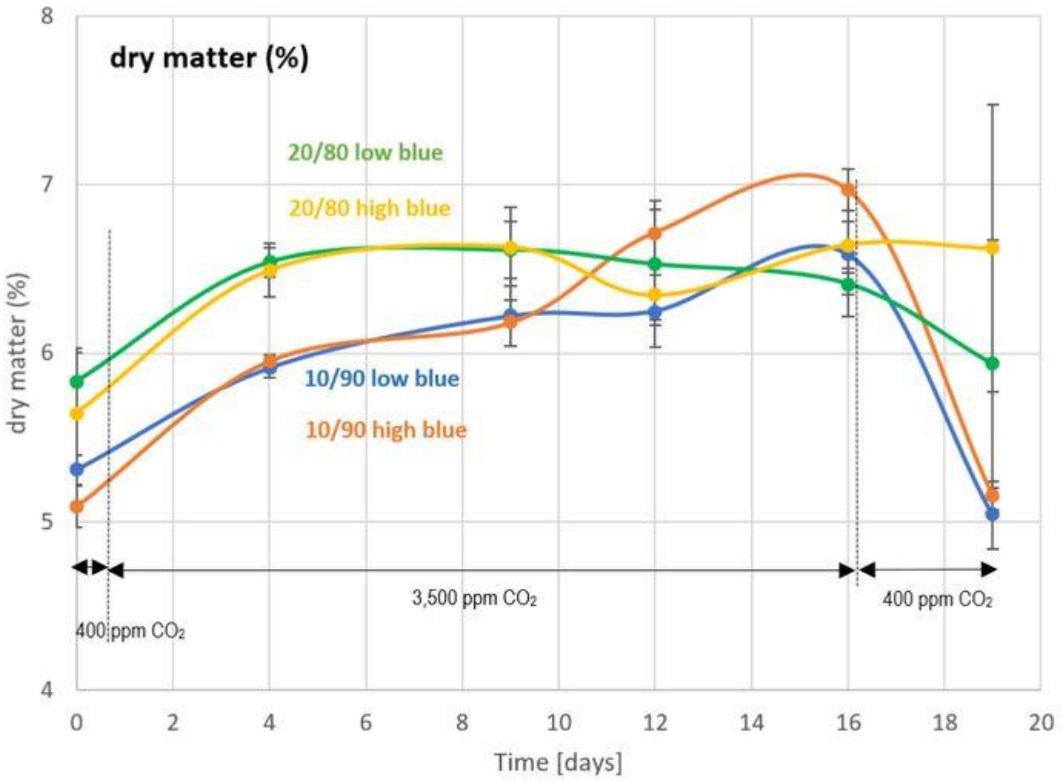

Fig.41: Development of dry matter at repeated (cyclic) harvesting, related to 3,500ppm CO_2 at two NH_4^+/NO_3^- ratios and two light regimes.

At 400ppm CO_2 exposure, the dry matter content with a NH_4^+/NO_3^- ratio of 20/80 with an average of 5.7% is approx. 8.7% relatively higher, compared to 10/90 with an average of 5.2%. After increasing the CO_2 exposure to 3,500ppm, dry matter content for both NH_4^+/NO_3^- ratios increased statistically significant to 6.4 and to 6.9%.

As also displayed in fig.41, when lowering CO_2 level from 3,500 ppm again to 400 ppm, the promoting effect was reversed.

A further result is that, for the maximum growth rate achieved at 3,500 ppm CO_2 and the effect of a more constant long-term stable pH value, the NH_4^+/NO_3^- 10/90 nutrient solution was again confirmed to be the optimal one under the other culture conditions.

5.3 Nutritive Factors

5.3.1 Amino acids and pure protein content

The results of the amino acid spectrum reflect the situation of a *Lemna minor* culture that had already been operated under optimal conditions at the starting point of the experiment. The average frond age in the population at this point was 28 days.

Tab.9: Amino acid spectrum in a dried sample (moisture content 8.5%) of *Lemna minor* H_2O at the starting point of the experiment. Highlighted are amino acids essential in human nutrition.

Amino acids	Content (g/100g DM)
Methionine	0.38
Cysteine	0.34
Aspartic acid	3.4
Threonine	1.2
Serine	1.2
Glutamic acid	2.6
Glycine	1.5
Alanine	1.5
Valine	1.3
Isoleucine	1.1
Leucine	2.0
Tyrosine	0.81
Phenylalanine	1.3
Lysine	1.4
Histidine	0.53
Arginine	1.8
Proline	1.1
Ornithine	<0.02
γ Amiobutyric acid	0.34
Taurine	0.12
Total sum of amino acids	***23.92***

The sum of 23.92 g/100g pure protein at 8.5% humidity of the sample results in 26.14% for total DM. The most prominent amino acids in *Lemna minor* are highlighted.

In order to determine the relative trends as well as the absolute values of pure protein contents, the calibration of the Bradford analysis by using bovine albumin, resulted in an $R^2 = 0.9927$ (see Fig. 42).

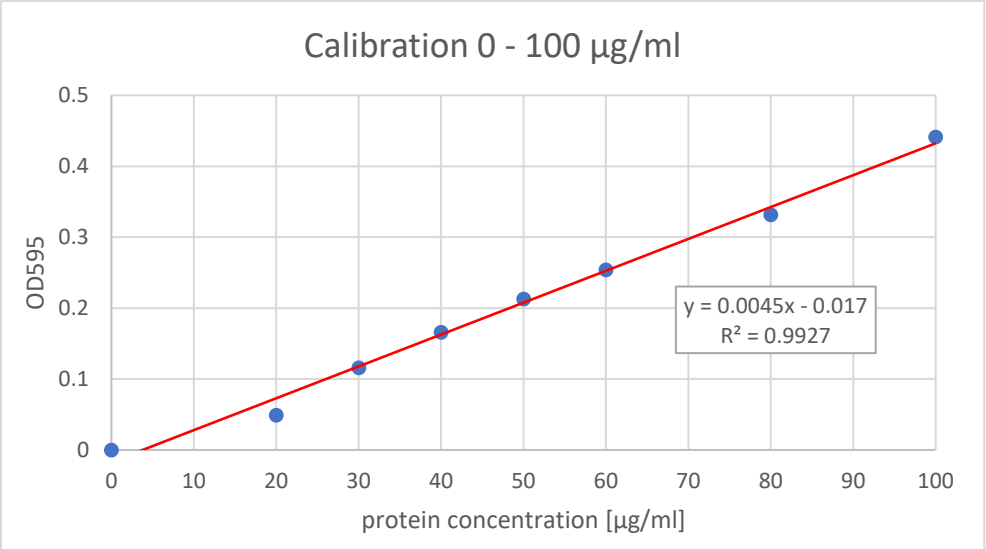

Fig.42: Calibration curve for Bradford analysis with use of bovine albumin

To adjust protein analysis onto the *Lemna* matrix, BSA – spiked samples were used and compared to pure *Lemna* material. As shown in Fig.43 below, the underestimation by *Lemna* pure needs to be compensated by a linear correction factor of +9.4%.

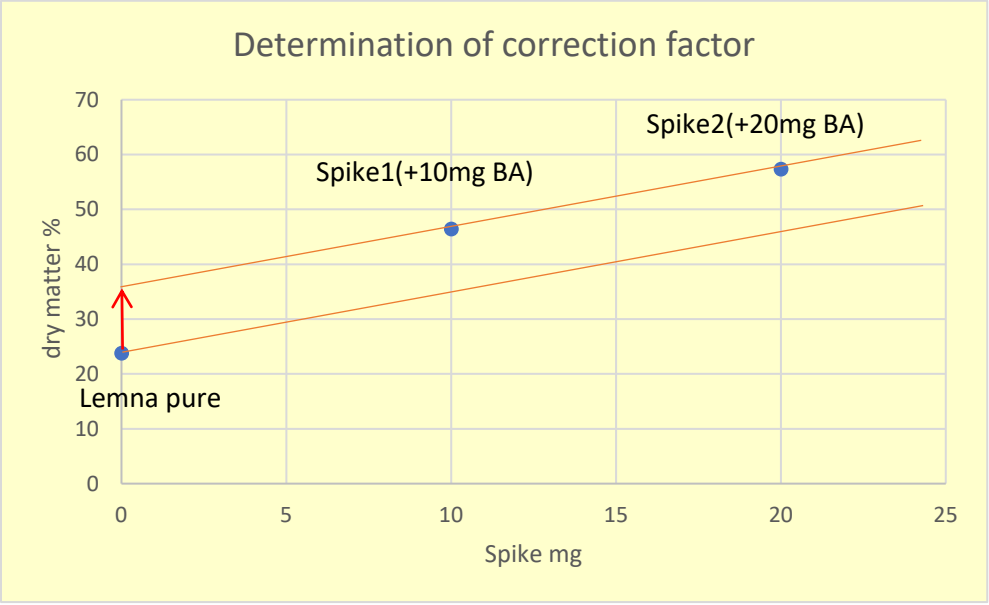

Fig.43: Determination of correction factor of the calibration between bovine serum albumin and plant biomass *Lemna minor.*

In all treatments the protein content of harvested *Lemna minor* biomass (Bradford analysis) tended to increase from harvest to harvest of a continuously repeated (cyclic) partial harvest. (Fig.44)

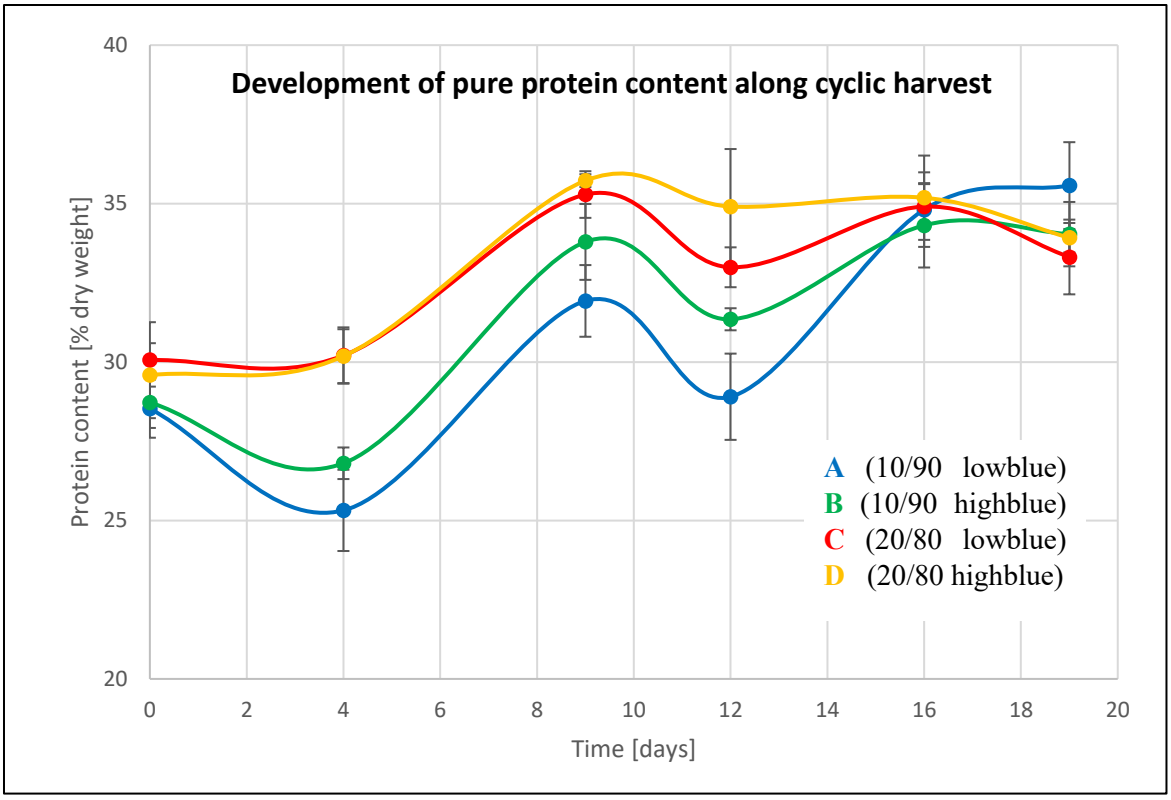

Fig.44: Development of the pure protein content in harvested biomass along continuous repeated (cyclic) harvesting in laboratory set-up (Bonn).

"The pure protein content increased with repeated 3 to 5 d harvest intervals while the average frond age decreased, like shown further below. This effect was observed irrespective of the further treatments under investigation (Fig.44).

Tab.10: Influence of NH_4^+/NO_3^- ratios on relative protein contents at high blue (hb) and low blue (lb) conditions

Treatment	NH_4^+/NO_3^- -ratio	Light regime	Rel. increase of protein content in %
A	10/90	Low-blue	+ 24.7
B	10/90	High-blue	+ 18.1
C	20/80	Low-blue	+ 10.8
D	20/80	High-blue	+ 14.6

In the upscaled set- up (Kalkar), a similar trend was obtained with an increase of the pure protein content over a repeated harvesting sequence, the same at the Berlin site. The NH_4^+/NO_3^- ratio of 10/90 (A and B) proved to be the best one for a maximum effective increase

of pure protein in the more juvenile fronds.

A further detailed analysis of the second upscaling (Kalkar) confirms the results of the lab-scale. Particularly, an increase of nearly all amino acids related to younger fronds is obtained.

The blue bars display the amino acid composition at the starting point of the culture, the orange bars display the ones for the first harvest sequence from the 1st to 3rd, and the gray bars of the second sequence from the 4th to 6th harvests.

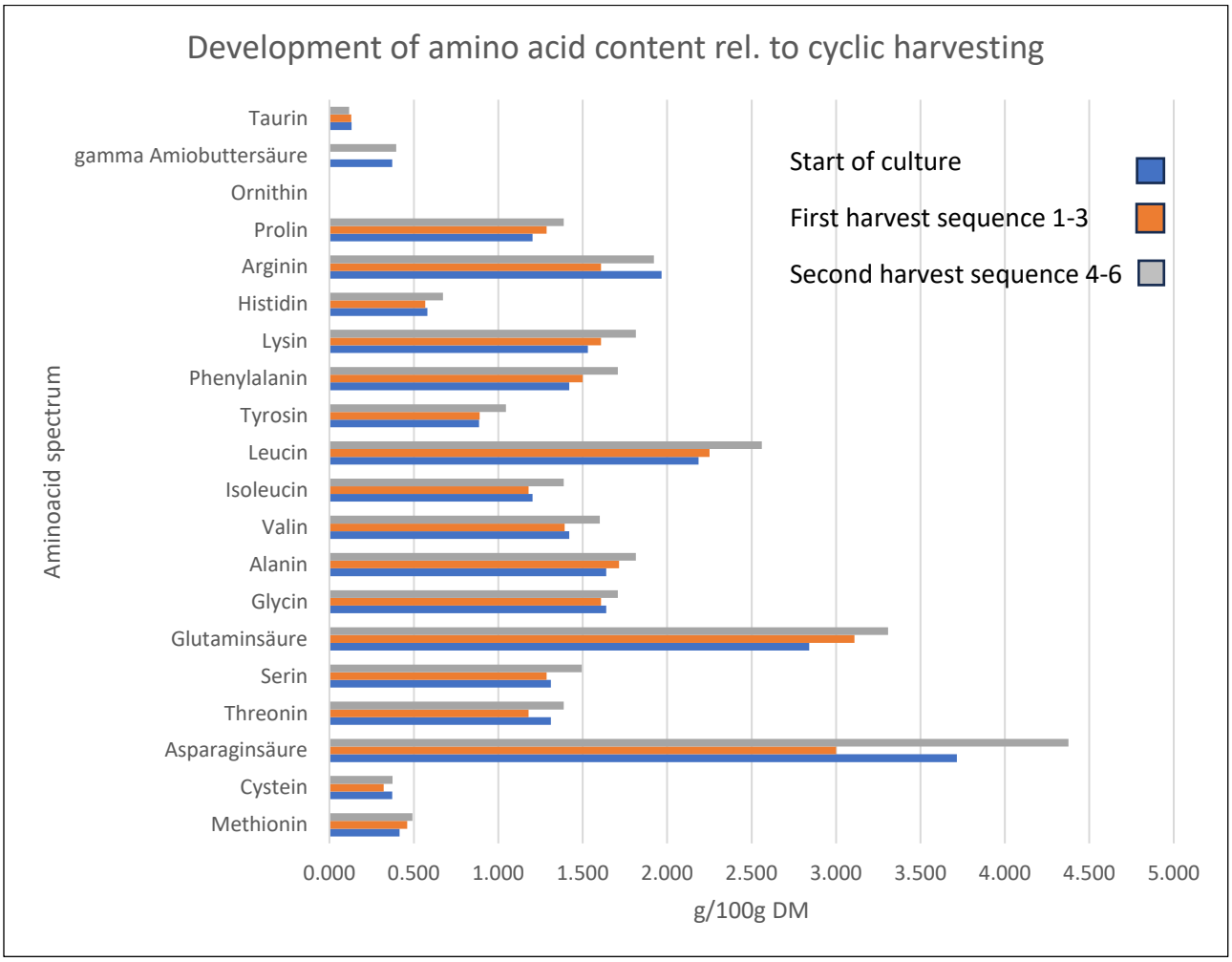

Fig.45: Amino acid distribution and development related to cyclic harvesting sequences of upscaled set-up at Kalkar. Origin data set from GBA in German, Gesellschaft für Bioanalytik mbH, Hamburg.

Most of the relevant amino acids are found in *Lemna minor* biomass (Fig.45). The most prominent ones are aspartic acid, glutamic acid, leucine, phenylalanine, lysine, and proline. Most of the amino acids increased significantly, on average, between the start of harvest up to the 4th - 6th harvests. A significant relative increase was obtained for glutamic acid with

+16%, lysine +19%, leucine +17%, and aspartic acid with +18% as a consequence of the lower average frond age by sequential partial harvesting.

5.3.2 Fatty acids

Tab.11 below shows the complete analysis of fatty acids from the same sample at starting point. Only 6 out of possible 51 fatty acids are prominently represented in *Lemna minor.* These are lauric acid, palmitic acid, stearic acid, oleic acid, linoleic acid, and alpha-linolenic acid. Most important is the O6/O3 ratio of 0.63, which is of particular importance for its use as feed and food. All others are tested but below the detection limit of 0.1g/ 100 g DM.

Tab.11: Fatty acid spectrum of *Lemna minor* from the same sample at **starting point**.

Fatty acid	Content [g/100 g DM]
C 4:0 Butyric acid	<0.1
C 6:0 Capronic acid	<0.1
C 8:0 Caprylic acid	<0.1
C10:0 Capric acid	<0.1
C 11:0 Undecanoic acid	<0.1
C 12:0 Lauric acid	0.219
C 13:0 Tridecanoic acid	<0.1
C 14:0 Myristic acid	<0.1
C 14:1 Myristoleic acid	<0.1
C 15:0 Pentadecanoic acid	<0.1
C 15:1 Cis 10-pentadecanoic acid	<0.1
C 16:0 Palmitic acid	0.656
C 16:1 Palmitoleic acid	<0.1
C 16:2 Hexadecadienoic acid	<0.1
C 16:3 Hexadecatrienoic acid	<0.1
C 16:4 Hexadecatetaenoic acid	<0.1
C 17:0 Heptadecanoic acid (Margaric acid)	<0.1
C 17:1 Heptadecenoic acid	<0.1
C 18:0 Stearic acid	0.109
C 18:1 Oleic acid	0.546
C 18:1 Petroselinic acid	<0.1
C 18:1 cis 11-Octadecenoic acid	<0.1
C 18:1 13 Octadecenoic acid	n.f.
C 18:1 (trans) Isomer	n.f.
C 18:2 Linoleic acid (O-6)	0.546
C 18:2 (trans/trans) isomer	n.f.
C 18:2 (cis/trans) isomer	n.f.
C 18:2 (trans/cis) isomer	n.f.
C 18:3 alpha-linoleneic acid (O-3)	0.874
C 18:3 Linolenic acid (O-4) = gamma Linolenic acid	<0.1
C 18:3 Linolenic acid (O-6) = (cis/cis/trans) isomer	<0.1

C 18:4 Stearic acid/Octadecatetraenoic acid	<0.1
C 20:0 Arachidic acid	<0.1
C 20:1 Eicosenoic acid	<0.1
C 20:2 Eicosadienoic acid (O-6)	<0.1
C 20:3 Eicosatrienoic acid	<0.1
C 20:3 Eicosatrienoic acid (O-3)	<0.1
C 20:4 Eicotetraenoic acid (O-3)	<0.1
C 20:4 Arachidonic acid (O-6)	<0.1
C 20:5 Eicosapentaenoic acid (O-3)	<0.1
C 21:0 Henicoic acid	<0.1
C 22:0 Behenic acid	<0.1
C 22:1 Docosanoic acid, incl. following isomer	<0.1
C 22:1 Erucic acid	<0.1
C 22:2 Docosadienic acid (O-6)	<0.1
C 22:4 Docosatetraenoic acid (O-6)	<0.1
C 22:5 Docosapentaenoic acid	n.f.
C 22:6 Docosahexaenoic acid (O-3)	<0.1
C 23:0 Tricosanoic acid	<0.1
C 24:0 Lignoceric acid	<0.1
C 24:1 Nerve acid	<0.1

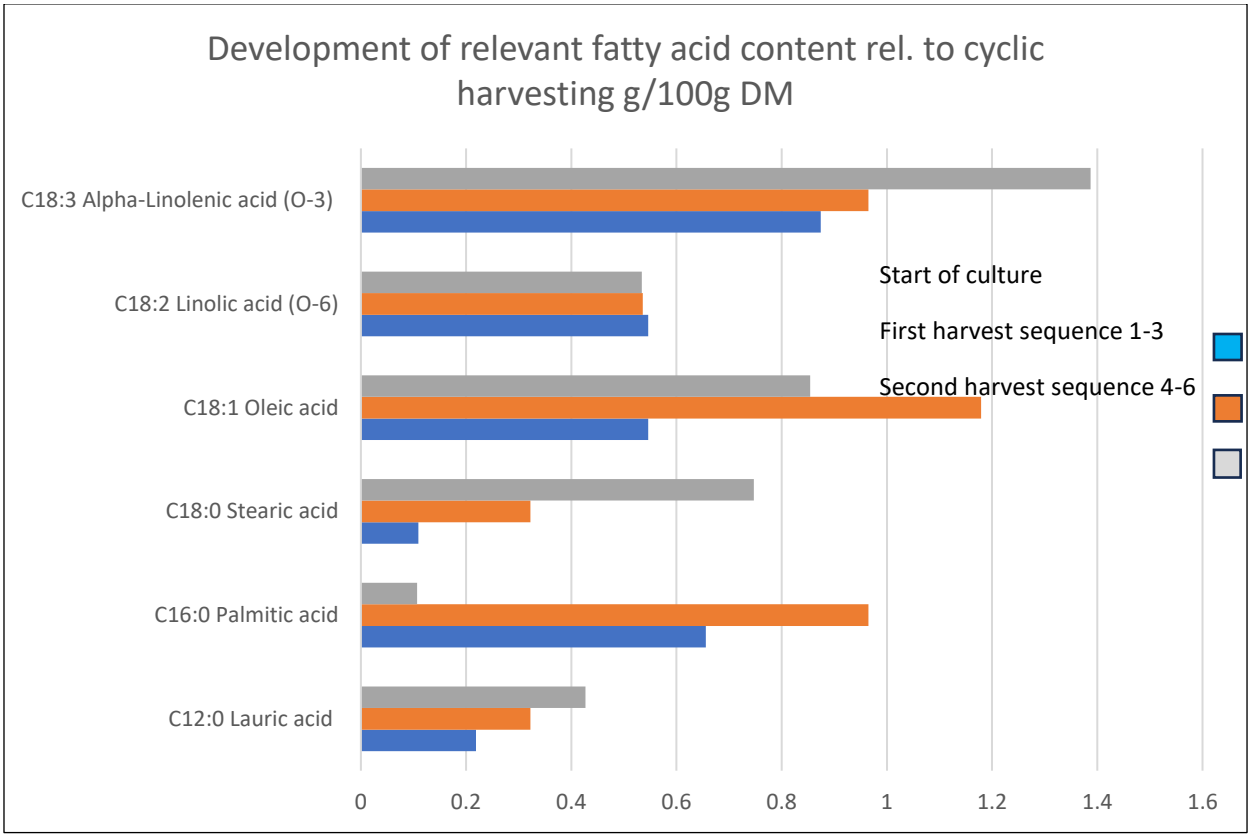

Fig.46: Development of fatty acid composition along repeated short harvest intervals.

A significant increase of about +59% was obtained for C18:3 alpha linolenic acid (Ω3) between start of the culture and the 4th – 6th harvest intervals. A strong increase of C18:0 stearic acid by 685% was obtained, but at a relatively low total concentration of 0.7g/100g DM. Along the same harvest sequence, palmitic acid decreased by about 613% in those younger fronds. C18:2 linoleic acid (Ω6) remained nearly at the same concentration in old and young fronds. As a consequence, the Ω3/Ω6 ratio which is relevant for food quality further increased from 1.6 to 2.6.

5.3.3 Vitamins

The most prominent/important vitamins are high-lighted.

Tab.12: Concentration of vitamins in DM

Vitamin E	mg/100 g	<5,0
Vitamin A	mg/100 g	<5,0
Vitamin B1 (thiamine)	mg/100 g	0,31
Vitamin B2 (riboflavin)	mg/100 g	0,89
Vitamin B6	mg/100 g	0,64
Vitamin D3	µg/100 g	<0,50
Vitamin B12 (enzymatically)	µg/100 g	38,5
Vitamin B12 (LC-MS)	µg/100 g	14,0
Vitamin K1	µg/100 g	1.590
Vitamin K3	mg/100 g	<0,01
Ascorbic acid	mg/100 g	<0,1
Pantothenic acid	mg/100 g	1,4
Niacin	mg/100 g	5,8
Biotin	µg/100 g	32
Ubiqinone, Coenzyme Q10	mg/100 g	1,2
Alpha-Carotin	mg/100 g	<0,01
Beta-Carotin	mg/100 g	7,8

Tab.13: Further nutritive factors in DM

Caloric value	kJ/100 g	966
Carbohydrates	g/100 g	6,1
Sugar, total	g/100 g	4,0
Fructose	g/100 g	1,7
Glucose	g/100 g	2,3
Saccarose	g/100 g	<0,2
Maltose	g/100 g	<0,5
Lactose	g/100 g	<0,5
Fiber	g/100 g	38,5
Crude Ash	g/100 g	17,6

As is further shown below, about 2/3 of the crude ash are made up by K, Ca, and Mg.

5.4 Antinutritive factors

5.4.1 Oxalic acid

The oxalic acid concentration in *Lemna minor* is relevant for the use as novel food. In addition, the correlation to calcium oxalate has been verified *(DeKock et al., 1973), (Francesci et al., 1987), Massey et al., 1993)*. Specific cells within the tissue for calcium oxalate deposit in *Lemna minor (Mazen et al., 2004)* have been verified as well, the so-called idioblasts. The idioblast cell measures 80µm in length having a width of 30µm, and calcium oxalate was present as a raphide crystal package inside with a length of 38µm and a width of 20µm.

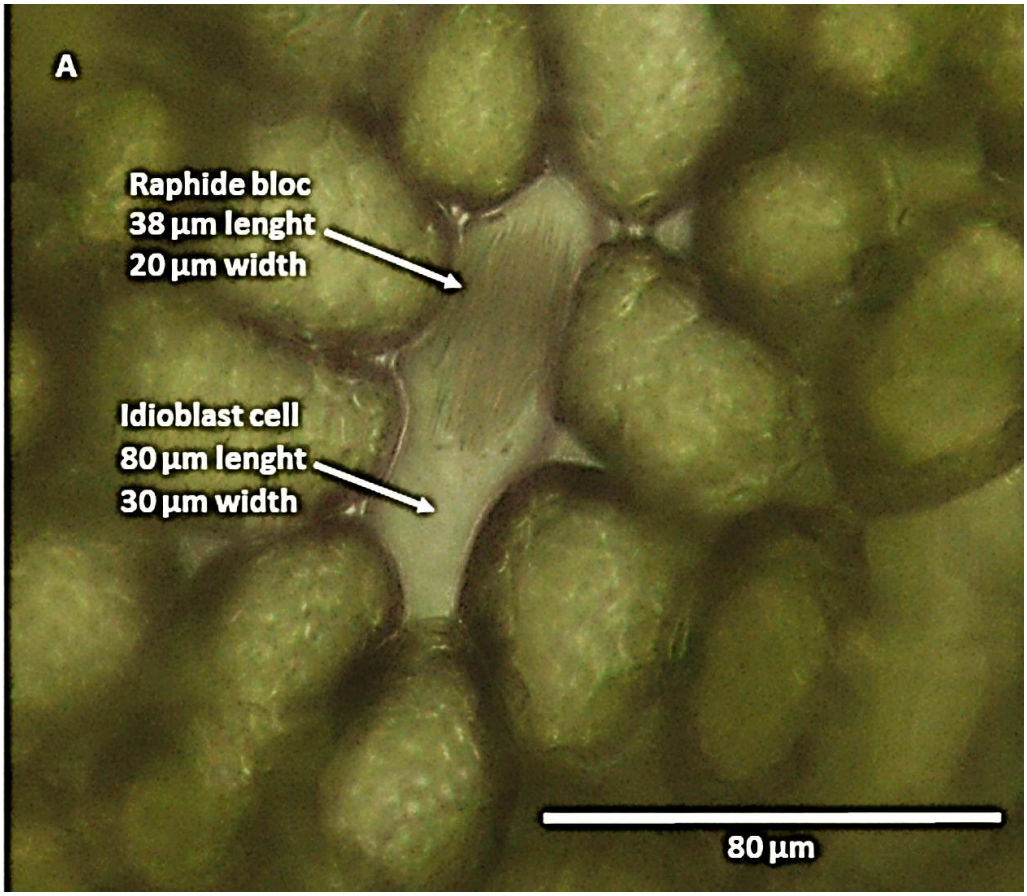

Fig.47: A microscopic image of the tissue structure of *Lemna minor* from the experimental set-up with a so-called idioblast cell in between, with a completely visible calcium oxalate-raphide structured crystal package deposited inside (400f, Olympus CX31 RTSF, camera Cellsens Entry V1, software Cellsens V1.12).

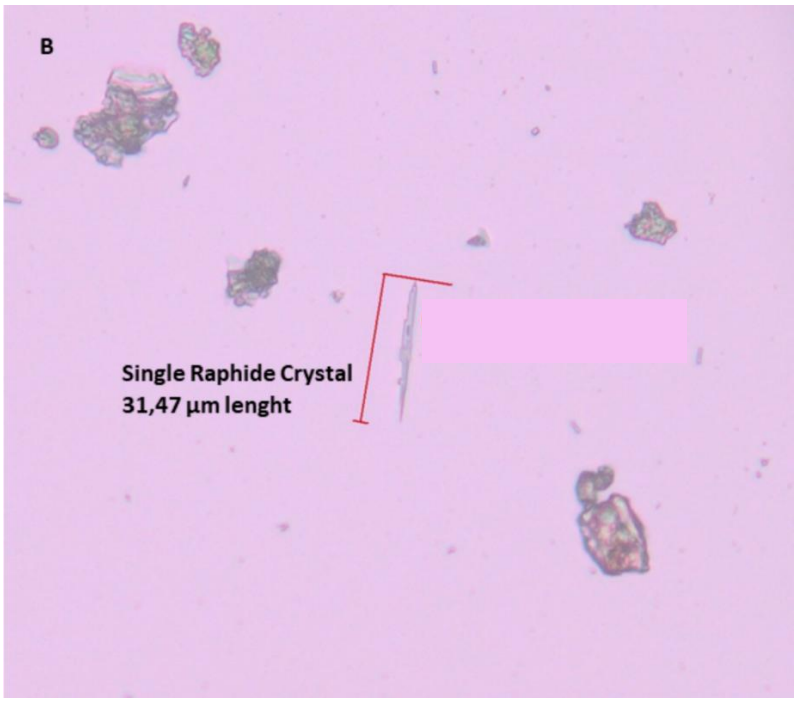

Fig.48: (400f, Original measure data from microscope software, particles of ground *Lemna* DM. Single needle structure of calcium oxalate raphide at a size of 31µm, which corresponds as being a part of the of the raphide bloc located in the idioblast cell as shown in Fig.47.

The concentration of oxalic acid varied between the different treatments and over time of repeated partial harvesting. The resulting trend in all treatments was a decrease in concentration of soluble oxalic acid over the continuous partial harvests. With start of culturing the various NH_4^+/NO_3^- ratios of 10/90 (A, B), 20/80 (C, D), and 30/70 (E, F), under the low and high blue light regimes, the first partial harvests (1/3) of the culture surfaces were taken. As shown in Fig.49, samples E and F with an NH_4^+/NO_3^- ratio of 30/70 died after the second harvest in long term cultivation and were not considered further. Sample B started with 169.7µg•g^{-1} as the highest, and sample A started with 124.8 µg•g^{-1} as the lowest concentration of soluble oxalic acid. After 25 d, the resulting soluble oxalic acid levels were clearly and mainly influenced by the light regime: low blue resulted in higher levels, and high-blue further minimized the oxalic acid contents. Varying the NH_4^+/NO_3^- ratios and the light quality, influenced the levels of free oxalic acid over consecutive harvests (Fig.49).

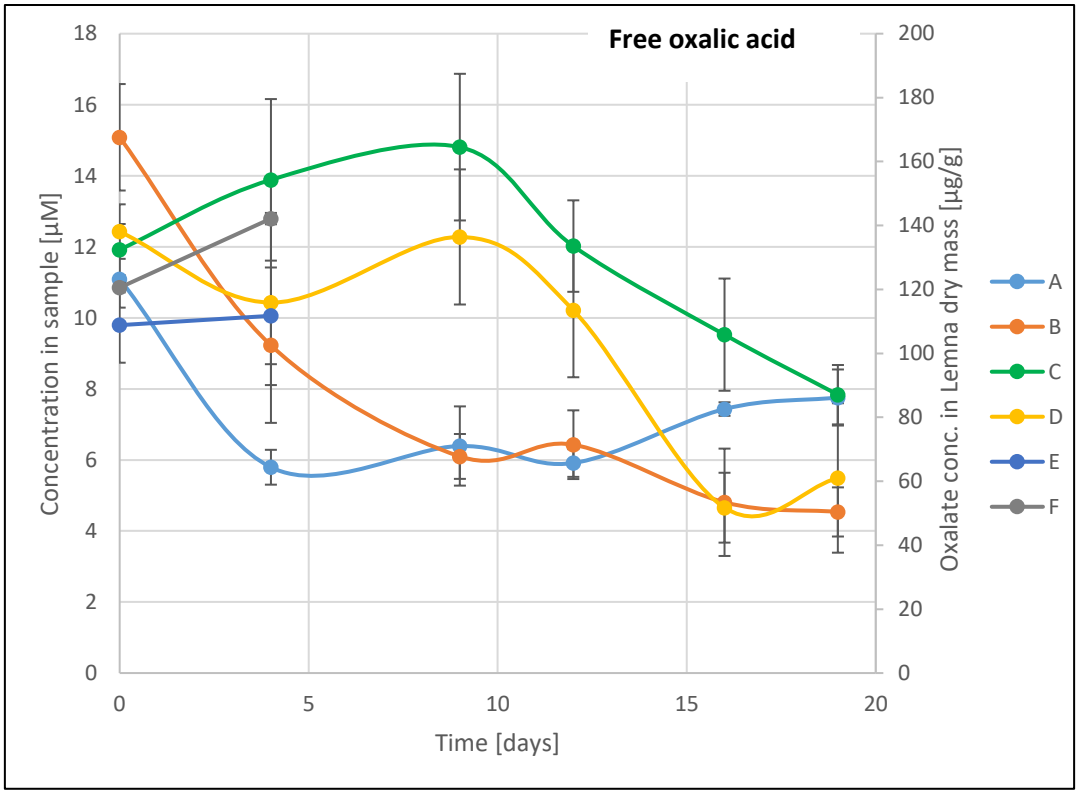

Fig.49: Free oxalic acid concentration of samples from cultures, grown under different NH4+/NO3- ratios and light quantities; A (10/90, low-blue) and B (10/90, high-blue) converge at the same decreased level of concentration; samples C (20/80, low-blue) and D (20/80, high-blue) show the same trend at a still lower level. Samples E (30/70, low-blue) and F (30/70, high-blue) died already after the second harvest.

Keeping the CO_2 concentration at 3500 ppm, soluble oxalic acid contents were manly influenced by the level of blue light, less so by the NH_4^+/NO_3^- ratio. Although the cultures did not start exactly from the same oxalic acid level, the influence of the blue light level was prominent. The strongest reduction in soluble oxalic acid contents was obtained at high blue light and a NH4/NO3 ratio of 1/9.

5.4.2 Mineral elements

The accumulation of heavy metals should be minimized in *Lemna* cultures. The shown concentrations of metals in repeatedly harvested *Lemna* biomass were only determined for the 1st, 4th and 6th harvest, displaying the trends between starting harvest and final harvest.

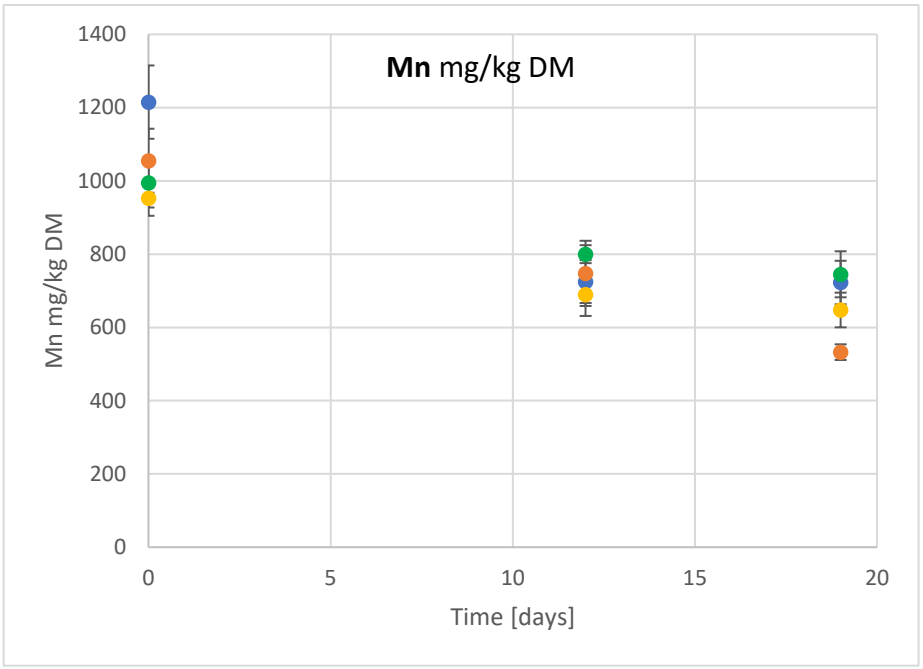

Fig.50: Mn concentration in DM vs. culturing time and repeated (cyclic) partial harvesting along time scale.

The concentration of Mn in DM was reduced by about -50% between start of partial harvesting and end of the harvest sequence resulting in a lower average frond age (see fig. 71). This result was relevant to meet the ESFA requirements for novel food.

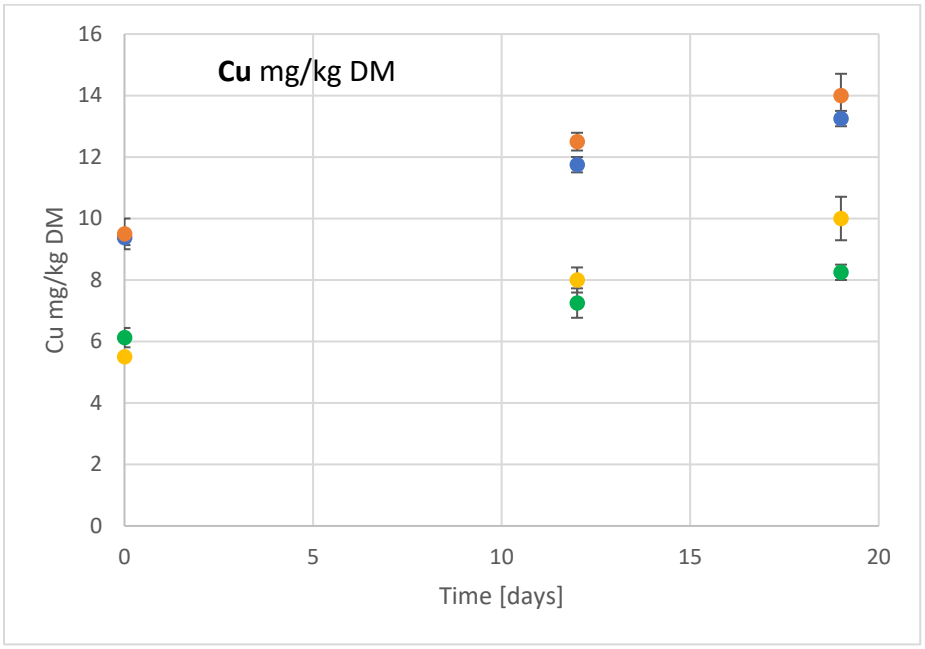

Fig. 51: Cu concentration in DM vs. culture time including cyclic harvest along time scale.

The concentration of Cu in DM slightly increased by about 30-45% between start of partial harvesting and end of harvest sequence since the absolute concentration of 6-13 $\mu g \cdot g^{-1}$ DM is low and non-toxic. The trends for increase of Cu concentration are the same for both

NH_4^+/NO_3^- ratios of 10/90 and 20/80, but their total Cu concentrations were different; about 29% lower for 20/80 than for 10/90 although the Cu concentrations in both nutrient solutions were the same.

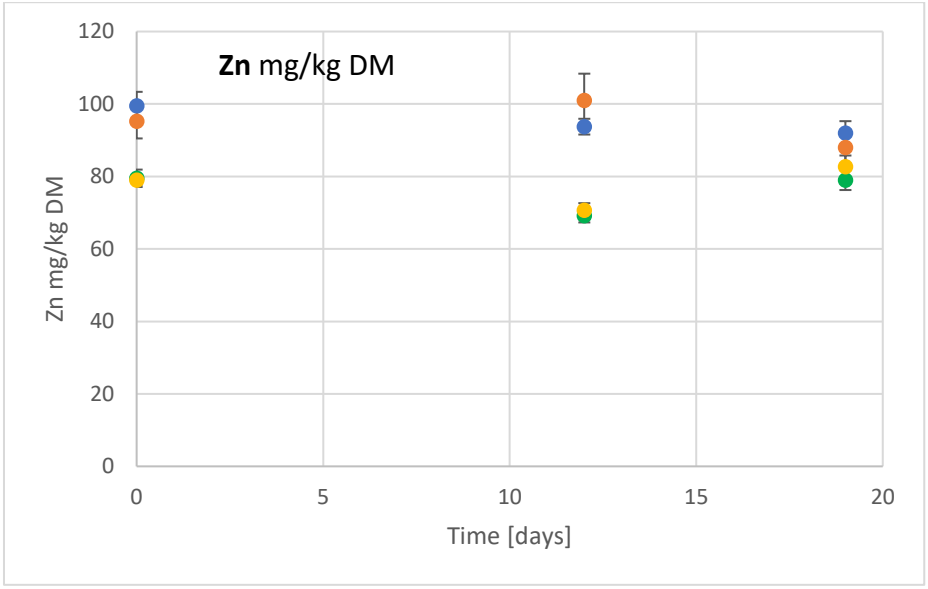

Fig.52: Zn concentration in DM vs. culture time including cyclic harvest along time scale.

The Zn concentration remained largely the same over the time.

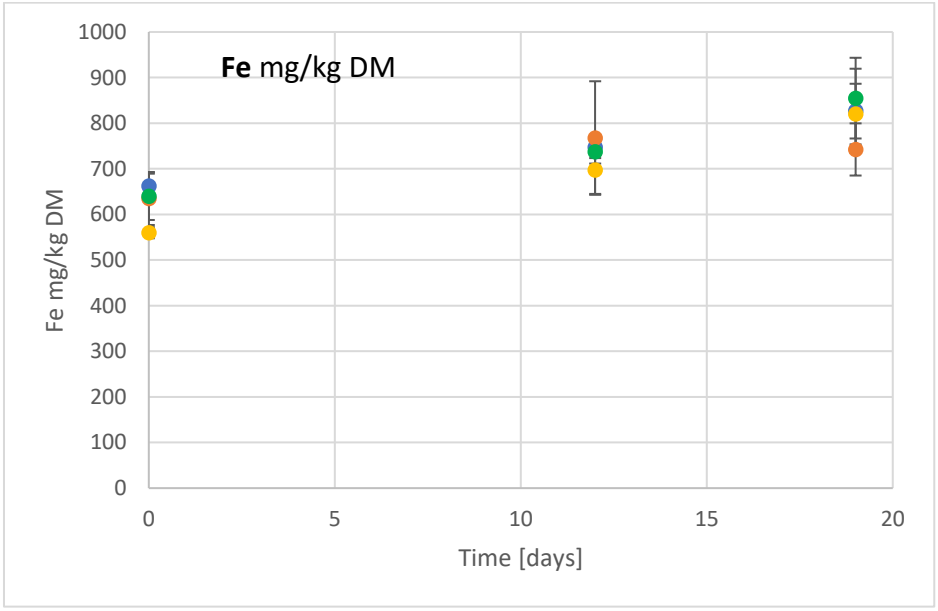

Fig.53 : Fe concentration in DM vs. culture time including cyclic harvest along time scale.

The Fe concentration increased slightly over time in every sample (treatment), differences between treatments were not statistically significant.

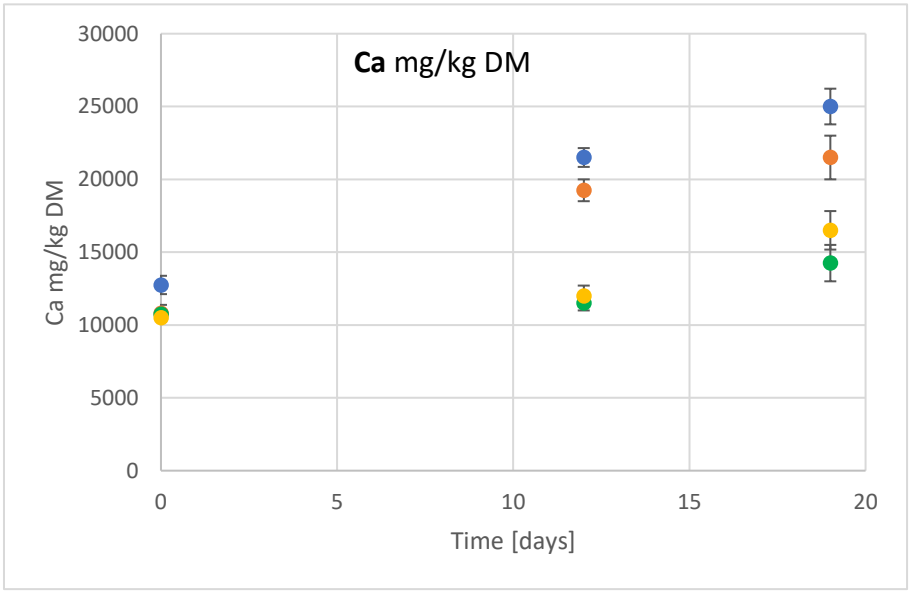

Fig.54: Ca concentration in DM vs. culture time including cyclic harvest with differences between treatments.

The Ca concentrations increased about 100% for 10/90, and about 50% for 20/80 over time of partial harvesting. Furthermore, a slight difference between light regimes (low-blue, high-blue) was observed, amounting to about 15% for 10/90 and 15% for 20/80.

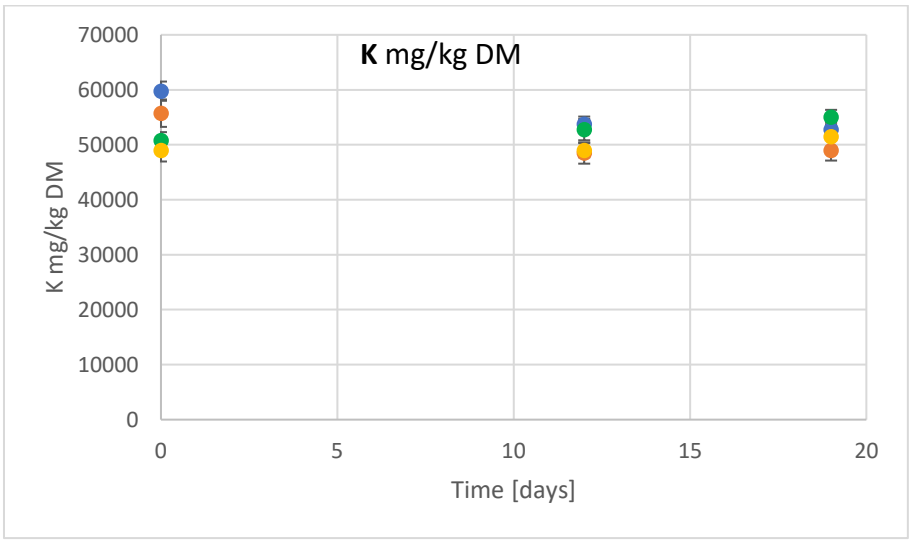

Fig.55: K concentration in DM vs. culture time including cyclic harvest, no significant differences between treatments!

The K concentrations remained largely constant irrespective of the treatment.

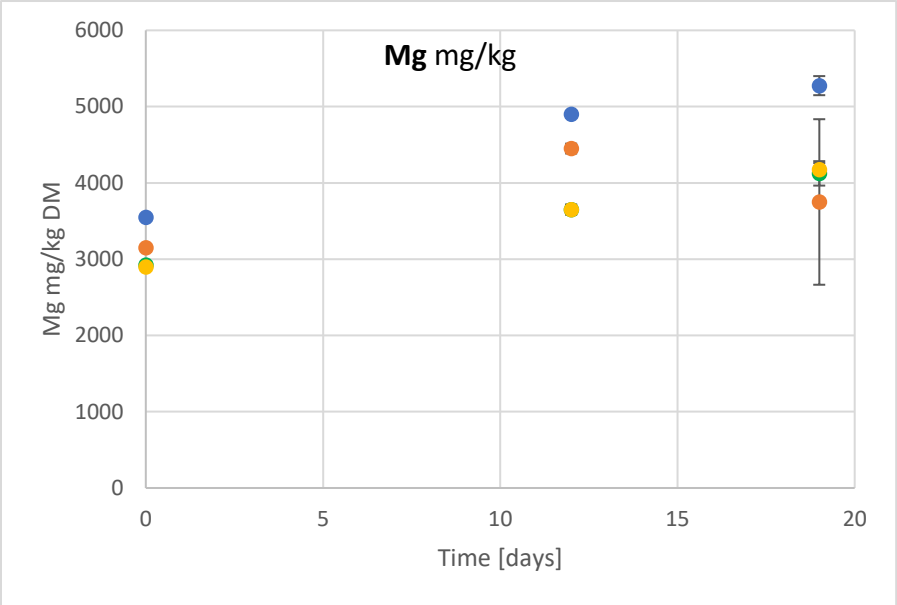

Fig.56: Different increase of Mg concentrations in *Lemna minor* DM between different treatments.

The concentration of Mg increased from start of the cultivation towards last cyclic harvest from 3,550 mg/kg DM to 5,275 mg/kg DM in the 10/90 nutrient solution at the low-blue light regime, and from 3,150 mg/kg to 3,750mg/kg DM at the high-blue light regime.

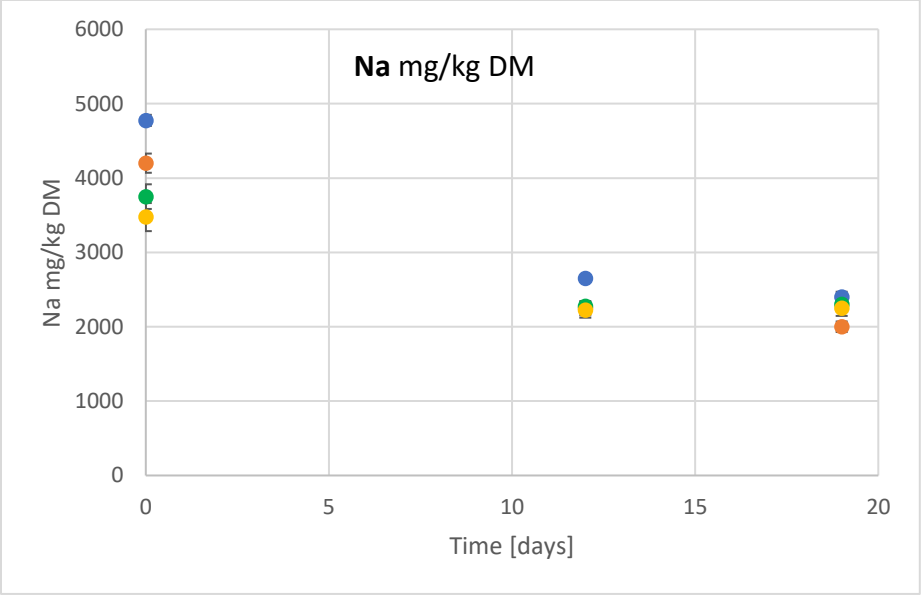

Fig.57: Decrease of Na concentration in DM vs. culture time including cyclic harvest.

The Na concentration decreased with the same trend for 10/90 and 20/80. No further dependency on the light regime was found.

5.4.3 Bacteriological contamination

Since in upscaled cultivation systems only a non-axenic cultivation is practicable, bacteriological contamination was relevant due to the requirements for novel food. The regular treatment of the nutrient solution by ozonation and ultraviolet exposure before NH_4^+/NO_3^- replacement, especially in the Berlin set-up (use of fish manure), the relevant contamination was effectively reduced in the resulting *Lemna minor* DM. A further short pasteurization of the FM at 70° for 10 minutes after harvest resulted in the reduction of the bacteriological load to practically zero, as shown in Tab.14 below.

Tab. 14: Germ counts (**C**olony **f**orming **u**nits) in *Lemna minor* DM, after ozonation of the nutrient solution and pasteurization of the biomass.

Escherichia coli	CFU/g	<10
Bacillus cereus, presumtive	CFU/g	<10
Staphylokokken, coagulase positive (37°C)	CFU/g	<10
Salomonella	/25g	negative
Listeria spp.	/25g	n.f.
Listeria monocytogenes	/25g	n.f.

5.5 Modelling of growth, growth rate, average frond age

5.5.1 Data flow

Correlative results between experimental data and model data

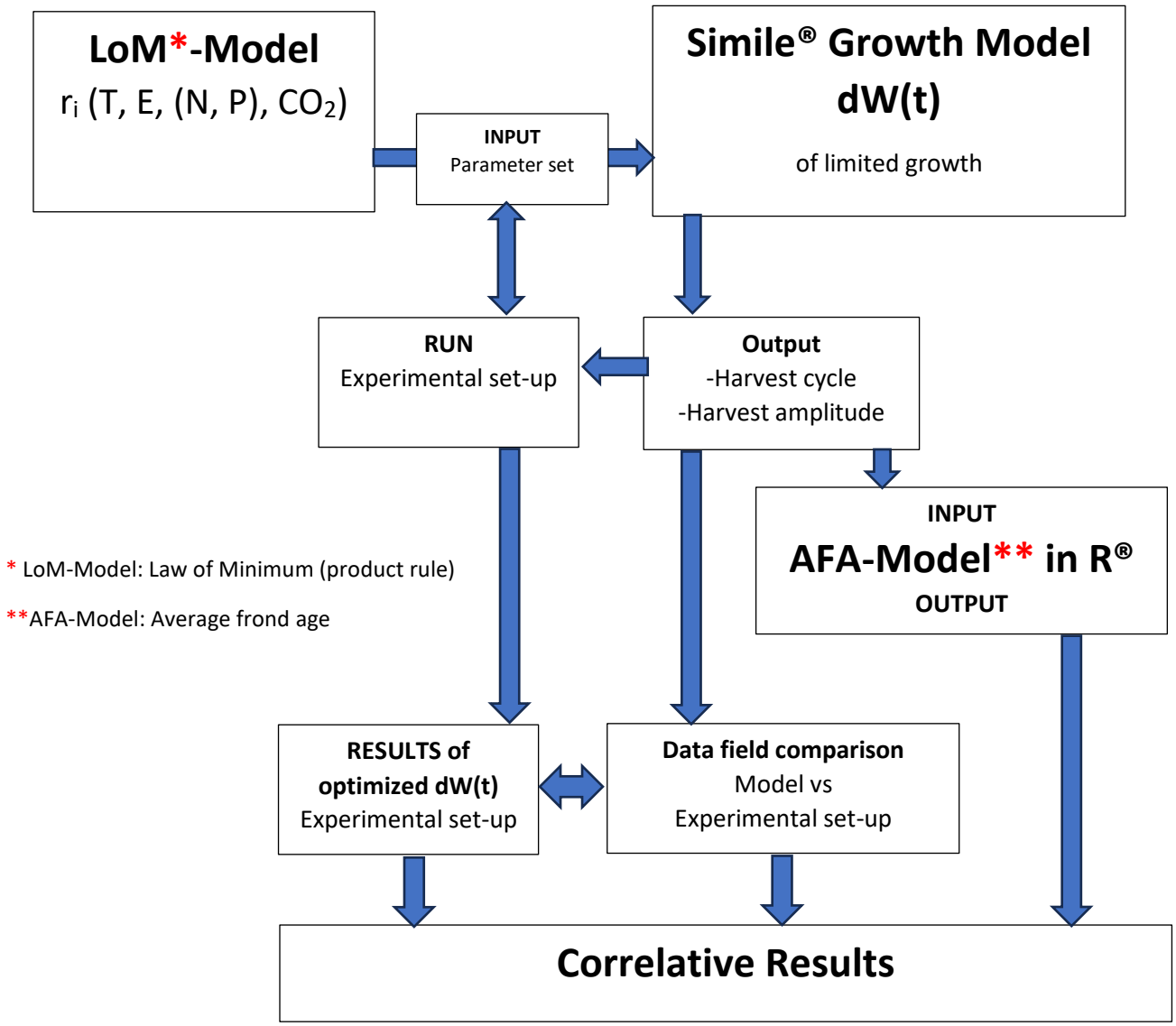

Fig. 58: Model structure for growth model, including LOM- and AFA-model as a result of reverse design of growth rate measurements.

The model was a result of the differential equation of limited growth, adapted to the specific culture conditions for *Lemnoideae*. The growth rate of *Lemna minor* culture is dependent on essential base parameters, such as light, temperature, and nutrition. A further dependency is

given by the CO_2 concentration. Since the growth rate was dependent on all these base parameters, using a LOM model was a consequent result at the starting point of the modelling, setting the relevant input data for the central Simile® growth model (see Fig. above). After different results were obtained for different repeated (cyclic) harvest for nearly all measured data, the use of an average frond age model was a further result of the complex modelling. From the biomathematical perspective, cyclic harvesting influences the average frond age (AFA) of the remaining culture. This resulted in the logic structure of the modelling. Furthermore, the AFA model was able to consistently explain every result for all of the experimental series.

5.5.2 LOM model of growth parameters in growth rate r_i

Relevant growth parameters and coefficients (see eq.14 in Chapter 3.1.5, in Materials and methods)

Temperature: $r_i(T)=r_{i0}*\alpha(T)$, for T= 29, 25, 20°C,

Light: $r_i(E)=r_{i0}*\beta(E)$, for 80 and 129 $\mu mol \cdot m^{-2} \cdot s^{-1}$,

Nutrition: $r_i(N,P)=r_{i0}*\Upsilon(N, P)$,

and CO_2: $r_i(CO_2)=r_{i0}*\delta(CO_2)$,

were calculated based on literature values *(Docauer, 1983)*, *(Lasfar, 2007)*, compared and aligned with author's own results from the laboratory set-up in Bonn and the upscaled set-ups in Kalkar and Berlin.

The productivity factor, as a product of

$$pf = \alpha*\beta*\Upsilon*\delta \qquad \text{eq.32}$$

results in the factors for the effective growth rate in the modelling of different experimental set-ups, considering each experimental environmental condition. Using a theoretical maximal growth rate r_{i0} ($g \cdot m^{-2} \cdot d^{-1}$), the effective growth rate was obtained by

$$r_i = pf * r_{i0} \qquad \text{eq.33}$$

Tab.15 below shows the results for several growth rates under the experimental conditions in all experimental set-ups. If any further intermediate values for all coefficients were be considered, the possible permutations of the table would expand exponentially. This problem was effectively solved by linear interpolations and reflects all possible growth rates.

Since the range of values used in the table is already located in the quasi-linear range of the theoretical growth curves, intermediate values can easily be calculated by simple interpolation.

Tab. 15: Overview of resulting growth rate r_i under main culture condition, to be introduced into the Simile®

T (°C)	α(T)	E(µE)	β(E)	(N/P)	ϒ(N, P)	CO_2(ppm)	δ(CO2)	pf	r_{i0}	r_i (g $m^{-2}d^{-1}$)
29	1	390	1.00	5	0.8231	3500	1	0.8231	380	**312.78**
25	0.86	390	1.00	5	0.8231	3500	1	0.7079	380	**268.99**
20	0.74	390	1.00	5	0.8231	3500	1	0.6091	380	**231.46**
29	1	129	0.92	5	0.8231	3500	1	0.7573	380	**287.76**
25	0.86	129	0.92	5	0.8231	3500	1	0.6512	380	**247.47**
20	0.74	129	0.92	5	0.8231	3500	1	0.5604	380	**212.94**
29	1	80	0.80	5	0.8231	3500	1	0.6585	380	**250.22**
25	0.86	80	0.80	5	0.8231	3500	1	0.5663	380	**215.19**
20	0.74	80	0.80	5	0.8231	3500	1	0.4873	380	**185.16**
29	1	390	1.00	10	0.8164	3500	1	0.8164	380	**310.23**
25	0.86	390	1.00	10	0.8164	3500	1	0.7021	380	**266.80**
20	0.74	390	1.00	10	0.8164	3500	1	0.6041	380	**229.57**
29	1	129	0.92	10	0.8164	3500	1	0.7511	380	**285.41**
25	0.86	129	0.92	10	0.8164	3500	1	0.6459	380	**245.46**
20	0.74	129	0.92	10	0.8164	3500	1	0.5558	380	**211.21**
29	1	80	0.80	10	0.8164	3500	1	0.6531	380	**248.19**
25	0.86	80	0.80	10	0.8164	3500	1	0.5617	380	**213.44**
20	0.74	80	0.80	10	0.8164	3500	1	0.4833	380	**183.66**
29	1	390	1.00	5	0.8231	400	0.63	0.5186	380	**197.05**
25	0.86	390	1.00	5	0.8231	400	0.63	0.446	380	**169.46**
20	0.74	390	1.00	5	0.8231	400	0.63	0.3837	380	**145.82**
29	1	129	0.92	5	0.8231	400	0.63	0.4771	380	**181.29**
25	0.86	129	0.92	5	0.8231	400	0.63	0.4103	380	**155.91**
20	0.74	129	0.92	5	0.8231	400	0.63	0.353	380	**134.15**
29	1	80	0.80	5	0.8231	400	0.63	0.4148	380	**157.64**
25	0.86	80	0.80	5	0.8231	400	0.63	0.3568	380	**135.57**
20	0.74	80	0.80	5	0.8231	400	0.63	0.307	380	**116.65**
29	1	390	1.00	10	0.8164	400	0.63	0.5143	380	**195.45**
25	0.86	390	1.00	10	0.8164	400	0.63	0.4423	380	**168.08**
20	0.74	390	1.00	10	0.8164	400	0.63	0.3806	380	**144.63**
29	1	129	0.92	10	0.8164	400	0.63	0.4732	380	**179.81**

25	0.86	129	0.92	10	0.8164	400	0.63	0.4069	380	**154.64**
20	0.74	129	0.92	10	0.8164	400	0.63	0.3502	380	**133.06**
29	1	80	0.80	10	0.8164	400	0.63	0.4115	380	**156.36**
25	0.89	80	0.80	10	0.8164	400	0.63	0.3662	380	**139.16**
20	0.73	80	0.80	10	0.8164	400	0.63	0.3004	380	**114.14**

5.5.3 Cyclic harvesting: Model vs. reality

5.5.3.1 Laboratory set-up (Bonn)

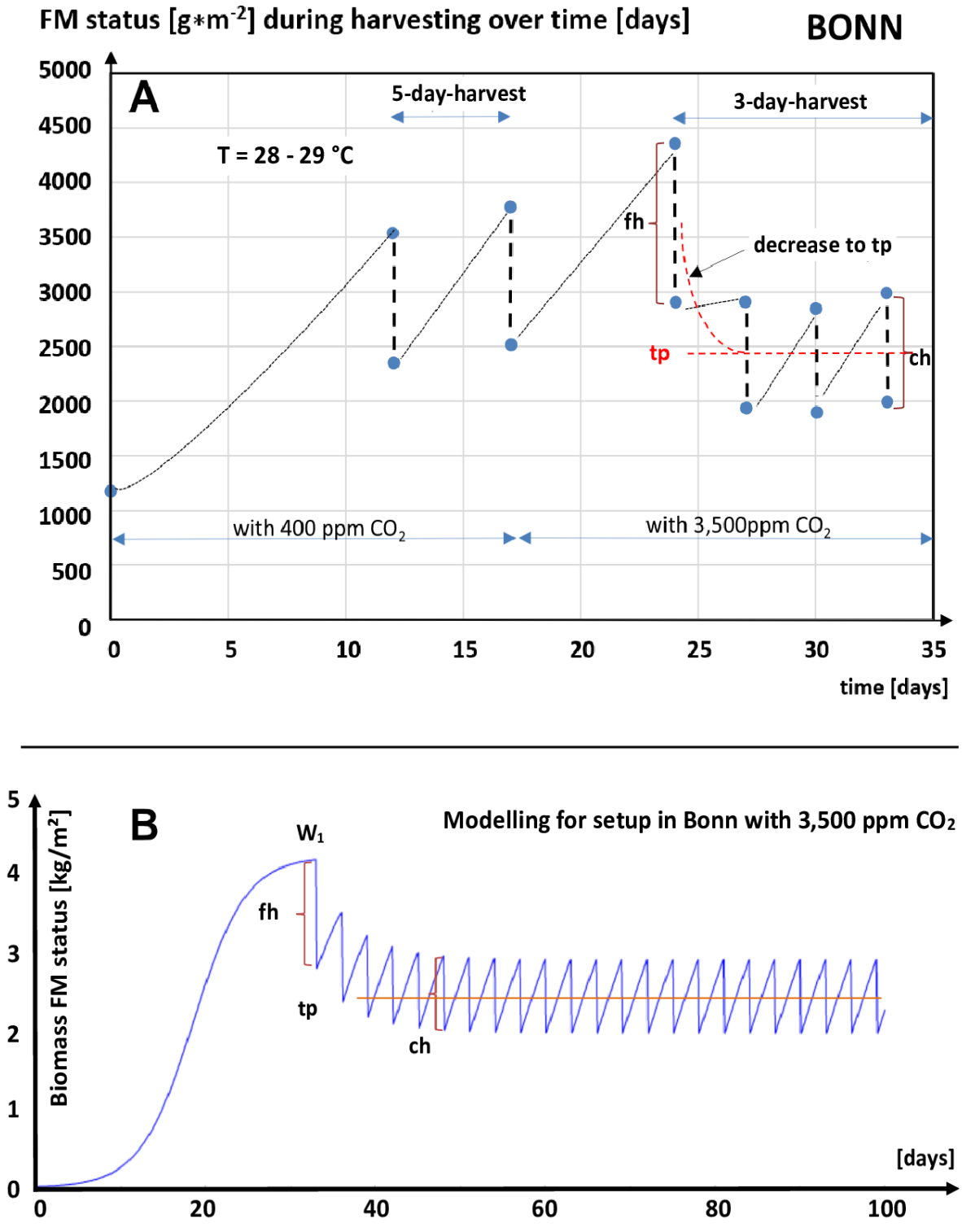

Fig.59: A: Transition from the harvest curve at 400ppm CO_2 to the harvest curve at 3,500ppm CO_2

B: Model of harvest curve at 3,500ppm CO_2. W_1 is the FM coverage status at starting point of harvest.

Fig 59 A displays the harvest impact as a resulting sawtooth curve at 400ppm and 3,500ppm. Firstly, the harvest at 3,500ppm started at a higher capacity, but dropped as predicted by the model towards tp, which is the point of the strongest regrowth rate in the sigmoidal growth curve. The respective harvest amount (FM) resulted from the difference in the FM coverage before and after partial harvest, given by the sawtooth curve.

The model was started, like shown in Fig. 59B with parameters at average values as follows.

Tab.16: Model parameters for the Simile® growth model at **BONN** set-up

Capacity	W_{max}	3,850 $g \cdot m^{-2}$
Harvest max	r_{i0}	380 $g \cdot m^{-2} \cdot d^{-1}$
Temperature	T	29°C
Light	µmol s^{-1} m^{-2}	129 $\mu mol \cdot m^{-2} \cdot s^{-1}$
CO_2	ppm	400 / 3,500
N/P	ratio	5/1
Productivity factor*	pf	0.727
Effective growth rate	$r_i = r_{i0} * pf$	276.3 $g \cdot m^{-2} \cdot d^{-1}$

*Resulted from LOM model, considering parameters from the BONN set-up. The comparison between Harvest real and Harvest model resulted in a small underestimation of the model prediction at the first harvest under 3,500ppm CO_2. Second and third harvests amounts decreased, where real data matched the model predictions with only a marginal under- and over-estimation. The harvested biomass at the 4th harvest point, again, was slightly under-estimated by the model (see fig.60).

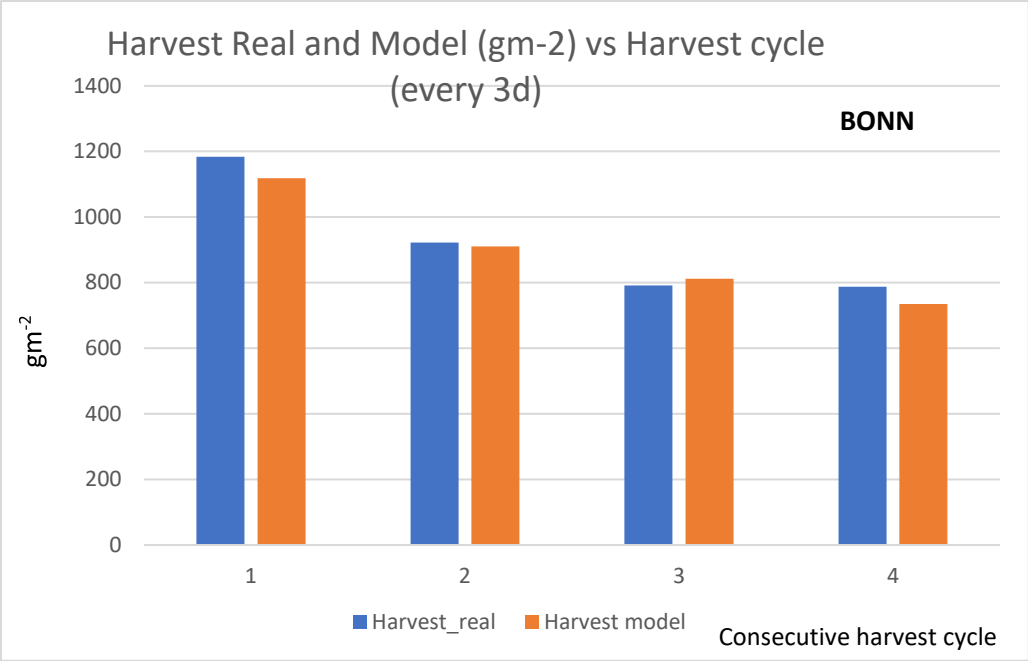

Fig.60: Comparison of real harvested biomass with the model prediction for the laboratory set-up in BONN.

Instead, the more important "coefficient of determination" can be calculated. In order to obtain the coefficient of determination (R^2) between the model prediction and the real data measurements, both non-linear curves must be plotted against each other. The non-linearity of both curves in relation to each other could thus be linearised, so that a deviation from linear regression was determined. In doing so, the coefficient of determination (R^2) for the laboratory set-up was obtained by linear regression to R^2=0.96 (at lab set-up).

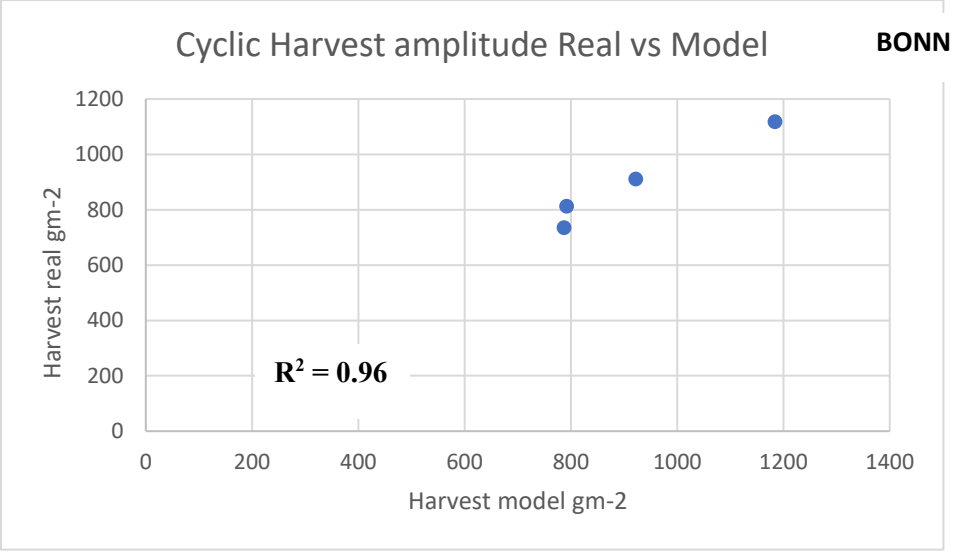

Fig.61: Coefficient of determination (R^2) between harvest real and harvest model by linear regression after linearisation of both curves.

A R^2 of 0.96 indicates a good match between the model prediction and the real measurement, which is a combined result of controlling the parameters along the predetermined culture parameters with a high accuracy in the laboratory set-up.

5.5.3.2 First upscaling set-up (Berlin)

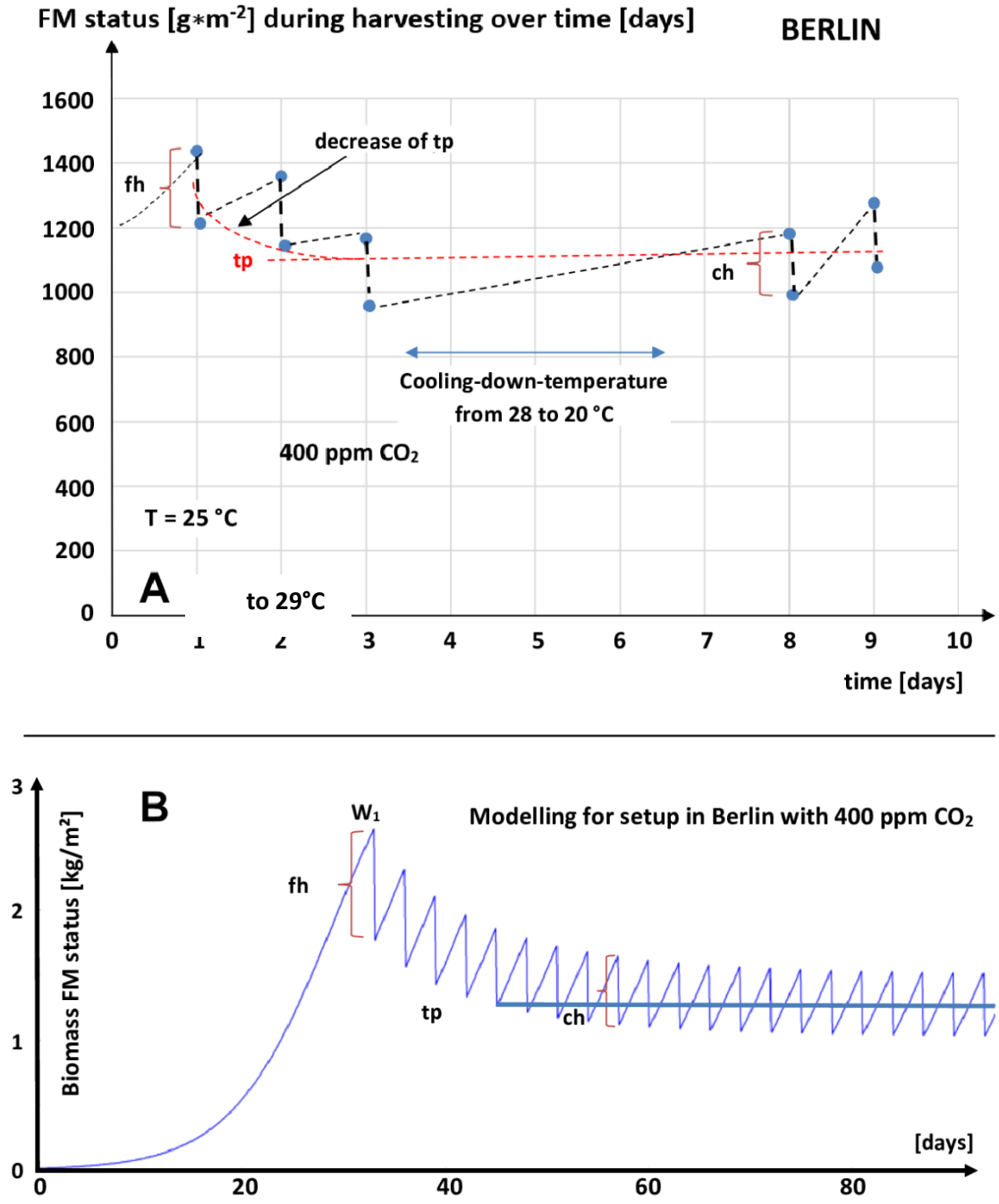

Fig.62A: Harvest curve at 400 ppm CO_2, fig.62B: Model of harvest curve at 400ppm CO_2. W_1 is the FM coverage status at starting point of harvest. W1: FM status of coverage of FM Biomass at start of harvest, fh: first harvest amount, tp: turning point, ch: consolidated harvest.

Fig.62A displays the cyclic harvest impact on the coverage as a resulting sawtooth curve at 400ppm CO_2. First harvest was started at a higher coverage status, but dropped, as predicted by the model in Fig.62B, resulting by consolidation towards tp, which is the point of the strongest regrowth rate in the sigmoidal curve. So the model in Fig.62B predicts an equilibration for a harvest interval of 3 days and 33% harvested surface around the tp of the sigmoidal growth curve, shown in Fig.62A.

The respective harvest amount (FM) resulted from the difference of the FM coverage before and after partial harvest given by the sawtooth curve.

The model for the Berlin set-up was started with parameters at average values as follows. The respective capacity was mainly reduced by a lower temperature, which tends to drop to 20°C. CO_2 was reduced to 400ppm. For this reason, the productivity factor pf - resulting from the LOM model - was reduced, as considered by linear interpolation according to Tab.17.

Tab.17: Model parameter for the Simile® growth model at the first upscaled **BERLIN** set-up

Capacity	W_{max}	2,400g m^{-2}
Harvest max	r_{i0}	380g•m^{-2}•d^{-1}
Temperature	T	25 - 29°C
Light	µmol s^{-1} m^{-2}	129 µmol•m^{-2}•s^{-1}
CO_2	ppm	400 - 800
N/P	ratio	5/1
Productivity factor*	pf	0.474
Effective growth rate	$r_i = r_{i0}$*pf	180.12 g•m^{-2}•d^{-1}

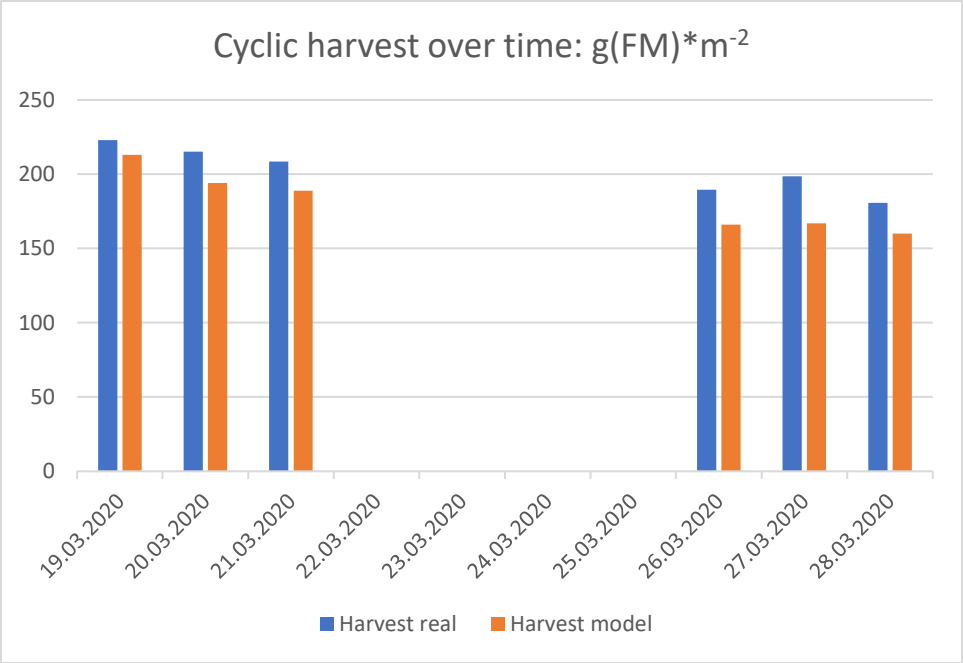

Fig.63: Comparison of modelled and experimental FM yields at the upscaled set-up in BERLIN.

The comparison between harvest real and harvest model resulted in a small under-estimation of the model prediction over all harvests. Both the harvest real curve and the harvest model curves decreased from starting harvest towards the equilibrium value. Since the culture conditions in the BERLIN set-up were far away from the optimum, in contrast to the laboratory set-up in BONN, the model nevertheless showed the same trend and prediction of the harvested amount of FM.

Instead of standard deviation or standard error, the relevant statistical determination was developed based on the more important coefficient of determination R^2, calculated between the model prediction and the real data measurements; also in this set-up, non-linear curves were plotted against each other. Linearisation resulted from linear regression, as for the laboratory set-up results in R^2 value.

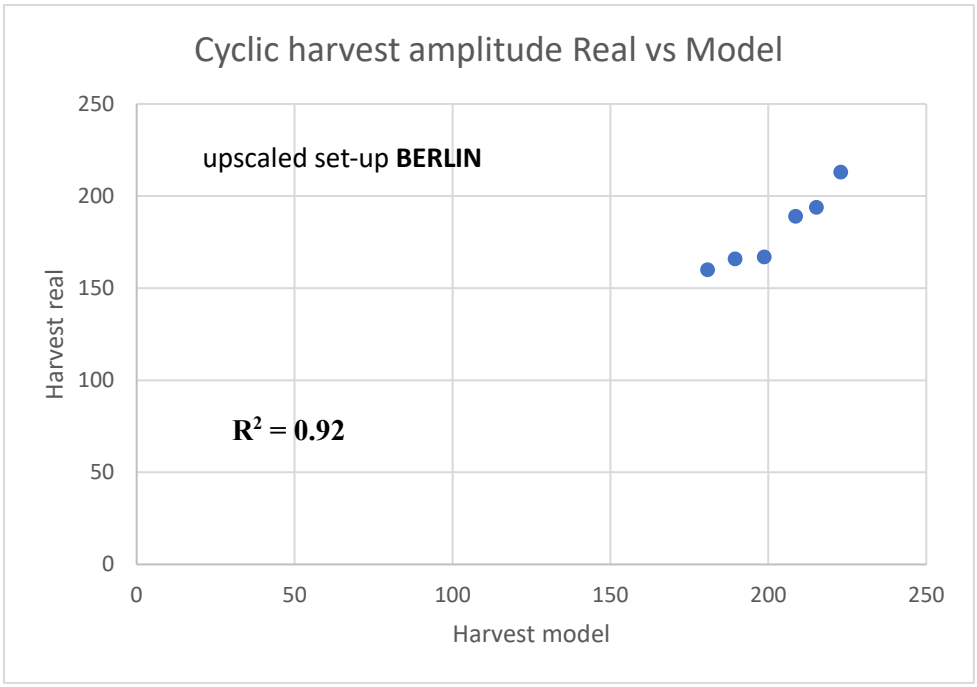

Fig.64: Comparison of modelled and harvested FM g/m^{2}d production under the Berlin setup.

5.5.3.3 Second upscaling set-up (Kalkar)

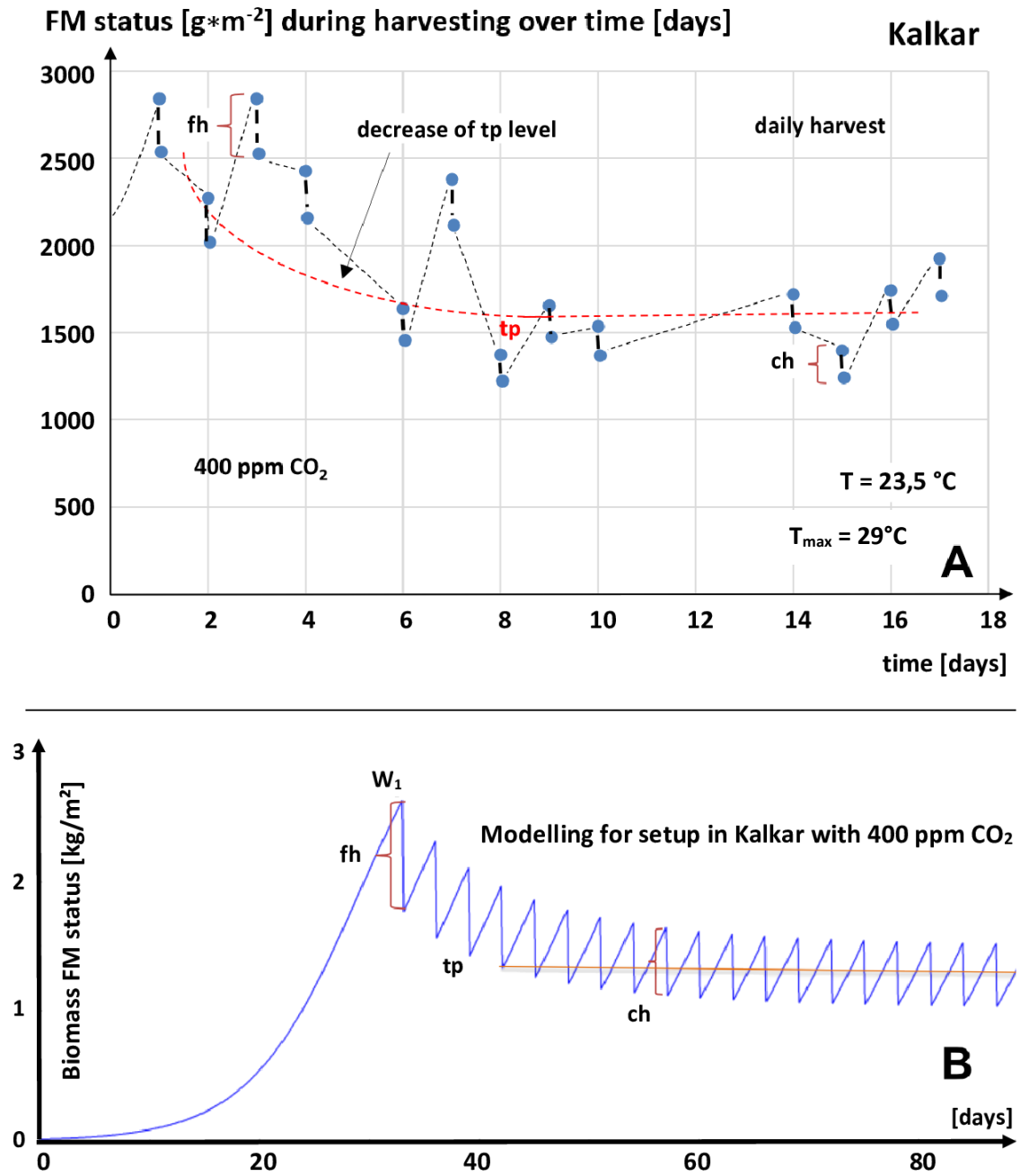

Fig.65: FM status during harvesting compared to model curve, up-scale Kalkar.

Tab.18: Model parameters for the Simile® growth model at the second upscaled **KALKAR** set-up

Capacity	W_{max}	2.842 $g \cdot m^{-2}$		
Harvest max	r_{i0}	380 $g \cdot m^{-2} \cdot d^{-1}$		
Temperature	T	23.5 – 29 °C	$\alpha(r_i(T))$ =	0.92
Light	$\mu mol \cdot s^{-1} \cdot m^{-2}$	129 (average)	$\beta(r_i(E))$ =	0.92
N/P	ratio	5	$\delta(r_i(N/P))$ =	0.8231
CO_2	ppm	400	$\Upsilon(r_i(CO_2))$ =	0.63
Productivity factor*	pf		0.4420	
Effective growth rate	$r_i = r_{i0} * pf$	167.26 g m^{-2} d^{-1}		

A comparison of the harvest model and the real harvests only showed the same trend. The values between model results and the real harvest results show strong fluctuations, and not a consequent over- or underestimation along the complete culture/harvest period.

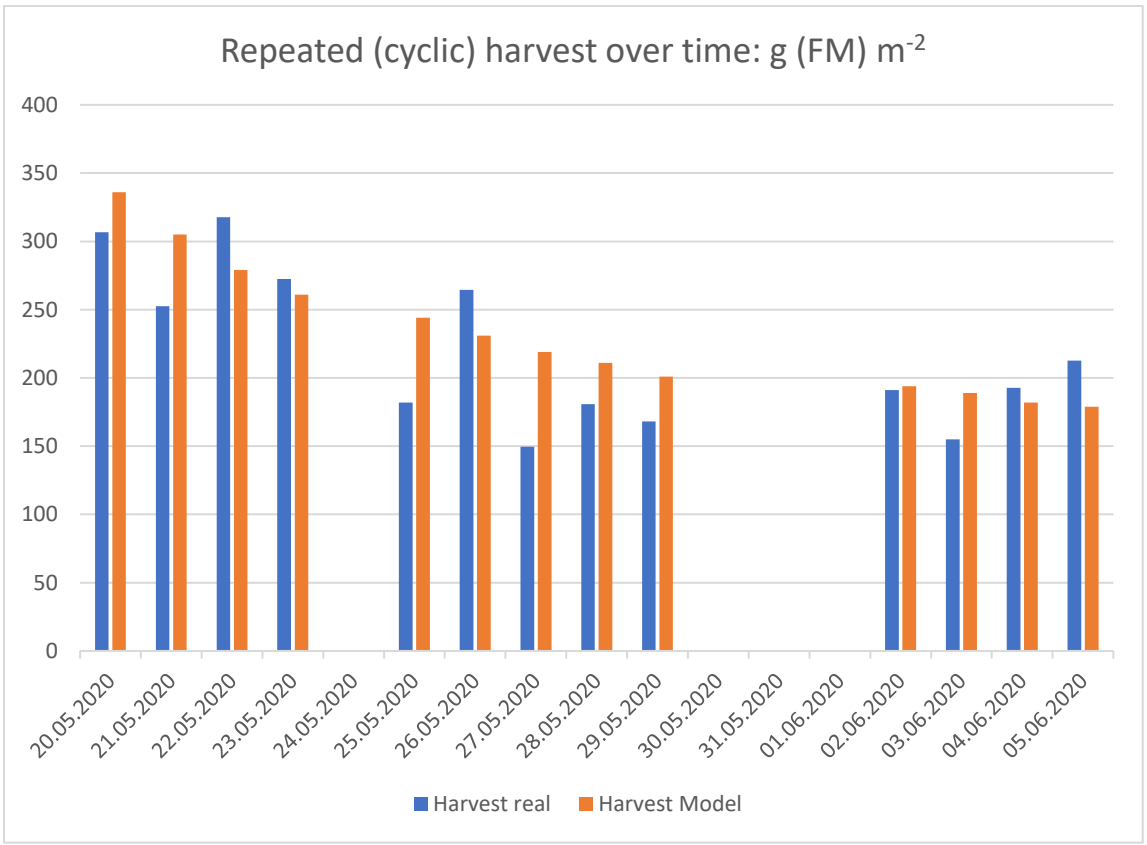

Fig.66: Comparison of the real harvest sequence and model prediction; variations are due to the higher variability of the growth conditions.

The same methodology as in the laboratory set-up was used here, resulting in the R^2 value.

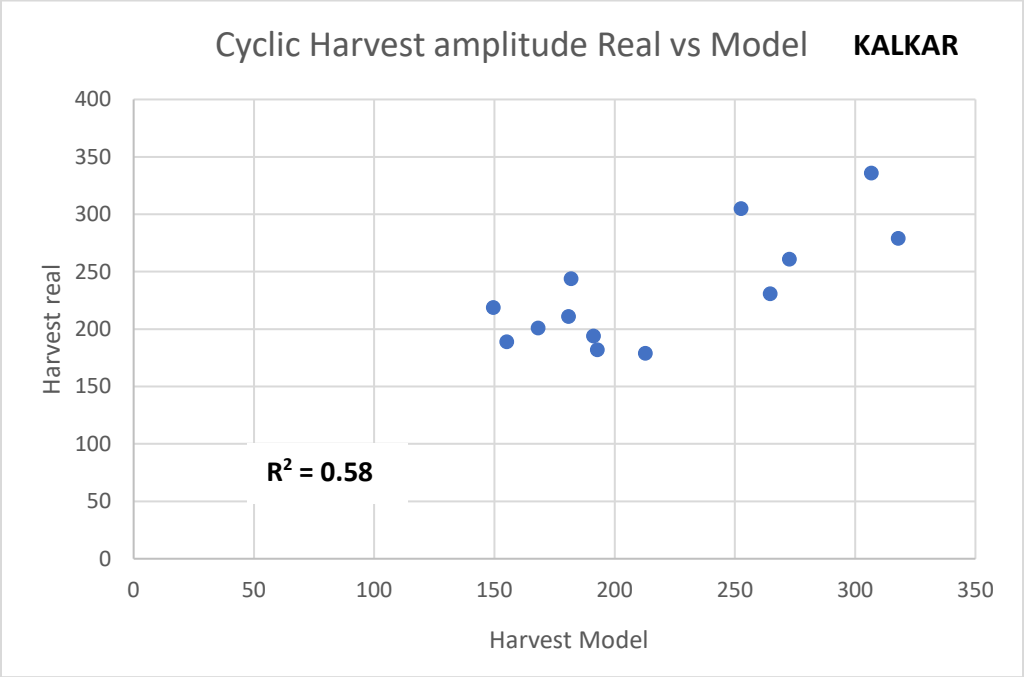

Fig. 67: Coefficient of determination for up-scale Kalkar, measured and calculated in FM g/m²d

A conclusive final overview on the results from modelling at all set-ups related to the growth rate are shown below.

Tab.19: Calculated k factors := α, β, γ, δ, considering the different conditions at the different set-up locations and the pertaining productivity factor $\prod_{j=T,E,NP,CO2} k(ri(j))$ using eq.14.

	$\|\alpha(ri(T$	$\|\beta(ri(E$	$\|\gamma(ri(N,P)$	$\|\delta(ri(CO$	Productivity factor	Measured ri (average)
Bonn	0.96	0.92	0.8231	1.0	0.727	276 g/m²day
Kalkar	0.92	0.92	0.8231	0.63	0.440	167 g/m²day
Berlin	0.92	0.92	0.8231	0.68	0.474	180 g/m²day

5.5.4 Average frond age model

The yield (FM) was obtained by harvesting a part of the population (e.g., 1/3) of *Lemna minor*. At the beginning, the average frond age was about 28 days. Thus, after the 1st harvest, the remaining population in the culture propagates with a high growth rate, fully replacing the partial harvested amount within 3 days. As a result, until the 2nd harvest, 1/3 of the regrowing

population has an average frond age of (1+3)/2 = 2.0 days, which effectively reduces the real average frond age from harvest to harvest. The average frond age of the harvested biomass is following a strongly decreasing hyperbolic curve as resulting from eq.27 (Chapter 4.1.7). The result is displayed as program in R® as in Tab. 20.

Tabl.20:Calculation in R®, for n harvests:

```
alter <- function(A, T, f, alpha, n) {
  AE <- numeric(n+1)
  AE[1] <-A
  beta <- T/(A+(1-alpha)*T)
  for(i in 2:(n+1)) {
    AE[i] <- f * (1-beta) * (AE[i-1]+T) + (1 - f + f*beta)*alpha*T
  }
  AE
}
```

Given repeated (cyclic), harvesting as a dynamic population impact, the harvest period must be much smaller than the individual life time. But smaller partial harvest amplitudes as such are contra-productive. Considering that, it is obvious to assume that the effect of lowering the average frond age can be reached faster by greater harvest amplitudes within the related minimum harvest period.

The following results from the AFA model apply to all relevant experimental conditions: Results from the AFA model with the condition: no harvest, f=1 (see below). If the culture is not harvested, the average age of the fronds in the population remains constant, because senescent fronds are replaced by new daughter fronds, provided that the capacity (maximum population density) remains constant. Furthermore, the mortality of Lemna was considered in the extended model, as shown in eq.27. The results of the AFA model, displayed below, are using real parameter from the experimental set-ups. The following plots are original plots directly from the program R®, displaying the plot and the run of numbers, here marked as Index = consecutive days, related to the resulted average frond age.

Vertical axis: Average frond age. Horizontal axis (Index: Consecutive days): repeating (cyclic) harvest impact.

```
f0 <- alter(28, 3, 1, 1/2, 20)
f0
```

```
##  [1] 28 28 28 28 28 28 28 28 28 28 28 28 28 28 28 28 28 28 28 28 28
```

```
plot(f0)
```

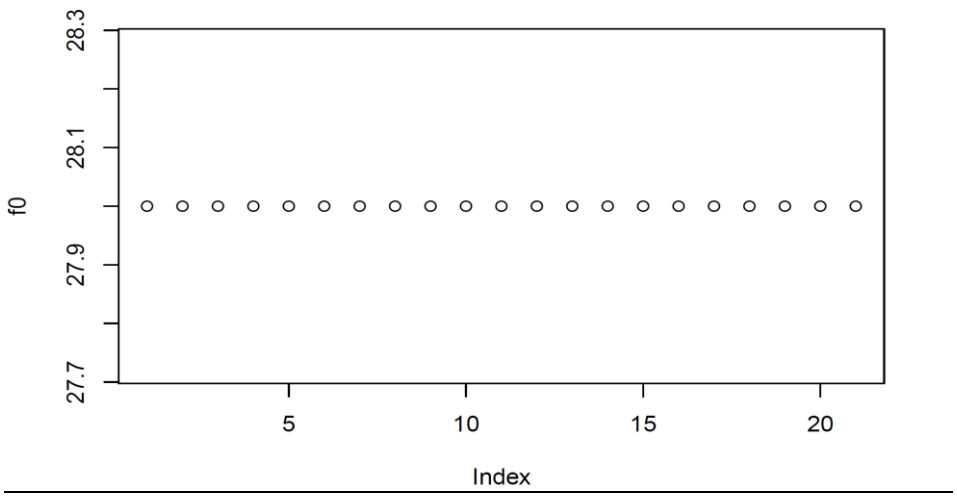

Fig.68: Above: Average frond age number series. Below: Plot of average frond age remain constant at 28d, resulted by "no" harvests regrowth replace died fronds

First example: cyclic harvesting of **1/10** of the culture, **f=9/10**, remaining after harvest.

```
f1 <- alter(28, 3, 9/10, 1/2, 20)
f1
```

```
##  [1] 28.00000 25.35000 23.20754 21.47542 20.07504 18.94287 18.02754 17.28752
##  [9] 16.68923 16.20553 15.81447 15.49831 15.24270 15.03605 14.86898 14.73390
## [17] 14.62470 14.53641 14.46503 14.40732 14.36066
```

```
plot(f1)
```

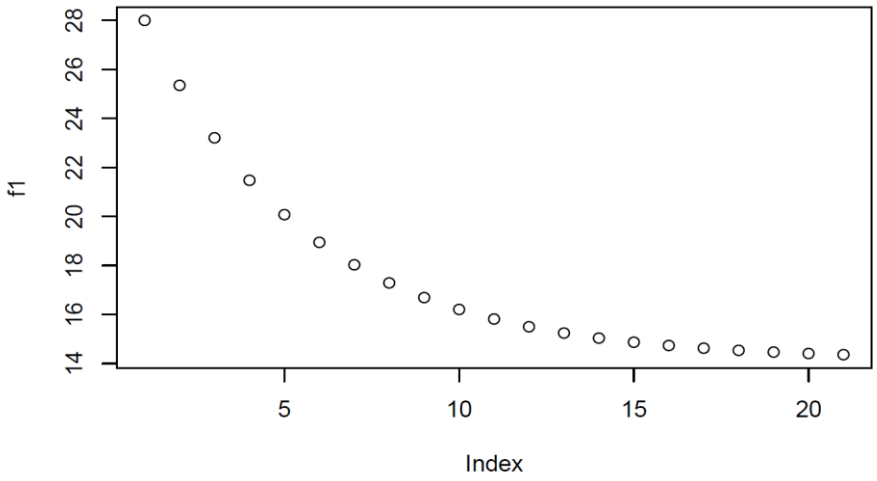

Fig.69: Plot of average frond age, decreasing by repeated (cyclic) harvest impact daily, 1/10 of the culture surface. Above: Average frond age number series descending. Below: Plot of average frond age descending towards 14d asymptotically.

Second example: cyclic harvesting of **1/3** of the culture surface, **f=2/3**,_where the partial harvest is 1/3 of the entire population and f=2/3 is the remaining population per tray. This harvest sequence reflects the practice of the cyclic (repeating) harvesting in the experimental set ups at Bonn and Berlin.

```
f2 <- alter(28, 3, 2/3, 1/2, 20)
f2
```

```
##  [1] 28.000000 19.166667 13.876648 10.708614  8.811373  7.675173  6.994736
##  [8]  6.587243  6.343208  6.197062  6.109540  6.057126  6.025736  6.006938
## [15]  5.995680  5.988939  5.984901  5.982483  5.981035  5.980168  5.979649
```

```
plot(f2)
```

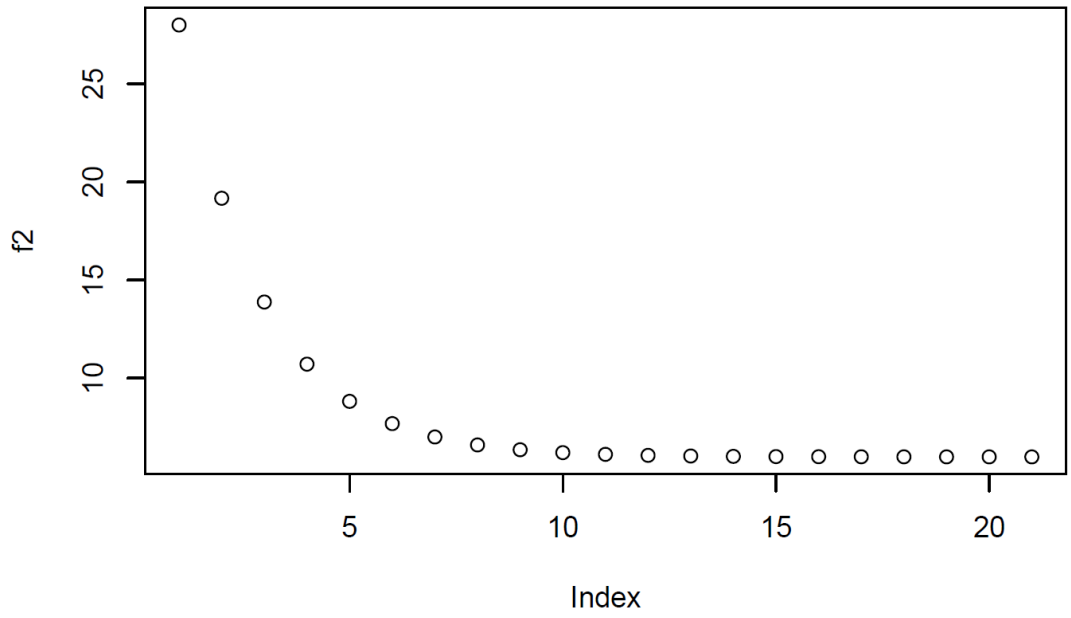

Fig.70: Partial harvest every 6d of 1/3 of the culture. Plot of average frond age, decreasing by cyclic (repeated) harvest impact. Above: Average frond age number series descending. Below: Plot of average frond age descending towards 3d asymptotically.

Third example: cyclic harvesting of **2/3**, **f=1/3,** harvest cycle time 3 days.

```
f3 <- alter(28, 3, 1/3, 1/2, 20)
f3
```

```
##  [1] 28.000000 10.333333  5.043315  3.459298  2.984987  2.842962  2.800435
##  [8]  2.787701  2.783888  2.782746  2.782404  2.782302  2.782271  2.782262
## [15]  2.782259  2.782258  2.782258  2.782258  2.782258  2.782258  2.782258
```

```
plot(f3)
```

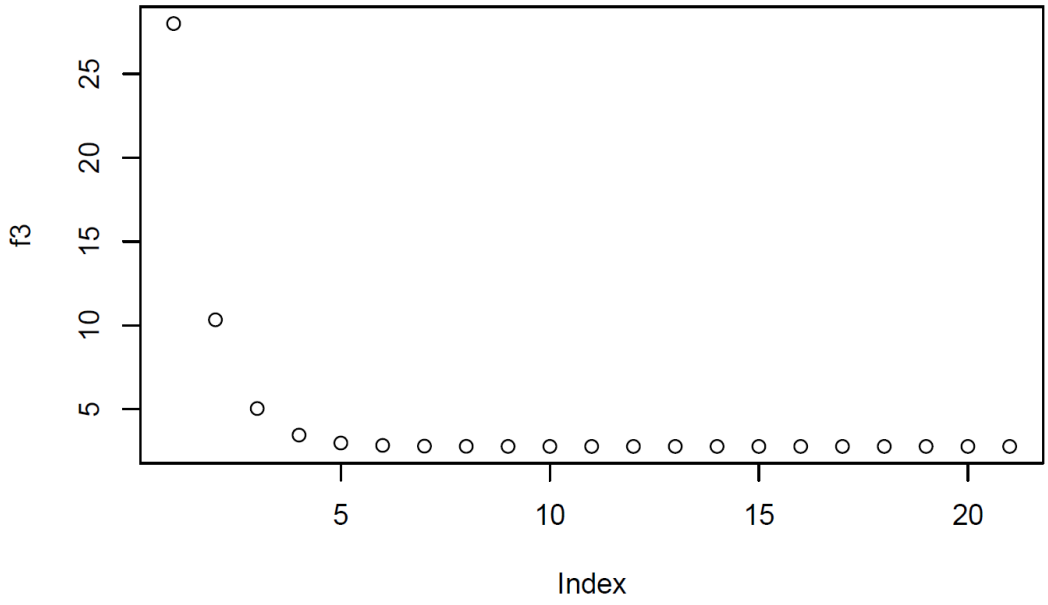

Fig.71: Parial harvest of 2/3 of culture surface every 3d. Plot of average frond age, decreasing by cyclic (repeated) harvest impact. Above: Average frond age number series descending. Below: Plot of average frond age descending towards 2.78d asymptotically.

The average frond age will drop fast by harvesting each time 2/3 of the population, but will exceed the regrowth capacity when harvesting every third day. As a consequence, the population would run to zero after 4 or 5 harvests.

Fourth example: harvest everything, as a theoretical verification of the model

```
f4 <- alter(28, 3, 0/3, 1/2, 20)
f4
```

```
##  [1] 28.0  1.5  1.5  1.5  1.5  1.5  1.5  1.5  1.5  1.5  1.5  1.5  1.5  1.5  1.5  1.5
## [16]  1.5  1.5  1.5  1.5  1.5  1.5
```

```
plot(f4)
```

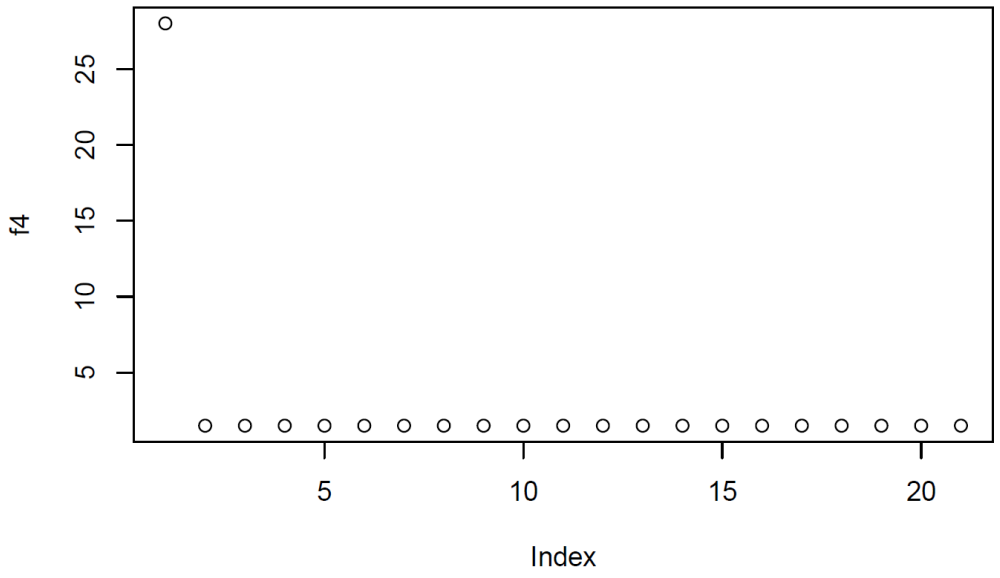

Fig.72: Plot displays harvesting 3/3 daily only as theoretical/mathematical check of the validity of the model, if model ran to lowest average frond age.

Fifth example: harvest 1/3, f=2/3, harvest cycle time **5** days: These harvest conditions were partly used in all set-ups at 400ppm CO_2.

```
plot(alter(28, 5, 2/3, 1/2, 20))
```

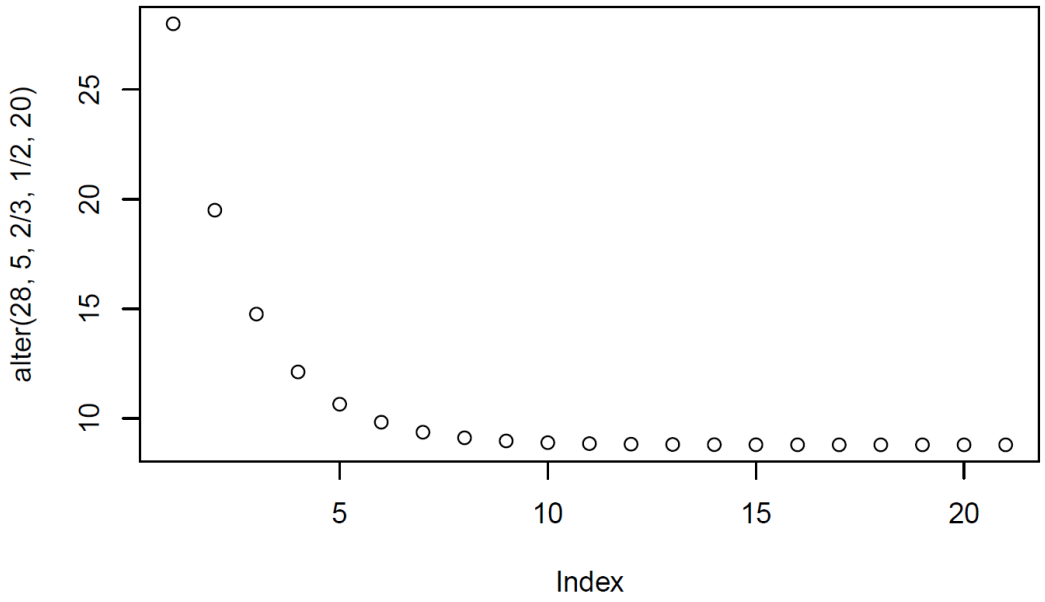

Fig.73: Plot of average frond age depending to partial harvest of 1/3 of the culture every 5d.

Sixth example: harvest 1/3, f=2/3, harvest cycle time **5** days: These comparative runs make the different influences of the mortality on the culture conditions visible, using a maximum average frond age of 28 days versus 56 days.

```
plot(alter(56, 5, 2/3, 1/2, 20))
```

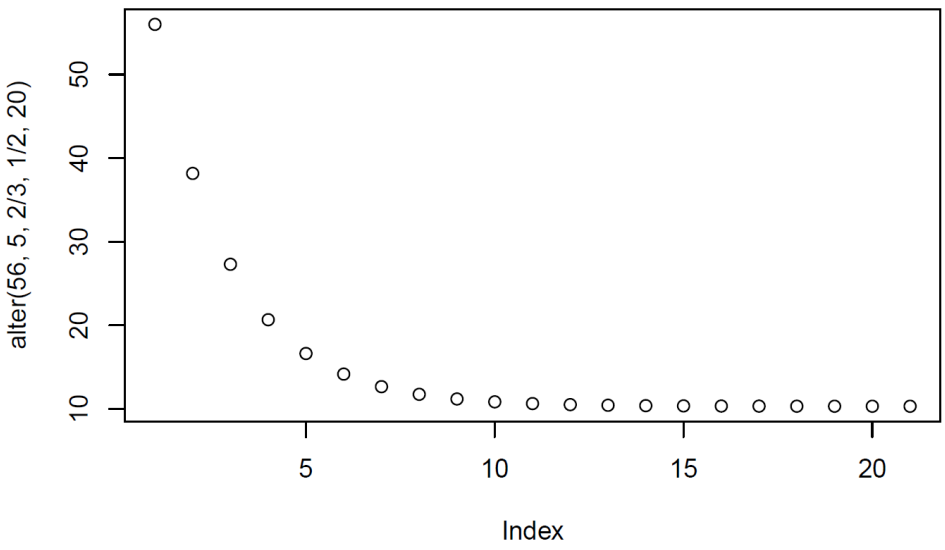

Fig.74: Plot of same conditions like Fig.73, but with assumption of maximum lifecycle of 56d

```
plot(alter(28, 5, 2/3, 8/10, 20))
```

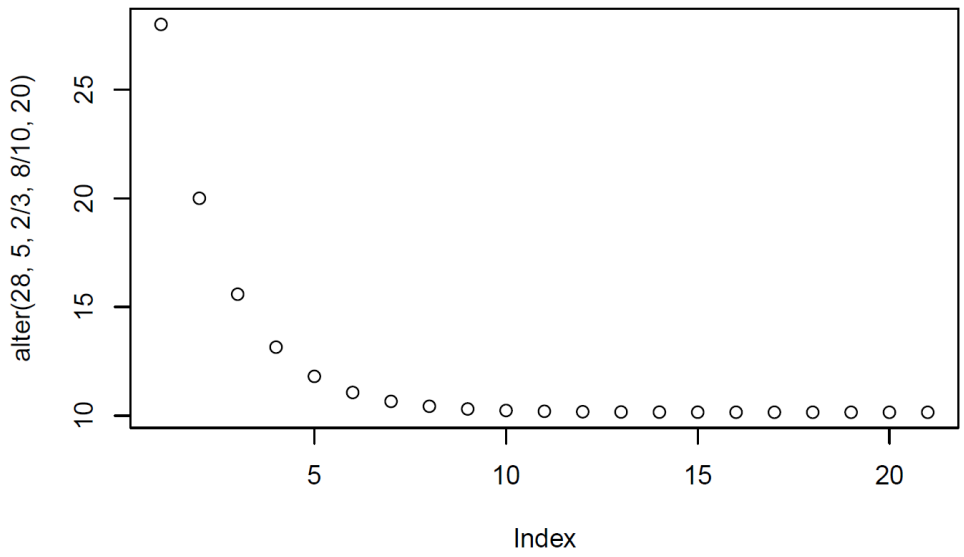

Fig.75: This plot displays only a theoretical case, with check of model validity of assumption of different growth/regrowth dynamics by lower tp in regrowth.

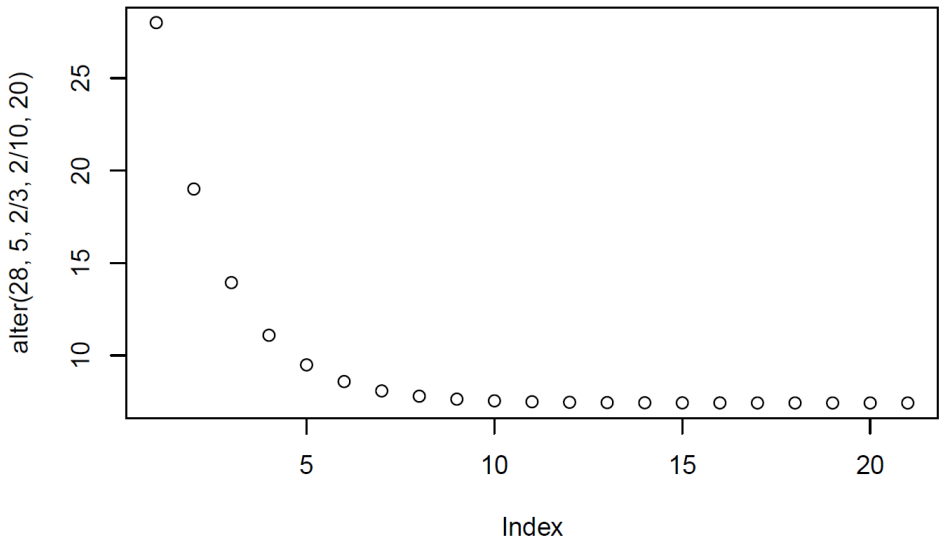

Fig.76: Plot shows the same model assumption as in fig.75 but with higher tp in the growth/regrowth curve.

Thus, between simple and extended AFA model are visible, but marginal. A further result from these runs is that the model runs as such are qualitatively nearly the same for different specific lifetimes of cultured *Lemna* species.

For the application case in the laboratory set-up, the simplified model and the extended model "second application" showed the best match. The reason is also visible: within the first 7

harvests every 3 days, senescence has barely any influence after 28 days if the culture is cultivated for no longer than 28 days.

At this point, it must be emphasised once again that the average age of the fronds could not be determined directly through experimentation. Instead, it was calculated from the constant harvest cycle times and the regrowth obtained after harvesting from the respective time intervals.

5.5.4.1 AFA model results applied to biomass quality.

The following tables show the quality parameters of metal uptake, free oxalic acid concentration and protein content in relation to the model runs of the AFA model. The respective concentrations are assigned to the respective modelled average frond age.

Pure protein content: increased by rejuvenation of the population by repeated (cyclic) harvest.

Tab.21: Average frond age applied to the protein content of cyclically harvested biomass resulted from AFA model (Bradford: Lab set-up Bonn)

Harvest	*AFA (days)*	*% DM (10/90)*	*% DM (20/80)*
1st harvest/status	28	28.5 +/- 0.9	28.7 +/- 0.5
2nd harvest	19	25.3 +/- 1.3	26.8 +/- 0.5
3rd harvest	14	31.9 +/- 1.1	33.8 +/- 1.2
4th harvest	11	28.9 +/- 1.3	31.3 +/- 1.3
5th harvest	9	34.8 +/- 1.20	34.3 +/- 1.3
6th harvest	8	35.6 +/- 1.4	34.0 +/- 1.0

As shown in Tab. 21, the AFA model resulted in a reduction of the average frond age of the harvested biomass from 28d to 8d of the 6th partial harvest, which relates to an increase of pure protein in %DM from 28.5 +/-0.9 to 35.6 +/-1.4, being slightly higher for NH_4^+/NO_3^- = 10/90 ratio.

Free oxalic acid concentration in DM decreased at same time by rejuvenation of the population by cyclic (repeated) harvest, between start of harvesting at an average frond age of 28d down to 8d. Data in tab.22 were obtained by using nutrient solution at 10/90 and 20/80 NH_4^+/NO_3^- ratios at optimum culture conditions as mentioned before. Lowering the average

frond age by repeated partial harvesting every 3d lowered the oxalic acid concentrations for both NH_4/NO_3 ratios, but it was more pronounced at the 10/90 ratio.

Tab.22: content of **free oxalic acid** in cyclic partial harvested biomass versus AFA model (LCMS: Lab set-up Bonn)

Harvest	***AFA (days)***	***µg/g DM (10/90)low-blue***	***µg/g DM (10/90)high-blue***
1st harvest/status	28	124.7 +/- 7.8	169.6 +/- 14.6
2nd harvest	19	65.2 +/- 4.8	103.8 +/- 10.9
3rd harvest	14	71.9 +/- 10.8	68.6 +/- 6.1
4th harvest	11	66.5+/- 3.8	72.3+/- 9.4
5th harvest	9	83.6 +/- 1.8	54.1 +/- 14.7
6th harvest	8	87.30 +/- 7.7	51.0 +/- 6.7

The strongest reduction of free oxalic acid contents by over 40% was obtained at the 10/90 ratio under high-blue irradiation at an AFA of 8d. Compared to the initial value with an AFA of 28d, there was a more than 3 fold decrease.

Dependency of metal accumulation on the average frond age shows a decrease for Mn and Na and a slight increase for Cu, Fe, Ca, and Mg concentrations, while the Zn and K concentrations were not significantly altered.

Tab.23: **Mn** concentration in DM of cyclic partial harvested biomass, depending on the average frond age.

Harvest	***AFA (days)***	***mg/kg DM (10/90)low-blue***	***mg/kg DM (10/90)high-blue***
1st harvest/status	28	1,215.0	1,055.0
3rd harvest	14	747.0	747.5
6th harvest	8	722.0	532.5

As a result, Mn was reduced by -40 to -50% along the continuous partial harvest at an average frond age of 8d.

Tab.24: **Na** concentration in DM of cyclic partial harvested biomass depending on the average frond age.

Harvest	***AFA (days)***	***mg/kg DM (10/90)low-blue***	***mg/kg DM (10/90)high-blue***
1st harvest/status	28	4,775	2,650
3rd harvest	14	2,650	2,250
6th harvest	8	2,250	2,000

A significant reduction of about -50% was also reached for Na at the low-blue light regime by cyclic partial harvesting towards an average frond age of 8d. At the high-blue light regime, the accumulation of Na as such started at a lower level.

Tab.25: **Cu** concentration in DM of cyclic partial harvested biomass depending on the average frond age.

Harvest	***AFA (days)***	***mg/kg DM (10/90)low-blue***	***mg/kg DM (10/90)high-blue***
1st harvest/status	28	9.4	9.5
3rd harvest	14	11.8	12.5
6th harvest	8	13.3	14.0

Cu concentration in DM increased slightly along cyclic harvesting by about 40% but favourably remained at a total low level.

Tab.26: **Fe** concentration in DM of cyclic partial harvested biomass depending on the average frond age.

Harvest	***AFA (days)***	***mg/kg DM (10/90)low-blue***	***mg/kg DM (10/90)high-blue***
1st harvest/status	28	640.00	640.00
3rd harvest	14	737.50	747.50
6th harvest	8	825.00	742.50

Also, Fe concentrations in DM increased slightly along cyclic partial harvesting by about between +16 und +29%, but remained at a safe level for human consumption.

Tab.27: **Ca** concentration in DM of cyclic partial harvested biomass depending on the average frond age.

Harvest	***AFA (days)***	***mg/kg DM (10/90)low-blue***	***mg/kg DM (10/90)high-blue***
1st harvest/status	28	12,8	10,5
3rd harvest	14	21,5	19,3
6th harvest	8	25,0	21,5

Ca concentrations in DM increased along cyclic partial harvesting by about 50% and contributed to the crude ash mentioned above.

Tab.28: **Mg** concentration in DM of cyclic partial harvested biomass depending on the average frond age.

Harvest	***AFA (days)***	***mg/kg DM (10/90)low-blue***	***mg/kg DM (10/90)high-blue***
1st harvest/status	28	3,55	3,15
3rd harvest	14	4,90	4,45
6th harvest	8	5,28	3,75

Mg concentrations in DM increased along cyclic partial harvesting by about +19% for the low-blue, and by +48% for the high-blue light regimes.

Tab.29: **Zn** concentration in DM of cyclic partial harvested biomass depending on the average frond age.

Harvest	***AFA (days)***	***mg/kg DM (10/90)low-blue***	***mg/kg DM (10/90)high-blue***
1st harvest/status	28	99.5	95.3
3rd harvest	14	93.8	101.0
6th harvest	8	92.0	88.0

Zn concentrations in DM remain more or less constant along cyclic partial harvest within given statistical fluctuations.

Tab.30: **K** concentration in DM of cyclic partial harvested biomass depending on the average frond age.

Harvest	*AFA (days)*	*mg/kg DM (10/90)low-blue*	*mg/kg DM (10/90)high-blue*
1st harvest/status	28	59,750	55,750
3rd harvest	14	53,750	49,000
6th harvest	8	55,000	49,000

K concentrations in DM decreased slightly along partial cyclic harvest by about -8.6% for low-blue, and by -13.8% for high-blue.

6. DISCUSSION

6.1 Introduction

In order to feed the world's growing population in the upcoming decades, higher agricultural yields of protein crops for human consumption and animal feed are required. Due to their high protein content and quick growth rates, duckweeds (*Lemnoideae*), which are floating aquatic higher plants, may become more important in the future since the amount of land accessible for farming is expected to decline rather than rise.

Finding the ideal conditions for producing consistently high yields with the quality attributes needed for novel food in a permanent culture was the challenge of the present work.

It is hardly impossible to determine and validate the optimal culture parameters like temperature, CO_2 exposure, amount and quality of light, and nutrient levels all together in a purely experimental approach as there are so many possible parameter combinations. Therefore, a modelling approach had to be developed, too, to optimise the cultivation process.

6.2 Description of the growth of *Lemna* cultures

6.2.1 Growth curve of a population

As shown in Chapter 4 and eq.4, populations develop along a differential equation under limiting growth conditions (*Murray, 2011; Verhulst, 1845; Maltus, 1807; Bacaër & Bacaër, 2011)*. The solution of that differential equation is a sigmoidal curve (e-function with constrained capacity), the so - called logistic function. This curve starts with a strong exponential increase up to a purported "turning point". The most important functional factor in this e-function is the growth rate r_i, which is composed of all growth-relevant variables such as temperature, light, CO_2, and the ratio of macronutrients. Once the exponential expansion reached this turning point, it was halted by the so-called resource damping caused by increasing population density *(Driver et al., 2005)*. This ends asymptotically at the stated capacity of the population. The *tangens hyperbolicus* characterises the growth rates at a given point of curves.

Because there are many individuals per culture (>100,000 per m^{-2}), *Lemna minor* cultures followed this growth curve closely. Therefore, rather than counting or measuring the individua, growth can be quantified by measuring the increase in biomass and not the number of individuals.

Over a long-term cultivation in the experimental set-ups, it has been shown that a continuous partial harvest of the population, accounting for growth before and regrowth after partial harvest, may result in the best yield. The repeated (cyclically) harvested population thus follows a sigmoidal growth curve with a super-imposed sawtooth curve caused by the harvest impact.

As a result, both the associated partial harvest amounts and the ideal partial harvest frequency were based on the cultures' response to the harvest schedule. The optimum fit between harvest frequency and harvest amounts was thus found through modelling and will be explained in the second part of this chapter.

6.2.2 Competition between Lemna and Algae

Preventing the formation of competitive algal biomass is crucial for the ongoing growth of *Lemna* cultures under non-axenic conditions. In all experiments, *Lemna minor* preferred a

slightly acidic nutrient medium around pH 6.5, while algae, particularly *Chlorella vulgaris*, prefer strongly alkaline nutrient media at pH 9 or higher. The prolific growth of algae bears two implications once the pH level rises over pH 8 and 9. First, the growing algal population outgrows the *Lemna* population and especially raises pH during the light phase. Second, a larger population of algae competes for nutrients. As a result, the *Lemna* population gradually declines, and might even die off completely.

We found that *Lemna* grows quickly while the algae are suppressed when the temperature is maintained at its optimum of 29°C, the total N concentration is kept low, the pH constant in the weakly acidic range, and light adjusted even below the saturation point.

6.2.3 Influence of harvest frequency on average age of the fronds in a population

A life span of *Lemna minor* until its senescence was found to be 29d on the average. But different species of the *Lemnoideae* group have different life spans. As an example: for *Lemna gibba*, average life span was found to be 52d *(Chmilar & Laird, 2019; Barks & Laird, 2014), and Barks et al. (2018)* mentioned a life span of 23d for *Lemna turionifera*. This means that, the specific total biomass for *Lemna* that can be determined within the life span of 29-30d while the specific total biomass for *Lemna gibba* is reached over 52 days.

Harvest frequency (repeating harvest intervals) and harvest quantity are linked, as was previously mentioned in Chapter 4.1.5 and Fig.19, and have an impact on the population's average frond age. When starting to harvest of a population after it grew to fully cover the surface, the fronds had a relatively high average age of around 28 days, which is near the maximum life time. The population is encouraged to regenerate and replace the harvested individuals as quickly as possible until the next harvest occurs, for example, every three days. Therefore, the average frond age of the new regrowth, is between one and three days. The resulting model calculations demonstrate how quickly the average frond age of the total population decreases if this is continuously repeated. The quality of the resulting biomass is significantly influenced by this decrease in average frond age, like further discussed below.

6.2.4 Influence of environmental parameters (temperature, light, CO_2, pH) on growth

Temperature

According to *Docauer (1983)* and *Lasfar (2017)*, the optimum temperature for growing *Lemna minor* is approximately 29°C. In the presented model, we obtained a temperature factor: if the temperature drops from 29°C to 20°C, this factor (see eq.6) indicates a decline by around -30%. *Lemna's* growth drastically decreases at temperatures below 20°C, and completely stops below 10°C. The temperature occasionally went out of the chosen settings in the up-scaled set-ups in Kalkar and Berlin, but usually it still ranged within roughly +/- 5 K (°C). The growth rate in these up-scalings was therefore far more erratic, compared to the optimum conditions on the lab scale. As previously stated, competitive algal growth is supported by any deviation from the optimum parameters. In other words, the more *Lemna* growth was promoted by keeping conditions close to optimal parameter levels, the more algal growth could be suppressed in the culture.

Light

Photosynthetic C-fixation as depending on light intensity varies between species. It is characterised by a particular saturation point. As *Lemnoideae* are C3 plants *(Bauer et al., 1976; Wedge & Burries, 1982; Bauer & Martha, 1981; Bauer et al., 1983),* raising CO_2 levels can effectively increase their carbon fixation, even more so by being an aquatic plant where stomata remain permanently open.

One might assume that the same photon-flux-densities would produce the same growth. But in the experiments rates with the identical PAR values but varying amounts of blue light at 440 nm, the biomass DM rose by almost 10% at the 3:4 ratio of 440 nm/660 nm ("High Blue") as opposed to the 1:4 ratio ("Low Blue"). The increased photonic energy at shorter wavelengths can be made responsible for this effect. However, to avoid algal development, light was restricted to 129µmol $m^{-2}s^{-1}$ in the experiments.

CO_2

Adult *Lemna minor* may continually absorb CO_2 because they cannot close their stomata, without experiencing drought stress as an aquatic species. This is consistent with *Frost-*

Christensen & Floto's (2007) investigation of aquatic plants' cuticular membranes' resistance to CO_2 diffusion and its implications for CO_2 acquisition. *Lemna minor* is a floating macrophyte rather than a submerged one *(Zeiger et al., 1987; Borisjuk et al., 2018; Le, 2010).* As a result, mesophyll resistance is the only flux resistance that limits CO_2 uptake and transfer through the constantly open stomata. Once *L. minor* forms multilayered covers, the fronds tilt so that channels (ducts) are formed between them, allowing gas diffusion, even with up to 7 layers (see chapter RESULTS, Fig. 40). This indicates that the lower echelons of the culture are not fully submerged and still exposed to an air layer.

It was demonstrated that the growth rate r_i rises with increasing CO_2 concentrations. An average photon-flux-density PAR of around 129 $\mu mol \bullet m^{-2} \bullet s^{-1}$ already exceeds 90-95% of the saturation (Γ-point), as demonstrated by *Docauer (1983)* and *Landolt (1987)* and validated by the experiments of this work. A possible increase in light saturation at higher CO_2 concentrations could be postulated, even if it could not be assessed in the current experiments, as higher light levels would cause a large rise in the co-population of *algae*. If the algal growth increases, the regrowth rate of *Lemna* decreases as indicated by a reduced biomass. Running cost-benefit analyses for energy input and yield, the potential gain by light intensities near the saturation point would only increase CO_2 fixation by about 5%. This is almost neglectable compared to the increase by about 60% with CO_2 concentrations increased to about 3000 ppm. There is as well an influence of N nutrition on the photosynthetic gain: the DM content for an NH_4^+/NO_3^- ratio of 2:8 was about 6% greater than at an NH_4^+/NO_3^--ratio of 1:9 at a CO_2 concentration of 400 ppm. At 3500 ppm CO_2 and a NH_4^+/NO_3^--ratio of 1/9, FM yield was raised by roughly +46%. As the dry matter content increased as well from 5.4% to 6.9% TS, the total DM yield was raised by even +59%.

It could be observed that a change from light green to dark green occurs under low light conditions. It can be interpreted that this relates to *Lemnoideae*'s low light tolerance, indicating that there are more stacks per grana in their thylakoid membrane. Granal stacks may allow PSII from neighbouring stack membranes to unite vertically with a light harvesting antenna, increasing the antenna's effective cross-section without obstructing the diffusion of PQ (plastoquinone) *(Mullineaux, 2005). Gu et al. (2022)* came to the conclusion that light conditions can affect the number of grana stacks and the size of each thylakoid. *Jia et al. (2012)*

and *Chow et al. (2012)* had previously shown that leaves may grow massive grana to adapt to low light levels, and this was in line with their findings *(Colpo et al., 2023)*. PSII supercomplexes frequently generate protein arrays under low light, which may be a tactic to avoid molecular crowding *(Kirchhoff et al., 2007; Krysiak et al., 2025).* The photo-protective xanthophyll species in the membrane and the tiny lipophilic electron carrier PQ may diffuse more easily thanks to the lipidic channels in the arrays *(Tietz et al., 2015)*.

Since this work produced high and sustained yields under the specified low light conditions, these aforementioned literature data indicate a positive effect on specific processes in the PS system of *Lemnoideae,* coinciding with the efficiency of *Lemna* spp. in photosynthesis.

A special case was the root growth of *Lemna minor* under nitrogen deprivation at a high CO_2 concentration of 2,400 ppm. While their roots are typically between 10 and 20 mm long, the cultures showed root lengths of about 50cm after just 12 days of N-deficit, as seen in Fig. 39 (Chapter 5). In a review, *Sun et al. (2020)* mentioned root elongations under N-deficiency. The authors came to the conclusion that the nitric oxide signalling pathways and many phytoregulators act in a synergistic or antagonistic way to cause crop root elongation. However, it is still unknown for *Lemna* how a higher CO_2 concentration plus N-deficit might cause a 25–50 fold increase in root elongation.

pH

To keep the pH level constant around 6.0 - 6.5 is of paramount importance for long term *Lemna* production with the aim to minimize algal growth in our axenic cultures. Thus, rapid and strong pH variations have to be avoided. A rapid rise in pH was observed with a high N_{total} concentration at more than 2 mM N. Algal growth was then strongly enhanced, particularly under long-term cultivation for longer than four weeks. To maintain the pH constant over a longer time, the N_{total} concentration should not exceed 1.14 mM. Thus, N (and other nutrients) uptake by the culture had to be compensated by adding N (and other nutrients) twice or three times a day. Thus, the N level could be kept almost constant at the relatively low concentration (compared to other recommendations: *Appenroth, 2015; Appenroth et al., 1996)* and minimize competing growth of algae (see as well 6.2.5.).

6.2.5 Influence of nutrients on growth

For a continuous growth of *Lemna* cultures under non-axenic conditions it is of utter importance to prevent the growth of competing algal biomass. As pointed out above, a low total N concentration and a constant pH in the weakly acidic range support a fast growth of *Lemna* while suppressing the development of competing algae. This explains why the NH_4^+/NO_3^- ratio of 1:9 produced the best results; it maintained the pH constant at the desired level of about 6.5, while higher nitrate levels caused the medium to become alkaline. The similar ratio was utilised by *Appenroth (2015)* although his overall N level was eight times higher. According to our observations, under non-sterile conditions other than in the case of *Appenroth (2015)*, this would quickly result in a tremendous algal bloom.

Nutrient solutions for *Lemnoideae* mostly indicated in the literature deviate often distinctly from the optima found in the present study. As mentioned above, compared to the concentration of N_{total} of 1.14 mM as found to be optimum in our studies, partly, most other nutrient solutions *Hoagland&Arnon (1938), Schenck&Hildebrandt (1969), Steinberg (1946)* and N-Medium, considered in *Appenroth (2015)* and *Appenroth et al. (1996)* use significantly higher N concentrations (Tab.31). Due to the refeeding nutrients twice to three times a day the growth of our cultures was highly prolific, preventing deficiencies, while the aforementioned authors mostly changed nutrient solutions at much larger intervals or just grew *Lemna* spp. just once and/or under sterile conditions. A significantly increased growth by rising CO_2 concentrations in turn increases the demand for nutrients which has to be taken into account when growing *Lemna spp.* in continuous cultures.

Tab.31: Comparison of most recently used nutrient solutions in literature versus optimization in this work (Used Salts in detail see appendix Tab.35).

	Hoagland	Mod. Steinberg	Schenck-Hildebrand	N-Medium	Schmidt KM
Elements	**mM**	**mM**	**mM**	**mM**	**mM**
N (NO_3^-)	18	5.96	13.8	10	1.04
N (NH_4^+)	-	-	1.3	-	0.1
P	1	0.73	1.3	0.15	0.23
K	1	0.80	12.4	8.15	0.73
Mg	2	0.41	0.8	1.0	0.4
J	-	-	0.003	1.0	-
S	2	1.04	0.8	1.0	0.45
Ca	4	1.25	0.68	1.0	0.52
	µM	**µM**	**µM**	**µM**	**µM**
B	50	1.94	40	5	46
Mn	10	0.91	30	13	9.15
Cu	0.4	-	0.4	-	0.32
Zn	1.5	0.63	1.74	-	0.77
Mo	5	-	0.2	0.4	0.58
Co	-	-	0.21	-	-
Fe	20	2.81	26	25	18
Cl	20.4	1.82	-	26	18.3
Na	-	2.44	-	50	1.16

Lemna minor is a low light tolerant plant *(Quingyang Zhou et al., 2017; Bloom-Zandstra, Lampe, 1985)*, and thus it uses nitrate as an energetically "cheap" osmoticum. Like in many other low light tolerant plants this may as well result in a massive accumulation of nitrate, which is prohibitive when duckweed is considered for human or animal nutrition. *Devlaminck (2020)* gave evidence that, at a nitrate concentration of about 9mM, luxury uptake of NO_3^- into the vacuoles of *Lemna* cells increased significantly. *Appenroth et al. (2017)* formerly used a NH_4^+/NO_3^- ratio of about 1/9, but at a significantly higher N_{total}, as in a modified Schenck-Hildebrand nutrient solution of about 15mM NO_3^-. Such high NO_3^- concentrations can only be operated under axenic culture conditions due to the otherwise dominating algal growth.

Since *Lemna minor* is low light tolerant, an efficient energy transfer is of paramount importance especially under low light conditions. Thus, P supply plays an important role for optimum growth rates, *Budde & Chollet (1988).* Over a series of harvests, the highest continuous yield was obtained at a N/P ratio of 5:1. In the present study, this ratio kept the pH at an optimum level of 6.5, even under an elevated CO_2 level of 3,500 ppm at 29°C, where

we obtained a FM growth of 300gm^{-2}d^{-1}. Compared to *Appenroth et al. (2017)*, who maintained a N/P ratio of roughly 12:1, this ratio is lower. Lemna had far greater P absorption rates at the same N/P ratio of roughly 5/1, according to data from *Paterson et al. (2020)*.

Lemna minor needs a rather high amount of K. Thus, a N/K ratio of 1:0.64 resulted to be the optimum for growth, which could be shown by K concentrations remaining constant in the nutrient solution when being continuously replenished.

Mg concentration seems to be especially relevant for *Lemna minor* under low light conditions. This may not be surprising, since the major function of Mg is his role as central atom in the chlorophyll molecule. Since *Michael (1941),* it has been manifested that the proportion of the total Mg bound in chlorophyll depended on the supply of Mg. Under low light conditions, the proportion of the Mg bound in chlorophyll was >50% higher *(Dorenstouter et al., 1985)*. As shown by *Cammarano et al. (1972)*, Mg has an essential function as a bridge element for the aggregation of ribosome subunits and thus the protein synthesis, which was one of the main factors to be optimized in the present work. Besides, Mg^{2+} is required as a cofactor in all ATP requiring processes. It also had to be considered that high K concentrations competed with Mg by dissociation of subunits, which could lower protein synthesis rates *(Xie et al. 2021).*

The concentrations of the micronutrients B, Cu, Zn, Mn, Fe, Mo in the presently used nutrient solution are largely based on the most currently recommended concentrations in pertaining publications.

Partial harvest amplitudes (amount) at repeated (cyclic) harvest intervals (i.e., the time of regrowth until the next harvest) caused a significant decrease in the accumulation of the main critical micronutrients, such as Mn and Zn, which should not exceed the critical levels for food consumption (see Tab.32, Mn<102µg/g, Zn<340 µg/g DM, *(European Commission, Directorate-General for Health and Food Safety, 2025)*). As Mo did not accumulate, and as we could not observe any signs of deficiency, Mo can be added at the actually used concentration. *Khellaf & Zerdaoui (2009)* determined the toxic limits for *Lemna* as 3.1µMol/l for Cu and 1.5µMol/l for Zn. With 0.32µMol/l for Cu and 0.77µMol/l for Zn, we stayed significantly below these toxic limits, neither observing deficiencies nor toxicities.

Consequently, the replenishment of Fe must be adjusted to match the actual demand. Nevertheless, the uptake itself is known to be highly regulated in higher plants *(Cornelis et al., 2009; Kobayashi & Nishizawa, 2012)* to prevent toxic levels being reached physiologically. For this reason, it was important to determine the limits of Fe deficiency experimentally.

Fe deficiency was found at 4 µM, resulting in a significant 21% decrease in biomass (FM). This was verified to be independent of the two different light regimes LB (Low-Blue) and HB (High-Blue). While the concentrations of Mn, Zn and Cu are lower in younger fronds, the concentration of Fe was higher by about 29%. Furthermore, increases in both iron concentration and pure protein content occurred together through repeated partial harvesting.

The primary function of B is to enable the cross-linking of the pectic polysaccharide RG-II within cell walls *(Kobayashi et al., 1996; Ishii & Matsunaga, 1996; Ishii et al., 1999; O'Neill et al., 2001),* where over 90% of the RG-II in the plant cell wall is cross-linked by a borate bridge *(O'Neill et al., 2004; Matsunaga et al., 2004).* Thus, especially young differentiating tissues show the highest B demand, where withholding B leads to cell wall alterations within minutes *(Findeklee & Goldbach 1996).* There are indications as well that some of the B acts at the level of the plasma membrane and the cytoskeleton of the cell *(Bassil et al., 2004; Voxeur & Fry, 2014; Wimmer et al., 2009, Yu et al., 2003, 2001)*. According to *Findeklee & Goldbach (1996), Goldbach et al. (2001), Yu et al. (2003),* and *Cakmak & Römheld (1997)*, an accumulation of phenolics under B deficiency is also typical for many plant species. However, it was assumed in this work, considering *Cakmak & Römheld (1997)*, that a phenol accumulation in B-deficient tissue may have adverse impacts on plants, particularly during the reproductive growth stage with a long-term exposure to high light intensity. The changes in the calyptra of *Lemna minor* (Fig.35, 36) have not been reported yet and are quite striking, and may be related to both, the role in RGII cross-linking as well as acting on the cytoskeleton and/or plasmalemma.

While a clear reduction in biomass yield is visible under both light regimes (low-blue and high-blue) under Fe deficiency, B deficiency only reduced growth at low-blue (I(440nm)/I(660nm) = 1/4). At high blue light (I(440nm)/I(660nm) = 3/4), no effects of B

deficiency were observed. It should be noted that both deficiency experiments were performed under otherwise optimal nutritional conditions with an additional CO_2 supply of 3,500 ppm. It could be assumed that increased irradiance of the blue line at 440 nm results in more photonic energy being consumed by an increased CO_2 fixation rate. At high blue irradiation, the effects of B deficiency on biomass were not significant.

6.3 Influence on quality characteristics

The quality of the biomass is another priority, in addition to optimising crop yields for a continuous production. The working hypotheses state that the aim was to comply with the EFSA's Novel Food standards for *Lemna minor* while maximising nutritive elements and avoiding anti-nutritive components.

The average frond age, N_{total} concentration, NH_4^+/NO_3^- ratio, oxalate/oxalic acid and heavy metal accumulation were the main factors that determine quality.

It was demonstrated that a key factor influencing quality was the average frond age, which was highly altered by repeating partial harvesting of the culture population as mentioned before. The continuous harvesting of one third of the *Lemna* biomass prevents the accumulation of older fronds and thus most of the population remains in a more juvenile stage.

Lemnoidea are considered as rich sources of proteins, and literature studies often report amounts considerably above 40% in DM. This can be misleading if the values are based on merely the determination of total N, multipled by a constant factor (typically 6.25), to yield the crude protein content.

In the present work, the pure protein content was determined acc. to Bradford. According to *Jones et al. (1989),* using the series of triplicates, the problem with the calibration to plant protein could effectively be solved by using spikes for recalibration. As a result, the pure protein content was measured in the present work instead of crude protein.

6.3.1 Novel Food requirements

Minimizing anti-nutritive factors: oxalic acid, heavy metals, and Na:

Heavy metal and oxalate/oxalic acid levels must be kept within the following limits for human consumption, particularly when it comes to novel foods:

Tab.32: Metal concentrations accumulated from the nutrient solution in µg/g from EFSA 2023/2025 *(European Commission, Directorate-General for Health and Food Safety, 2025)* for a mix of *Lemna minor* (0-30%) – *Lemna gibba* (70-100%), compared to pure *Lemna minor* from the present work of the 1st and 5th harvest, relating to DM.

Metals	Mix *L. gibba/L.minor*	*Lemna minor 1st harvest* [µg·g^{-1} DM]	*Lemna minor 5th harvest* [µg·g^{-1} DM]
Mn	< 102	952	532
Zn	< 340	80	92
Fe	< 901	663	855
Cu	< 42	10	13

For the elements Mn, Zn, Fe, and Cu, the pure *Lemna minor* grown in our experiment is still within the EFSA standards, as seen in Tab. 32. The only element above the allowed level is Mn. The Novel Food regulation only considers a mixture of *Lemna gibba* and *Lemna minor*. As a result, there is no way to compare the pure *Lemna minor* biomass of the present work. Moreover, it can be assumed that the EFSA test volumes were not generated in a cultivation setting that maximised yield. Mn deficiency was not examined in this work, but it can be expected that, if Mn concentration were reduced in the nutrient solution to its minimum level for sufficiency, the EFSA recommendations might most likely be met also for pure *Lemna minor* biomass.

As oxalate consumption has been connected to kidney stone development, oxalic acid concentration is limited in food safety regulations *(Prezioso et al., 2015; Taylor & Curham 2013).*

Tab.33: Oxalic acid concentrations in µg/g DM from *Vanhanen (2016)* for several mixes of green smoothie juices and for spinach (*Mirahmadi et al. 2022*), compared to pure *Lemna minor* from this work from the 1st to the 5th harvests and the EFSA recommendation.

*,**green fruit-juice mix, FJ1, FJ2 *(Vanhanen, 2018)*.

Oxalic acid	Green mix smoothies [µg·g^{-1} *DM*]	*Lemna minor 1st harvest* [µg·g^{-1} DM]	*Lemna minor 5th Harvest* [µg·g^{-1} DM]
FJ1*	130	170	51
FJ2**	830		
Spinach	65-129		
EFSA	<1,900		

To meet oxalic acid EFSA standards, the oxalic acid concentration of *Lemna minor* could be reduced very effectively by repeated (cyclic) harvesting. Thus, the oxalic acid concentration remained far below the levels allowed in green mix smoothies as examined by *Vanhanen (2018),* same as for spinach *(Mirahmadi et al., 2022).*

As *Lemna* spp. fronds age, both the synthesis of free oxalic acid and the buildup of calcium oxalate increase *(Mazen et al., 2003)*. Reducing the average frond age was shown to drastically reduce the oxalic acid concentration in *Lemna* biomass (by 34% under low blue light and by 64% under high blue light).

Increasing the NH_4^+/NO_3^- ratio from 10/90 to 20/80 in the nutrient solution, a greater NH_4^+ ratio typically lowers the content of organic acids in plant tissues *(Franceschi, 1987)*. The glycolate oxidase pathway to oxalic acid was functional, and the product was available for crystal formation, according to *Franceschi's (1987)* analysis of the metabolism of oxalic acid and calcium oxalate production in *Lemna minor*. Later, *Franceschi (1989)* discovered that the production of calcium oxalate in *Lemna minor* is a fast and reversible process that depends, among other things, on (cytosolic) Ca^{2+} activities. Additionally, it was demonstrated by *Bong et al. (2015)* that Ca decreased spinach's soluble oxalate content. *Kazumi (1996)* documented that in *Lemna minor*, D-glucosone is converted to L-ascorbic acid and oxalic acid. According to a time course research on *Lemna* pulse - labelled with D-[1-^{14}C)]glucosone, the rise in oxalate is almost equal to the reduction in labelled L-ascorbate. *Kazumi (1996)* postulated that D-

glucosone in *Lemna* converted L-ascorbate to oxalate without the presence of glycolate or glyoxylate as intermediates.

Our findings suggest that the percentage of blue light in the entire spectrum may have an impact on the quantities of free oxalic acid. According to *Kostmann et al. (2001)* and *Keates et al. (2000)*, additional research should examine if the ratio of I(440nm)/I(680nm) influences the synthesis of L-ascorbic acid. Dry matter contents increase by around 30% from the first to the fifth harvest when CO_2 levels are raised to 3,500 ppm. Meanwhile, there is a 64% drop in the oxalic acid content. The amount of dry matter in the *Lemna* culture rapidly dropped within just three days after reducing CO_2 to ambient levels of 400 ppm between the fifth and sixth harvests once more, while the concentration of oxalic acid remained low.

The *soluble* oxalic acid concentration of various green juices in pulps from fruit mixes was measured by *Vanhanen (2018)* (pp. 67–73). For green fruit mix juices, the values ranged from about 130.7µg•g^{-1} (FM) to 828.5µg•g^{-1} (FM), whereas for discarded pulp, the values ranged from approximately 292µg•g^{-1} (FM) to 1,262.5µg•g^{-1} (FM). Even though the average DM content of *Lemna* fronds was 7% (at 3,500 ppm CO_2), the oxalate levels remain at or below the range of fruit juices, with a maximum of 169.7µg•g^{-1} being decreased to 51µg•g^{-1}.

Therefore, by optimising growth conditions and harvest schedules to maintain the fronds at a relatively juvenile state, Ca-oxalate/oxalic acid levels in *Lemna* can be maintained at levels safe for human consumption.

The use of drinking water or H_2O_{demin}, indoor farming conditions (non-axenic), and mineral fertiliser are the key processes to meet the HACCP standards.

As it has been shown, ongoing regrowth following many harvests shifts the *Lemna* population towards more juvenile fronds in the culture. As juvenile fronds have much lower **Mn** contents, the criteria for Novel Food regulations can be met. The Mn concentration in the nutrient medium has to be adjusted, though, that the repeated harvesting assures the minimum Mn demand, which is crucial i.a. for photosynthesis, particularly for *Lemna* as a low light tolerant plant.

For **Na**, the same outcome was achieved. In young fronds, the Na concentration is about 50% lower than in old ones. This is in line with other findings *(Liu et al., 2017)* which show that

Lemna tends to hyperaccumulate Na with increasing age, resulting in salt stress at concentrations over 10–100 mM NaCl. The maximum absorption reached unexpected quantities of almost 4000 mg/kg DM maximum although the concentrations of Na in the nutritional solution reported in the literature were very low. This indicates that *Lemna* has a high predisposition towards hyperaccumulation of Na.

Given use of *Lemna* spp. for Novel Food and human nutrition in general, it is crucial to combine a low-Na and high-K diet to maintain a low Na/K ratio in the diet in order to effectively control blood pressure and lower cardiovascular events *(Kim et al., 2024)*. *Lemna minor* can meet this requirement, especially when harvested in a way to keep fronds age low.

Lemna minor's **K** concentration is remains largely constant, irrespective of harvest cycles and average frond age. This applies for **Zn** too. One has to take care, though, that all the material which comes into contact with the nutrient solution, including the rain water cistern should not release additional Zn. Both, nutrient solutions as well as distilled or rain water, are able to corrode galvanized surfaces and thus can be loaded with toxic Zn concentrations.
K has a major effect on turgor formation, osmoregulation *(Marschner, 2012, Chapt 6.6.6; Kanai et al., 2007)* and enzyme activation energy *(Gajdanovicz et al., 2010; Peoples & Koch 1979).* Additionally, K is a co-factor in the synthesis of proteins. It has been shown that photosynthesis is significantly reduced under a K shortage. *(Wyn Jones et al., 1979)*. Moreover, an effective C fixation depends heavily on a sufficient K supply.

After six partial harvests, younger fronds had higher levels of Cu, Mg, and Fe compared to the 28d old population at the beginning of the experiment. After six harvests, the average frond age was determined to be 4 days. Since the absolute concentration of Cu, which is between 6 and 13 mg/kg DM, is low and non-toxic, this just reflects the necessary uptake. It complies with the Novel Food Use criteria for human consumption (see tab. 32). By the way, the *WHO (2004)* and *Coad & Pedley (2014)* both strongly advise adequate iron absorption to prevent anaemia, particularly in women.

Juvenile fronds were found to have 100% greater **Ca** contents, while the concentration of oxalic acid was lowered to half of its initial level in the “younger” populations after repeated frequent harvesting compared to the “old” population. It is assumed that calmodulin functions as a transporter to the so-called specialised idioplasts for precipitating Ca^{2+} as calcium oxalate

(Foster, 1956), (Mazen et al. 2004), (Thor, 2019), (Francesci & Schuren, 1986), (Francesci, 1987), (Francesci, 1989), (Li & Francesci, 1990), (Francesci, 2001), (Francesci, Horner, 1979), (Ledbetter & Porter, 1970). This suggests that Ca detoxification occurs quickly and effectively in *Lemna* spp.. Therefore, in order to maintain the resulting calcium oxalate concentrations according to the Novel Food criteria, the amount of Ca should be restricted. Repeated harvesting in about 3 to 4 d intervals in addition helps to maintain oxalate levels within a safe range.

Although the nutrient concentration of 0.4 mM Mg was shown to be the optimum, this is at the lower range of 0.4 – 2 mM documented in the literature (see Tab.31). However, the nutritional solutions from the literature that use much greater total K concentrations also have higher total N concentrations, ranging from 7 to 14 mM. In addition, often the nutrient solutions were kept for a long time without replenishing the nutrients that have been taken up, in contrast to the present approach where nutrient uptake was compensated up to three times a day. *Kurvits&Kirkby (1980)* had already showed that other cations, primarily K^+, could suppress the uptake of Mg^{2+}. *Dölger et al. (2024)* updated and confirmed this for total K concentrations.

Optimization of nutritive factors: protein content and fatty acids:

At a ratio of NH_4^+/NO_3^- of 1:9, the pure protein content under the ideal harvest schedule approached 35.6% starting with the fourth harvest. The maximum levels of pure protein might be achieved by optimising additional factors like temperature, other nutrients, light, and CO_2. Higher protein concentrations were also documented in the literature, although these reports were mostly based on total N concentrations *(Petersen et al., 2021; Petersen et al., 2022)*.

Most amino acids, including lysine, phenylalanine, leucine, valine, and aspartic acid, also rose with a lower average age of the fronds (harvests 4 to 6 in our experiments, Fig.45 in chapter 5.3.1.)). The same should apply for upscaled set ups, too.

C18:3 alpha-linolenic acid (Ω3) was around 60% greater in the younger fronds, and since C18:1 oleic acid (Ω6) stayed constant, the high Ω3/Ω6 ratio is advantageous for both human and animal nutrition.

Lemna minor had 38.5 and 1,590µg/100g of vitamins B12 and K1, respectively. *Watanabe (2007)* discovered that fishmeat has a B12 value of approximately 42 µg/100g, which is almost the same for *Lemna minor*. Furthermore, biotin was found at a concentration of about 32µg/100g, which is comparable to nuts like almonds and greater than that of fish meat *(Watanabe et al., 2014)*. *Bogacz-Radomska & Harasym (2018)* reported that the beta-carotin content was approximately 7.8 mg/100g, which is close to the 9.9 mg/100g found in carrots. Given the much less sturdy cell walls in the aquatic plant *Lemna* spp., the nutritional availability might be even better, especially when the food is not processed much. This has to be shown, though, by feeding studies of perch, which were beyond the scope of this thesis.

In summary, the average frond age is of great importance for both the nutritive and anti-nutritive characteristics. Therefore, the notion that optimal harvest intervals can affect the average frond age of *Lemna minor* in order to produce a maximum protein content while minimising the accumulation of anti-nutritive elements could be fully confirmed in every setup.

6.4 Modelling

6.4.1 Model approach

When cultivating *Lemna minor* with more than 100,000 individua per m^2, a multitude of culture parameters must be determined and optimized. Accordingly, the culture system is a mathematically rigorous and robust system with predictable high accuracy under steady *in vivo* conditions. The resulting vast number of potential permutations can only be handled with numerical modelling. Several models were created in total.

To calculate the growth rate r_i, the first model (LOM) records the ideal temperature, the ideal NH_4^+/NO_3^- - and the N/P ratio, the dependence on light, and the dependence on CO_2 concentration. The extended growth model (main model) is then used to establish the ideal harvest intervals and amplitudes (partial harvest quantities) based on the growth rate r_i that was calculated in this manner. As seen, since the plant-specific capacity (W_{max}) is the key term in the differential equation for limited growth, it must be provided as an input value for the modelling together with the pertinent curve for the analytical solution. This is

applicable to any possible enlargement of the cultivated area. Furthermore, coverage and capacity are essential for determining the actual potential yields.

6.4.2 Comparison of the model with other model approaches

It has been shown that, in contrast to recent research such as in *Femeena et al. (2023)* and *Petersen et al. (2022)*, accurate modelling requires consideration of all experimental setup boundary conditions. This includes a thorough understanding of the capacity (maximum cover) on a growth area *(Drievers et al., 2005)* which must be entered as the crucial number W_{max} into the model equation, as well as a precise analytical solution of the differential equation of the sigmoidal growth curve. The sigmoidal growth curve as such could be confirmed by any of our experiments. The growth rates reported by *Petersen et al. (2022)* and *Femeena et al. (2023)* were expressed as relative growth rates, calculated as an average between a single end harvest point and a starting point. In contrast to that, we determined the point of maximum growth by curve discussion of the analytical solution of the sigmoidal curve, at the turning point tp. This turning point is located at half of capacity (W_{max}) of the culture and indicates the point of the highest growth rate.

6.4.3 Consistency of model results and real data

Related to the findings by *Driver et al. (2009)* exponential growth of *Lemna minor* is slowed down by resource limitations, and ends when reaching maximum culture density (capacity). Along a sigmoidal growth function, every point is related to dn and is proportional to the current n status value. The value of n is then the total current number of individua at any moment, and not an average of the densities at the beginning and the harvest. Working with this yields a significantly higher accuracy in describing the real population growth process. By treating the harvest around tp as a point of maximum growth rate, and keeping the cyclic harvesting process will provide a maximum stimulation for the population to grow constantly with a maximum possible growth rate. Only this results in a maximum yield integrated over time.

Most important for appropriate modelling is to consider all growth-influencing parameters to obtain the proper growth rate r_i. Similar to the most essential nutrients, photonic energy, CO_2, and temperature were considered as a mathematical product rule for the resulting growth rate r_i (see eq.14). The analytical solution opened the possibility of a detailed curve

discussion, not only obtaining the point of maximal growth, but also to find further ranges like maximum harvest amount (harvest amplitude) around tp, obtained by the second derivation of the growth function. This limit resulted as 53% of the capacity (W_{max}). The proper definition of boundary conditions was most relevant for the numeric modelling.

The highest growth rates were obtained in the non-axenic culture under the following completely controlled conditions on a lab scale in Bonn:
215$gm^{-2}d^{-1}$ at 400ppm CO_2, and 323$gm^{-2}d^{-1}$ at 3,500 ppm CO_2.

The model achieved this as a prediction with 96% accuracy at lab scale. So far, in upscaled set-ups, the *in vivo* conditions have not reached the optimum for any parameter. Nevertheless, the drop in final yield could also be predicted with high accuracy. The misfit from the optimum could then be reduced using feedback control, for example by increasing the culture temperature and adjusting the quantity and quality of light.

These values could be obtained in upscaled set-ups since the aforementioned *in vivo* conditions could be controlled to be near the optimum value. It was shown in detail that yield loss could be predicted precisely when temperature, CO_2, or photonic energy were above or below the optima. This consideration results in the aforementioned product rule for all the individual contributions to the growth rate.

Tab.15 in chapter 5 resulted from modelling for all possible permutations and combinations of the culture parameters used in this study. For each set of parameters, a specific growth rate r_i was obtained. With these resulting values for r_i, each set-up could be simulated by the model. The resulting models were compared to the most relevant measurements of the set-ups. A comparison of the model with all experimental set-ups for lab-scale and for the 1st and 2nd upscales resulted in different coefficients of determination R^2.

The model prediction for lab-scale reached the highest accuracy between model and reality with a value of $R^2 = 0.96$. That means that the model nearly perfectly describes the reality at the lab-scale with fully controlled conditions.

For the 1st upscaling of a stacked culture system installed in the fish culture section of the ETF aquaponic system in Berlin, the obtained value was $R^2 = 0.92$. This shows a high accuracy for an up-scaled set up. Nevertheless, the chosen parameter set resulted in a slight

underestimation of r_i. This can be explained by more fluctuating and slightly lower temperatures under these conditions. With less fluctuations of temperature, the R^2 value would have been even higher. In the 2nd up-scaled system at Kalkar, the correlation coefficient was much lower with $R^2 = 0.58$. The unexplained part can be attributed to much higher fluctuations in the environmental conditions, e.g. temperature. This resulted in over- and underestimations over the cultivation period. The reasons were a drop of temperature during the night and a high hysteresis in temperature control. In the mornings the culture solution only heated up very slowly. Likewise, there were as well periods with overheating when there was a high irradiation to the greenhouse. In contrast to the set-ups at Berlin and Bonn, light quality varied in the greenhouse.

6.4.4 Proof of model by using literature data

For further proof of the accuracy of the developed growth model, data from literature *(Petersen et al., 2022)* were introduced for the calculation of resulting growth rates r_i.

Tab.34: Model results of data from *Petersen et al., (2022),* compared with data from this work.

	Petersen et al 2022 (Pet.)	Schmidt, Bonn (Sch.)
Culture time	40d including pre-culture	33d including pre-culture
Culture surface	25.5m^2 set-up: upscale	0.5m^2 set-up: lab
Harvest method	Irregular harvest with varying harvest amounts	Repeated (cyclic) harvest with regular amplitude and interval.
CO_2 concentration	400ppm	3,500ppm
Density of culture at time of harvest	calculated 1.39 kg m^{-2}	measured 2.64 kg m^{-2}
Average growth rate r_i	0.035 kg $d^{-1}m^{-2}$	0.313 kg d^{-1} m^{-2}
Water temperature	23°C	29°C
Photon flux rate	105 µmol•m^{-2}•s^{-1}	129 µmol•m^{-2}•s^{-1}
Photon flux rate in total d^{-1}	4,536,000 mol d^{-1}	7,430,400 mol d^{-1}
Photo period	12:12	16:8

Comparing the listed growth parameters of both set-ups, two important differences are obvious:

Firstly: Any of the culture parameters in the set-up from *Petersen et al. (2022)* were far below

the parameters in the set-up in this work, i.e., lower temperature, lower photon flux rate, lower total photon flux per day, and lower CO_2 concentration. Since the growth rate is defined by the product rule according to eq.14, any of the values which were kept significantly below 1.0 (theoretical max value) resulted in an important drop of the possible growth rate as follows:

Petersen et al. 2022

α =0.66, β =0.58, γ =0.80, δ =0.63

=> $ri(Pet.) = ri_0 \cdot 0.193$

Schmidt

α =1.0, β =0.92, γ =0.823, δ =1.0 (see tab.15)

=> $ri(Sch.) = ri_0 \cdot 0.76$

$$\frac{ri(Sch.)}{ri(Pet.)} = 3.9$$

In doing so, already around 50% of the lower effective growth rate obtained by *Petersen et al. (2022)* could already be explained by calculating the resulting growth rates by the culture parameters used.

Secondly: Only a small number of harvestings were employed by *Petersen et al. (2022).* As a consequence, the coverage density of the culture (g m^{-2}) at the time of harvest was only about half of the culture density in this work. So, a further factor of about 2.0 would explain it.

So, using the data from *Petersen et al. (2022)*, harvest amplitude (amount), and interval (cycle time) would then result in a further drop of effective ri, which could be recalculated by modelling with a theoretical prediction of an undercut of factor

$\frac{ri(Sch.)}{ri(Pet.)} = 8.22$

As the ratio of both growth rates r_i from tab.34 resulted in

$\frac{ri(Sch.)}{ri(Pet.)} = 8.94$

By that, the model could explain 92% of the difference of the compared growth rates.

For this reason, r_i is dynamically changing.

In the long run, using an average "relative growth rate" for calculations will produce inaccurate findings. It might also be demonstrated that capacity varies, making each set of characteristics unique. The resulting capacity varies with changes in the species utilised in the culture, temperature, CO_2 concentration, photon flux density, and nutrient concentrations. As a result, tp also varies. Maximum ri and the system's overall growth dynamics will alter in parallel with the individual population's resulting capacity. The model approach reflects this fact.

6.4.5 Consideration on how the model could be adapted to the more variable conditions in the upscaled approaches

In this specific culture system with regulated temperature, light intake, plant nutrition, and CO_2 exposure, it could be demonstrated that the model accurately reflects the growth, including harvesting, of *Lemna minor*, at the lab scale set up in Bonn. As a consequence of the resulting high coefficient of determination, R^2, it may be further shown that the precision in forecasting the biomass over time originates from the proper definition of the sigmoidal growth function. Predictions outside the experimental boundaries specified in this study can thus be provided.

To improve the model's efficacy for up-scaled settings, the average optimum parameter should not be used if significant variances are anticipated. Rather, changing the parameters to reflect the actual situation should cause the model to restart in each of those scenarios. New values for the harvest interval and amount (amplitude) would then be produced by the model. This would improve the model/reality fit and raise the R^2 score.

As a further consequence, the cultivation remains predictable, even if the set-up of the culture system was changed. The fact that the same culture method (optimised culture parameters, including cyclic harvest intervals) was determined to be the best and produced a maximum yield, a maximum pure protein content, and a minimal antinutritive component was one of the work's key findings. As a result, the model may be able to accurately reflect

reality and, conversely, make predictions by expanding the parameters beyond the conducted trials to include future factors.

In addition to forecasting the ideal harvest amplitude and interval, this modelling typically takes optimal growth parameters into account. The model predicts that the harvest amplitude will rapidly decrease until it reaches a detrimental stage if harvest is initiated well below the turning point tp. This was verified in the experiments.

If such a situation arises, modelling reveals two strategic options.

Option 1:

Stop the harvest sequence until the culture has grown back to a coverage value of more than 30% above tp. The harvest series can then be restarted. After a few new partial harvests, the harvest amplitude will consolidate symmetrically around tp as described in the results (see Fig. 59A, 62A, 65A). The same growth parameters are assumed in the model.

Option 2:

Stop the harvest sequence until the culture has grown back to the aforementioned coverage value. If necessary, a new model run is started with the current (changed) growth parameters. The harvest sequence is restarted using the newly determined values for the harvest interval and amplitude.

Option 1 is selected if the growth parameters remain unchanged and the harvest sequence was only carried out because the initial coverage was too low. Option 2 is selected if at least one of the growth parameters for temperature, light, nutrition or CO_2 has changed. Option 2 is also the best strategy for achieving a higher R^2 value in upscaled systems.

The present model can thus be used for controlling the cultivation of the *Lemna* in a partially or fully automated process. Thus far, there has been only an approach for microalgae: for the first time, *Tebbani et al. (2014)* described a model-guided microalgae cultivation. A method with optimal control for heterotrophic microalgae production was described by *Abdollahi & Dubljevic (2012)*.

Based on the work presented above in this thesis, a patent application was submitted to the European Patent Office (EPO) DE10 2020 133 132.0 and PCT/EP2021/085464. The

EPO's *Biotechnology Division* analyzed novelty and inventiveness over the state of the art. The publications which were closest to the submitted patent were the controlled mass production of *Lemna minor* with defined amino and fatty acid profiles (Chakrabarti et al. 2018) besides the already mentioned two publications on micro algae production (*Abdollahi & Dubljevic 2012, Tebbani et al. 2014)*. It was stated by the EPO, though, that the approach in the submitted patent was different as it considers a regularly repeated feedback control by full model runs if the culture parameters like temperature, light, CO_2, and nutrition vary. Thus, the submitted patent was confirmed to meet all requirements for novelty and inventiveness, and was granted by EPO on 06.11.2024.

Finally, fig. 77 illustrates pure model runs as a form of an overview and outlook, in which harvest amplitudes (partial harvest volumes) and harvest frequency, as well as their effect on the overall harvest over a long period of time (1 year), are given.

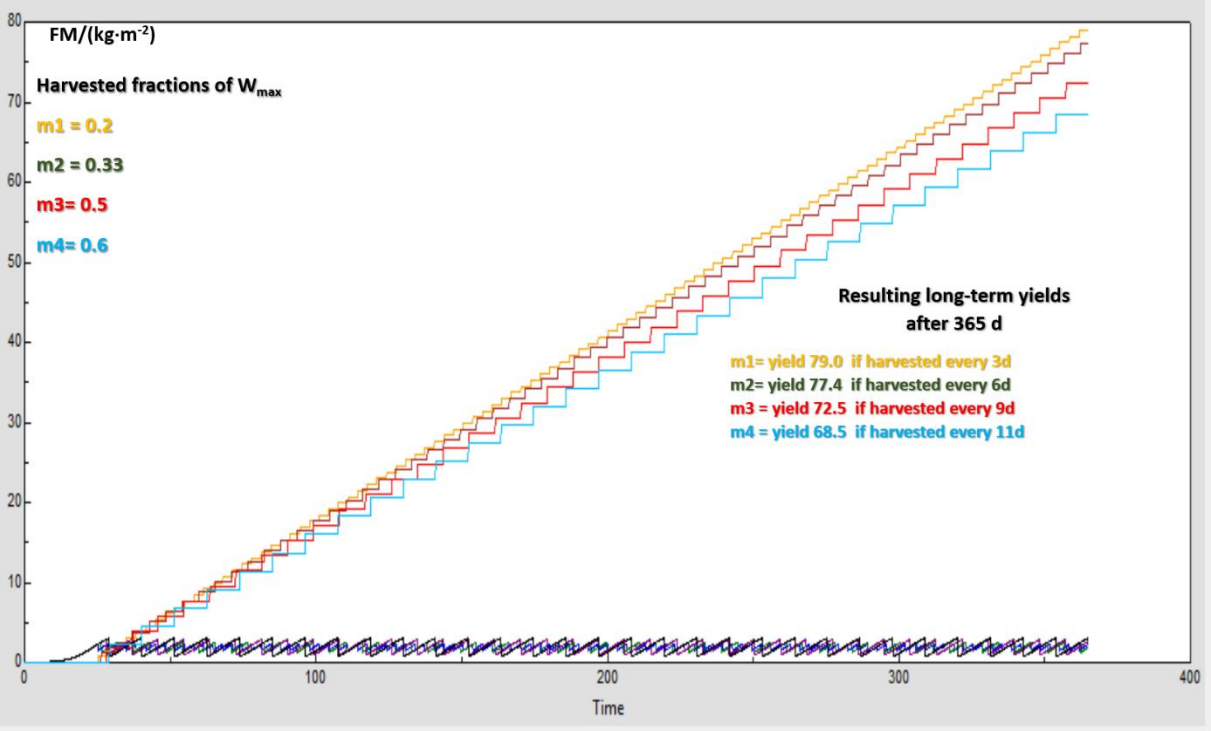

Fig.77: Model runs using different harvest fractions (portions) of Wmax (capacity of population), at different harvest intervals. The set of curves below shows the harvest curves, which, for four different partial harvest quantities m1-m4, naturally also have different harvest intervals that are offset from one another. The set of curves above shows the resulting different staircase curves representing the total harvest quantities.

It gives clear proof, that the model may aid as well to pick the best harvest frequency and amounts. It comes out that a more frequent harvesting with a smaller proportion of the

Lemna population to be gathered instead of wider intervals between harvests but larger proportions will lead to a larger total yield. Over a year, the yield difference may amount to roughly +20%, which can be important for an economic success.

7. CONCLUSIONS

To produce sufficient quantities of *Lemnoideae*, especially *Lemna minor*, indoors, culturing can only really be done non-axenically. *Lemnoideae* are also known to tolerate low light levels. Therefore, they can be cultivated as 'future crops' in a space-saving manner, even in stacks, with a minimum of additional illumination.

High growth rates and good quality were achieved for the following factors, when set at favourable values light exposure, CO_2 concentration and the nutrients N, P, K, Mg, Fe and B.

To prevent algal growth, the trays' surfaces must always be covered, and the N concentration should be kept constant at 1.14 mM. If the NH_4^+/NO_3^- ratio is limited to 1:9, the pH should remain under slightly acidic conditions. Harvesting one third of the covered surface area every three days, at the point of the highest growth rate (Ri), resulted in optimum protein content while minimising undesirable oxalate and manganese contents.

Regarding B, it was found that a significant deficiency only occurred when plants were irradiated with lower proportions of blue light (440 nm), rather than in the high-blue spectrum. Overall, the highest yields and best biomass quality were achieved with the high-blue (440nm) spectrum at 3,500 ppm CO_2. Further experiments are necessary to investigate the peculiarity of B deficiency observed. These experiments would provide information about the biological connection between light energy input in the short-wave ultraviolet (UV) range, i.e. the high-energy part of the spectrum, and boron requirements.

Based on the experimental results, a combination of analytical and numerical modelling was employed to examine the impact of various production parameters on achieving a sustained maximum yield over the long term. The SIMILE® program was used to adjust the model to meet the specific requirements of this culturing process. The growth of a *Lemna* population follows a sigmoidal curve. When combined with the delta function of repeated harvesting, the curve became sawtooth-shaped. The resulting model accurately describes the obtained

growth data (R^2 = 0.96) and likewise describes literature data quite well. It therefore provides a basis for an automatic control and dosing system.

It has been demonstrated that such a culture system can produce a continuous supply of protein-rich biomass from *Lemna minor.* An initial upscaled setup in Berlin demonstrated that nutrient-rich wastewater, such as that from an indoor fish farm, could be used to feed the cultures after sanitation, nitrification, and minor adjustments including the addition of nutrients which are at a too low level.

An integrated *Lemna* cultivation system in an aquaponics facility can utilise nutrient-rich wastewater and benefits from the elevated 29°C temperature required for perch cultivation. Furthermore, the CO_2 produced by fish farming supports the growth of *Lemna* cultures, as demonstrated at ECF Farm Systems in Berlin.

Such a system can also use low-caloric waste heat from sources such as return pipes at power stations and server farms, provided the temperature reaches around 40°C.

However, open questions remain regarding the extent to which the cultivation parameters optimised in this study for *Lemna minor* can be transferred to other *Lemnoideae* species, and how the cultures perform at higher CO_2 concentrations with increased light levels. Solving those questions could make a promising source of novel food and/or protein rich healthy feed.

8. LIST OF FIGURES AND TABLES

8.1 Figures

8.1.1 Literature review

8.1.2 Materials and Methods

8.1.3 Results

8.2 Tables

8.2.1 Literature review

8.2.2 Material & methods

8.2.3 Results

8.2.4 Discussion

8.2.5 Appendix

8.3 Equations

8.3.1 Literature review

8.3.2 Materials and methods

8.3.3 Results

9. LITERATURE

(Citation APA Standard)

(Journal abbreviations: Woodward Library, Univ. Brit. Columbia)

Abdollahi, J., & Dubljevic, S. (2012). Lipid production optimization and optimal control of heterotrophic microalgae fed-batch bioreactor. Chem. Eng. Sci., 84, 619-627. https://doi.org/10.1016/j.ces.2012.09.005

Acosta, K., Appenroth, K. J., Borisjuk, L., Edelman, M., Heinig, U., Jansen M. A. K., Oyama, T., Pasaribu, B., Schubert, I., Sorrels, S., Sree, K. S., Xu, S, Todd, P. M., & Lam, E. (2021). Return of the *Lemnaceae*: duckweed as a model plant system in the genomics and postgenomics era. The Plant Cell*, 33*(10), 3207–3234. https://doi.org/10.1093/plcell/koab189

Abdollahi, J., & Dubljevic, S. (2012). Lipid production optimization and optimal control of heterotrophic microalgae fed-batch bioreactor. *Chem.* Eng. Sci., 84, 619-627. https://doi.org/10.1016/j.ces.2012.09.005

Adams, K. L., & Wendel, J. F. (2005). Polyploidy and genome evolution in plants. Curr. Opin. Plant Biol., 8(2), 135–141. https://doi.org/10.1016/j.pbi.2005.01.001

Aguilera-Morales, M. E., Canales-Martínez, M. M., Ávila-González, E., & Flores-Ortíz, C. M. (2018). Nutrients and bioactive compounds of the *Lemna gibba* and *Ulva Lactuca* as possible ingredients to functional foods. Lat. Am. J. Aquat. Res., 4(46), 709-716. http://dx.doi.org/10.3856/vol46-issue4-fulltext-8

Alford, A., Borofsky, M., Furrow, E., & Lulich, J. (2020). Naturally-occurring Calcium Oxalate Stones in Animals: A quantitative Review of Submission to the Minnesota Urolith Center from 2011 to 2018. J. Urol., 203(4), e128-e129. https://doi.org/10.1097/JU.0000000000000830.09

Andriani, Y., Irawan, B., Iskandari, Zidni, I., & Partasasmita, R. (2019). Diversity of duckweed (Araceae-Lemnoideae), morphological characteristics and its potentials as food sources for herbivorous fishes in West Java, Indonesia. Biodiv., 20(6), 1617-1623. DOI:10.13057/biodiv/d200618

Ansari, A. A., & Khan, F. A. (2008). Remediation of eutrophic water using *Lemna minor* in a controlled environment. Afr. J. Aquat. Sci., 33(3), 275-278. https://doi.org/10.2989/AJAS.2008.33.3.11.623

Appenroth, K. J., & Augsten, H. (1996). Wasserlinsen und ihre Nutzung. Biologie in unserer Zeit, 26(3), 187-195. https://onlinelibrary.wiley.com/doi/epdf/10.1002/biuz.19960260311

Appenroth, K. J., & Lam, E. (2012). Wasserlinsen als Nutzpflanzen: Ein “Unkraut” mit vielen verborgenen Qualitäten. Biologie in unserer Zeit, 42(3), 181-187. https://doi.org/10.1002/biuz.201210480

Appenroth, K. J., Sree, K.S., Böhm, V., Hammann, S., Vetter, W., Leiterer, M., & Jahreis G. (2017). Nutritional value of duckweeds (Lemnoideae) as human food. Food Chem., 217, 266-273. https://doi.org/10.1016/j.foodchem.2016.08.116

Appenroth, K. J., Ziegler, P., & Sree, K. S. (2021). Accumulation of starch in duckweeds (*Lemnaceae*), potential energy plants. Physiol. Mol. Biol. Plants, 27, 2621–2633. https://doi.org/10.1007/s12298-021-01100-4

Appenroth, K. J., Sree, K. S., Bog, M., Ecker J., Seeliger, C., Böhm, V., Lorkowski, S., Sommer, K., Vetter, W., Tolzin-Banasch, K., & Kirmse, R. (2018). Nutritional value of the duckweed species of the genus *Wolffia* (*Lemnaceae*) as human food. Front. Chem., 6, 483. https://doi.org/10.3389/fchem.2018.00483

Appenroth, K. J., Borisjuk, N., & E. Lam (2013). Telling duckweed apart: genotyping technologies for the *Lemnaceae*. Chin. J. Appl. Environ. Biol., 19(1), 1–10. DOI: 10.3724/SP.J.1145.2013.00001

Appenroth, K. J., Krech, K., Keresztes, A., Fischer, W., & Koloczek, H. (2010). Effects of nickel on the chloroplasts of the duckweeds *Spirodela polyrhiza* and *Lemna minor* and their possible use in biomonitoring and phytoremediation. Chemosphere, 78(3), 216–223. https://doi.org/10.1016/j.chemosphere.2009.11.007

Arnott, H. J., & Pautard, F. G. E. (1970). Calcification in Plants. In: Schraer H. ed. Biological calcification cellular and molecular aspects. New York, NY, USA: Appleton-Century Crofts, 375-446. https://link.springer.com/chapter/10.1007/978-1-4684-8485-4_8

Arnott, H. J. (1982). Three systems of biomineralization in plants with comments on the associated organic matrix. In: Nancollas GH, ed. Biological Mineralization and Demineralization. Berlin, Germany: Springer Verlag, 199-218. https://link.springer.com/chapter/10.1007/978-3-642-68574-3_10

Ashby, E., & Oxley, T.A. (1935). The interaction of factors in the growth of Lemna. VI. An analysis of the influence of light intensity and temperature on the assimilation rate and the rate of frond multiplication. Ann. Bot., 49, 309-336. https://www.jstor.org/stable/43237578

Asimi, O. A., Khan , I. A., Bhat, T. A., & Husain N. (2018). Duckweed (*Lemna minor*) as a plant protein source in the diet of common carp (Cyprinus carpio) fingerlings. J. Pharmacog. Phytochem., 7, 42-45. https://www.phytojournal.com/archives?year=2018&vol=7&issue=3&part=A&ArticleId=4170.

Aslam, S., & Zuberi A. (2017). Effect of duckweed by replacing soybean in fish feed on growth performance of Grass carp (Ctenopharyngodon idella) and Silver carp (Hypophthalmichthys molitrix). Int. J. Fish. Aquat. Stud., 5, 278-282. https://www.fisheriesjournal.com/archives/2017/vol5issue5/PartD/5-4-90-214.pdf

Bacaër, N. (2011). Verhulst and the logistic equation (1838). A short history of mathematical population dynamics, 618, 89-96. London: Springer.
Verhulst and the logistic equation (1838) | SpringerLink

Barks, P. M., & Laird, R. A. (2014). Senescence in duckweed: age related declines in survival, reproduction and offspring quality. Funct. Ecol., 29(4), 540-548. https://doi.org/10.1111/1365-2435.12359

Barks, P. M.,Dempsey Z. W., Burg T. M., & Laird, R. A. (2018). Among-strain consistency in the pace and shape of senescence in duckweed. J. of Ecol., 106(5), 2132-2145. https://doi.org/10.1111/1365-2745.12937

Bassil, E., Hu, H., & Brown, P. H. (2004). Use of phenylboronic acids to investigate boron function in plants. Possible role of boron in transvacuolar cytoplasmic strands and cell-to-wall adhesion. *Plant Physiol.*, *136*(2), 3383-3395.
https://doi.org/10.1104/pp.104.040527

Bauer, R., Huber, W., & Sankhla, N. (1976). Effect of abscisic acid on photosynthesis in *Lemna minor* L.. Zeitschrift für Pflanzenphysiologie, 77(3), 237-246.
https://doi.org/10.1016/S0044-328X(76)80200-0

Bauer, H., Martha, P. (1981). The CO_2 compensation point of C3 plants - a re-examination I. Interspecific variability. Zeitschrift für Pflanzenphysiologie, 103(5), 445-450.
https://doi.org/10.1016/S0044-328X(81)80167-5

Bauer, H., Martha, P., Kirchner-Heiss, B., & Mairhofer, I. (1983). The CO_2 compensation point of C3 plants — a re-examination II. Intraspecific variability. Zeitschrift für Pflanzenphysiologie, 109(2), 143-154.
https://doi.org/10.1016/S0044-328X(83)80203-7

Beltran-Peña, A., Rosa, L., & D'Odorico, P. (2020). Global food self-sufficiency in the 21st century under sustainable intensification of agriculture. Environ. Res. Lett., 15(9), 095004.
DOI 10.1088/1748-9326/ab9388

de Beukelaar, M. F. A., Zeinstra, G. G., Mes, J. J., & Fischer, A. R. H. (2019). Duckweed as human food. The influence of meal context and information on duckweed acceptability of Dutch consumers. Food Qual. Preference, 71, 76-86.
https://doi.org/10.1016/j.foodqual.2018.06.005

Bloom-Zandstra, M., & Lampe, E.M. (1985). The role nitrate in osmoregulation of lettuce (*Lactuca sativa* L.) grown at different light intensities. J. exp. Bot., 36(7), 1043-1052. https://doi.org/10.1093/jxb/36.7.1043

Bog, M., Appenroth, K. J., & Sree, K. S. (2019). Duckweed (*Lemnaceae*): its molecular taxonomy. Front. Sustainable Food Syst., 3, 117.
https://doi.org/10.3389/fsufs.2019.00117

Bogacz-Radomska, L., & Harasym, J. (2018). β-Carotene—properties and production methods. *Food Qual. Saf.*, *2*(2), 69-74.

Bokhari, S. H., Ahmad, I., Mahmood-Ul-Hassan, M., & Mohammad, A. (2016). Phytoremediation potential of *Lemna minor* L. for heavy metals. Int. J. Phytorem., 18(1), 25-32.
DOI: 10.1080/15226514.2015.1058331

Bong, W.-C., Vanhaven, L., & Savage, G. P. (2015). Addition of calcium compounds to reduce soluble oxalate in a high oxalate food system. Food Chem., 221, 54-57. https://doi.org/10.1016/j.foodchem.2016.10.031

Bontsema, J., Van Ooteghem, R. J. C., Hemming, J., Van Henten, E. J., van't Ooster, A., & Janssen, H. J. J. (2010). On-line Monitoring of the Energy and Moisture Flows in Greenhouses. IFAC Proceedings Volumes, 43(26), 262-267.
https://doi.org/10.3182/20101206-3-JP-3009.00046

Borchert, R. (1985). Calcium-induced patterns of calcium-oxalate crystals in isolated leaflets of *Gleditsia triacanthos* L. and *Albizia julibrissin Durazz*. Planta 165, 301-310. https://link.springer.com/article/10.1007/BF00392226

Borchert, R. (1986). Calcium acetate induced calcium uptake and formation of calcium-oxalate crystals in isolated leaflets of *Gleditsia triacanthos* L. Planta 168, 571-578. https://link.springer.com/article/10.1007/BF00392278

Borisjuk, A., Peterson, A., Jiyang, L., Gupron, Q., Luo Q., Shi, L., Chen, G., Kischenko, O., Zhou, Y., & Shi, J. (2018). Structural and biochemical properties of duckweed surface cuticula, Front. Chem. 2018, 6, 317.
https://doi.org/10.3389/fchem.2018.00317

Bot, G. P. (1983). Greenhouse climate: from physical processes to a dynamic model. Wageningen University and Research. www.proquest.com
https://www.proquest.com/openview/07210f8befd94aab61b27172a6891e1f/1?pq-origsite=gscholar&cbl=2026366&diss=y

Bottini, M. C. J., Greizerstein, E. J., Aulicino, M. B., & Poggio, L. (2000). Relationships among genome size, environmental conditions and geographical distribution in natural populations of NW Patagonian species of *Berberis* L. (*Berberidaceae*). Ann. Bot., 86(3), 565-573.
https://doi.org/10.1006/anbo.2000.1218

Brechner, E., (2001). Kompaktlexikon der Biologie, Band 2. Spektrum Akademischer Verlag. Heidelberg (Lemma:„Enzyme“).

Budde, R. J. A., & Chollet, R. (1988). Regulation of enzyme activity in plants by reversible phosphorylation. Physiol. Plant. 72, 435-439.
https://doi.org/10.1111/j.1399-3054.1988.tb05857.x

Bünning, E., 1967. The Physiological Clock, 2nd edn. Springer-Verlag, New York. https://link.springer.com/book/10.1007/978-3-662-22511-0

Bong, W.-C., Vanhaven, L., & Savage, G. P. (2015). Addition of calcium compounds to reduce soluble oxalate in a high oxalate food system. Food chem., 221, 54-57. https://doi.org/10.1016/j.foodchem.2016.10.031

Bradford, M. M. (1976). A rapid and sensitive method for the quantitation of microgram quantities of protein utilizing the principle of protein-dye binding. Anal. Biochem., 72(1-2), 248-254. https://doi.org/10.1016/0003-2697(76)90527-3

BVL (2017) Berichte zur Lebensmittelsicherheit (2017). Bundesweiter Überwachungsplan Gemeinsamer Bericht des Bundes und der Länder, pp 13-14.

Von Caemmerer, S. (2000). Biochemical Models of Leaf Photosynthesis; Techniques in Plant Sciences No 2., CSIRO Publishing: Collingwood, Australia.

Von Caemmerer, S., & Farquhar, G. D. (1981). Some relationships between the biochemistry of photosynthesis and the gas exchange of leaves. Planta 1981, 153, 376-387. https://link.springer.com/article/10.1007/bf00384257

Cakmak, I., & Römheld, V. (1997). Boron deficiency-induced impairments of cellular functions in plants. *Plant Soil*, *193*(1), 71-83. https://link.springer.com/article/10.1023/A:1004259808322

Calabrese, M. G., & Ferranti, P. (2019). Novel Foods: New Food Sources. Encyclopedia of Food Security and Sustainability, 1, 271-275. Doi: 10.1016. B978-0-08-100596-5.22128-8.

Caldwell, O.W. (1899). On the life-history of *Lemna minor*. Int. J. Plant Sci., 27, 37–66. https://doi.org/10.1086/327786

Camacho-Cristóbal, J., & González-Fontes, A. (1999). Boron deficiency causes a drastic decrease in nitrate content and nitrate reductase activity, and increases the content of carbohydrates in leaves from tobacco plants. Planta, 209, 528–536. https://doi.org/10.1007/s004250050757

Cammarano, P., Felsani, A., Gentile, M., Gualerzi, C., Romeo, A., & Wolf, G. (1972). Formation of active hybrid 80-S particles from subunits of pea seedlings and mammalian liver ribosomes. Biochimica et Biophysica Acta (BBA)-Nucleic Acids and Protein Synthesis, 281(4), 625-642. https://doi.org/10.1016/0005-2787(72)90160-8

Cao, H. X., Fourounjian, P., & Wang, W. (2018). The importance and potential of duckweeds as a model and crop plant for biomass-based applications and beyond: Handbook of Environmental Materials Management (pp. 1-16). Springer, Cham. https://doi.org/10.1007/978-3-319-58538-3_67-1

Coad, J., & Pedley, K. (2014). Iron deficiency and iron deficiency anemia in women. *Scand. J. Clin. Lab. Invest.*, *74*(sup244), 82-89.

Carr, I., Glencross, B., & Santigosa, E. (2023). The importance of essential fatty acids and their ratios in aquafeeds to enhance salmonid production, welfare, and human health. Front. Anim. Sci., 4, 1147081. DOI 10.3389/fanim.2023.1147081

Ceschin, S., Abati, S., Leacche, I., & Zuccarello, V. (2018). Ecological comparison between duckweeds in central Italy: The invasive *Lemna minuta* vs. the native *L. minor*. Plant

Biosyst. - Int. J. Dealing Aspects Plant Biosyst., *152*(4), 674-683. https://doi.org/10.1080/11263504.2017.1317671

Chairiyah, N., Harijati, N., & Mastuti, R. (2013). Variation of calcium oxalate (CaOx) crystals in porang (*Amorphophallus muelleri* Blume). American Journal of Plant Sciences, *4*(09), 1765. http://dx.doi.org/10.4236/ajps.2013.49217

Chairiyah, N., Harijati, N., & Mastuti, R. (2016). Variation of calcium oxalate (CaOx) crystals in porang corms (*Amorphophallus muelleri* Blume) at different harvest time. American Journal of Plant Sciences, *7*(2), 306-315. DOI: 10.4236/ajps.2016.72030

Chakrabarti, R., Clark, W. D., Sharma, J. G., Goswami, R. K., Shrivastav, A. K., & Tocher, D. R. (2018). Mass production of *Lemna minor* and its amino acid and fatty acid profiles. Front. chem., 6, 479. https://doi.org/10.3389/fchem.2018.00479

Chen, Y., Bian, Z., Marcelis, L. F., Heuvelink, E., Yang, Q., & Kaiser, E. (2024). Green light is similarly effective in promoting plant biomass as red/blue light: a meta-analysis. J. Exp. Bot., *75*(18), 5655-5666. https://doi.org/10.1093/jxb/erae259

Chmilar, S. L., &Laird, R.A. (2019). Demographic senescence in aquatic plant Lemna gibba L. (Araceae). Aqua. Bot., 153, 29-32. https://doi.org/10.1016/j.aquabot.2018.11.004

Choudhury, S., Goswami, S., Choudhury, A. R., & Paul, S. (2022). Light-Harvesting Antenna Complex and Its Role in Environmental Stress. In Photosynthesis and Respiratory Cycles during Environmental Stress Response in Plants (pp. 79-97). Apple Academic Press.

Chow, W. S., Jia, H., & Liggins, J. R. (2012). Acclimation of leaves to low light produces large grana: the origin of the predominant attractive force at work. openresearch-repository.anu.edu.au. doi: 10.1098/rstb.2012.0071

Christensen, A. H., Sharrock, R. A., & Quail, P. H. (1992). Maize polyubiquitin genes: structure, thermal perturbation of expression and transcript splicing, and promoter activity following transfer to protoplasts by electroporation. Plant Mol. Biol., 18, 675–689.

Colpo, A., Molinari, A., Boldrini, P., Živčak, M., Brestič, M., Demaria, S., Baldisserotto,C., Pancaldi, S., Ferroni, L. (2023). Thylakoid membrane appression in the giant chloroplast of *Selaginella martensii* Spring: A lycophyte challenges grana paradigms in shade-adapted species. Plant Science, 336, 111833. https://doi.org/10.1016/j.plantsci.2023.111833

Compeer, A. E., & de Best, J. H. (2018). Report Blauwe Keten: Applications of proteins, amino acids and starch from duckweed. Avans University of Applied Sciences, Vlaanderen,Nederland.

Cornelis, P., Matthijs, S. & Van Oeffelen, L. (2009). Iron uptake regulation in *Pseudomonas aeruginosa*. Biometals **22**, 15–22. https://doi.org/10.1007/s10534-008-9193-0

Cornish-Bowden, A. (2015), One hundred years of Michaelis Menten. Perspectives of Science, 4, 3-9. https://doi.org/10.1016/j.pisc.2014.12.002

Coughlan, E., Walsh, E., Bolger, P., Burnell, G., O'Leary, N., O'Mahoney, M., Paolacci, S., Wall, D., & Jansen, M. A. K. (2022). Duckweed bioreactors: Challenges and opportunities for large-scale indoor cultivation of *Lemnaceae*. J. Cleaner Prod., Vol 336, 130285 https://doi.org/10.1016/j.jclepro.2021.130285

Covington, M. F., Panda, S., Liu, X. L., Strayer, C. A., Wagner, D. R., & Kay, S. A. (2001). ELF3 modulates resetting of the circadian clock in Arabidopsis. *The Plant Cell*, *13*(6), 1305-1316. https://doi.org/10.1105/TPC.000561

Datko, A. H., Mudd, S. H., & Giovanelli, J. (1980). *Lemna paucicostata* Hegelm. 6746: development of standardized growth conditions suitable for biochemical experimentation. Plant physiol., 65(5), 906-912. https://doi.org/10.1104/pp.65.5.906

DeKock, P. C., Ohta, Y., Inkson, R. H. E., & Knight, A. H. (1973). The effect of oxalate and ethylenediaminetetraacetic acid on the absorption of calcium into *Lemna*. Physiol. Plant., 28(3), 379-382. https://doi.org/10.1111/j.1399-3054.1973.tb08574.x

Devlamynck, R., de Souza, M. F., Bog, M., Leenknegt, J., Eeckhout, M., & Meers, E. (2020). Effect of the growth medium composition on nitrate accumulation in the novel protein crop *Lemna minor*. Ecotoxicol. Environ. Saf., 206, 111380. https://doi.org/10.1016/j.ecoenv.2020.111380

DLG (Liste: Positivliste für Einzelfuttermittel, (2023), Nummer 08.10.01, updated May 2023, 15. Auflage) www.dlg.org/fileadmin/downloads/landwirtschaft

Docauer, D. M. (1983). A nutrient basis for the distribution of the *Lemnaceae*, University of Michigan Pro Quest Dissertations Publishing, Degree Year 1983. 8324164, 34-46 https://deepblue.lib.umich.edu/bitstream/handle/2027.42/159531/8324164.pdf?sequence=1&isAllowed=y

Doi, K., Izawa, T., Fuse, T., Yamanouchi, U., Kubo, T., Shimatani, Z., ... & Yoshimura, A. (2004). Ehd1, a B-type response regulator in rice, confers short-day promotion of flowering and controls FT-like gene expression independently of Hd1. Genes & Development, 18(8), 926-936.

Dorenstouter, H., Pieters, G. A., & Findenegg, G. R. (1985). Distribution of magnesium between chlorophyll and other photosynthetic functions in magnesium deficient "sun" and "shade"leaves of poplar. J. Plant Nutr., 8(12). https://doi.org/10.1080/01904168509363409

Dölger, J. L., Pitann, B., & Mühling, K. H. (2024). Potassium induced suppression of magnesium uptake and translocation is limited in oat (*Avena sativa* L.). *J. Plant Nutr. Soil Sci.*, *187*(4), 454-458. https://doi.org/10.1002/jpln.202400151

Driever, S. M., van Nes, E. H., & Roijackers, R. M. (2005). Growth limitation of *Lemna minor* due to high plant density. Aquat. Bot., 81(3), 245-251. https://doi.org/10.1016/j.aquabot.2004.12.002

Van Dyck, I., Vanhoudt, N., Batlle, J.V., Hormans, N., Nauts R., Van Gompel, A., Claesen, J., & Vangronsveld, J. (2021). Effects of environmental parameters on *Lemna minor* growth: An integrated experimental and modelling approach. J. Environ. Manage., 300, 113705. https://doi.org/10.1016/j.jenvman.2021.113705

https://open.efsa.europa.eu/

https://open.efsa.europa.eu/questions/EFSA-Q-2020-00512

European Commission, Directorate-General for Health and Food Safety, Ursula von der Leyen (2025). Commission Implementing Regulation (EU) 2025/153 of 29 January 2025 authorising the placing on the market of *Lemna minor* and *Lemna gibba* plants as novel food and amending Implementing Regulation (EU) 2017/2470. https://eur-lex.europa.eu/eli/reg_impl/2025/153/oj/eng

(EU)Commission Implementing Regulation (EU) 2017/2470 of 20 December 2017 establishing the Union list of novel foods in accordance with Regulation (EU) 2015/2283 of the European Parliament and of the Council on novel foods, EFSA Journal 2022, 20(11), 7598. (OJ L 351, 30.12.2017, p. 72) http://data.europa.eu/eli/reg_impl/2017/2470/oj) https://doi.org/10.2903/sp.efsa.2024.EN-8963.

Erismann, K. H., & Finger, A. (1968). Lemnaceen in kontinuierlicher Kultur. Ber. Schweiz. Bot. Ges, 78, 5-15.

Evans, J. R., Kaldenhoff, R., Genty, B., & Terashima, I. (2009). Resistances along the CO_2 diffusion pathway inside leaves. J. Exp. Bot, *60*(8), 2235-224. https://doi.org/10.1093/jxb/erp117

Ewert, F. (2004). Modelling plant responses to elevated CO_2: How important is leaf area index?, *Ann. Bot.*, 93(6), 619–627. https://doi.org/10.1093/aob/mch101

FAO, F. (2018). The future of food and agriculture: alternative pathways to 2050. Food and Agriculture Organization of the United Nations, Rome, 228.

Farquhar, G. D., & Von Caemmerer, S. (1982). Modelling of photosynthetic response to environmental conditions. Physiological Plant Ecology II: Water relations and carbon assimilation (549-587). Berlin, Heidelberg: Springer Berlin Heidelberg. DOI: 10.1007/978-3-642-68150-9_17

Ferreira, R. B., & Shaw, N. M. (1989). Effect of osmotic stress on protein turnover in *Lemna minor* fronds. Planta, 179(4), 456-465. https://link.springer.com/article/10.1007/BF00397585

Foster, A. S. (1956). Plant idioblasts: remarkable example of cell specialization. Protoplasma 46, 184-193. https://link.springer.com/article/10.1007/BF01248877

Fourounjian, P., Slovin, J., & Messing, J. (2021). Flowering and seed production across the *Lemnaceae*. Int. J. Mol. Sci., 22, 2733. https://doi.org/10.3390/ijms22052733

Fourounjian, P. (2020). Small RNAs in Duckweeds. *In:* The Duckweed Genomes (157-164). Cham: Springer International Publishing. https://doi.org/10.3390/ijms22052733

Fowler, S., Lee, K., Onouchi, H., Samach, A., Richardson, K., Morris, B., Coupland, G. & Putterill, J. (1999). GIGANTEA: a circadian clock-controlled gene that regulates photoperiodic flowering in Arabidopsis and encodes a protein with several possible membrane-spanning domains. EMBO J., 18, 4679–4688. https://doi.org/10.1093/emboj/18.17.4679

Franceschi, V. R., & Horner, H. A. T. Jr (1980). Calcium oxalate crystals in plants. Bot. Rev. 46, 361-427. https://link.springer.com/article/10.1007/BF02860532

Franceschi, V. R., & Loewus, F. A. (1995). Oxalate biosynthesis and function in plants and fungi. In: Khan S. R., ed. Calcium oxalate in biological systems. Boca Raton, FL, USA: CRC Press, 113-130. https://www.taylorfrancis.com/chapters/edit/10.1201/9781003068747-6/oxalate-biosynthesis-function-plants-fungi-vincent-franceschi-frank-loewus

Franceschi, V. R., & Horner H. T. Jr. (1979). Use of *Psychotria puncata* callus in study of calcium oxalate crystal idioblast formation. Z. Pflanzenphysiol. 67, 61-75. https://doi.org/10.1016/S0044-328X(79)80153-1

Franceschi, V. R. (1987). Oxalic acid metabolism and calcium oxalate formation in *Lemna minor*. Plant Cell Environ., 10(5), 397-406. https://doi.org/10.1111/1365-3040.ep11603639

Franceschi, V. R. (1989). Calcium oxalate formation is a rapid and reversible process in *Lemna minor* L. Protoplasma 148, 130–137. https://doi.org/10.1007/BF02079332

Franceschi, V. R. (2001). Function of calcium oxalate crystals in plants. Trends Plant Sci, 6, 331. https://doi.org/10.1016/S1360-1385(1)02014-3

Frank, E. (1972). The formation of crystal idioblasts in *Canavalia ensiformis* D.C. at different levels of calcium supply. Zeitschrift für Pflanzenphysiologie, 67, 350-358. https://doi.org/10.1016/S0044-328X(72)80096-5

Frederic, M., Samir L., Louise M., & Abdelkrim A. (2006). Comprehensive modelling of mat density effect on duckweed (*Lemna minor*) growth under controlled eutrophication. Water Res. 40(15), 2901–2910. https://doi.org/10.1016/j.watres.2006.05.026

Frost-Christensen, H., & Floto, F. (2007). Resistance to CO_2 diffusion in cuticular membranes of amphibious plants and the implication for CO_2 acquisition. Plant, Cell & Environ. 30(1), 12-18. https://doi.org/10.1111/j.1365-3040.2006.01599.x

Fu, L., Huang, M., Han, B., Sun, X., Sree, K. S., Appenroth, K. J., & Zhang, J. (2017). Flower induction, microscope-aided cross-pollination, and seed production in the duckweed *Lemna gibba* with discovery of a male-sterile clone. Sci. Rep., 7(1), 3047. https://doi.org/10.1038/s41598-017-03240-8

Fuhrer, J. (1983). Light-inhibition of dark respiration in *Lemna minor* L.. Botanica Helvetica Band 93, Heft 1. http://doi.org/10.5169/seals-65235

Gajdanowicz, P., Michard, E., Sandmann, M., Rocha, M., Corrêa, L. G. G., Ramírez-Aguilar, S. J., Gomes-Porras, J.L., Gonzales, W., Thibaud, J-B., van Dongen, J.T., Dreyer, I. (2011). Potassium (K+) gradients serve as a mobile energy source in plant vascular tissues. *Proc. Nat. Acad. Sci.*, *108*(2), 864-869. https://doi.org/10.1073/pnas.1009777108

Gallaher, R. N. (1975). The occurence of calcium in plant tissue as crystals of calcium oxalate. Communications in Soil Science and Plant Analysis, 6, 315-330. https://doi.org/10.1080/00103627509366570

Gallaher, R. N., Perkins, H. F., & Jones, J. B. (1975). Calcium concentration and distribution in healthy and decline peach tree tissues 1. Hort. Science, 10(2), 134-137. https://doi.org/10.21273/HORTSCI.10.2.134

Gallaher, R. N., & Jones J. B. (1976). Total extractable and oxalate calcium and other elements in normal and mouse ear pecan tree tissues. J. Am. Soc. Hortic. Sci., 101, 6922-6926. https://doi.org/10.21273/JASHS.101.6.692

Grahl, H., & Wild, A. (1973). Lichtinduzierte Veränderungen im Photosynthese-Apparat von *Sinapis alba*. Berichte der Deutschen Botanischen Gesellschaft, 86(5-9), 341-349. https://doi.org/10.1111/j.1438-8677.1973.tb02417.x

Goudriaan J., & van Laar H. H. (1994). Modelling Potential Crop Growth Processes, ISBN 978-0-7923-3220-6, Springer-Science + Business media B.V.. DOI: 10.1007/978-94-011-0750-1

Gu, L., Grodzinski, B., Han, J., Marie, T., Zhang, Y. J., Song, Y. C., & Sun, Y. (2022). Granal thylakoid structure and function: explaining an enduring mystery of higher plants. New Phytol., 236(2), 319-329. https://doi.org/10.1111/nph.18371

Hanstein, J. (1871). Die Entwicklung des Keimes der Monokotylen und Dikotylen. Botanische Abhandl. aus dem Gebiet der Morph. u. Physiol. I: I-II 2. 6. I87I.

Hawkesford, M., Horst, W., Kichey, T., Lambers, H., Schjoerring, J., Møller, I. S., & White, P. (2012). Functions of macronutrients. In Marschner's mineral nutrition of higher plants (35-189). Academic press. https://doi.org/10.1016/B978-0-12-384905-2.00006-6

Hegelmaier, F. (1870). Die Lemnaceen. Eine monographische Untersuchungen. Leipzig. 5.

Hegelmaier, F. (1871). Die Fructificationsteile von *Spirodela*. Bot.Zeit. 29, 62I-629, 645-666.

Hepler, P. K. (2005). Calcium: a central regulator of plant growth and development. The Plant Cell, 17(8), 2142-2155. https://doi.org/10.1105/tpc.105.032508

Herreo, M., Thornton, P. K. (2013). Livestock and global change: Emerging issues for sustainable food systems. Proc. Natl. Acad. Sci. USA, 110, 20878-2088. https://doi.org/10.1073/pnas.1321844111

Hikosaka, K., Niinemets, U., & Anten, N. P. (2015). Canopy Photosynthesis: From Basics to Applications. Springer, 79-83, DOI: 10.1007/978-94-017-7291-4

Hillman, W. S. (1976). Calibrating duckweeds: light, clocks, metabolism, flowering. Science, 193(4252), 453–458, https://www.science.org/doi/abs/10.1126/science.193.4252.453

Hillman, W. S. (1961). Experimental control of flowering in *Lemna* III. A relationship between medium composition and the opposite photoperiodic responses of *Lemna perpusilla* 6746 and *Lemna gibba* G3. Am. J. Bot., 48, 413–419. https://doi.org/10.1002/j.1537-2197.1961.tb11659.x

Hillman, W. S. (1966). Photoperiodism in *Lemna*: reversal of night interruption depends on colour of the main photoperiod. Science, 154(3754), 1360–1362. https://www.science.org/doi/abs/10.1126/science.154.3754.1360

Hoagland, D. R., & Arnon, D. I. (1938). The water-culture method for growing plants without soil. Circ. Calif. Agric. Exp. Stn., 347, 32. https://www.cabdirect.org/cabdirect/abstract/19500302257

Hoagland D. R., & Arnon D. I. (1950). The water-culture method for growing plants without soil, Circular/University of California, College of Agriculture, Agricultural Experiment Station, Berkeley. 347(2), 347-353. https://cir.nii.ac.jp/crid/1370302866026676736

Hoang, P. T. N., Schubert, V., Meister, A., Fuchs, J., Schubert, A. (2019). Variation in genome size, cell and nucleus volume, chromosome number and rDNA loci among duckweeds. Sci. Rep., 9, 3234. https://doi.org/10.1038/s41598-019-39332-w

Horak, O., & Kinzel, H. (1971). Typen des Mineralstoffwechsels bei den Höheren Pflanzen. Österreichische botanische Zeitschrift, 119(4/5), 475-495. https://www.jstor.org/stable/43337760

Horner, H. T., & Wagner, B. L. (1995). Calcium oxalate formation in higher plants, In: Khan S. R., ed. Calcium oxalate in biological system. Boca Raton, FL, USA: CRC Press 53-72; https://www.taylorfrancis.com/chapters/edit/10.1201/9781003068747-4/calcium-oxalate-formation-higher-plants-harry-horner-bruce-wagner

Hossain, A., Krupnik, T. J., Timsina, J., Mahboob, M. G., Chaki, A. K., Farooq, M., ... & Hasanuzzaman, M. (2020). Agricultural land degradation: Processes and problems undermining future food security. Environment, climate, plant and vegetation growth, 17-61, Cham: Springer International Publishing. https://link.springer.com/chapter/10.1007/978-3-030-49732-3_2

Hönow R., & Hesse A. (2002). Comparison of extraction methods for determination of soluble and total oxalate in foods by HPLC-enzyme-reactor. Food Chem., 78(4), 511-521. http:dx.doi.org/10.1016/S0308-8146(02)00212-1

HPLE, High Level Panel of Experts (2017). Nutrition and food systems, Comm. World Food Secur., 44, 150.

Ishii, T., & Matsunaga, T. (1996). Isolation and characterization of a boron-rhamnogalacturonan-II complex from cell walls of sugar beet pulp. *Carbohydr. Res.*, *284*(1), 1-9. https://doi.org/10.1016/0008-6215(96)00010-9

Ishii, T., Matsunaga, T., Pellerin, P., O'Neill, M. A., Darvill, A., & Albersheim, P. (1999). The plant cell wall polysaccharide rhamnogalacturonan II self-assembles into a covalently cross-linked dimer. *J. Biol. Chem.*, *274*(19), 13098-13104. https://www.jbc.org/article/S0021-9258(18)36851-0/fulltex

Jia, H., Liggins, J. R., & Chow, W. S. (2012). Acclimation of leaves to low light produces large grana: the origin of the predominant attractive force at work. Philos. Trans. R. Soc. London, Ser. B, 367(1608), 3494-3502. https://doi.org/10.1098/rstb.2012.0071

Jones, C. G., Hare, J. D., & Compton S. J. (1989). Measuring plant protein with the Bradford assay. J. Chem. Ecol., 15(3). https://link.springer.com/article/10.1007/BF01015193

Johnson, S., Saikia, N., Mathur, H. B., & Agarwal, H. C. (2009). Fatty acids profile of edible oils and fats in India. Centre for Science and Environment, New Delhi, 3-31. http://www.indiaenvironmentportal.org.in/files/fatty_acids_profile.pdf

Jung, S. (2022). Neuausweisung nitratbelasterter und eutrophierter Gebiete. Landwirtschaftskammer Nordrhein-Westfalen. https://www.landwirtschaftskammer.de/landwirtschaft/ackerbau/duengung/duengeverordnung/gebietsausweisung-2022

Kanai, S., Ohkura, K., Adu-Gyamfi, J. J., Mohapatra, P. K., Nguyen, N. T., Saneoka, H., & Fujita, K. (2007). Depression of sink activity precedes the inhibition of biomass production in tomato plants subjected to potassium deficiency stress. *J. Exp. Bot.*, *58*(11), 2917-2928.

Kaufmann (1868). Entwicklungsgeschichtliche Untersuchungen über die Lemnaceen. Bot. Zeit. 26: 382-384. 4. 1868.

Khan, M. A., Wani, G. A., Majid, H., Farooq, F. U., Reshi, Z. A., Husaini, A. M., & Shah, M. A. (2020). Differential bioaccumulation of select heavy metals from wastewater by *Lemna minor*. Bull. Environ. Contam. Toxicol., *105*(5), 777-783. https://doi.org/10.1007/s00128-020-03016-3

Kamal, M., Ghaly, A. E., Mahmoud, N., & Cote R. (2004). Phytoaccumulation of heavy metals by aquatic plants. Environ. Int., 29, 1029-1039. https://doi.org/10.1016/S0160-4120(03)00091-6

Kazumi, S. (1996). Formation of L-ascorbic acid and oxalic acid from D-glucosone in *Lemna minor*. Phytochem., 41(1), 145. https://doi.org/10.1016/0031-9422(95)00537-4

Keates S. A., Tarlyn N. M., Loewus F. A., & Franceschi V. R. (2000). L-ascorbic acid and 1-galactose are sources of oxalic acid and calcium oxalate in *Pistia stratiotes*. Phytochem., 53, 433–440. https://doi.org/10.1016/S0031-9422(99)00448-3

Khellaf, N., & Zerdaoui, M. (2009). Growth response of duckweed *Lemna minor* to heavy metal pollution. Iran. J. Environ. Health. Sci. Eng., 6(3), 161-166.

Khvatkov, P., Chernobrovkina, M., Okuneva, A., & Dolgov, S. (2019). Creation of culture media for efficient duckweeds micropropagation (*Wolffia arrhiza* and *Lemna minor*) using artificial mathematical optimization models. Plant Cell, Tissue Organ Cult. *(PCTOC)*, *136*(1), 85-100. DOI:10.1007/S11240-018-1494-6

Kim, I. (2007). Development of the root system in *Spirodela polyrhiza* (L.) Schleiden (*Lemnaceae*). J. Plant Biol., 50, 540-547. https://link.springer.com/article/10.1007/BF03030707

Kim, B. S., Yu, M. Y., & Shin, J. (2024). Effect of low sodium and high potassium diet on lowering blood pressure and cardiovascular events. Clin. Hypertens., *30*(1), 2. https://link.springer.com/article/10.1186/s40885-023-00259-0

Kirchhoff, H., Haase, W., Wegner, S., Danielsson, R., Ackermann, R., & Albertsson, P.-A. (2007). Low light-induced formation of semicrystalline photosystem II arrays in higher plant chloroplasts. Biochemistry, 46(39), 11169-11176. https://doi.org/10.1021/bi700748y

Kobayashi, M., Matoh, T., & Azuma, J. I. (1996). Two chains of rhamnogalacturonan II are cross-linked by borate-diol ester bonds in higher plant cell walls. *Plant Physiol.*, *110*(3),

1017-1020.
https://doi.org/10.1104/pp.110.3.1017

Kobayashi, T., Nishizawa, N.K. (2012). Iron uptake, translocation, and regulation in higher plants. Annu. Rev. Plant Biol., 63, 131-152.
https://doi.org/10.1146/annurev-arplant-042811-105522

Korner, O., Challa, H., & van Ooteghem, R. J. (2002). Modeling temperature effects on crop photosynthesis at high radiation in a solar greenhouse. Acta Hortic., 137-144. https://www.researchgate.net/profile/Oliver-Koerner/publication/40128314_Modeling_temperature_effects_on_crop_photosynthesis_at_high_radiation_in_a_solar_greenhouse/links/576bb99c08aefcf135bff5a1/Modeling-temperature-effects-on-crop-photosynthesis-at-high-radiation-in-a-solar-greenhouse.pdf

Kostman T. A., Tarlyn N. M., Loewus F. A., & Franceschi V. R. (2001). Biosynthesis of 1-ascorbic acid and conversion of carbons 1 and 2 of 1-ascorbic acid to oxalic acid occurs within individual calcium oxalate crystal idioblasts. Plant Physiol., 215, 634–640.
https://doi.org/10.1104/pp.125.2.634

Kostmann, T. A., & Koscher, J. R. (2003). 1-galactono-c-lactone dehydrogenase is present in calcium oxalate crystal idioblasts oft wo species. Plant Physiol. Biochem., 41, 201-206.
https://doi.org/10.1016/S0981-9428(03)00011-1

Kot, M. (2001). Elements of mathematical ecology. Cambridge University Press DOI:10.1017/CBO9780511608520

Krysiak, M., Oung, H. M. O., & Kirchhoff, H. (2025). What are grana in chloroplasts of vascular plants good for?. Ann.Bot., 137 (3) 571-590.
https://doi.org/10.1093/aob/mcaf229

Kudla, J., Batistič, O., & Hashimoto, K. (2010). Calcium signals: the lead currency of plant information processing. The Plant Cell, 22(3), 541-563.
https://doi.org/10.1105/tpc.109.072686

Kuo-Huang, L. L., & Zindler-Frank, E. (1998). Structure of crystal cells and influences of leaf development on crystal development and vice versa in *Phaseolus vulgaris* (Leguminosae). Botan. Acta, 111, 337-345.
https://doi.org/10.1111/j.1438-8677.1998.tb00718.x

Kuehdorf, K., Appenroth, K. J. (2012). Influence of salinity and high temperature on turion formation in the duckweed *Spirodela polyrhiza*, Aquat. Bot., 97(1), 69-72.
https://doi.org/10.1016/j.aquabot.2011.10.003

Kufel, L., Strzałek, M., Wysokińska, U.E., Oknińska, S., Ryś, K. (2012). Growth rate of duckweeds (*Lemnaceae*) in relation to the internal and ambient nutrient concentrations–testing the Droop and Monod models. Pol. J. Ecol., 60(2), 241-249.

Kurvits, A., & Kirkby, E. A. (1980). The uptake of nutrients by sunflower plants (*Helianthus annuus*) growing in a continuous flowing culture system, supplied with nitrate or ammonium as nitrogen source. J.Plant Nutr.Soil Sci.143(2), 140–149

Landolt, E. (1980). Biosystematic Investigations in the Family of Duckweeds (*Lemnaceae*), Veroffentlichungen des Geobotanischen Institutes ETH, Stiftung Rubel, Zurich, Switzerland.

Landolt, E. (1986). The family of *Lemnaceae* – A Monographic study, vol. 1. Veröffentlichungen des Geobotanischen Institutes ETH Stiftung Rubel, Zürich Switzerland.

Landolt E., & Kandeler R. (1987). Biosystematic investigations in the family of duckweed (*Lemnaceae*) – Vol. 4: The Family of *Lemnaceae* – A Monographic Study; Geobotanisches Institut ETH: Zürich, Germany. https://pascal-francis.inist.fr/vibad/index.php?action=getRecordDetail&idt=8238403

Landolt, E., Lüönd, A., & Kandeler, R. (1987). Biosystematic investigation in the family of duckweeds, Veröffentlichungen des Geobotanischen Instituts der ETH Zürich, Stiftung Ruebel; Heft 70,71,80,95 https://agris.fao.org/search/en/providers/122438/records/647751b4bc45d9ecdbc0ad74

Lange, O. L., Nobel, P. S., Osmond, C. B., & Ziegler, H. (1982). Eds., Physiological Plant Ecology II. Water Relations and Carbon Assimilation New Series; Springer: Berlin, Heidelberg, Germany, 12B, 550-587. https://doi.org/10.1007/978-3-642-68150-9

Lasfar, S., Monette F., Millette, L., & Azzouz, A. (2007). Intrinsic growth rate: A new approach to evaluate the effects of temperature, photoperiod and phosphorus-nitrogen concentrations on duckweed growth under controlled eutrophication. Water Res., 41(11), 2333-2340. https://doi.org/10.1016/j.watres.2007.01.059

Le, J. S. (2010). Stomatal Opening Mechanism of CAM Plants. J. Plant Biol., 53, 19–23 DOI 10.1007/s12374-010-9097-8

Lee, R. (2011). The outlook for population growth. Science. 333(6042), 569-573. DOI: 10.1126/science.1208859

Leitch, A. R., & Leitch, I. J. (2008). Genomic plasticity and the diversity of polyploid plants. Science, 20(5875), 481–483. https://www.science.org/doi/abs/10.1126/science.1153585

Leng, R. A. (1999). Duckweed: A tiny aquatic plant with enormous potential for agriculture and environment. Animal Production and Health Division, University of Tropical Agriculture Foundation, PhnomPenh (Combodia). FAO Rome (Italy). 108. http://www.fao.org/ag/AGAinfo/resources/documents/DW/Dw2.htm

Leng, R. A., Stambolie, J. H., & Bel, R. (1995). Duckweed - a potential high-protein feed resource for domestic animals and fish. Livestock Research for rural development, 7(1). https://citeseerx.ist.psu.edu/document?repid=rep1&type=pdf&doi=2d1edec8b0755b33c1c84e838361f059478f917b

Lepeduš, H., Vidaković-Cifrek, Ž., Šebalj, I., Antunović Dunić, J., & Cesar, V. (2020). Effects of low and high irradiation levels on growth and PSII efficiency in *Lemna minor* L. Acta Botan. Croat., 79(2), 185-192. https://doi.org/10.37427/botcro-2020-016

Les, D. H., Crawford, D. J., Landolt, E., Gabel, J. D., & Kimball, R. T. (2002). Phylogeny and systematics of *Lemnaceae*, the duckweed family. Syst. Bot., 27(2), 221–240 https://doi.org/10.1043/0363-6445-27.2.221

Li, P., Liu, C., Luo, Y., Shi, H., Li, Q., PinChu, C., ... & Fan, W. (2022). Oxalate in plants: metabolism, function, regulation, and application. J. Agric. Food. Chem., 70(51), 16037-16049. https://doi.org/10.1021/acs.jafc.2c04787

Li, X. X., Zhang, D., Lynch-Holm, V. J., Okita, T. W., & Franceschi, V. R. (2003). Isolation of a crystal matrix protein associated with calcium oxalate precipitation in vacuoles of specialized cells. Plant Physiol., 133, 549-559. https://doi.org/10.1104/pp.103.023556

Li, X. X., & Franceschi V. R. (1990). Distribution of peroxisomes and glycolate metabolism in relation to calcium oxalate formation in *Lemna minor* L. Eur. J. Cell Biology, 51, 9–16. PMID: 2184039

Liebers, M., Hommel, E., Grübler, B., Danehl, J., Offermann, S., & Pfannschmidt, T. (2023). Photosynthesis in the biomass model species *Lemna minor* displays plant-conserved and species-specific features. Plants, 12(13), 2442. https://doi.org/10.3390/plants12132442

Liu, C., Dai, Z., & Sun, H. (2017). Potential of duckweed (*Lemna minor*) for removal of nitrogen and phosphorus from water under salt stress. J. Environ. Manage., 187, 497-503. https://doi.org/10.1016/j.jenvman.2016.11.006

Liu, Y., Sanguanphun, T., Yuan, W., Cheng, J. J., & Meetam, M. (2017). The biological responses and metal phytoaccumulation of duckweed *Spirodela polyrhiza* to manganese and chromium. Environ. Sci. Pollut. Res., 24, 19104-19113. https://doi.org/10.1007/s11356-017-9519-y

Litchman, E. (2007). Resource competition and the ecological success of phytoplankton. Evolution of Primary Producers in the Sea, 351-375, Academic Press, https://doi.org/10.1016/B978-012370518-1/50017-5

Longin, J., & Neirinckx, L. (1977). Essai de typologie physiologique des plantes, basée sur leur métabolisme calcique foliaire. Bulletin de la Société Royale de Botanique de Belgique/Bulletin van de Koninklijke Belgische Botanische Vereniging, 228-238. https://www.jstor.org/stable/20793684

López-Pozo, M., Adams III, W. W., & Demmig-Adams, B. (2023). *Lemnaceae* as novel crop candidates for CO_2 sequestration and additional applications. Plants, 12(17), 3090. https://doi.org/10.3390/plants12173090

Lüönd, A. (1983). Das Wachstum von Wasserlinsen (*Lemnaceae*) in Abhaengigkeit des Naehrstoffangebots, insbesondere Phosphor und Stickstoff. Vol. 3. Veroeffentlichungen des Geobotanischen Instutes der ETH, Stiftung Ruebel, Zurich, Biosystematic investigations in the family of duckweeds (*Lemnaceae*). https://www.research-collection.ethz.ch/bitstream/handle/20.500.11850/137770/1/eth-36051-01.pdf

Lüönd, A. (1983). Das Wachstum von Wasserlinsen (*Lemnaceae*) in Abhängigkeit des Nährstoffangebots, insbesondere Phosphor und Stickstoff. Diss. Naturwissenschaft ETH Zürich, Nr 7302, 0000, https://doi.org/10.3929/ethz-a-000290579

Malthus, T. R. (1807). An essay on the principle of population, as it affects the future improvement of society. With remarks on the speculations of mr. Godwin, m. Condorcet, and other writers. By TR Malthus (Vol. 2).

Mariani, F., Fattorini, S., Di Giulio, A., & Ceschin, S. (2021). Development and reproduction of *Cataclysta lemnata*, a potential natural enemy of the invasive alien duckweed *Lemna minuta* in Italy. The Eur. Zool. J., 88(1), 216–225. https://doi.org/10.1080/24750263.2021.1872721

Marschner, P. (2012). Mineral Nutrition of Higher Plants, third edition, chapter 6.5.5 Membrane Stabilization, Elsevier Amsterdam, 174-175.

Marschner, P. (2012). Marschners Mineral Nutrition of Higher Plants, third edition, chapter 6.1.5 N Supply, Plant Growth and Composition. Elsevier Amsterdam, 148-151.

Marschner, P. (2012). Marschners Mineral Nutrition of Higher Plants third edition, chapter 6.1.1 Nitrate Transport in Plants. Elsevier Amsterdam, 136-146.

Mäenpää, P., & Aro, E. M. (1986). Chlorophyll-protein complexes, chlorophyll a/b ratio and chloroplast ultrastructure in *Lemna minor* L. grown under different light conditions. J. Plant Physiol., 123(2), 161-168. https://doi.org/10.1016/S0176-1617(86)80137-7

Martirosyan E. V., Ryzhova N. N., Skryabin K. G., & Kochieva E. Z. (2008). RAPD analysis of genome polymorphism in the family *Lemnaceae*. Russ. J. Genet., 44, 360-364. https://doi.org/10.1134/S1022795408030198

Massey L. K., Roman-Smith H., & Sutton R. A. L. (1993). Effect of dietary oxalate and calcium on urinary oxalate and risk of formation of calcium oxalate kidney stones. J. Am. Diet. Assoc., 93, 901-906. https://doi.org/10.1016/0002-8223(93)91530-4

Matsunaga, T., Ishii, T., Matsumoto, S., Higuchi, M., Darvill, A., Albersheim, P., & O'Neill, M. A. (2004). Occurrence of the primary cell wall polysaccharide rhamnogalacturonan II in pteridophytes, lycophytes, and bryophytes. Implications for the evolution of vascular plants. *Plant Physiol.*, *134*(1), 339-351. https://doi.org/10.1104/pp.103.030072

Mattoo, A. K., Hoffman-Falk, H., Marder, J. B., & Edelman, M. (1984). Regulation of protein metabolism: coupling of photosynthetic electron transport to in vivo degradation of the rapidly metabolized 32-kilodalton protein of the chloroplast membranes. Proc. Natl. Acad. Sci., 81(5), 1380-1384. https://doi.org/10.1073/pnas.81.5.1380

Mazen A. M. A., Zhang D., & Franceschi V. R. (2003). Calcium oxalate formation in *Lemna minor*: physiological and ultrastructural aspects of high capacity calcium sequestration. New Phytol., 161, 435-448. DOI: 10.1046/j.1469-8137.2003.00923.x

McAinsh, M. R., & Pittman, J. K. (2009). Shaping the calcium signature. New Phytologist, 181(2), 275-294. https://doi.org/10.1111/j.1469-8137.2008.02682.x

McLay, C. L. (1976). The effect of pH on the population growth of three species of duckweed: *Spirodela oligorrhiza*, *Lemna minor* and *Wolffia arrhiza*. Freshwater Biol., 6(2), 125-136. https://doi.org/10.1111/j.1365-2427.1976.tb01596.x

Merry, R, Dobbels, A. A., , Sadok, W., Naeve, S., Stupar, R. M., & Lorenz, A. J. (2021). Iron deficiency in soybean. Crop Sci., 62(1), 36-52. https://doi.org/10.1002/csc2.20661

Mes, J. J., Esser D., Somhorst, D., Oosterink, E., van der Haar, S., & Ummels, M. (2022). Daily intake of *Lemna minor* or spinach as vegetable does not show significant difference on health parameters and taste preference. Plant Foods Hum., 77, 121–127. https://doi.org/10.1007/s11130-022-00952-9

Michael, G. (1941). Über die Aufnahme und Verteilung des Magnesiums und dessen Rolle in der höheren grünen Pflanze. Z. Pflanzenernaehr., Dueng., Bodenkd. 25, 65-120. https://doi.org/10.1002/jpln.19410250202

Miller, O. F. (2023). Effects of Heavy Metal Uptake on Growth, Chlorophyll Content, and Calcium Oxalate Crystals in *Lemna minor* (Duckweed). https://digitalcommons.otterbein.edu/stu_honor/152/

Mirahmadi, S. F., Hassandokht, M., Fatahi, R., Naghavi, M. R., & Rezaei, K. (2022). High and low oxalate content in spinach: an investigation of accumulation patterns. *Journal of the Science of Food and Agriculture*, *102*(2), 836-843. https://doi.org/10.1002/jsfa.11419

Mitrovic, S. M., Allis, O., Furey, A., & James, K. J. (2005). Bioaccumulation and harmful effects of microcystin-LR in the aquatic plants *Lemna minor* and *Wolffia arrhiza* and the filamentous alga *Chladophora fracta*. Ecotoxicol. Environ. Saf., 61(3), 345-352.

Miwa, K., Serikawa, M., Suzuki, S., Kondo, T., & Oyama, T. (2006). Conserved expression profiles of circadian clock-related genes in two *Lemna* Species showing long-day and short-day photoperiodic flowering responses. *Plant and Cell Physiol.*, 47(5), 601–612. https://doi.org/10.1093/pcp/pcj027

Morris, S. J., & Blackwood, C. B. (2007). The ecology of soil organisms. Soil microbiology, ecology and biochemistry , 195-229. Academic Press. https://doi.org/10.1016/B978-0-08-047514-1.50012-3

Müller, J., & Kuttler, C. (2015). Structured models in ecology. Methods and Models in Mathematical Biology, 297-414. Springer, Berlin, Heidelberg. https://link.springer.com/chapter/10.1007/978-3-642-27251-6_3

Mueller, P., Feller, U., & Erismann, K. H. (1977). Influence of different CO_2-concentrations on growth and composition of *Lemna minor* L. grown on nitrate or ammonium. Z. Pflanzenphysiol. Bd. 85, S.233-241. https://doi.org/10.1016/S0044-328X(77)80249-3

Mullineaux, C. W., Pascal, A. A., Horton, P., & Holzwarth, A. R. (1993). Excitation-energy quenching in aggregates of the LHC II chlorophyll-protein complex: a time-resolved fluorescence study. Biochimica et Biophysica Acta (BBA)-Bioenergetics, 1141(1), 23-28. https://doi.org/10.1016/0005-2728(93)90184-H

Muranaka, T., & Oyama, T. (2018). Monitoring circadian rhythms of individual cells in plants. J. Plant. Res., 131, 15–21. https://doi.org/10.1007/s10265-017-1001-x

Muranaka, T., Ito, S., Kudoh, H., & Oyama, T. (2022). Circadian-period variation underlies the local adaptation of photoperiodism in the short-day plant *Lemna aequinoctialis*. *Iscience*, *25*(7). https://doi.org/10.1016/J.Isci.2022.104634

Nakata, P. A. (2003). Advances in our understanding of calcium oxalate crystal formation and function in plants. Plant Sci., 164, 901-909. https://doi.org/10.1016/S0168-9452(03)00120-1

Nakata, P. A., Kostman, T. A., & Franceschi, V. R. (2003). Calreticulin is an important component of the high capacity calcium sequestration mechanism in specialized plant cells. Plant Biochemistry and Biophysics, 41, 425-430. https://www.jstor.org/stable/1514327

Nisbet, R. M., & Gurney, W. S. C. (1986). The formulation of age-structure models. *In*: Mathematical Ecology, 95-115. Springer, Berlin, Heidelberg. https://link.springer.com/chapter/10.1007/978-3-642-69888-0_5

Noonan, S. C., & Savage, G. P. (2002). Oxalate content of foods and its effect on humans. Asia Pacific J. Clin. Nutr., 8(1), 64-74. https://doi.org/10.1046/j.1440-6047.1999.00038.x

Ohri, D., & Khoshoo, T. N. (1986). Genome size in gymnosperms. Plant Syst. Evol., 153(1-2), 119–132. https://link.springer.com/article/10.1007/BF00989421

O'Neill, M. A., Eberhard, S., Albersheim, P., & Darvill, A. G. (2001). Requirement of borate cross-linking of cell wall rhamnogalacturonan II for *Arabidopsis*

growth. *Science*, *294*(5543), 846-849.
DOI: 10.1126/science.1062319

O'Neill, M. A., Ishii, T., Albersheim, P., & Darvill, A. G. (2004). Rhamnogalacturonan II: structure and function of a borate cross-linked cell wall pectic polysaccharide. *Annu. Rev. Plant Biol.*, *55*(1), 109-139.
https://doi.org/10.1146/annurev.arplant.55.031903.141750

Otto, S. P. (2007). The evolutionary consequences of polyploidy. Cell, 131(3), 452-462. https://doi.org/10.1016/j.cell.2007.10.022

van Ooteghem, R. J. (2010). Optimal control design for a solar greenhouse. IFAC Proceedings Volumes, 43(26), 304-309.
https://doi.org/10.3182/20101206-3-JP-3009.00054

Pagliuso, D., Grandis, A., Fortirer, J. S., Camargo, P., Floh, E. I. S., & Buckeridge, M. S. (2022). Duckweeds as promising food feedstocks globally. Agronomy 12, 796. https://doi.org/10.3390/agronomy12040796

Paterson, J. B., Camargo-Valero, M. A., & Baker, A. (2020). Uncoupling growth from phosphorus uptake in *Lemna*: Implications for use of duckweed in wastewater remediation and P recovery in temperate climates. Food Energy Secur., 9(4), e244. https://doi.org/10.1002/fes3.244

Pennisi, S.V., & McConnell, D.B. (2001). Inducible calcium sinks and preferential calcium allocation in leaf primordial of *Dracena sanderiana* Hort, Sander ex M.T. Mast (Dracaenaceae). Hortscience 36, 1187-1191.
https://doi.org/10.21273/HORTSCI.36.7.1187

Peoples, T.R. and Koch, D.W. (1979). Role of potassium in carbon dioxide assimilation in Medicago sativa L. Plant Physiol.. 63, 878-881.

Petersen F., Demann J., Restemeyer D. J., Ulbrich A., Olfs H.-W., Westendarp H., & Appenroth K.-J. (2021). Influence of the nitrate-N to ammonium-N ratio on relative growth rate and crude protein content in the duckweeds *Lemna minor* and *Wolffiella hyalina*. Plants, 10, 1741.
DOI: 10.3390/plants10081741

Petersen F., Demann J., Restemeyer D., Olfs H. W., Westendarp H., Appenroth K. J., & Ulbrich A. (2022). Influence of light intensity and spectrum on duckweed growth and proteins in a small-scale, re-circulating indoor vertical farm. Plants, 11(8), 1010
https://doi.org/10.3390/plants11081010

Paolacci, S., Stejskal, V., & Jansen, M. A. K. (2021). Estimation of the potential of *Lemna minor* for effluent remediation in integrated multi-trophic aquaculture using newly developed synthetic aquaculture wastewater. Aquacult. Int., 29, 2101–2118. https://doi.org/10.1007/s10499-021-00736-z

Polutchko, S. K., Stewart, J. J., McNamara, M., Doherty Garcia, N., López-Pozo, M., Adams III, W. W., & Demmig-Adams, B. (2022). *Lemna* as a sustainable, highly nutritious crop:

Nutrient production in different light environments. Nutraceuticals, 2(4), 350-364. https://doi.org/10.3390/nutraceuticals2040027

Porter, J. R., Xie L., Challinor, A. J., Cochrane, K., Howden, S. M., Iqbal ,M. M., Lobell, D. B., Travasso, M. I., Aggarwal, P., & Hakala, K. (2015). Food Security and Food Production Systems In Climate Change 2014-Impacts, Adaption and Vulnerability: Part A: Global and Sectoral Aspects; Cambridge University Press: Cambridge, UK; New York, NY, USA, 485-534.
https://eprints.whiterose.ac.uk/110945/

Prezioso, D., Strazzullo, P., Lotti, T., Bianchi, G., Borghi, L., Caione, P., Carini, M., Caudarella, R., Ferraro, M., Gambaro, G., Gelosa, M., Gut-Tilla, A., Illiano, E., Martino, M., Meschi, T., Messa, P., Miano, R., Napo-Dano, G., & Nouvenne, A. (2015). Dietary treatment of urinary risk factors for renal stone formation. A review of CLU working group. Arch. Ital. Urol. Androl., 87, 105–120.
https://doi.org/10.4081/aiua.2015.2.10519.

Quitadamo, I. J., Kostman, T. A., Schelling, M. E., & Franceschi, V. R. (2000). Magnetic bead purification as a rapid and efficient method for enhanced antibody specificity for plant sample immunoblotting and immunolocalization. Plant Sci., 153(1), 7-14. https://doi.org/10.1016/S0168-9452(99)00243-5

Raven, P. H., Evert, R.F., Eichhorn, S.E. (2005). Biology of Plants, 7th Edition, Macmillan

Raven, J., Osborne, B., & Johnston, A. (1985). Uptake of CO_2 by aquatic vegetation. Plant Cell Environ., 8(6), 417-425.
https://doi.org/10.1111/j.1365-3040.1985.tb01677.x

Rayburn, A. L., & Auger, J. A. (1990). Genome size variation in *Zea mays* ssp. mays adapted to different altitudes. Theor. Appl. Genet., 79(4), 470-474.
https://link.springer.com/article/10.1007/BF00226155

Richards, F. J. (1959). A flexible growth function for empirical use. J. Exp. Bot., 10(2), 290-300. https://doi.org/10.1093/jxb/10.2.290

Roncel, M., Gonzáles-Rodrígues, A. A., Naranjo, B., Bernal-Bayard, P., Lindahl, A. M., Hervas, M., Navarro, J. A., & Ortega, J. M. (2016). Iron deficiency induced a partial inhibition of photosynthetic electron transport and a high sensitivity to light in the diatom *Phaeodactylum tricornutum*. Front. Plant Sci., (Sec. Plant Cell Biology), 7. https://doi.org/10.3389/fpls.2016.01050

Rühle, W., & Wild, A. (1979). Measurements of cytochrome f and P-700 in intact leaves of *Sinapis alba* grown under high-light and low-light conditions. Planta, 146, 377-385. https://link.springer.com/article/10.1007/BF00380848

Sadigov, R. (2022). Rapid growth of the world population and its socioeconomic results. The Scientific World Journal.
https://doi.org/10.1155/2022/8110229

Sapeta, H., Yokono, M., Takabayashi, A., Ueno, Y., Cordeiro, A. M., Hara, T., Tanaka, A., Akimoto, S., Oliveira, M. M., & Tanaka, R. (2023). Reversible down-regulation of

photosystems I and II leads to fast photosynthesis recovery after long-term drought in *Jatropha curcas*. J. Exp. Bot., 74(1), 336–351. https://doi.org/10.1093/jxb/erac423

Saqrane, S., Ouahid, Y., El Hassni, M., El Hadrami, I., Bouarab, L., del Campo, F. F., ... & Vasconcelos, V. (2007). Phytotoxic effects of cyanobacteria extract on the aquatic plant *Lemna gibba*: microcystin accumulation, detoxication and oxidative stress induction. Aquat. Toxicol., 83(4), 284-294.

Schenck, R. U., & Hildebrandt, A.C. (1969). Production of protoplasts from plant cells in liquid culture using purified commercial cellulases 1. Crop. Sci., 9, 629–631. https://doi.org/10.2135/cropsci1969.0011183X000900050036x

Schmidt, K. M. (2010). Certificate on the grant of community plant variety rights. CPVO decision (No:29760)

Schmidt, K. M. (2020). Method for operating a culture facility for aquatic plants, and culture facility itself (DE 10 2020 133 132 A1). Deutsches Patent- und Markenamt. https://register.dpma.de/DPMAregister/pat/register?AKZ=1020201331320, filed

Schmidt, K. M. (2021). Method for operating a culture facility for aquatic plants, and culture facility itself (WO2022123076A1). European Patent Office, granted as EP. https://worldwide.espacenet.com/publicationDetails/originalDocument?FT=D&date=20220616&DB=&locale=en_EP&CC=WO&NR=2022123076A1&KC=A1&ND=4#

Schmidt, K. M., Rogmans, M., Wilhelm, H. J. (2018). Method for operating a culture system for protein-rich aquatic plants, as well as the culture system itself (DE 10 2018 003 368 B3). Deutsches Patent- und Markenamt, https://register.dpma.de/DPMAregister/pat/register?AKZ=1020180033687, granted

Schmidt, K. M., Rogmans, M., Wilhelm, H. J. (2018). Method for operating a farm with a combined fish farming and plant culture plant (DE 10 2018 007 939 A1). Deutsches Patent- und Markenamt, https://register.dpma.de/DPMAregister/pat/register?AKZ=1020180079393, filed

Schmitt, W. (2013). Mechanistic TK/TD-model simulating the effect of growth inhibitors on Lemna populations; Ecological Modelling, 255, 1-10. https://doi.org/10.1016/j.ecolmodel.2013.01.017

Simile® https://www.simulistics.com/

Schopfer, P., Brennicke, A., Pflanzenphysiologie, Spektrum Akademischer Verlag, 7. Aufl. 2010, S. 264 ff.

Severi, A., & Fornasiero, R. B. (1983). Morphological variations in *Lemna minor* L. and possible relationships with abscisic acid. Caryologia 36(1), 57-64. https://doi.org/10.1080/00087114.1983.10797644

De Silva, D. L. R., Hetherington, A. M., & Mansfield, T. A. (1996). Where does all the calcium go? Evidence of an important regulatory role for trichomes in two calcicoles. Plant, Cell

& Environment, 19(7), 880-886.
https://doi.org/10.1111/j.1365-3040.1996.tb00424.x

Smith, S. D. P. (2022). The influence of light and nutrient availability on floating plant dominance in forested temporary and semipermanent wetlands. Hydrobiologia 849, 2595–2608.
https://doi.org/10.1007/s10750-022-04881-1

Smith, V. H., & Schindler, D. W. (2009). Eutrophication science: where do we go from here? 24(4), 201-207.
https://doi.org/10.1016/j.tree.2008.11.009

Sońta, M., Rekiel, A., & Batorska, M. (2019). Use of duckweed (*Lemna* L.) in sustainable livestock production and aquaculture – a review. Ann. Anim. Sci., 19(2), 257–271. DOI: 10.2478/aoas-2018-0048

Soong, J. L., Fuchslueger, L., Marañon-Jimenez, S., Torn, M. S., Janssens, I. A., Penuelas, J., & Richter, A. (2020). Microbial carbon limitation: The need for integrating microorganisms into our understanding of ecosystem carbon cycling. Global change biol., *26*(4), 1953-1961.
https://doi.org/10.1111/gcb.14962

Sree, K. S., Appenroth K. J. (2014). Increase of starch accumulation in the duckweed *Lemna minor* under abiotic stress. Albanian J. Agric. Sci., 13, 11–14.

Sree, K. S., Sudakaran, S., Appenroth, K. J. (2015). How fast can angiosperms grow? Species and clonal diversity of growth rates in the genus Wolffia (*Lemnaceae*). Acta Physiol. Plant., 37, 204.
https://doi.org/10.1007/s11738-015-1951-3

Sree, K. S., Dahse, H. M., Chandran, J. N., Schneider, B., Jahreis, G., & Appenroth, K. J. (2019). Duckweed for human nutrition: no cytotoxic and no anti-proliferative effects on human cell lines. Plant Foods Hum. Nutr., 74(2), 223-224.
https://doi.org/10.1007/s11130-019-00725-x

Sree, K. S., & Appenroth, K. J. (2020). Worldwide genetic resources of duckweed: stock collections. In The Duckweed Genomes (39-46). Cham: Springer International Publishing.
https://doi.org/10.1007/978-3-030-11045-1_3

Steinberg, R. A. (1946). Mineral requirements of *Lemna minor*. Plant Physiol., 21(1), 42.
https://www.ncbi.nlm.nih.gov/pmc/articles/PMC437718/

Stewart, J. J., Adams, W. W. III, López-Pozo, M., Doherty Garcia, N., McNamara, M., Escobar, C. M., & Demmig-Adams, B. (2021). Features of the Duckweed Lemna That Support Rapid Growth under Extremes of Light Intensity. Cells, 10, 1481.
https://doi.org/10.3390/cells10061481

Stewart, J. J., Adams, W. W. III, Escobar, C. M., López-Pozo, M., & Demmig-Adams, B. (2020). Growth and essential carotenoid micronutrients in *Lemna gibba* as a function of growth

light intensity. Front. Plant Sci., 11, 480.
https://www.frontiersin.org/articles/10.3389/fpls.2020.00480/full

Stomp, A. M. (2005). "The duckweeds: a valuable plant for biomanufacturing. Biotechnology Annual Review, 11, 69–99.
https://doi.org/10.1016/S1387-2656(05)11002-3

Sun, X., Chen, F., Yuan, L., & Mi, G. (2020). The physiological mechanism underlying root elongation in response to nitrogen deficiency in crop plants. *Planta*, *251*(4), 84. https://link.springer.com/article/10.1007/s00425-020-03376-4

Szabo, S., Roijackers, R., Scheffer, M., & Borics, G. (2005). The Strength of limiting factors for duckweed during algal competition, Arch. Hydrobiol., 164(1), 127-140.
DOI: 10.1127/0003-9136/2005/0164-0127

Taylor E. N., & Curhan G. C. (2013). Dietary calcium from dairy and nondairy sources, and risk of symptomatic kidney stones. J. Urol., 190, 1255–1259.
https://doi.org/10.1016/j.juro.2013.03.074

Tebbani, S., Lopes, F., Filali, R., Dumur, D., & Pareau, D. (2014). Nonlinear predictive control for maximization of CO_2 bio-fixation by microalgae in a photobioreactor. *Bioprocess. Biosyst. Eng.*, *37*(1), 83-97.
https://link.springer.com/article/10.1007/s00449-013-0928-0

Thor, K. (2019). Calcium—nutrient and messenger. Front. Plant Sci., 10, 440.
https://doi.org/10.3389/fpls.2019.00440

Tikhonov, A. N. (2015). Induction events and short - term regulation of electron transport in chloroplasts: an overview. Photosynth. Res., 125, 65-94.
https://link.springer.com/article/10.1007/s11120-015-0094-0

Turck, D., Bohn, T., Castenmiller, J., De Henauw, S., Hirsch-Ernst, K. I., Knutsen, H. K., Maciuk, A., Mangelsdorf, I., McArdle, H. J., Naska, A., Pelaez, C., Pentieva, K., Siani, A., Thies, F., Tsabouri, S., & Vinceti. M. (2022). Safety of *Lemna minor* and *Lemna gibba* whole material as novel food pursuant to Regulation (EU) 2015/2283. EFSA J., 20(11). https://doi.org/10.2903/j.efsa.2022.7598

Türker, O. C., Yakar, A., & Gür, N. (2017). Bioaccumulation and toxicity assessment of irrigation water contaminated with boron (B) using duckweed (*Lemna gibba* L.) in a batch reactor system. J. Hazard. Mater., 324(B), 151-159.
https://doi.org/10.1016/j.jhazmat.2016.10.044

Ueda, K., & Nagai, T. (2021). Relative sensitivity of duckweed *Lemna minor* and six algae to seven herbicides. J. Pestic. Sci., 46(3), 267-273.
https://doi.org/10.1584/jpestics.D21-018

Ueno, K., Ito S., & Oyama, T. (2022). An endogenous basis for synchronisation characteristics of the circadian rhythm in proliferating *Lemna minor* plants. New Phytol., 233(5), 2203-2215.
https://doi.org/10.1111/nph.17925

Ullah, H., Gul, B., Khan, H., Ur Rehman, K., Hameed, I., Zeb, U., & Roomi, S. (2023). Impact of pH on the growth and nutritional profile of *Lemna minor* L. as a sustainable alternative for Pakistan's feed sector. Aquacult. Int., 31(4), 1879-1891. https://doi.org/10.1007/s10499-023-01063-1

Ullah, H., Gul, B., Khan, H., & Zeb, U. (2021). Effect of salt stress on proximate composition of duckweed (*Lemna minor* L.). Heliyon, 7(6). https://doi.org/10.1016/j-heliyon.2021.e07399

Vanhanen, L. P. (2018). Oxalate content of green juices and strategies for reduction of soluble oxalate content: A thesis submitted in partial fulfilment of the requirements for the Degree of Doctor of Philosophy at Lincoln University (Doctoral dissertation, Lincoln University). https://www.researchgate.net/publication/336724079

Vassilieva, O. (2011). Modelling and analysis of population dynamics in advective environments. University of Ottawa (Canada). ProQuest Dissertations Publishing, 2011. NR98243 https://www.proquest.com/openview/c8198ec1ee816065d2d8696410d7c8e5/1.pdf?pq-origsite=gscholar&cbl=18750

VDLUFA. Methodenbuch Band 3 "Die Chemische Untersuchung von Futtermitteln"; VDLUFA-Verlag: Darmstadt, Germany, 2012

Verhulst, P. F. (1845). La loi d'accroissement de la population. Nouveaux Memories de l'Académie Royale des Sciences et Belles-Lettres de Bruxelles, 18, 14-54. https://www.persee.fr/doc/marb_0770-8157_1845_num_18_1_3438

Verhulst, P. F. (1845). Recherches mathématiques sur la loi d'accroissement de la population. Mémoires de l'académie royale de Belgique, 18(1), 1-40.

Vidaković Cifrek, Ž., Sorić, S., & Babić, M. (2013). Growth and photosynthesis of *Lemna minor* L. exposed to different light conditions and sucrose supplies. Acta Botan. Croat., 72(2), 211-219. https://doi.org/10.2478/v10184-012-0018-4

Vivar-Quintana, A. M., Absi, Y., Hernández-Jiménez, M., & Revilla, I. (2023). Nutritional value, mineral composition, fatty acid profile and bioactive compounds of commercial plant-based gluten-free flours. Appl. Sci., 13(4), 2309. https://doi.org/10.3390/app13042309

Volk, G. M., Lynch-Holm, V. J., Kostman, T. A., Goss, L. J., & Franceschi, V. R. (2002). The role of druse and raphide calcium oxalate crystals in tissue calcium regulation in *Pistia stratiotes* leaves. Plant biol., 4(01), 34-45. DOI: 10.1055/s-2002-20434

Voxeur, A., & Fry, S. C. (2014). Glycosylinositol phosphorylceramides from Rosa cell cultures are boron-bridged in the plasma membrane and form complexes with rhamnogalacturonan II. *The Plant Journal*, *79*(1), 139-149. https://doi.org/10.1111/tpj.12547

Wada, M., & Kagawa, T. (2001). Light-controlled chloroplast movement. In *Comprehensive Series in Photosciences*, 1, 897-924. Elsevier https://doi.org/10.1016/S1568-461X(01)80030-2

Walsh, E., Coughlan, N. E., O'Brien, S., Jansen, M. A. K., & Kühnhold, H. (2001). Density dependence influences the efficacy of wastewater remediation by *Lemna minor*. Plants, 10(7), 1366. https://doi.org/10.3390/plants10071366

Wang, W., Kerstetter, R. A., & Michael, T. P. (2011). Evolution of genome size in duckweeds (*Lemnaceae*). J. Bot., *2011*(1), 570319. doi:10.1155/2011/570319

Wang J., Zhou Y., Dong C., Shen Q., & Putheti R. (2009). Effects of NH_4^+-N/ NO_3^--N ratios on growth, nitrate uptake and organic acid levels of spinach (*Spinacia oleracea* L.). Afr. J. Biotechnol., 8(15), 3597-3602. https://www.ajol.info/index.php/ajb/article/view/61860

Wang, W., Wu, Y., Yan, Y., Ermakova, M., Kerstetter, R., & Messing, J. (2010). DNA barcoding of the *Lemnaceae*, a family of aquatic monocots. BMC Plant Biol., 10, 1-11. https://link.springer.com/article/10.1186/1471-2229-10-205

Wang, Y., Wang, X., Yang, R., Niu, L., & Wang, W. (2020). Comparison of protein extraction methods for 2DE-based proteomic analysis of duckweed *Spirodela polyrhiza*, a small aquatic model plant, Aquat. Bot., 163, 103216. https://doi.org/10.1016/j.aquabot.2020.103216

Warsi, O. M., & Dykhuizen, D. E. (2017). Evolutionary implications of Liebig's law of the minimum: Selection under low concentrations of two non-substitutable nutrients. Ecol. Evol., 7(14), 201, 5296-5309. https://doi.org/10.1002/ece3.3096

Watanabe, F. (2007). Vitamin B12 sources and bioavailability. Exp. Biol. Med., *232*(10), 1266-1274.

Watanabe, T., Kioka, M., Fukushima, A., Morimoto, M., & Sawamura, H. (2014). Biotin content table of select foods and biotin intake in Japanese. *Int J Anal Bio-Sci Vol*, *2*(4).

Watanabe, E., Isoda, M., Muranaka, T., Ito, S., & Oyama, T. (2021). Detection of uncoupled circadian rhythms in individual cells of *Lemna minor* using a dual-color bioluminescence monitoring system. Plant and Cell Physiol., 62(5), 815-826. https://doi.org/10.1093/pcp/pcab037

Webb, M. A. (1999). Cell mediated crystallization of calcium oxalate in plants. Plant Cell, 11, 751-761. https://doi.org/10.1105/tpc.11.4.751

Wedge, R. M., & Burris, J. E. (1982). Effects of light and temperature on duckweed photosynthesis. Aquat. Bot., 13, 133-140. https://doi.org/10.1016/0304-3770(82)90047-X

Wersal, R. M., & Turnage, G. (2021). Using contact herbicides for control of duckweed and watermeal with implications for management. Journal of Aquatic Plant Management, 59(1), 40-45. https://www.apms.org/wp-content/uploads/japm-59-01-40-full.pdf

White, P. J., & Broadley, M. R. (2003). Calcium in Plants. *Ann. Bot.*, 92(4), 487–511. https://doi.org/10.1093/aob/mcg164

White, P. J., & Broadley, M. R. (2009). Biofortification of crops with seven mineral elements often lacking in human diets – iron, zinc, copper, calcium, magnesium, selenium and iodine. 182(1), 49-84. https://doi.org/10.1111/j.1469-8137.2008.02738.x

Wimmer, M. A., Lochnit, G., Bassil, E., Mühling, K. H., & Goldbach, H. E. (2009). Membrane-associated, boron-interacting proteins isolated by boronate affinity chromatography. *Plant Cell Physiol.*, *50*(7), 1292-1304. https://doi.org/10.1093/pcp/pcp073

World Health Organization, & Unicef. (2004). Focusing on anaemia: towards an integrated approach for effective anaemia control: joint statement by the World Health Organization and the United Nations Children's Fund. In *Focusing on anaemia: towards an integrated approach for effective anaemia control: joint statement by the World Health Organization and the United Nations Children's Fund* (pp. 1-sheet).

Wyn Jones, R. G., Brady, C. J., & Speirs, J. (1979). Ionic and osmotic relations in plant cells. *Recent advances in the biochemistry of cereals*, 63-103. Academic Press, London and Orlando.

Xie, K., Cakmak, I., Wang, S., Zhang, F., & Guo, S. (2021). Synergistic and antagonistic interactions between potassium and magnesium in higher plants. The Crop Journal, 9(2), 249-256. https://doi.org/10.1016/j.cj.2020.10.005

Xu, J., Shen, Y., Zheng, Y., Smith, G., Sun, X. S., Wang, D., ... & Li, Y. (2023). Duckweed (*Lemnaceae*) for potentially nutritious human food: A review. Food Reviews International, 39(7), 3620-3634. DOI: 10.1080/87559129.2021.2012800

Xu, Y., Ma, S., & Huang, M. et al. (2015). Species distribution, genetic diversity and barcoding in the duckweed family (*Lemnaceae*). Hydrobiologia 743, 75–87. https://doi.org/10.1007/s10750-014-2014-2

Xu, J., Cui, W., Cheng, J. J., & Stomp, A. M. (2011). Production of high-starch duckweed and its conversion to bioethanol. Biosyst. Eng., 110(2), 67-72. https://doi.org/10.1016/j.biosystemseng.2011.06.007

Xu, J., & Shen, G. (2011). Growing duckweed in swine wastewater for nutrient recovery and biomass production. Bioresour. Technol., 102(2), 848-853. https://doi.org/10.1016/j.biortech.2010.09.003

Xu, J., Shen, Y., Zheng, Y., Smith, G., Sun, X. S., Wang, D., ... & Li, Y. (2023). Duckweed (*Lemnaceae*) for potentially nutritious human food: A review. Food Rev. Int., 39(7), 3620-3634. https://doi.org/10.1080/87559129.2021.2012800

Yahaya, N., Hamdan, N. H., Zabidi, A. R., Mohamad, A. M., Suhaimi, M. L. H., Johari, M. A. A. M., ... & Yahya, H. (2022). Duckweed as a future food: Evidence from metabolite profile, nutritional and microbial analyses. Future Foods, 5, 100128.

Yang, J., Zhao, X., Li, G., Hu, S., & Hou, H. (2021). Frond architecture of the rootless duckweed *Wolffia globosa*. BMC Plant Biol., 21(1), 387. https://doi.org/10.1186/s12870-021-03165-5

Yang, D. H., Andersson, B., Aro, E. M., & Ohad, I. (2001). The redox state of the plastoquinone pool controls the level of the light-harvesting chlorophyll a/b binding protein complex II (LHC II) during photoacclimation. Photosynth. Res., 68, 163-174. https://doi.org/10.1023/A:1011849919438

Ye, X., Gao, Z., Xu, K., Li, B., Ren, T., Li, X., ... & Lu, J. (2024). Photosynthetic plasticity aggravates the susceptibility of magnesium-deficient leaf to high light in rapeseed plants: the importance of Rubisco and mesophyll conductance. The Plant J., 117(2), 483-497. https://doi.org/10.1111/tpj.16504

Ye X, Chen X-F, Deng C-L, Yang L-T, Lai N-W, Guo J-X, & Chen L-S. (2019). Magnesium-deficiency effects on pigments, photosynthesis and photosynthetic electron transport of leaves, and nutrients of leaf blades and veins in *Citrus sinensis* seedlings. *Plants*. 8(10), 389. https://doi.org/10.3390/plants8100389

De Yoreo, J. J., & Vekilov, P. G. (2003). Principles of crystal nucleation and growth. Rev. Mineral. Geochem., 54(1), 57-93. https://doi.org/10.2113/0540057

Yu, G., Liu, H., Venkateshan, K., Yan, S., Cheng, J., Sun, X. S., & Wang, D. (2011). Functional, physiochemical, and rheological properties of duckweed (*Spirodela polyrhiza*) protein. Transactions of the ASABE, 54(2), 555-561. doi: 10.13031/2013.36459

Yu, Q., Baluška, F., Jasper, F., Menzel, D. and Goldbach, H.E. (2003), Short-term boron deprivation enhances levels of cytoskeletal proteins in maize, but not zucchini, root apices. Physiol. Plant., 117: 270-278. https://doi.org/10.1034/j.1399-3054.2003.00029.x

Yu, Q., Wingender, R., Schulz, M., Baluška, F. and Goldbach, H.E. (2001), Short-term boron deprivation induces increased levels of cytoskeletal proteins in *Arabidopsis* roots. Plant Biol., 3: 335-340. https://doi.org/10.1055/s-2001-16452

Zeiger, E., Farquhar, G.D., & Cowan I.R. (1987). Stomatal Functions. Stanford University Press, 229. https://books.google.de/books?hl=de&lr=&id=mp-aAAAAIAAJ&oi=fnd&pg=PR9&dq=Zeiger,+E.,+Farquhar,+G.D.,+Cowan+I.R.+(1987).+Sto

matal+Functions.+Stanford+University+Press,+pp+229,+&ots=T97-r-bfap&sig=sdsiROfvK-N2GlocgwxvYL3gKbc#v=onepage&q&f=false

Zenir, M. C., López-Pozo, M., Polutchko, S. K., Stewart, J. J., Adams III, W. W., Escobar, A., & Demmig-Adams, B. (2022). Productivity and nutrient quality of *Lemna minor* as affected by microbiome, CO_2 level, and nutrient supply. Stresses, 3(1), 69-85. https://doi.org/10.3390/stresses3010007

Zeskan, A. (2016). Duckweed: An efficient hyperaccumulator of heavy metals in water bodies. Plant Metal Interaction, 411-429, Elsevier. https://doi.org/10.1016/B978-0-12-803158-2.00016-3

Ziegler, P., Adelmann, K., Zimmer, S., Schmidt, C., & Appenroth, K. (2015). Relative *in vitro* growth rates of duckweeds (*Lemnaceae*) – the most rapidly growing higher plants. Plant Biol. 17, 33–41. https://doi.org/10.1111/plb.12184

Zindler-Frank, E. (1975). On the formation of the pattern of crystal idioblasts in *Canavalia ensiformis* DC. VII. Calcium and oxalate content of the leaves in dependence of calcium nutrition. Z. Pflanzenphysiol. 77(1), 80-85. https://doi.org/10.1016/S0044-328X(75)80128-0

Zindler-Frank, E., Honow R., & Hesse A. (2001). Calcium and oxalate content of leaves of *Phaseolus vulgaris* at different calcium supply in relation to calcium oxalate crystal formation. J. Plant Physiol. 158, 139-144.

Zhao, Z., Shi, H. J., Wang, M. L., Cui, L., Zhao, H., & Zhao, Y. (2015). Effect of nitrogen and phosphorus deficiency on transcriptional regulation of genes encoding key enzymes of starch metabolism in duckweed (*Landoltia punctata*). Plant Physiol. Biochem., 86, 72-81. https://doi.org/10.1016/j.plaphy.2014.11.007

Zhou, Q., Gao, J., Zhang, R., & Zhang, R. (2017). Ammonia stress on nitrogen metabolism in tolerant aquatic plant—*Myriophyllum aquaticum*. Ecotoxicol. Environ. Saf., 143, 102-110. https://doi.org/10.1016/j.ecoenv.2017.04.016

10. APPENDICES

10.1 Analytical Integration in detail

Starting with basic differential equation for limited growth,

(Verhulst 1838, Murray J.D. Mathematical Biology, third edition 2004, pp 3-5))

$$\frac{dW(t)}{dt} = r_i * W(t) * (1 - \frac{W(t)}{Wmax})$$

(Term $r_i * \frac{\boldsymbol{W(t)}}{\boldsymbol{Wmax}}$ *van den Top, 2014* is implemented as well in the differential equation)

Solution path of improved analytical solution:

$$\frac{dW(t)}{dt} = r_i * W(t) - \frac{r_i}{Wmax} * W(t)^2 \qquad /$$

$$\Rightarrow \quad -\frac{Wmax}{r_i} * \frac{dW(t)}{dt} = W(t)^2 - Wmax * W(t) \qquad / : (W(t)^2 - Wmax * W(t)) \; / * (-\frac{r_i}{Wmax})$$

$$\Rightarrow \quad \int \frac{1}{W^2 - Wmax * W(t)} * dW(t) = \int -\frac{r_i}{Wmax} * dt \quad / \text{ Integration on both sides}$$

$$\Rightarrow \quad -\frac{2}{Wmax} * artanh\left(\frac{2W(t) - Wmax}{Wmax}\right) = -\frac{r_i}{Wmax} * t + C \quad /$$

$$\Rightarrow \quad artanh\left(\frac{2W(t) - Wmax}{Wmax}\right) = \frac{r_i}{2} * t - C * \frac{Wmax}{2} \quad / \text{ creation of reverse function on both sides}$$

$$\Rightarrow \quad \frac{2W(t) - Wmax}{Wmax} = \tanh(\frac{r_i}{2} * t + \frac{Wmax}{2} * C)$$

$\Rightarrow$

Final solution:

⇨ $W(t) = \frac{Wmax}{2} * (\tanh(\frac{r_i}{2} * t + \frac{Wmax}{2} * C) + 1)$

Additional hint: The analytical solution of the limited growth propagation differential equation is a **tangens hyperbolicus** function as it is

Verification of calculation:

First deviation of eq.2:

$W'(t) = \frac{Wmax}{4} r_i * (1 - \tanh^2(\frac{r_i}{2} * t + \frac{Wmax}{2} * C))$

Abbreviation: $X = (\frac{r_i}{2} * t + \frac{Wmax}{2} * C)$

eq.2 and eq.3 filled into eq.1

⇨ $\frac{Wmax}{4} r_i * (1 - \tanh^2(X)) = \frac{Wmax}{2} r_i(tanh\, X + 1) - \frac{r_i}{Wmax} * \frac{Wmax^2}{4} (\tanh^2(X) + 2\tanh(X) + 1$

$$= \frac{Wmax}{4} r_i(2\tanh(X) + 2 - \tanh^2(X) - 2\tanh(X) - 1$$

$$= \frac{Wmax}{4} * r_i(1 - \tanh^2(X))$$

q. e. d.

The so obtained solution already shows the importance of "**$W_{max}/2$**" as value for the turning point Wp of maximum gradient of biomass propagation, considered as multiplication factor as well as in the argument of the tan-hyp function.

10.2 Development/Evaluation of growth factor ri:

Series of r_i factors are dependent to T, E(light), CO_2 and Nutrition.

For temperature and **photoperiod** influence to the model:

$r_i(T) \propto * T * \theta 1^{\left(\frac{T-Top}{Top}\right)^2} * \theta 2^{\left(\frac{T-Top}{Top}\right)}$ *van 't Hoff Arrhenius*

$r_i(E) \propto * E * \theta 3^{\left(\frac{E-Eop}{Eop}\right)^2} * \theta 4^{\left(\frac{E-Eop}{Eop}\right)}$ *Lasfar et al (2014)*

Further simplification for T and E.
If T near to T_{op}, and E near to E_{op}, we assume $T=T_{op}$ and $E=E_{op}$.
=> $\Theta_i = 1$
=> $r_i(T) \propto * T$
and $r_i(E) \propto * E$

Under this assumption $r_i(T)$ and $r_i(E)$ get quasi linear in T and E, near optimum. This keeps in line with Michaelis-Menten kinetics at asymptotic branch near Optimum.

For **nutrition** influence to r_i with N and P:

$$r_i(P,N) = \alpha P,N * \frac{CP}{(CP+KP)} * \frac{KIP}{(KIP+CP)} * \frac{CN}{(CN+KN)} * \frac{KIN}{(KIN+CN)}$$ *Lasfar (2014)*

with

$\alpha_{P,N}$	intrinsic growth rate
C_P	P concentration
C_N	N concentration
K_{IP}, K_P, K_N, K_{IN}	constants for saturation and inhibition of P and N.

r_{i0}	possible maximum growth rate
$\alpha(r_i(T))$	α-factor, contribution of temperature to the growth rate
$\beta(r_i(E))$	β-factor, contribution of photonic energy to the growth rate
$\gamma(r_i(N,P))$	γ-factor, contribution of nutrient ratios to the growth rate
$\delta(r_i(CO_2))$	δ-factor, contribution of CO_2 concentration to the growth rate

For **CO_2** influence to r_i:
Consideration as diffusion model:

$$RCO_2 = \frac{Rcut*Rs}{(Rcut+Rs)} + Rcarboxyl$$

CO_2-Conductivity = 1/CO_2-Resistance

⇨ to be measured !!!

Final consideration as **product rule for r_i**, related to Liebig's law of minimum:

$$r_i = r_{i0} * |\alpha(r_i(T))| * |\beta(r_i(E))| * |\gamma(r_i(N,P))| * |\delta(r_i(CO2))|$$

to be filled in:

$$W(t) = \frac{Wmax}{2} * (\tanh(\frac{r_i}{2} * t + \frac{Wmax}{2} * C) + 1)$$

$$=> \boldsymbol{W(t)} = \frac{\boldsymbol{Wmax}}{2} * (\boldsymbol{tanh}(\frac{r_{i0}}{2} * (\prod_{T,E,N,P,CO2} k * r_i(j)) * \boldsymbol{t} + \frac{\boldsymbol{Wmax}}{2} * \boldsymbol{C}) + 1)$$

with the time-dependent exponent

$$\frac{r_{i0}}{2} * (\prod_{T,E,N,P,CO2} k * r_i(j)) * \boldsymbol{t}$$

and the aforementioned time-independent exponent

$$\frac{\boldsymbol{Wmax}}{2} * \boldsymbol{C}$$

10.3 Comparison of standard nutrient solution

Tab.35 Comparison of used salts in standard nutrient solution compared to nutrient solution of this work

	Hoagland	**Mod. Steinberg**	**Schenck-Hildebrand**	**N-Medium**	**Schmidt KM**
Salts	**mM**	**mM**	**mM**	**mM**	**mM**
$Ca(NO_3)_2$ $4H_2O$	4	1.25	0.68	1.0	0.52
$(NH_4)_2SO_4$	-	-	-	-	0.05
$(NH_4)H_2PO_4$	-	-	1.3	-	-
K_2SO_4	-	-	-	-	0.25
KCl	-	-	-	-	-
KH_2PO_4	1	0.66	-	0.15	0.23
K_2HPO_4 $3H_2O$	-	0.072	-	-	-
KNO_3	10	3.46	12.4	8.0	-
$MgSO_4$ $7H_2O$	2	0.41	0.8	1.0	0.4
KI	-	-	0.003	-	-
	µM	**µM**	**µM**	**µM**	**µM**
H_3BO_3	50	1.94	40	5	46
$MnSO_4$	-	-	30	-	-
$MnCl_2$	10	0.91	-	13	9.15
$CuSO_4 \cdot 5H_2O$	0.4	-	0.4	-	0.32
$ZnSO_4$ $\cdot 7H_2O$	1.5	0.63	1.74	-	0.77
$Na_2MoO_4 \cdot 2H_2O$	5	0.18	0.2	0.4	0.58
$(NH_4)_6Mo_7O_{24}$ $4H_2O$	-	-	-	-	-
$CoCl_2$ $6H_2O$	-	-	0.21	-	-
FeNaEDTA	20	2.81	26	25	-
EDTA-Na2	-	1.22	2.75	25	-
Fe-EDDHA	-	-	-	-	18

10.4 List of equipment and reagents

Tab.36: Equipment and reagents used in lab-scale, first up-scale, second up-scale

Equipment: culturing and sample preparation	
Gas-cylinder CO_2	80 Bar, 5.0, Air liquide, Krefeld, Germany,
Pressure reducing valve	Air liquide, Krefeld, Germany
Flowmeter	SCENTY®, HTK Hamburg, Germany
CO_2 Flow and dosing controller (Bonn, Kalkar)	MAPAX® control Flowbox, HTK Hamburg, Germany
CO_2 water system (Kalkar)	CARBORAIN® Danfoss, Type CT-A30, 078B8002, P_{in} 3 Bar
Growth-Box, aluminum profiles	ITEM-Industrie Profile, Solingen, Germany

Growth-Box, UV Foil	**Folitec Agrarfolien-Vertriebs GmbH, Westerburg, Germany**
Heating mats for plant cultivation	Bio-Green, by Beckmann GmbH & Co KG, Wangen im Allgäu, Germany
RCD circuit breaker	240V/10A, ABB AG, Germany
Flexible tubing	Tygon® and silicon tubes, Merck (St Gobain)
Perestaltic pump, 30 channel	(reassembled from Flow analyzer), Skalar Analytical B.V., Breda, Netherlands
LED Light bars, Kalkar	NetLED Low-Blue + NetledVFC,NVS2423V/NM0002204, Pirkkala, Finland
LED light table, adjust. 400, 440, 660, 730 nm +3000K (530nm)	Mobile LED Rack M-RU, Rhenac Green-tech AG, Hennef, Germany
LED Light bars, Berlin, Kalkar	LedInPro, Typ Grow T8-LL315 (High-blue), Zhengzhou, Henan, China
Preculture (Aquarien)	Hornbach, Krefeld
Single LED-light Bar (precultures)	Rhenac Green-tech AG, Hennef, Germany
Harvesting means (adjustable)	Stainless steel, Custom made according to specification, ABB-AG, Ratingen, Germany
Sample bags	Pergamin 95x132, Carl Roth GmbH+Co KG, Germany
Vials	20ml HD polyethylene vials 20 ml, Carl Roth GmbH+Co KG, Germany
Data logger	Dostmann Log 210, Carl Roth GmbH+Co KG, Germany
Magnetic stirrer (incl Hotplate)	ROTILABO® MH15, Carl Roth GmbH+Co KG, Germany
Micropipettors, set-up Kalkar & Uni Bonn	Adjustable 0.001-5ml ROTILABO®, Carl Roth GmbH+Co KG, Germany
Micropipettors Uni DUE (Duisburg-Essen)	Set: 0.5µl-5ml Eppendorf, Merck KG
Centrifuge Uni DUE	Centrifuge 5430R; Eppendorf, Hamburg, Germany
Ultrasonic cleaner Uni DUE	
Shaking platform	DuoMax 1030; Heidolph, Schwabach, Germany
IR-Dryer , Kalkar	RADWAG® MA 50.R
Culture trays in experimental set-up	Borosilicate glas, Duran®, Carl Roth GmbH+Co KG, Germany
Desiccator 1. generation	Exsikkator Glass, DN 250, 8l, ROTILABO®, Carl Roth GmbH+Co KG, Germany
Desiccator 2. generation	Exsikkator Star Vitrum 42l, Carl Roth GmbH+Co KG, Germany
Camera	Leica SL2 + Vario 24-70mm asph. Olympus E5+Makro 25mm, 1:1.4
Lab. glass: Soda-lime, Borsilicate Duran®	Rotilabo®, Carl Roth GmbH+Co KG, Germany
Plant trays	TRAY0001-000, Fuchs OHG, Linsengericht, Germany
Culture trays	Borsilicate, DURAN®
Mesh (Bonn, Harvesting)	Flow Meshtrade™ FM-100, PP-Mesh 1/3mm x 1mm, 70% void volume, (Diversified Biotech, Dedham Ma, USA)
Microperforated foil (Berlin, harvesting and dewatering)	Aquaplus®, TGU GmbH+Co. KG, Greven, Germany

Mesh (100% PES) (Berlin, Kalkar, Drying)	HaGa®, HaGa-Welt GmbH+Co.KG, Elze, Germany
Amberglass Bottles 1l (Stocksolutions)	Soda lime glass, Carl Roth GmbH+Co KG, Germany
Glass tanks 2l (Nutrient solution tracking)	DURAN®, GLS 80, Carl Roth GmbH+Co KG, Germany

Analyzers and Probes	
Scale (Kalkar, Bonn)	Kern eW, accuracy 10 mg Carl Roth GmbH+Co KG, Germany
Scale (Uni DUE, DM for oxalate- and protein determination)	Metteler Toledo, MS104TS/00
pH-probe	Aqua Lytic AL 10 pH, Carl Roth GmbH+Co KG, Germany
EC-probe	Hanna, Hi 99300 EC/TDS Meter [µS], Carl Roth GmbH+Co KG, Germany
T-probe	Hanna, Hi 99300 EC /TDS Meter [°C] Carl Roth GmbH+Co KG, Germany
Photometric calibration solution for NH_4^+, NO_3^-, K	Hanna, Germany
Microscope	Olympus CX 31 RTSF
Microscope camera	Olympus CellSens Entry V1
Bradford Analyzer	Infinite 200 PRO microplate reader (Tecan, Crailsheim, Germany)
LCMS Analyzer	LC 2040C 3D + FCV-20AH2 Valve Unit + LCMS 2020, Shimadzu, Duisburg, Germany
ICP-Analyzer	Albotec GmbH, Germany
Photometer 1 (PAR)	Licor LI-1500, USA, Head Licor Quantum Q 107 010
Photometer 2 (incl Software adapt. to Excel®)	Mavospec Base 15579, Gossen, Germany
CO_2-Probe	Testo T-440 + probe head 06321270, Testo SE&Co.KGaG, Titisee-Neustadt, Germany
Calliper	Nonius Caliper, Accuracy: <0,1mm, Mitutoyo Europe GmbH, Neuss, Germany
Vials for LCMS and Bradford	1.5ml reaction tubes (Sarstedt, Nümbrecht, Germany)
Vortex mixer	Vortex Genie 2; Scientific Industries, Bohemia, NY, USA
96-well-plates (Bradford-analysis)	Carl Roth GmbH & Co. KG
Laboratory tissues (dewatering of harvest)	Kimberly Clarke professional, 200 Kimtech Science 20,5x 20 cm), Carl Roth GmbH+Co KG, Germany

Software	
Photometersoftware	Gossens for Mavospec base, last update Jan. 2019
Modelling Software	SIMILE®64 v6.12., Jun. 2023, University of Bonn
Office version (Word®, Excel®, Publisher®)	
R®	Update status Jan. 2023, University of Bonn

Software Bradford	Originally related software to Infinite 200 PRO microplate reader (Tecan, Crailsheim, Germany), status February 2023
Software LCMS	Originally related software to LC 2040C 3D + FCV-20AH2 Valve Unit + LCMS 2020, Shimadzu, Duisburg, Germany, status January 2022
ICP-Software	Originally related software, status March 2023
Software data logger	Dostmann, Carl Roth GmbH & Co. KG
Software Camera	Software Leica SL2, Vario Elmarit-SL, 1:2.8-4/24-90 asph, regular update, last update Febr. 2023
Software Microscope camera	Software CellSens V1.12

Reagents	
Calcium nitrate tetrahydrate $Ca(NO_3)_2$ 4 H_2O	Carl Roth GmbH & Co. KG
Ammonium sulfate $(NH_4)_2SO_4$	Carl Roth GmbH & Co. KG
Potassium hydrogen phosphate KH_2PO_4	Carl Roth GmbH & Co. KG
Potassium sulfate K_2SO_4	Carl Roth GmbH & Co. KG
Magnesium sulfate $MgSO_4$ $7H_2O$	Merck KG
Boronic acid H_3BO_3	Merck KG
Manganium chloride tetrahydrate $MnCl_2$ $4H_2O$	Merck KG
Zink sulfate heptahydrate $ZnSO_4$ $7H_2O$	Carl Roth GmbH & Co. KG
Copper sulfate $CuSO_4$	Carl Roth GmbH & Co. KG
Sodium molybdate Na_2MoO_4 $2H_2O$	Carl Roth GmbH & Co. KG
NaFe(III)-EDDHA	Sequestren 138 (6%), Merck KG
Styrene-divinylbenzene (anion exchange resin)	Amberlite® IRA 743, Sigma-Aldrich, Steinheim Germany, (Merck)
C_{18} ec SPE columns	1ml Chromabond C_{18} ec SPE column (Macherey-Nagel, Düren, Germany)
Solution / Bradford analysis	Roti®-Quant, Carl Roth GmbH + Co. KG,
Bovine serum albumin (BSA)	Sigma-Aldrich, Steinheim, Germany
DiH_2O, Bonn	Uni Bonn, Campus Klein-Altendorf
Ultrapure DiH_2O Uni DUE	Milli-Q® Lab Water Solutions, Merck KG
Acetronitrile (Eluent)	Acetonitrile 50% (v/v) in Milli-Q® Lab water
NaOH	0.1 mM, Merck
Acetone	Sigma-Aldrich, Steinheim, (Merck) Germany
Ethanol	Carl Roth GmbH + Co. KG
Hydrogen peroxide H_2O_2	Carl Roth GmbH + Co. KG
Glass vials and inserts incl crimp caps	Macherey-Nagel, Düren, Germany
Sulfuric acid (pH-Stabilization Kalkar)	Merck KG
Trichloroacetic acid	Carl Roth GmbH + Co. KG
Nitric acid (38%, for agricultural use)	CHEMIESHOP24.de
Aqua regia	Albotec GmbH
$CaCO_3$ (pH-stabilization Kalkar)	Merck KG
CO_2 Gas (for food application)	Air Liquide, Germany, purity level 5.0
Calibration solution for EC	Carl Roth GmbH + Co. KG
Calibrations solution for pH	Carl Roth GmbH + Co. KG
Grease for perestaltic pump	Skalar Analytical B.V., Breda, Netherlands
Bacteria Nitrosomonas (Berlin)	ECF Farm-systems GmbH, Berlin

Bacillus Thuringiensis (Kalkar) (Cataclysta Lemnata (Linnaeus, 1758))	Xentari®

Further Set ups Kalkar & Berlin :

Installations (Kalkar & Berlin)	
Greenhouse (Kalkar & Berlin)	Typ Venloblock, KTBL Netherlands
Culture trays /racksystem (Kalkar)	H97.000.010.0010, Meteor Systems BV, 4879 NG Etten Leur, Netherlands
Greenhouse Controler Kalkar	Hortraco Horti, Sirius-GC + SmartLink
Green House Controler Berlin	ECF Farm Systems, Berlin
Harvest- and Harvestwash Conveyer (Berlin)	Own construction
Ozonator (Berlin)	ECF Farm Systems, Berlin
Biofilter (Berlin)	ECF Farm Systems, Berlin
UV-Burner (Berlin)	ECF Farm Systems, Berlin

10.5 Certificate of used plant variety for experimental set-up

CPVO
Community Plant Variety Office

CERTIFICATE ON THE GRANT OF COMMUNITY PLANT VARIETY RIGHTS

THE COMMUNITY PLANT VARIETY OFFICE HEREBY ACKNOWLEDGES THE GRANT OF COMMUNITY PLANT VARIETY RIGHT BY ITS DECISION N° EU **29760** OF **10 MAY 2011** TAKEN IN ACCORDANCE WITH COUNCIL REGULATION (EC) N° 2100/94 ON COMMUNITY PLANT VARIETY RIGHTS, WITH EFFECT FROM THE DATE OF THE DECISION REFERRED TO ABOVE, FOR

Maria Rogmans
Spierheide 54
DE - 47546 Kalkar

AS HOLDER OF THIS RIGHT,

REPRESENTED BY

Patentanwalt Karl Michael Schmidt

BEING DOMICILED OR HAVING HIS SEAT OR ESTABLISHMENT IN

Buchenweg 65
DE - 47447 Moers

IN RESPECT OF THE VARIETY OF ***Lemna minor L.*** BEARING THE DESIGNATED DENOMINATION:

HENRY DACAPO

FOR A PERIOD EXPIRING ON **31 DECEMBER 2036** AT THE LATEST.

THE COMMUNITY PLANT VARIETY RIGHT HAS UNIFORM EFFECT WITHIN THE TERRITORY OF THE EUROPEAN COMMUNITY AND MAY NOT BE TRANSFERRED IN RESPECT OF THIS TERRITORY OTHERWISE THAN ON SUCH UNIFORM BASIS. IT CAN BE EXERCISED AND ENJOYED BY THE HOLDER IN ACCORDANCE WITH COUNCIL REGULATION N° 2100/94 ON COMMUNITY PLANT VARIETY RIGHTS.

THIS ACKNOWLEDGEMENT DOES NOT AFFECT THE REQUIREMENT OF THE HOLDER TO PAY THE FEES DUE FOR EACH YEAR OF DURATION OF THE COMMUNITY PLANT VARIETY RIGHT.

President of the
Community Plant Variety Office

Bart KIEWIET

CPVO
Community Plant Variety Office

DECISION
(No: 29760)

The competent Committee for determining applications for the grant of Community Plant Variety Rights has decided, pursuant to article 62 of Council Regulation (EC) No 2100/94 (the Regulation), to grant such a right in relation to -

the variety: **HENRY DACAPO** (Application number: **2010/0855**)

of species: ***Lemna minor L.***

to: (Applicant) **Maria Rogmans**
Spierheide 54
DE - 47546 Kalkar

Date: **10 MAY 2011**

In connection with the grant of this Community Plant Variety Right the Committee has approved, pursuant to article 63 of the Regulation, the variety denomination:

HENRY DACAPO

Signed:

Dirk THEOBALD Martin EKVAD Carlos GODINHO

Taken under the authority of the President of the Office,

Community Plant Variety Office • Office Communautaire des Variétés végétales
Bart KIEWIET
Community Plant Variety Office • Office Communautaire des Variétés végétales

The attention of the applicant is drawn to their possibility to appeal against this decision. Notice of appeal shall be filed by the applicant in writing to the attention of the Community Plant Variety Office within two months of the service of the decision.
The attention of the applicant is drawn to the possibility of an appeal against this decision by a third party to whom it is of direct and individual concern. Notice of such appeal shall be filed in writing to the attention of the Community Plant Variety Office within two months of the publication of the decision.
Appeals are subject to a fee.

nak tuinbouw

FINAL REPORT ON THE TECHNICAL EXAMINATION IN THE FRAMEWORK OF PLANT BREEDERS' RIGHTS

INCOMING
C.P.V.O. / O.C.V.V.
31 JAN. 2011
N°

1.	Reference no. reporting authority	:	LMN00005
2.	Requesting authority	:	OCVV / CPVO
3.	Reference no. requesting authority	:	2010/0855
4.	Breeders reference	:	Henry Dacapo
5.	Date of application	:	06-05-10
6.	Applicant	:	Hermann-Josef Wilhelm, KALKAR
7.	Agent	:	
8.	Botanical name of taxon	:	Lemna minor L.
9.	Common name of taxon	:	Duck weed
10.	Variety denomination	:	Henry Dacapo
11.	Breeder	:	Hermann-Josef Wilhelm, KALKAR
12.	Testing authority	:	Naktuinbouw, NL
13.	Testing station and place	:	Naktuinbouw, ROELOFARENDSVEEN, NL
14.	Period of testing	:	2010
15.	Date and place of issue of document	:	17-01-2011, Roelofarendsveen, NL

16. RESULTS OF THE TECHNICAL EXAMINATION AND FINAL CONCLUSION

a.	**Report on Distinctness:** Is the variety clearly distinguishable from any other variety whose existence is known to us:	Yes
b.	**Report on Uniformity:** Is the variety sufficiently uniform with regard to the particular features of its sexual reproduction or vegetative propagation:	Yes
c.	**Report on Stability:** Is the variety stable in its essential characteristics:	Yes

17. REMARKS

A variety description is included in case of a positive report.

18. Signature The Team Leader

Dr. Ir. R.M.A.P. Haegens

Community Plant Variety Office • Office Communautaire des Variétés Végétales •

nak tuinbouw

1. Reference number requesting authority	LMN00005
2. Reference number requesting authority	2010/0855
3. Breeder's reference	Henry Dacapo
4. Applicant	Hermann-Josef Wilhelm, Kalkar

5. Botanical name of taxon	Lemna minor L.
6. Common name fo taxon	Duck weed
7. Variety denomination	Henry Dacapo
8. Document number and date of protocol or guideline	
9. Document number and/or date of national guideline	NAT/LMN/1
10. Testing authority	Naktuinbouw, NL
11. Test station and place	Naktuinbouw, ROELOFARENDSVEEN, NL
12. Period of testing	2010
13. Date and place of issue of document	17-01-2011, Roelofarendsveen

14. Group	-

nak tuinbouw

15. Characteristics included in the protocol or guideline

No.	Characteristics	States of expression	Note	Remarks
1	Root: length	short to medium	4	
2	Root: color (in full grown stage)	green	1	
3	Root: length of root tip	medium	5	
4	Root: color of tip	green	1	
5	Leaf: length	short	3	
6	Leaf: width	very narrow to narrow	2	
7	Leaf: shape	circular	1	to ovate
8	Leaf: intensity of green color of upper side	dark	4	
9	Leaf: color of lower side	green	1	
10	Leaf: intensity of color of lower side	not observed	N	
11	Leaf: color of margin	green	2	
12	Leaf: shape of apex	rounded	3	
13	Leaf: intensity of anthocyanin coloration of upper side	absent or very weak	1	
14	Leaf: intensity of anthocyanin coloration of lower side	absent or very weak	1	

nak tuinbouw

16. Similar varieties and differences in relation to those varieties

Denomination of similar variety	Characteristics in which the similar variety is different	State of expression of similar variety	State of expression of candidate variety
Henry Allegro	Leaf: shape	2	1 to ovate
Henry Allegro	Leaf: length	4	3
Henry Allegro	Leaf: width	3	2

17. Additional information

a) Additional data:
The variety is vegetatively propagated.

b) Remarks:
-

10.6 Official Product specification

***Lemna minor* flour basic, executed for UNIPER**

1. **Product**

1.1 Naming:

Lemna minor flour Basic

1.2 Suggested Declaration

Ground *Lemna*

1.3 Product description

The *Lemna minor* is dried and then finely ground. The entire cultivation process takes place indoor in greenhouses under controlled HACCP conditions. Thermal sterilisation, drying and grinding are preferably carried out at the place of cultivation.

1.4 Sustainability

Innovative vertical farming ensures high ground area efficiency and resource efficiency, minimises water consumption and prevents nutrients from entering the subsoil. In line with the EU Sustainability Goals, the environment and biosphere are relieved and production is also local.

Detailed life cycle assessment prepared by the Institute for Energy and Environmental Research, Heidelberg.

2. Human Food requirements

2.1 Certification

Wolffia arrhiza and *Lemna minor* + *Lemna Gibba* mix is certified as novel Food. Currently no certification for *Lemna minor* yet. Organic certification according to the EU organic logo, "Naturland" or similar is being sought. However, HACCP-certified inclusion in the positive list for feed materials is available.

2.2 Use of the product

Vegan protein product, meat substitutes, Sports nutrition, Smoothies, texturized products, baked goods.

The Fraunhofer Institute for Process Engineering and Packaging, IVV Freising, is currently carrying out relevant tests to clarify functional properties.

2.3 Sensory properties

Appearance:	light green powder
Odour:	typical of the species without foreign odour
Consistency:	finely ground powder
Particle size:	99.6% < 250µm

2.4 Nutritional information

High protein content, good Ω6/Ω3 fatty acid ratio, high vitamin B12 content.

2.5 GMO

Lemna minor flour basic is GMO-free according to regulation (EG) Nr. 1829/2003 and 1830/2003.

2.6 Allergens

Lemna minor flour basic is produced exclusively from pure plant material. The plants are grown indoors under strictly controlled conditions. Further processing means that contamination with known allergens can be ruled out.

Lemna minor is therefore free from animal protein and known allergens.

2.7 Freedom from animal testing

Lemna minor ground basic: freedom from animal testing.

2.8 BSE/TSE free

Lemna minor ground basic is 100% vegan and therefore free from BSE and TSE.

2.9 Nanoparticle

Free from nanoparticle

2.10 Irradiation

Lemna minor ground basic was not irradiated

3. Storage, Food shelf life, packaging

Storage	cool, dry, protected from light and tightly sealed
Shelf life	in the original packaging, the product has a shelf life of at least 24 months from the production date
Packaging	in accordance with the legal provisions of the EU

Lemna minor ground basic is a natural product. The above information may therefore be subject to natural fluctuations.

This specification does not release the purchaser of the product from his own responsibility and duty of care in handling the product.

10.7 Novel food registration for *Lemna minor/Lemna gibba mix*

Novel Food request examination executed by:

(EU) Commission Implementing Regulation (EU) 2017/2470 of 20 December 2017 establishing the Union list of novel foods in accordance with Regulation (EU) 2015/2283 of the European Parliament and of the Council on novel foods, EFSA Journal 2022;20(11):7598,

(OJ L 351, 30.12.2017, p. 72)
https://doi.org/10.2903/sp.efsa.2024.EN-8963

Novel food certification executed by:

European Commission, Directorate-General for Health and Food Safety, Ursula von der Leyen (2025). Commission Implementing Regulation (EU) 2025/153 of 29 January 2025 authorising the placing on the market of Lemna minor and Lemna gibba plants as novel food and amending Implementing Regulation (EU) 2017/2470
https://eur-lex.europa.eu/eli/reg_impl/2025/153/oj/eng

11. ACKNOWLEDGEMENTS

First and foremost, I want to express my gratitude to my doctoral supervisor, Prof. Dr. Heiner E. Goldbach, for his invaluable assistance during the entire project. He was an engaged conversation partner and a continuous counsel due to his extensive experience and knowledge. As the first examiner, I am particularly grateful to Prof. Dr. Ralf Pude, whose enthusiasm for the topic enabled this effort. I also thank his employees at the Klein-Altendorf campus's exterior laboratories. First and foremost, I'am grateful to Dr. Thorsten Kraska and Karl-Josef Wiesel for providing the technological resources needed to conduct the research. From that point on, Christian Heck and HGoTech GmbH gave me the LemnaLab facility and light tables to use in the culture studies.

Additionally, I am grateful to Dr. Gaiser of the University of Bonn's Department of Plant Production (INRES) for enrolling me in the course 'Cropping Systems Analysis and Modelling'. I was able to use the Simile® program to apply my analytically determined growth with lecturer Gunther Krauss as part of the lecture exercises. Any subsequent expansion into an all-encompassing growth model was based on this.

I also thank Mr. Wilhelm and Ms. Rogmans of Oxygenesis GmbH Kalkar. Since 2007, I have had the opportunity to collaborate with them on the co-design of multiple aquatic culture systems. At the start of this endeavour, the initial trials were also done there. Several *Lemnaceae* species registered with the CPVO were donated by Maria Rogmans and Hermann-Josef Wilhelm for the trials conducted there as well as the subsequent trials at the University of Bonn. The Naktuinbouw in Rolafsfarensveen, Netherlands, which conducted the variety testing and classification for the CPVO, is also acknowledged.

Additionally, Nicolas Leschke, Frank Brauer, and Carsten Mehl from ECF-Farm Systems GmbH's aquaponics facility in Berlin are greatly appreciated. There, I was able to construct a *Lemna* culture system's scaling stage and conduct the first long-term culture experiments using processed fish slurry as a source of nutrients. The *Lemna* biomass generated in cascade use was meant to serve as the primary source of nutrients for an edible fish that was initially fed perch. Additionally, Barramundi Aquakultur GmbH in Hainburg is to be thanked for testing *Lemna* biomass as fish feed.

In addition, I appreciate the ISCDRA's invitation to attend their 2019 international meeting at the Weizmann Institute in Israel. For four days, I was able to talk about the unique field of *Lemnaceae* with professionals from around the world using my own lecture and poster. Prof. Dr. em. Marvin Edelmann deserves special recognition.

A special thanks goes out to UNIPER TECHNOLOGIES GmbH in Gelsenkirchen and UNIPER KRAFTWERKE GmbH in Düsseldorf, who are dedicated to expanding the culture process in the LEMNERGY Project, which uses CO_2 and waste heat from power plants. I want to express my gratitude to Dr. Helmut Rode in particular for giving me the tools and analytical resources I needed for this effort, which have advanced the project. The European Climate, Infrastructure and Environment Executive Agency (CINEA), which authorised the EU financing application for additional upscaling, deserves special recognition. The "Competence Centre for Environmental Management NRW" is also acknowledged in this context for their candidacy for the NRW Innovation Award 2022.

Additional gratitude is due to Hannes Möller and Ansgar Rinklake, who not only provided me with CO_2, but also granted me permission to utilise the CO_2 gassing control system from HTK Hamburg, as well as to AIR LIQUIDE Deutschland GmbH, Krefeld.

For the combined oxalic acid and protein analyses, special thanks are due to Dr. Isabelle Heker from the lab of Prof. Dr. Rainer U. Meckenstock, University of Duisburg-Essen; Institute of Environmental Microbiology and Biotechnology.

Felix Gräven, Lydia Bertram, Gökcan Cem, and Peter Schmidt, my bachelor's students, deserve special recognition for their ambitious and high-achieving exam papers.

I would want to sincerely thank my parents, my entire family, Katrin, and my children, David, Benjamin, and Henry. I want to express my gratitude to my wife, Katrin Blanke, for her unwavering patience and support throughout the preparation and completion of this thesis, especially for her insightful and beneficial conversations regarding language clarity. My youngest son, Henry, deserves special recognition for finishing his school internship at my experimental facility at the University of Bonn.